

**GEOLOGICAL SETTING, COMPOSITIONAL FEATURES
AND K-Ar DATING OF PEGMATITE BODIES AROUND
OSOGBO-OKINNI AREA,
SOUTHWESTERN NIGERIA**

BY

KEHINDE ABAYOMI OWOYEMI

B.Sc. (Hons), Ilorin, M.Sc. (Mineral Exploration), Ibadan

MATRIC NO: 148582

**A thesis in the department of geology submitted to the faculty of science, university of
Ibadan, in partial fulfilment of the requirements for the award of the degree of**

DOCTOR OF PHILOSOPHY

of the

UNIVERSITY OF IBADAN

SEPTEMBER 2021

CERTIFICATION

I certify that this thesis was written by KEHINDE ABAYOMI OWOYEMI; Matric No:148582 under my supervision.

Prof. Olugbenga A. OKUNLOLA

B.Sc. (Ilorin), M.Sc. (ABU, Zaria), Ph.D. (Ibadan)

Department of Geology,

University of Ibadan,

Ibadan, Nigeria.

DEDICATION

I dedicate this work to God Almighty, the father of our Lord Jesus Christ, who through His Spirit helped me to fulfil the wish of my late mother.

ACKNOWLEDGEMENTS

I give all glory and thanks to God Almighty, the creator of all things who gave me life, health, and grace to undertake this research. God promised, and He fulfilled His promise, His holy name be praised.

I am very grateful to Professor Olugbenga AkindejiOkunlola, my supervisor, for challenging, encouraging and supporting me. His guidance and corrections which are invaluable brought out the best in me.

Words cannot express my appreciation to my darling wife Bolanle, who encouraged and supported me whole heartedly throughout this study. Thank you for enduring the littering of the house with books, journals, maps etc, and especially for my taking over the dining table/room as my study. I appreciate my children, Tosin, Tomi and Adewunmi for their prayers, encouragement, and good wishes.

I acknowledge and appreciate faculty members of the Geology department, Professors Olayinka, Adeyemi, Tijani, Ehinola, Nton; Drs Boboye, Bolarinwa, Olatunji, Oladunjoye, Osinowo, Oyediran, Adeigbe, and Adeleye, for their invaluable contributions to this work especially in the seminar room.

My profound appreciation goes to Mrs Maria Helena Bezerra Maia de Hollanda, the Director of the Geochronological Research Center, Institute of Geosciences, University of Sao Paulo, Brazil, who assisted in the geochronological analysis.

I appreciate Mrs Kemi Oni, for her hospitality during the period of my field work in Osogbo and environs, and Mrs Doyin Salami for logistics support. To all my colleagues and fellow students especially those who helped me during the field work, Gabriel, Efe, Segun, Austin, Wale, Oke and Bunmi, I say thank you. To all other members of my family, friends, and associates, for your prayers and kind wishes, I appreciate you all.

ABSTRACT

Pegmatites host a variety of economic rare metals and this has led to increased search and study of pegmatite belts globally. The Nigerian pegmatite belts continue to attract considerable attention due to their economic potentials. However, detailed geologic information on many of the pegmatites are still lacking and one of such are the pegmatite bodies of the Osogbo-Okinni area. Therefore, this study was aimed at geological evaluation of the pegmatite bodies around Osogbo-Okinni area southwestern Nigeria to elucidate their compositional features, mineralisation potentials and age of their emplacement.

Geological mapping on a scale of 1:25,000 was undertaken. Slides from 39 rock chips were made for petrographic study. Twenty-two whole pegmatite, 22 feldspar and 17 mica extracts of the pegmatite were crushed, pulverised, and homogenised. These were analysed for major, trace and rare earth elements using Inductively Coupled Plasma Atomic Emission Spectroscopy and Inductively Coupled Plasma Mass Spectroscopy. Age determination was achieved using the Cassinoli technique for unspiked K-Ar method on mica extracts. Data interpretation was by descriptive statistics and geochemical variation plots.

The pegmatite intruded granite gneiss, quartzite, amphibolite, and granite as low-lying, thin, and massive dykes. Quartz (25.0%), microcline (34.0%) and plagioclase (24.0%) were the main mineral constituents, while muscovite (5.0%), biotite (5.0%), and tourmaline (7.0%) were minor constituents. The mean concentration of SiO_2 , Al_2O_3 , Na_2O , K_2O and TiO_2 were 70.92, 15.95, 3.5, 4.23, and 0.02 wt%, respectively. Average whole pegmatite trace elements contents (ppm) were 283.95, 101.94, and 70.35 for Ba, W, and Ta. The light rare earth elements sum (18.92 ppm) was greater than that of heavy rare earth elements (2.22 ppm) indicating high fractionation for the pegmatites. The mica extracts average trace elements contents (ppm) was 510.86, 104.86, 376.88, 1101.97, and 272.41 for Sn, Sc, Li, Rb, Nb, respectively. Low K/Rb (50.37-340.77) and Mg/Li (1.23-36.54) ratios indicated fractionated pegmatites. The plots of $\text{Na}_2\text{O}+\text{K}_2\text{O}$ versus SiO_2 , $\text{Al}_2\text{O}_3/\text{Na}_2\text{O}+\text{K}_2\text{O}$ versus $\text{Al}_2\text{O}_3/\text{CaO}+\text{Na}_2\text{O}+\text{K}_2\text{O}$ and K/Rb versus Cs indicated igneous origin, peraluminous nature and placed the pegmatites in the muscovite class of lithium-caesium-tantalum pegmatite family. The pegmatites were products of syn-collisional and within-plate tectonic environments and are classified as complex and simple types based on enrichment in Ta, Nb, Sn and Li content. Furthermore, there were clear differences in fractionation indices of Mg/Li,

K/Rb, and K/Cs (1.23-10.64, 50.37-152.88 and 1,375.22-5,570.54) for the complex and the simple (13.75-36.54, 51.60-309, and 2,065.04-17,645.77) pegmatites. The complex pegmatite accounted for 36% of the total pegmatite samples analysed. The age of the pegmatites was put at 774-692 Ma, corresponding to evolution during the early Pan-African orogeny.

The Osogbo-Okinni pegmatites are of simple and complex types and are of early Pan African age. The complex ones have noticeable Ta-Sn-Nb and Limineralisation.

Keywords: Complex pegmatites, Pan african age, Fractionated pegmatite, Cassinoltechnique.

Word count: 441

TABLE OF CONTENTS

	PAGE
Title	i
Certification	ii
Dedication	iii
Acknowledgements	iv
Abstract	v
Table of Contents	vii-ix
List of Tables	x-xi
List of Figures	xii-xvii

CHAPTER ONE: INTRODUCTION

1.1	Study background	1
1.2	Aim of study	4
1.3	Objectives of study	4
1.4	Justification	4
1.5	Location and accessibility	5
1.6	Climate and vegetation	5
1.7	Relief and drainage pattern	7

CHAPTER TWO: LITERATURE REVIEW

2.1	Pegmatites	10
2.1.1	Definition	10
2.1.2	Composition	10
2.1.3	Texture	10
2.1.4	Formation of pegmatites	11
2.1.5	Classification of pegmatites	12
2.1.5.1	Pegmatite groups	12
2.1.5.2	Pegmatite classes and types	12

2.1.5.3	Pegmatite families	13
2.1.6	Pegmatites of Nigeria	16
2.1.7	Industrial potentials of pegmatites	19
2.2	K/Ar geochronology	20
2.2.1	Introduction	20
2.2.2	The conventional K/Ar method	21
2.2.2.1	Correction for atmospheric argon contamination	26
2.2.2.2	Loss of radiogenic argon ($^{40}\text{Ar}^*$)	27
2.2.2.3	Presence of excess radiogenic argon ($^{40}\text{Ar}^*$)	27
2.2.3	K-Ar Isochron dating	28
2.2.4	The $^{40}\text{Ar}/^{39}\text{Ar}$ method	30
2.2.4.1	Benefits of $^{40}\text{Ar}/^{39}\text{Ar}$ method	32
2.2.4.2	Limitations of $^{40}\text{Ar}/^{39}\text{Ar}$ method	32
2.2.5	The Cassinot technique	33
2.3	Previous works review	36
2.4	Regional geological setting of Nigeria	41
2.4.1	The Basement Complex	43
2.4.2	Younger Granites	47
2.4.3	Sedimentary basins	49

CHAPTER THREE: METHODOLOGY

3.1	Field mapping	51
3.2	Sample preparation	51
3.3	Petrographic studies	53
3.4	Geochemical analysis	53
3.5	Geochronology	53

CHAPTER FOUR: RESULTS AND DISCUSSION

4.1	Geology of Osogbo-Okinni area	55
4.1.1	Migmatite	58
4.1.2	Granite gneiss	63
4.1.3	Quartzite	63
4.1.4	Amphibolite	66
4.1.5	Granite	70
4.1.6	Pegmatite	72
4.1.6.1	Field occurrence	72
4.1.6.2	Petrography	77
4.2	Structures	85
4.3	Geochemistry	94
4.3.1	Granite Gneiss	94
4.3.2	Granites	112
4.3.3	Pegmatites	131
4.3.3.1	Whole rock chemistry	131
4.3.3.2	Mineral chemistry	152
4.3.3.2.1	Feldspar	152
4.3.3.2.2	Mica	153
4.3.4	The pegmatite groups of Osogbo-Okinni area	164
4.4	K-Ar geochronology of pegmatites of Osogbo-Okinni area	176
4.5	Indications from the study	180

CHAPTER FIVE: SUMMARY, CONCLUSION AND RECOMMENDATION

5.1	Summary	184
5.2	Conclusion	185
5.3	Recommendation	185
5.4	Contributions to knowledge	185
	REFERENCES	187

LIST OF TABLES

Table 4.1	Modal composition of associated rocks	62
Table 4.2	Modal composition of pegmatites	78
Table 4.3	Major oxide composition of granite gneisses	96
Table 4.4	Trace elements concentration in granite gneisses	97
Table 4.5	Rare earth elements composition of granite gneisses	99
Table 4.6	Ratios and sums of some major element oxides and some trace elements of granite gneisses	100
Table 4.7	Major oxide composition of granite	113
Table 4.8	Trace elements in granites	115
Table 4.9	Rare earth elements composition of granite	117
Table 4.10	Average major element composition of Osogbo-Okinni granite compared to other older granites in Nigeria	125
Table 4.11	Major oxide content of whole rock, feldspar extracts and mica extract	132
Table 4.12	Elemental ratios of selected major oxides of whole rock	136
Table 4.13	Major element oxide content of Osogbo-Okinni pegmatites compared to pegmatites from various locations in Nigeria	137
Table 4.14	Trace element content (ppm) of whole rock, feldspar, and mica extracts	139
Table 4.15	Rare earth element content (ppm) of whole rock, feldspar extracts, mica extracts	141
Table 4.16	Range of selected trace elements content and elemental ratios in whole rock of fertile granites and average value for upper continental crust compared to that of Osogbo-Okinni pegmatites	144
Table 4.17	Selected trace element contents and elemental ratio of K-feldspar of barren, fertile, and rare element pegmatites compared to Osogbo-Okinni pegmatite	155
Table 4.18	Selected trace element contents and elemental ratio of mica extracts of fertile granite, beryl-type, and spodumene-subtype pegmatites	

compared to Osogbo-Okinni pegmatite.

Table 4.19	Comparison of selected oxides and trace elements in complex and simple pegmatites of Osogbo-Okinni area.	165
Table 4.20	Comparison of major oxides and some trace element concentration of granite and pegmatites of Osogbo-Okinni area.	173
Table 4.21	Geochemical characteristics of some well-studied pegmatites compared with Osogbo-Okinni Pegmatites	175
Table 4.22	Unspike K-Ar ages of Osogbo-Okinni pegmatites	178
Table 4.23	Derived absolute age of Osogbo-Okinni pegmatites compared to other Neoproterozoic rocks of Nigeria, Africa, and South America	179

LIST OF FIGURES

Figure 1.1	Geological map of Nigeria showing the seven fields of pegmatites of Nigeria (after Okunlola, 2005)	3
Figure 1.2	Map of Osogbo-Okinni area, Southwestern Nigeria.	6
Figure 1.3	Land use and land cover map of Osogbo, 1986; Source: Authors lab work, 2018	8
Figure 1.4	Map of Osogbo-Okinni area showing drainage and relief	9
Figure 2.1	Pressure – Temperature diagram showing the fields of the four pegmatite classes proposed by Ginsburg, (1984) and Cerny, (1991a). the pegmatite classes are AB - abyssal, MS - muscovite, RE - rare element, and MI - miarolitic.	14
Figure 2.2	Geological times logarithmic scale and radiometric method range of application (after Odin 1990, 1994)	23
Figure 2.3	Decay scheme of potassium 40 (after Gillot et al, 2006)	24
Figure 2.4	Principle of atmospheric correction and signal calibration (after Gillot et al., 2006)	34
Figure 2.5	Generalized map of the geology of Nigeria (after Obaje, 2009).	42
Figure 2.6	Map of Schist belts of Nigeria (after Woakes et al., 1987)	45
Figure 2.7	Major Younger Granites localities in Nigeria (after Obaje, 2009)	48
Figure 3.1	Map of the Osogbo-Okinni area showing the sample points	52
Figure 4.1a	Quarry face of a massive pegmatite outcrop at Asipa, Okinni area	56
Figure 4.1b	Pegmatite outcrop by River Apala, Okinni area	56
Figure 4.2	Geological map of Osogbo-Okinni area, Southwestern Nigeria	57
Figure 4.3	Chilled margin of pegmatite around the migmatite xenolith (length of pen), (Dagbolu, SE of Oba).	59
Figure 4.4	Migmatite xenoliths in pegmatite shown by arrows (Asipa, SW of Oba)	60
Figure 4.5	Photomicrograph of a section of migmatite in transmitted light showing albite (A), quartz (Q), hornblende (H), biotite (B) and muscovite (M).	61
Figure 4.6	Part of granite gneiss outcrop at the northwestern edge of the study area.	64
Figure 4.7	Photomicrograph of a section of granite gneiss in transmitted light,	

Showing quartz (Q), microcline (Mic), biotite (B) and albite (A). 65

- Figure 4.7** Amphibolite intruded by pegmatite vein (1.4m width, between the marker and pencil). 67
- Figure 4.9a** Specimen of amphibolite (north of Oba) showing foliation of about 1mm thickness 68
- Figure 4.9b** Specimen of amphibolite showing banding of about 0.5-1.0cm thickness 68
- Figure 4.10** Photomicrograph of a section of amphibolite in transmitted light showing hornblende (H) with cleavage, plagioclase (PL) and quartz (Q) minerals. 69
- Figure 4.11** Photomicrograph of a section of granite in transmitted light showing microcline (Mic), quartz (Q) and biotite (B). 71
- Figure 4.12** Pegmatite veins in-filled with tourmaline mineralization (arrows) at Apala river, Okinni. 73
- Figure 4.13** Books of mica aggregate on pegmatite outcrop at Awosin, Northeast of Okinni 74
- Figure 4.14** Hand specimen of pegmatite of Osogbo-Okinni area showing books of muscovite, (arrows). 75
- Figure 4.15a.** Quartz vein in mountainous pegmatite (about 150x500m) at Awosin. 81
- Figure 4.15b** Thick quartz vein and later joints in the vein in pegmatite at Awosin 81
- Figure 4.16** Photomicrograph of a section of pegmatite in transmitted light, showing albite (A), muscovite (M) and quartz (Q). 79
- Figure 4.17** Photomicrograph of a section of pegmatite in transmitted light showing large crystals of microcline (Mic), quartz (Q) and albite (A). 80
- Figure 4.18a** Photomicrograph of a section of pegmatite in transmitted light showing microcline with perthitic structure (exsolution of albite lamellae (A) within microcline (Mic)) in cross polarized light, XPL 82
- Figure 4.18b** same as figure 4.17a, but in plane polarized light, PPL. 82
- Figure 4.19** Photomicrograph of a section of pegmatite in transmitted light showing albite (A), microcline (Mic), muscovite (M), and biotite (B). 83a

Figure 4.20	Photomicrograph of a section of pegmatite at Dagboluin transmitted light showing garnet (Grt), albite (A) and quartz (Q).	84
Figure 4.21	Joints pegmatites of Osogbo-Okinni area at Oba	87
Figure 4.22	Rose diagram for the orientation of joints in granite gneiss of Osogbo-Okinni area	88
Figure 4.23	Rose diagram for the orientation of joints in granite of Osogbo-Okinni area	89
Figure 4.24	Rose diagram for the orientation of joints in Pegmatite of Osogbo-Okinni area	90
Figure 4.25	Rose diagram for the orientation of veins in granite gneiss of Osogbo-Okinni area	91
Figure 4.26	Rose diagram for the orientation of veins in granite of Osogbo-Okinni area	92
Figure 4.27	Rose diagram for the orientation of veins in pegmatites of Osogbo-Okinni area	93
Figure 4.28	Plot of $Al_2O_3/(CaO+Na_2O+K_2O)$ v Al_2O_3/Na_2O+K_2O (after Shand, 1943)	101
Figure 4.29	Plot of Na_2O/Al_2O_3 vs K_2O/Al_2O_3 (after Garrels and Mackenzie, 1971)	102
Figure 4.30	Plot of P_2O_5/TiO vs MgO/CaO (after Werner, 1987)	103
Figure 4.31	AFM ternary plot for granite gneiss, (after Irvine and Baragar, 1976).	104
Figure 4.32	Plot of K_2O vs SiO_2 , (after Peccerillo and Taylor, 1976).	105
Figure 4.33	Classification plot of Fe_2O_3/MgO vs $(Zr+Nb+Y+Ce)$ for granite gneiss, (after Walden et al., 1987).	107
Figure 4.34	Rb vs Nb+Y tectonic discrimination diagram for granite Gneiss. WPG =Within Plate Granite,ORG=Ocean Ridge Granite, VAG= Volcanic Arc Granite, Syn-COLG= Syn Collisional Granite, (after Pearce et al. 1984)	108

Figure 4.35	Y vs Nb Tectonic discrimination diagram for granite gneiss. WPG = Within Plate Granite, ORG = Ocean Ridge Granite, VAG = Volcanic Arc Granite, Syn-COLG = Syn Collisional Granite, (after Pearce et al. 1984)	109
Figure 4.36	Chondrite normalized plot for granite gneiss, (chondrite values after Sun and McDonough, 1989).	110
Figure 4.37	Primitive mantle-normalized plot for granite gneiss, (after MacDonough et al., 1992)	111
Figure 4.38	Harker diagrams for granite, (arrow shows increasing fractional differentiation).	114
Figure 4.39	Plot of $\text{Na}_2\text{O}/\text{Al}_2\text{O}_3$ vs $\text{K}_2\text{O}/\text{Al}_2\text{O}_3$ (after Garrels and MacKenzie, 1971).	118
Figure 4.40	AFM diagram for granite of Osogbo-Okinni area, (after Irvine and Baraga, 1971)	119
Figure 4.41	Plot of K_2O vs SiO_2 for granite of Osogbo-Okinni area, (after Le Maitre et al., 1989)	120
Figure 4.42	Plot of total alkali vs silica for granites of Osogbo-Okinni area, (after Cox et al., 1979)	121
Figure 4.43	$\text{Na}_2\text{O} + \text{K}_2\text{O}$ vs SiO_2 diagram for granite of Osogbo-Okinni Area (after Middlemost, 1994)	122
Figure 4.44	Plot of Nb vs Y for granite of Osogbo-Okinni area, (after Pearce et al., 1984)	126
Figure 4.45	Plot of Rb vs Yb+Ta for granite of Osogbo-Okinni area, (after Pearce et al., 1984)	127
Figure 4.46	Plot of Rb vs Sr for granites of Osogbo-Okinni area showing the depth of emplacement (after Condie, 1973)	128
Figure 4.47	Chondrite-normalized rare earth element pattern for granites of Osogbo-Okinni area, (normalization values after Sun and McDonough, 1989)	129
Figure 4.48	Chondrite-normalised plot of incompatible trace elements for granite, (normalization values after Taylor and McLennan, 1985).	130

Figure 4.49	Na ₂ O+K ₂ O vs SiO ₂ diagram for whole rock pegmatites, (after Gillespie and Styles, 1999).	133
Figure 4.50	Plot of Al ₂ O ₃ /Na ₂ O+K ₂ O against Al ₂ O ₃ /CaO+Na ₂ O+K ₂ O, (after Maniar and Piccoli 1989).	142
Figure 4.51	K/Rb vs Cs diagram, (After Cerny, 1982).	143
Figure 4.52	Plot of Ta vs Ga,(after Moller and Morteani, 1987)	145
Figure 4.53	Plot of Ta vs Cs,(after Moller and Morteani, 1987).	146
Figure 4.54	Plot of Ta vs Rb+Cs for whole rock, feldspar, and mica extracts showing Ta mineralization,(mineralization lines after Beus, 1966 and Gordiyenko 1971).	148
Figure 4.55	Plot of Ta vs Rb for whole rock, feldspar, and mica extracts showing Ta mineralization,(mineralization lines after Beus, 1966, and Gordiyenko, 1971).	149
Figure 4.56	Plot of Ta vs K/Cs for whole rock, feldspar, and mica extracts showing Ta mineralization.	150
Figure 4.57	REE pattern for Whole Rock of Osogbo-Okinni pegmatites	151
Figure 4.58	Plot of K/Rb vs Cs in K-feldspar showing groups ‘a’ and ‘b’ pegmatites, (after Breaks et al, 2003).	154
Figure 4.59	Plot of K/Rb vs Rb/Sr for K-feldspar showing evolved pegmatites, (after Larsen, 2002)	156
Figure 4.60	Plot of Ba/Rb vs Rb/Sr for K-feldspar showing increasing evolution, (after Larsen, 2002)	157
Figure 4.61	Plot of K/Rb vs Pb showing the evolution trend of pegmatites with increase in Pb concentration in feldspar extract, (after Larsen, 2002)	158
Figure 4.62a	Plot of K/Rb vs Rb in Feldspar extracts of Osogbo-Okinni pegmatite	159
Figure 4.62b	Plot of K/Rb vs Rb in K-feldspar from Chaipaval, Sletteval, Bhoiseabhal in Scotland (Shaw et al., 2016), Kaatiala, Finland	

	(Lappalainen and Neuvonen, 1968) and Canada (Cerny et al., 2012b)	159
Figure 4.63	Ta mineralization in some mica extract samples above Gordiyenko, (1971) mineralization line.	161
Figure 4.64	Plot of K/Rb vs Cs showing positive correlation between cesium and rubidium and degree of fractionation in mica extract, (after Breaks et al., 2003).	162
Figure 4.65	Distributionmap of Niobium concentration in pegmatites of Osogbo-Okinni area	166
Figure 4.66	Distributionmap of Lithium concentration in pegmatites of Osogbo-Okinni area	167
Figure 4.67	Distributionmap of Tin concentration in pegmatites of Osogbo-Okinni area	168
Figure 4.68	Distributionmap of Tantalum concentration in pegmatites of Osogbo-Okinni area	169
Figure 4.69	Spider diagram of REE content of some simple pegmatites of Osogbo-Okinni area showing positive Eu anomalies.	170
Figure 4.70	Spider diagram of REE content of complex pegmatites of Osogbo-Okinni area showing negative Eu anomalies.	117

CHAPTER ONE

INTRODUCTION

1.1 Study Background

The use of rare metals, like tantalum, niobium, lithium, columbite, tin, tungsten, etc. hosted by pegmatites has developed substantially over recent years especially in applications to electronic products, medicinal equipment and alloys. As a result of this, there has been increase in demand and prospecting for these metals globally.

The continent of Africa is endowed with pegmatites highly enriched in rare metal minerals (von Knorring and Condliffe, 1987 Fetherston, 2004). Burundi, DRC, Rwanda, and Uganda have been producing tin (Sn) and Tantalum (Ta) for almost 100years. Furthermore, provinces of tantalum (Ta), niobium (Nb) and tin (Sn) are in other African nations like Ethiopia, Mozambique, Egypt, Somalia, Namibia, Madagascar, Nigeria, South Africa, and Zimbabwe. Deschamps et al. (2006) produced a database and map showing over 1500 locations of tantalum (Ta) and niobium(Nb) deposits in Africa.

Nigeria possesses vast reserves of solid minerals, which include, precious minerals, minerals for industrial and energy applications, base minerals, and metals. Between 1960 and early 1970s, Nigeria was a foremost exporter of tin, columbite, and coal. However, several political and economic factors, one of which is concentration on crude oil production for foreign exchange earnings, caused significant reduction in activities in this sector halfway into the 1970s, but successive governments of the federation have committed to revamping the sector(KPMG, 2017).To achieve this, the federal

government diversified the country's revenue base as part of the economy recovery plan and identified mining as an important revenue earning sector. Pegmatite is an important source of a large range of rare metals (Cerny, 1994). There is therefore a need to locate, delineate and constrain as many fertile pegmatite occurrences as possible in line with Nigeria's quest to diversify her economy through exportation of mineral resources for more forex earnings.

Nigeria is part of a formation of Pan-African orogenic belts during the merging of Gondwanaland in the Tonian (Neoproterozoic) to Cambrian period (1000-488Ma). These orogenic belts are generally made of rocks of Archean to Proterozoic age (4000-542Ma) modified during the Neoproterozoic to Cambrian (1000-488Ma) orogenic activities resulting in plutons which are essentially post-collisional granitoids (Kuster and Harms, 1998). These orogenic belts spreads from the African continent to the Brazilian orogenic belt of Latin America (de Wit et al., 2008). These Pan-African intrusions consist mainly of granites, granodiorites and tonalities intruded by pegmatites and aplite veins (Okunlola, 2005).

It was generally believed that Nigerian pegmatites result from magmatism of late Pan-African (Elueze, 2002). Okunlola and Udo-Udo, 2006, derived a late pan-African age for Komu pegmatite, $505-503 \pm 13$ Ma and Minna barren and rare-metal pegmatite was dated 560-450Ma (Melcher et al., 2013). However, recent studies reveal pegmatites of older ages in Ede, southwestern Nigeria which was dated 709 ± 29 -19Ma (Adetunji et al., 2016).

Earlier reports indicated that pegmatites enriched in rare metals can only be found along the SW-NE belt of Nigeria stretching up to 400 km to the tin field of Jos plateau (Wright, 1970). However, Garba, (2003) and Okunlola, (2005), recorded pegmatites beyond these limits. Okunlola, (2005) reported seven fields of mineralized pegmatites which include Kabba-Isanlu, Lema-Ndeji, Oke Ogun, Ibadan-Osogbo, Kushaka-BirninGwari, Keffi-Nassarawa, and Ijero-Aramoko (Figure 1.1). Generally, Nigerian pegmatites enriched in TaNb are complex albitised muscovite-quartz-microcline with

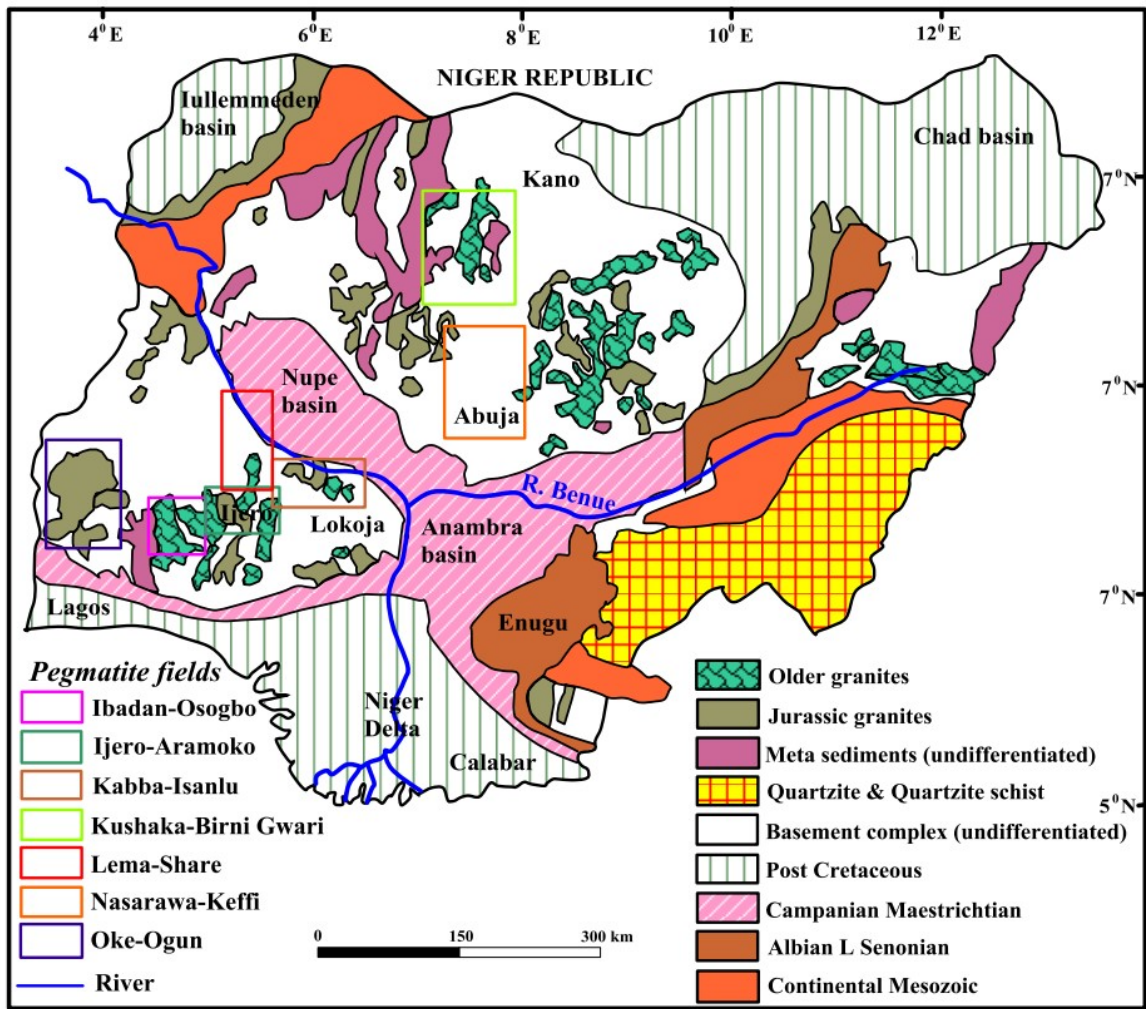


Figure 1.1 Geological map of Nigeria showing seven pegmatite fields of Nigeria.(after Okunlola, 2005)

unrecognisable to well delineated zonation (Okunlola and Jimba, 2006). Some of these fields, like Oke Ogun, Ibadan-Osogbo and Keffi-Nassarawa are being mined for rare and precious metals.

In the bid to further the geological evaluation of these pegmatite fields, the study of pegmatites of Osogbo-Okinni area which belong to the Ibadan-Osogbo pegmatite field is thus, being undertaken. The Ibadan-Osogbo pegmatite field is identified for further studies because of its numerous mountainous pegmatite outcrops covering a wide expanse of land especially in the Osogbo-Okinni-Oba area of the field. The understanding of composition, type, and geochronological placement of these rock suites will be new additions to the knowledge of Ibadan-Osogbo pegmatite field.

1.2 Aim of Study

The purpose of this study is geological appraisal of the pegmatite bodies around Osogbo-Okinni area southwestern Nigeria to elucidate their compositional features, mineralization potentials and age of their emplacement.

1.3 Objectives of Study

- i. To Identify the field/lithological relationship of the pegmatites and associated rocks of Osogbo-Okinni area.
- ii. To elucidate the petrographic and petrochemical features of these pegmatites
- iii. To determine the rare metal mineralisation potential of these pegmatites
- iv. To determine the age of these pegmatites

1.4 Justification

Among the pegmatite occurrences of Ibadan-Osogbo pegmatite field as identified by Okunlola (2005), the pegmatites of Osogbo-Okinni area have not been studied in detail like the Ibadan, Awo, Ede, and other pegmatite of Ibadan-Osogbo pegmatite field. Therefore, a detailed study of these pegmatites, as enumerated in the aim and objectives, has become necessary. The result of the study will unravel the mode of occurrence, origin, and emplacement of these pegmatites in the Earth's geochronological sequence.

Furthermore, this will reveal to greater details the general lithology and petrogenetic relationship of the pegmatite and associated rocks, and the economic potential of the rare metal (Ta-Sn-Nb) mineralisation.

1.5 Location and Accessibility

Osogbo-Okinni area is in Southwestern Nigeria, (Figure 1.2). It is situated between latitude $7^{\circ}45'N$ to $7^{\circ}57'N$ and longitude $4^{\circ}30'E$ to $4^{\circ}37'E$. Osogbo lies at the southern end of the study area while Okinni is at the west. The entire area is accessible through a good network of highways linking Osogbo with the other towns, motorable roads and bush paths leading to the numerous outcrops.

1.6 Climate and Vegetation

Osogbo's climate is tropical. This climate according to Köppen-Geiger climate classification is Aw type, (Koppen and Geiger, 1936). The southern part of Nigeria experiences maximum rainfall twice, with a short and a longer dry season in between. The first rainy period starts around March and continues to the end of July, this rainy season is followed by the August break, a short dry break in August lasting for two to three weeks. This break is succeeded by another period of rains from early September to mid-October. This cycle of rains and dry seasons ends with another dry season from late October to early March, (Agboola, 1979).

Southwestern Nigeria falls within the tropics with wet and dry seasons, a yearly rainfall between 150mm and 3000mm and temperature range between $21^{\circ}C$ and $34^{\circ}C$. The wet season is noted for a warm moist sea to land southwest monsoon from the Atlantic Ocean which ascends and produce copious rainfall because of its warmth and high humidity. The dry season is characterised by the northeast wind blowing almost continually from the Sahara Desert called the trade wind (Faleyimu et al., 2013).

The average annual temperature in Osogbo is $26.1^{\circ}C$ with 1241 mm of precipitation. January is the driest month with 9 mm precipitation. Peak precipitation is in September with an average of 202mm. March, with $28.3^{\circ}C$ average, is the hottest month while August with $23.7^{\circ}C$ average is the coldest (Ola and Adewale, 2014).

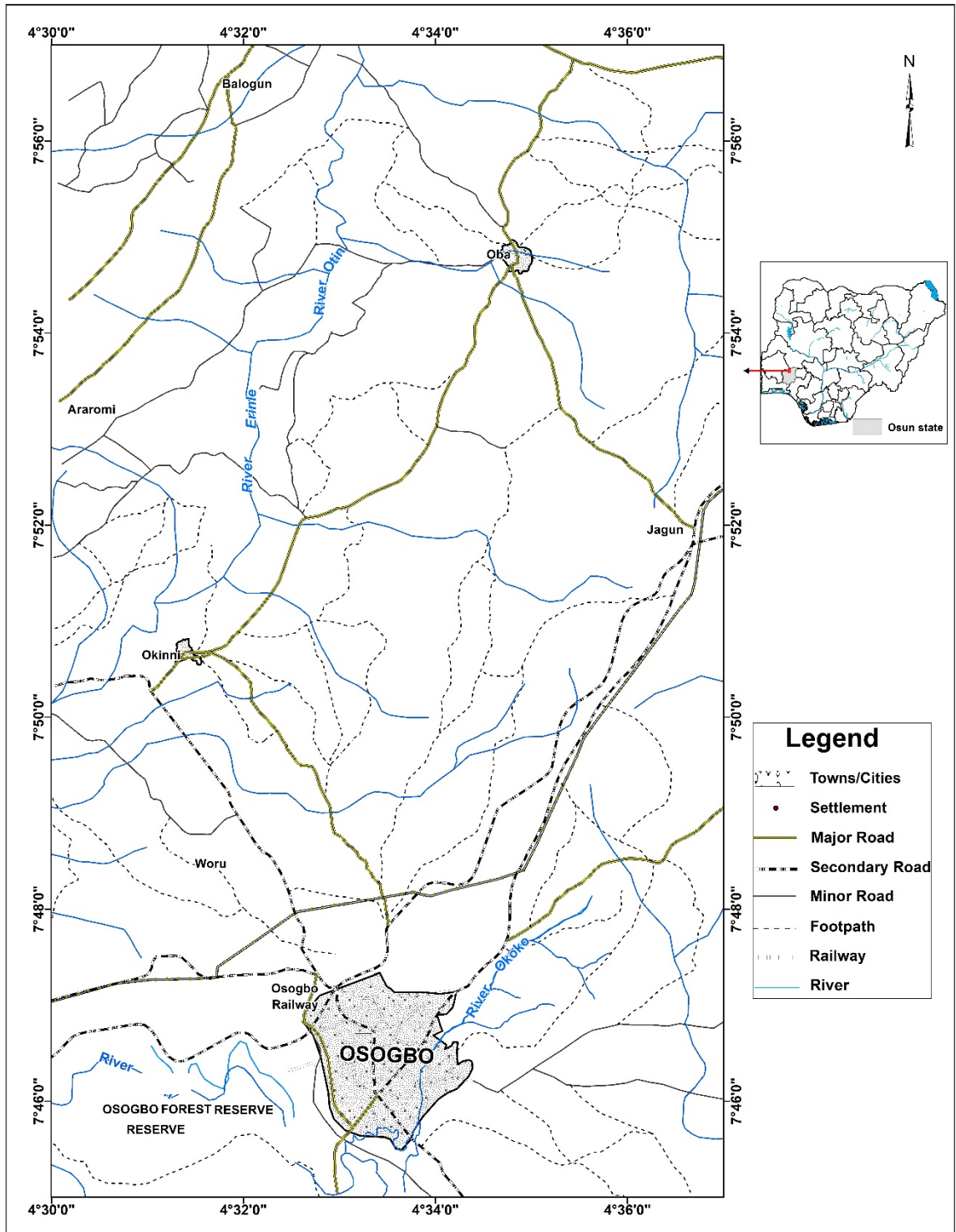


Figure 1.2. Map of Osogbo-Okinni area, Southwestern Nigeria

The vegetation of southwest Nigeria consists of freshwater wetland and mangrove forest at the fringes. This forest characterized by lowland extends northwards inland, while a secondary forest is located close to the derived southern Savannah at the northern end. Osogbo vegetation is a transition from rain forest and tropical equatorial in the South to Guinea and tropical Savanah towards the North, (Figure 1.3).

1.7 Relief and Drainage pattern.

The northern part of Osogbo-Okinni area hosts numerous domed hills and some flat-topped ridges, with prominent hills at Gbogbo, west of Oba. The land surface slopes from northern high altitude to low altitude in the south.

The entire land is drained by numerous rivers prominent among them is River Erinle, which takes its source from Erin area, northwest of the study area, flowing to the south along the west flank. Notable also are river Aleri, north of Oba, and river Okoko flowing into Osogbo area from the southeast. The drainage pattern is dendritic (Figure 1.4).

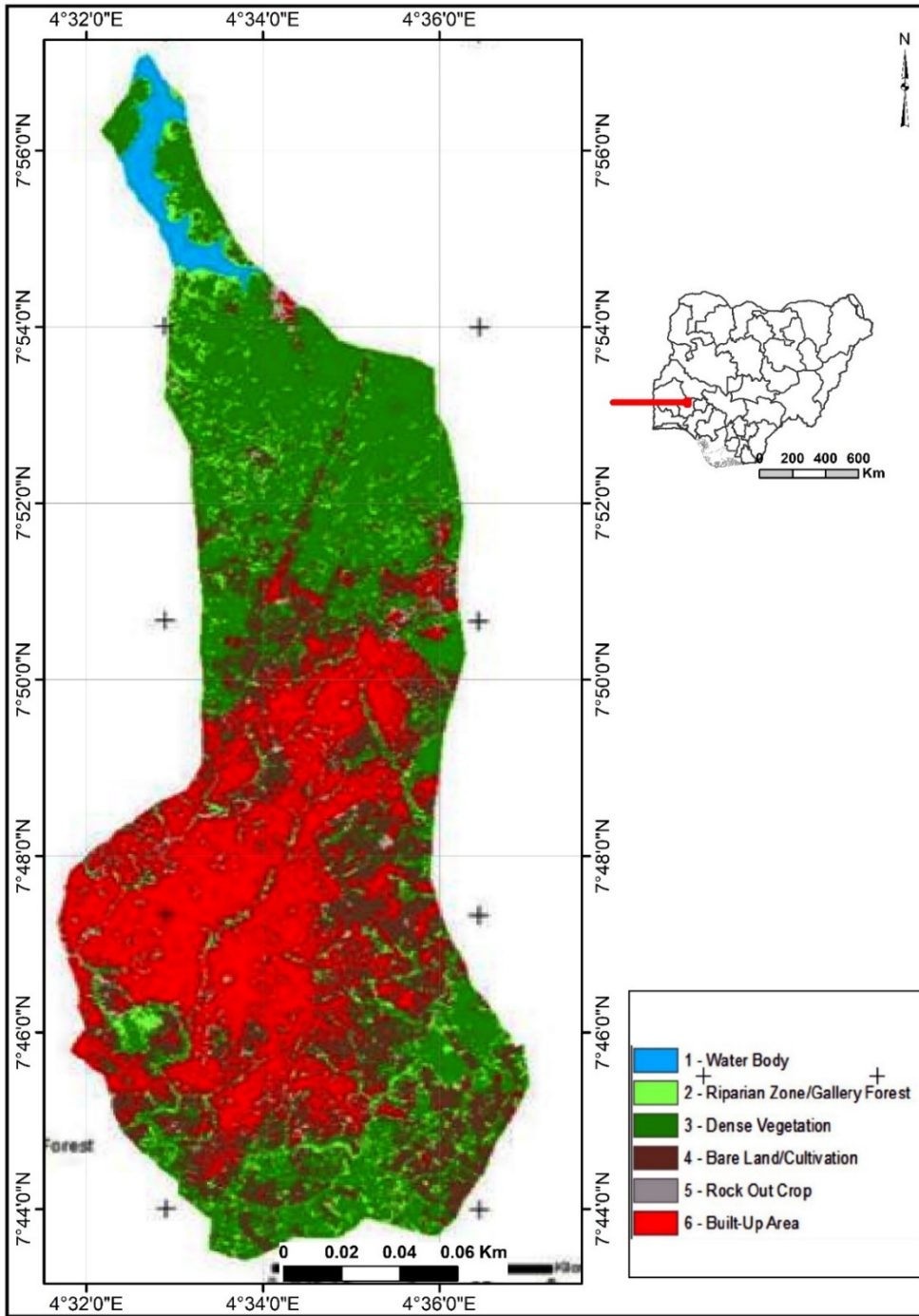


Figure 1.3 Land use and land cover map of Osogbo, 1986.

Source: Authors lab work, 2018

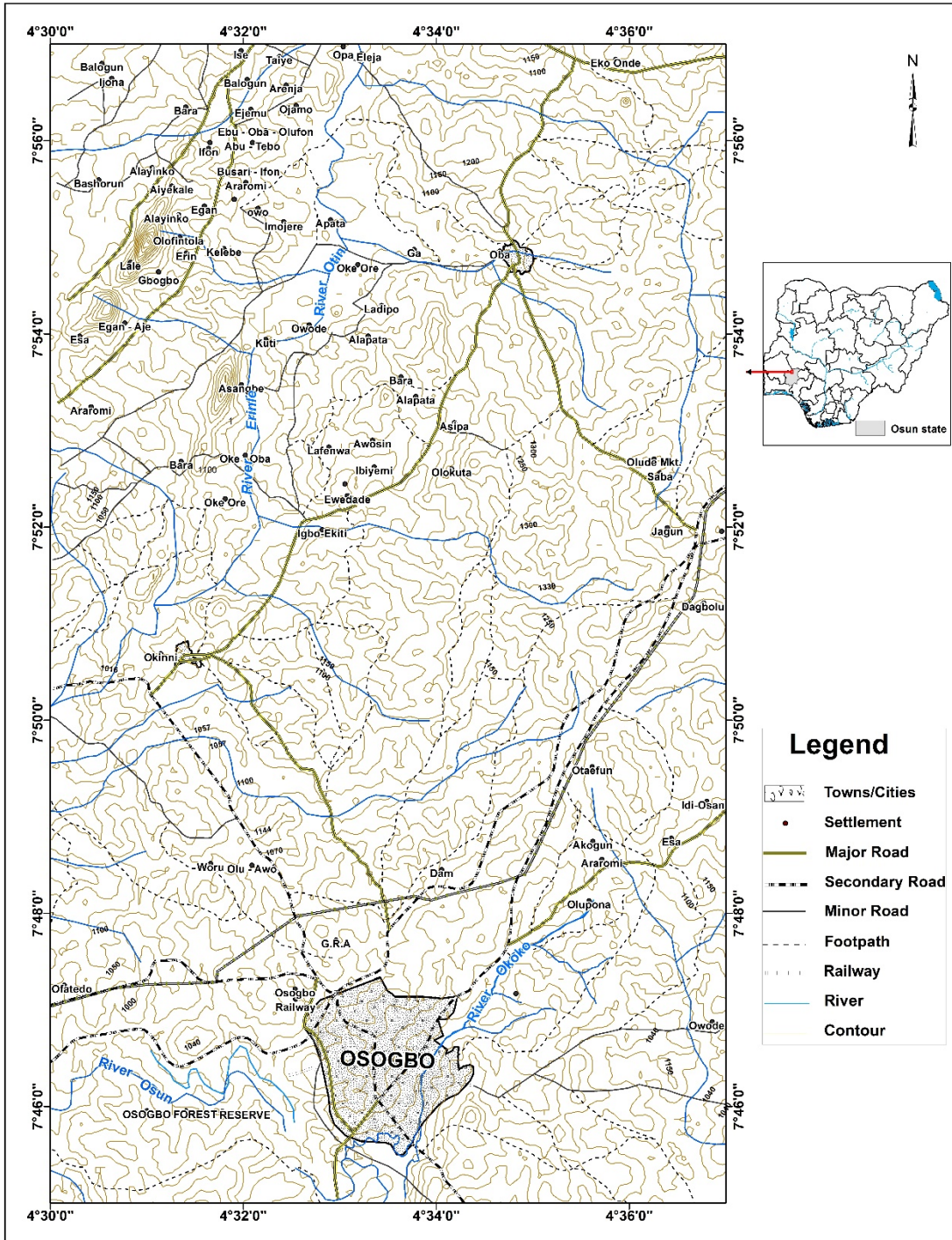


Figure 1.4 Map of Osogbo-Okinni area showing drainage and relief.

CHAPTER TWO

LITERATURE REVIEW

2.1 Pegmatite

2.1.1 Definition

Pegmatite is an igneous rock usually of granitic content differentiated by its very large but variable grain size from other igneous rocks, or by many of its crystals with skeletal, graphic, or other strong growth habit in defined directions. It intrudes igneous or metamorphic rocks as clearly defined homogeneous to zoned bodies (London, 2008).

2.1.2 Composition

Like the common igneous rocks, pegmatite consist of at least three major chemical components, and normally contain at least three of the common rock forming (silicate) minerals as major constituents. For example, the major chemical constituents of granites are SiO_2 , $\text{NaAlSi}_3\text{O}_8$, KAlSi_3O_8 and the prevailing minerals include quartz, sodic plagioclase, and K-feldspar. These minerals are the major component of pegmatite derived from granite, with minor constituents such as mica and garnet. Mineralization of pegmatite with rare metals like tantalum, tin, niobium, and lithium may occur where the pegmatite is highly fractionated.

2.1.3 Texture

What distinguished pegmatites from all other igneous rock types is their texture. The textural features geologists recognized among other textures as unique to pegmatites is the graphic intergrowth of feldspar and quartz crystals.

2.1.4 Formation of pegmatites

A magma chamber in which crystals are formed contain crystal mixtures in solid state and melt. Elements that chemically combine with other elements or minerals to form new minerals are called compatible elements. These elements which include Si, Al, Na, K become part of the structure of crystals of feldspar, quartz and mica which usually combine to form rocks. Elements remaining in the differentiated magma (partition into melt), are called incompatible. These elements include lithophile elements which have large ionic radii such as Cs^+ , Rb^+ , and Sr^{2+} ; elements such as Ta^{5+} , Nb^{5+} and P^{5+} with high ionic charge, and elements with small ionic radii plus low ionic charge such as Li^+ , Be^{2+} and B^{3+} (Simmons et al 2003). Similarly, elements enriched in vapour and are not compatible in melt or crystal phases are called volatiles, these include H_2O , F^- , Bo_3^{3-} , Po_4^{3-} which acts as fluxes by lowering the temperature of crystallization of pegmatite minerals and as catalysts for the formation of large crystals from the residual magma and enables it to flow for long distances which result in the intrusion of coarse-grained pegmatites in country rocks far away from their parent granite. On the other hand, non-volatiles are elements incorporated into melt or crystal phases.

Incompatible elements are separated from melt of granitic composition and are concentrated in pegmatites through a process called fractional crystallization. Barren granite having common minerals like feldspar, quartz, and mica is the first product to crystallize from the melt. The residual melt after the crystallization of barren granite produces fertile granite from rare elements and volatiles which were incompatible with the initial crystal phase. As the fractional crystallization progresses, compatible elements partition into minerals while the incompatible rare elements remain in the fertile granitic melt thereby enriching it. Finally, the residual melt with non-compatible elements crystallizes into minerals common to pegmatite like tantalite, cassiterite and pollucite. The level of fractionation at the last stage of granitic differentiation is revealed by the amount of rare element concentration (Cerny, 1991).

2.1.5 Classification of pegmatites

2.1.5.1 Pegmatite groups

The elementary unit of aggregation of pegmatite bodies on the basis of genesis is called the pegmatite group (Cerny, 1991a). Thus, groups of pegmatites have a common granitic source, and all such bodies are related geographically in space and are of the same time. Though the history and source of a pegmatite group is same, the internal fabric and composition of the pegmatites tend to change appreciably throughout the group.

Trueman and Cerny, (1982), derived a generalized model for chemical zonation within a single pegmatite group. Cerny, (1991a), revised by Cerny and Ercit, (2005) subsequently related the zoning pattern within a pegmatite group to the nature of the magma, the intrusion depth and the level of chemical fractionation. The location of a group of pegmatites occurring in a distinct tectonic terrane is described as pegmatite field. The pegmatites that are enriched in rare elements were subdivided into classes, types and subtypes based on their distinctive chemical and mineralogical signatures.

2.1.5.2 Pegmatite classes and types

Four classes of pegmatites were recognized in a scheme generated by Ginsburg, (1984), based primarily on mineralogical or textural features that he related to depth of emplacement. These are the rare element, abyssal, muscovite, and miarolitic classes. Cerny, (1991a), and Cerny and Ercit, (2005) amended this classification relating the classes of pegmatite with other petrogenetic data, for example, the stability fields of aluminosilicate polymorphs and the lithium aluminosilicates. A new class, the muscovite - rare-element class was added by Cerny and Ercit, (2005).

The abyssal class is defined in terms of the high metamorphic grade of their host rocks, but including pegmatites of intermediate depth, extending to upper-amphibolite conditions. The muscovite class are defined as pegmatites that are generally conformable to, and is deformed with, the host rocks defined by the progression of Kyanite-Sillimanite of the Barrovian metamorphic facies series and of high-pressure amphibolite facies.

The muscovite - rare-element class is distinguished from the muscovite class in that the former are intrusive bodies forming part of a continuum from granite to rare-element pegmatite whereas the latter are believed to be generated locally by anatexis of their hosts and are conformable with their host rocks.

The rare-element class of pegmatites are holocrystalline rocks composed of igneous rock-forming minerals mostly intruding hosts that record conditions of peak metamorphism appropriate for the lower-pressure portions of the greenschist and amphibolite metamorphic facies. This class is also the most diverse in composition, as these more fractionated pegmatites accentuate the various trace-element signatures of their source regions.

The miarolitic class is made up of pegmatites distinguished by an abundance of open or clay-filled and crystal-lined cavities called miaroles. These pegmatites occur as numerous small segregations within shallowly emplaced granitic plutons, (Figure 2.1)

2.1.5.3 Pegmatite families

Two groups are recognized among granitic pegmatites, and these are common pegmatites and rare element pegmatites. The common pegmatites are rocks of igneous origin with textures common to pegmatites consisting of minerals peculiar to granite. In addition to the standard rock forming minerals of granite, rare metal pegmatites will be enriched abundantly in elements that are normally in trace content in ordinary granites such as beryllium as beryl, lithium as spodumene, tantalum as tantalite and caesium as pollucite. Pegmatites belonging to rare-element class are grouped into two families based on their composition. These petrogenetic pegmatite families were proposed by Cerny, (1991a). These are known as the Lithium-Caesium-Tantalum LCT and Niobium-Yttrium-Fluorine NYF families characterized by enrichment of elements produced by fractionation within chemically distinct pegmatite groups. The LCT pegmatites have characteristic enrichment found mostly but not exclusively in S-type granites (Chappell and White, 1992, 2001), that originates from metasedimentary rocks rich in muscovite (London, 1995).

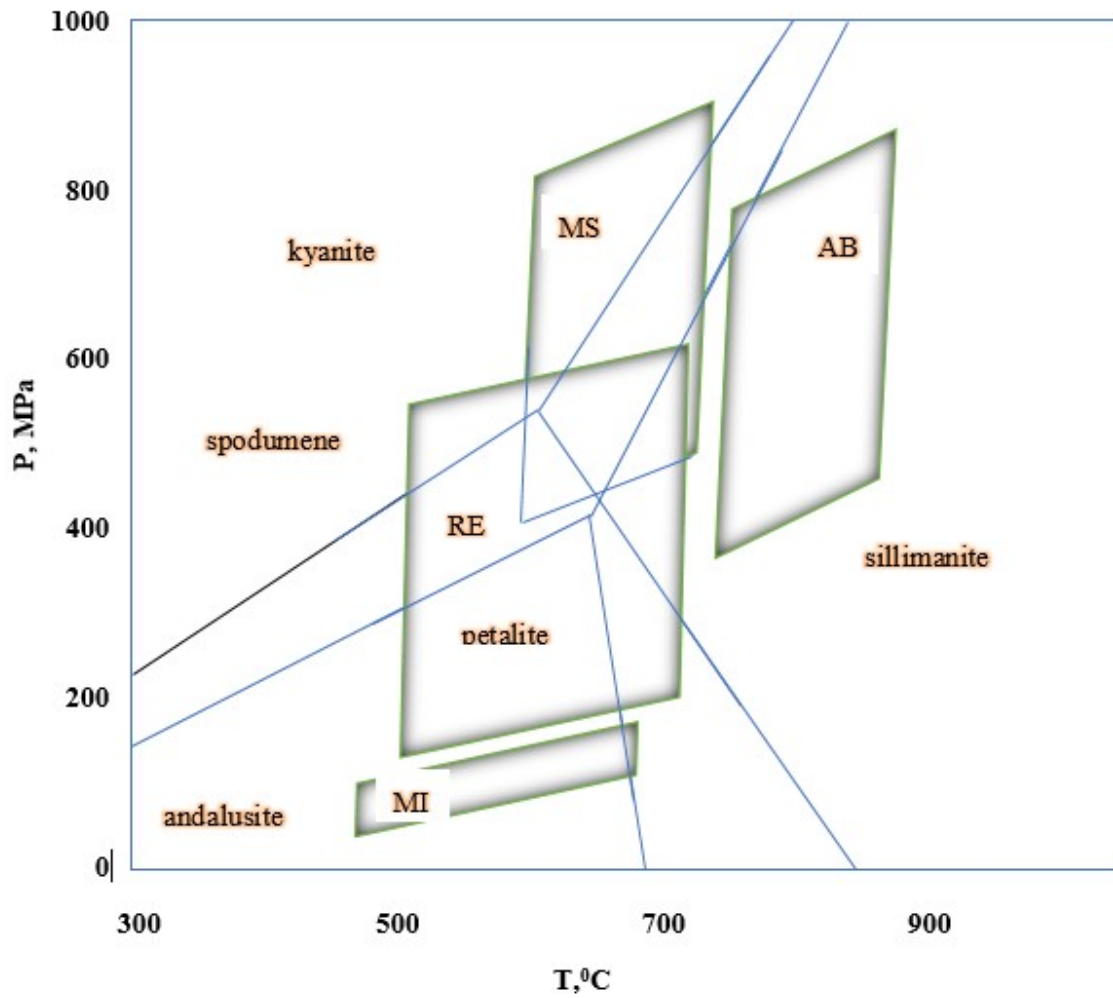


Figure 2.1 Pressure – Temperature diagram showing the fields of the four pegmatite classes proposed by Ginsburg, (1984) and Cerny, (1991a). The pegmatite classes are AB-abyssal, MS – muscovite, RE-rare element, and MI -miarolitic.

NYF pegmatites are characteristics of A-type granites and pegmatites of anorogenic origin otherwise known as ‘‘within plate’’ granites.

The LCT family pegmatites have Li, Cs and Ta as prominent rare metals in addition to Be, B, F, P, Mn, Ga, Rb, Nb, Sn, and Hf. Their content of tourmaline, muscovite, spessartine-rich garnet, and rarely gahnite ($ZnAl_3O_4$), andalusite or topaz points to peraluminous nature (London, 2005).

The lithium signature of the LCT family is expressed as the Li aluminosilicates spodumene (α - $LiAlSi_2O_6$) and petalite ($LiAlSi_4O_{10}$). High abundance of Li originates from the participation of micas in melting reactions at the source, and from the incompatibility of lithium in most other minerals that might remain as unmelted residue in the source (London, 1995, 2005b). The Cesium signature is derived from enrichment in granitic melts where muscovite and biotite as the principal reservoirs of cesium melts in the source magma (London, 1995, 2005b). In the rare-element pegmatites, Cs is incorporated into beryl and micas, and it eventually forms pollucite, in which Cs is a major component. Tantalum enrichment begins with anatexis where the melt contains biotite, followed by magmatic crystallization of biotite and muscovite. The Ta/Nb ratio is increased as biotite and muscovite crystallize from the melt while the Ti content is reduced. Rutile and titanite which are titanium bearing oxides have high content of Ta and can therefore deplete the melt of Ta from the early stages of fractionation. This seldom happens because the saturation of these oxides is suppressed by mica crystallization, thus allowing the melt to be enriched in Ta (Stepanov et al., 2014).

In addition to Niobium, Yttrium, and Fluorine, the NYF pegmatites have abundance of Beryllium, Titanium, Scandium, Zircon. One distinctive feature of NYF pegmatites is a common occurrence of amazonitic K-feldspar – Pb bearing blue-green K-feldspar (Hofmeister and Rossman, 1985a, Martin et al., 2008). The high fluorine content of NYF pegmatites is believed to come from melting reactions involving amphiboles and micas at temperatures appropriate for the base of the continental crust. Micas and amphiboles become richer in Mg with increasing temperature, and their F content increases with Mg

(Foley, 1991). These F-enriched minerals melt and impart their high F content to the magma at depth in the crust. NYF pegmatites are linked with granite magmatism that is thought to originate by deep melting of crust within continental rift zones, and usually with some chemical input from mantle sources (Martin and DeVito, 2005, Ercit, 2005). NYF pegmatites are of alkaline composition, manifested mostly by sodic pyroxenes and amphibole.

2.1.6 Pegmatites of Nigeria

Rare metal pegmatites occurrences were thought to be confined along the NE-SW striking belt, extending for about 400km ending in the tin mineral field of Jos, (Jacobson and Webb, 1946) though works undertaken by Garba, (2002), and Okunlola, (2005, 2017), reveal that Nigerian pegmatites extend beyond this boundary. In Nigeria, pegmatites occur as thin, low-lying, and massive dykes which intrude Pan African age rocks like granites, granodiorites and tonalites, (Okunlola, 2005).

Pegmatites of Nigeria host at least thirty economic minerals, prominent among these are gemstone minerals like tantalite, columbite, bismuth, cassiterite, tungsten, and the rare earth, cerium, caesium, and gallium. Other industrial minerals like feldspar, quartz, mica, and lepidolite are also hosted by this rock, sometimes up to ten of these minerals may be present at a time, (Okunlola, 2010, 2017).

Okunlola, (2005), reported on the metallogeny of Ta-Nb pegmatites of Nigeria and outlined seven main fields of pegmatites of Nigeria, using geochemical signatures, structural characteristics, and petrographic variations to delineate these fields. These seven distinct pegmatite fields are discussed below.

1. Kabba-Isanlu field.

The Itakpe area pegmatites of Central Nigeria form part of the Kabba-Isanlu field and it is discussed here as an example of pegmatites of this field. These pegmatites intrude the older assemblages of amphibolite-amphibolite schists, granitic gneisses, and banded iron formation. Petrographic studies show their constituents

to be majorly quartz and microcline with subordinate plagioclase and muscovite, while minor minerals include magnetite and hematite. Geochemical analysis of these pegmatites indicates high silica values while Na/K ratio which is less than 1.0 show poor albitization. These pegmatites may be barren because plots of K/Rb against Rb show poor fractionation trend as all samples plotted in the barren rare metal field, and Zr against Sr plot does not show evidence of post magmatic alteration. (Okunlola and Somorin, 2005)

2. Ijero-Aramoko field.

Bodies of pegmatites around Aramoko, Ara and Ijero areas of Southwestern Nigeria were studied as samples of the pegmatites of Ijero-Aramoko field. They were found to be low lying dykes commonly intruding older rocks of the migmatite gneiss complex and biotite granite. Quartz, microcline, albite, and muscovite are the main mineral constituents identified during petrographic studies. Geochemical analysis result show Ta-Nb mineralisation potential of these pegmatites with Ijero having greater potential value than pegmatites of Aramoko area. The pegmatites of this field especially of the Ijero area, are magmatic and can be classified as lepidolite sub-type of Cerny and Ercit, (2005) pegmatite classification scheme, (Okunlola and Jimba, 2006).

3. Oke-Ogun field.

Okunlola and Akintola, (2007), studied the Sepeteri pegmatites which forms part of the Oke-Ogun field. Amphibolite schists serve as the main rock type host to the Sepeteri pegmatites. Thin section studies show the major mineral constituents are quartz, microcline, albite, muscovite, and minor amounts of biotite. Geochemical analysis results reveal marginal to low level rare metal mineralization.

4. Lema-Ndeji field.

Pegmatites of Lema-Ndeji area of Central Nigeria are discontinuous dykes intruding the older assemblage of amphibolites, granite gneiss and quartzite semi discordantly. Thin section studies show quartz and muscovite as major constituent minerals and plagioclase, microcline, and tourmaline as subordinate. Accessory

minerals include ilmenite, magnetite, and tantalite. Geochemical analysis result of muscovite extract samples reveal enrichment in lithophiles such as Rb, Sr, Ba, Zr and rare metals such as Ta, Li and Nb, (Okunlola and Akintola, 2008).

5. Keffi-Nassarawa field.

The pegmatites of Keffi area of Central Nigeria, which is part of Keffi-Nassarawa field were studied by Okunlola and Ocan, (2009). The result reveals the presence of schist and older granites intruded by vertically dipping pegmatites and low-lying pegmatite bodies. They were found to have distinct mineralogical zones. Geochemical analysis reveal that the pegmatite bodies are generally more enriched in Sn-Li with lower content of Ta-Nb.

6. Ibadan-Oshogbo field.

Studies carried out by Akintola et al. (2011), on the pegmatite of Awo area revealed part of the characteristics of pegmatites of Ibadan-Oshogbo field. Awo area pegmatites occur as vertical intrusions, trending NNW-SSE, in older rocks of quartz schist, quartzite, banded gneiss and granite. Petrographic studies show that Awo pegmatite contain majorly quartz, plagioclase, microcline, biotite, muscovite, and minor minerals like garnet, cassiterite, and tourmaline. Geochemical analysis reveals the enrichment of the pegmatites in, Be, Cs, Rb, Ga, Zr, W, Ba, and Ta and Nb due to progressive rare alkali fractionation.

7. Kushaka – BirninGwari field.

The lithologic association into which Ta-Nb pegmatites intrude in this field consists of interlayered phyllitic and banded iron formation occurring as N-S trending ridges from Minna area to TshonBirniGwari area.

The Kushaka – BirninGwari field has one of the highest values of Ta/Nb ratio with values around 3.9 among the seven pegmatite fields meaning this field has the highest Ta mineralization potential. This assertion is confirmed with Ta versus K/Cs plot which shows that low K/Cs and high Ta values is consistent with higher enrichment of Ta in the pegmatite of this field. Furthermore, the high Ta/Nb ratio show preference for Ta concentration over Nb, (Okunlola, 2005).

2.1.7 Industrial potentials of pegmatites

Pegmatites have been attracting interest for the colourful gemstones and beautiful mineral specimens that they produce. Rare elements with unique applications in the aerospace, electronics and telecommunication industries are derived from pegmatites.

For the past years, high quality feldspar was the major mineral in pegmatites demanded by industries for the manufacture of pottery, vitrified sanitary ware, enamel ware, abrasives, glass, fertilizer, poultry additives, and as fillers and extenders in paints, plastics, and rubber. Physical and chemical properties of feldspar which make this mineral useful in the industry are suitable dispersibility, high resistance to abrasion, high chemical inertness, low viscosity at high filler loading, stable pH, resistance to frosting and appropriate refractive index.

Mica, a group of minerals related chemically, share a property that is called cleavage that enables them to separate into thin flexible sheets. Muscovite, a common species of Mica may occur in sheets one meter wide and more. In addition, mica's high melting point and very high electrical resistivity which are properties of a good electrical insulator makes it very relevant to the industry. It is used commonly in place of window glass, furnaces, and stove windows because of its high melting point.

A member of the mica group known as Lepidolite, has an element called Lithium. Lithium is used in medical application to treat manic depression. Also, it is used in the preparation of special lubricant, batteries and in alloying metals.

Quartz, another major constituent of pegmatite is used largely for glass making and as fillers in paint manufacture and abrasive for smoothening wood and metal.

A mineral that occurs normally in trace amount but can be concentrated to significant level of enrichment in pegmatite is beryl. Beryl occurs in various forms and colours and may possess necessary qualities of a gemstone used to make jewels. During the second world war and in the 1950s Beryl was the mineral in highest demand because of its

element constituent beryllium which is used to manufacture control rods in nuclear reactors and is combined with copper and other metals as alloys.

Garnet is an accessory mineral occurring in pegmatites. Almandine, a variety of garnet is used in industry as abrasive and in cutting and filter media.

Another useful accessory mineral in pegmatite is tourmaline. It occurs in various colours and beautiful multicolours; thus, it is used mainly as jewellery gemstone. It is said to also have some metaphysical applications especially black tourmaline.

A study of gemstone prospect of southwestern Nigeria, (Okunlola and Ogedengbe, 2003), has recorded more than ten types of gemstones namely, aquamarine, quartz, Kunzite, tourmaline, topaz, garnet, beryl, amethyst, heliodor, and emerald present in the Oke Ogun and Ibadan-Osogbo fields.

2.2 K/Ar geochronology

2.2.1 Introduction.

Potassium ${}_{19}\text{K}$, an alkali metal, is present abundantly in the earth crust constituting minerals like feldspars, feldspathoids, micas, clays and some evaporites (Heier and Adams, 1964). The more the quantity of potassium in a mineral or rock the more the silica in it. This means silicic rocks and minerals usually have more quantity of potassium than their equal amount in mafic rocks and minerals. A rock or mineral can gain or lose potassium through alteration processes. Potassium occurs as three known natural isotopes, ${}^{39}\text{K}$, ${}^{40}\text{K}$, and ${}^{41}\text{K}$, (Nier, 1935) and because of its heavy atomic weight, fractionation of potassium isotopes is insignificant. Potassium ${}^{40}\text{K}$ is however found to be radioactive with two products of the decay, ${}^{40}\text{Ca}$ and ${}^{40}\text{Ar}$ (Von Weizsacker, 1937).

Argon ${}_{18}\text{Ar}$ is an inert gas constituting <5% of the atmosphere as the third most abundant gas. It can be released from or added to rocks and minerals by alteration and thermal processes therefore every rock and mineral contains argon in some proportion. Argon has

three known natural isotopes, ^{40}Ar , ^{38}Ar and ^{36}Ar . Radiogenic $^{40}\text{Ar}^*$ as a product of decay of ^{40}K increases in amount with time. By using $^{40}\text{Ar}/^{36}\text{Ar}$ ratio of atmospheric argon, which is 295.5, the amount of ^{40}Ar produced by decay of a mineral or rock with time can be calculated by subtracting its known abundance in the atmosphere, (NMGRL, 2019).

The K/Ar geochronology method is centered on ^{40}K , a naturally occurring potassium isotope which is radioactive having a half-life of 1250 Ma and a branch decay to ^{40}Ca and ^{40}Ar . K/Ar geochronology method is premised on the accumulation of radiogenic argon ($^{40}\text{Ar}^*$) over geological time (McDougall and Harrison, 1999). It is the method of dating linking other radio-isotopic dating methods used to calibrate a large part of the Phanerozoic (Figure 2.2) of the geological time scale (Odin, 1990, 1994).

There are two classical techniques of K/Ar method used for geochronology.

1. The conventional potassium-argon method is the technique involving the separate measurement of potassium and argon from a homogeneously prepared sample.
2. The $^{40}\text{Ar}/^{39}\text{Ar}$ method based on measuring radiogenic argon $^{40}\text{Ar}^*$, and argon $^{39}\text{Ar}_k$ derived from potassium when the sample of the rock or mineral is irradiated in a fast neutron nuclear reactor.

A new analytical method using conventional K/Ar has been developed by Cassinoli, as reported in Cassinoli and Gillot, (1982) and Gillot and Cornette, (1986) to detect minute amounts of radiogenic argon which makes it easy to date very recent events down to past.

2.2.2 The Conventional K/Ar method

The occurrence of potassium isotopes ^{39}K , ^{40}K , and ^{41}K , in nature is in these proportions 93.2581%; 0.01167%; 6.7302%, respectively (Nier,1950; Garner et al., 1975). ^{40}K decays and produces ^{40}Ar with half-life of 1.25×10^9 years because it is radioactive. This means ^{40}K is presently approximately 1/12 of its original amount at Earth's formation 4.5 Ga, (Gillot et al., 2006). The decay of ^{40}K to stable ^{40}Ar is by a nuclear reaction involving electron capture and positron emission (Von Weizsacker, 1937; NMGRL, 2019). The decay of ^{40}K produces both ^{40}Ar and ^{40}Ca . The decay of eleven percent ^{40}K is

through electron capture resulting in active state of ^{40}Ar , which in turn de-activates by giving out a gamma ray. Eighty nine percent of ^{40}K decay to stable ^{40}Ca by negatron emission with an energy of 1.32 MeV (Figure 2.3). The decay constants are $\lambda_\beta = 4.962 \times 10^{-10} \text{yr}^{-1}$ for the process yielding ^{40}Ca and $\lambda_\epsilon = 0.581 \times 10^{-10} \text{yr}^{-1}$ for that resulting in ^{40}Ar (Steiger and Jaeger, 1977) thus, ten parts of ^{40}K decays to give nine parts of ^{40}Ca and one part of ^{40}Ar .

This suggest that the decay of ^{40}K to ^{40}Ca should be more appropriate for dating, however the difference in chemical behaviours of potassium and argon makes the decay of ^{40}K to ^{40}Ar more suitable. Fluids and argon are released towards the surface of the Earth and the atmosphere during geological processes like re-heating, but potassium will be incorporated into a secondary solid mineral. ^{40}K in the new secondary mineral will subsequently decay to produce radiogenic argon $^{40}\text{Ar}^*$. If the rock does not undergo further transformation, the last thermal event can be dated by measuring the amount of ^{40}K and ^{40}Ar present in the new mineral.

Increase in quantity of $^{40}\text{Ar}^*$ and ^{40}Ca from ^{40}K in a closed system where closed means argon, calcium and potassium have not been gained from outside the system or lost from the system, is given by equation 4.1,

$$^{40}\text{Ar}^* + ^{40}\text{Ca} = ^{40}\text{K}(e^{\lambda t} - 1) \quad 4.1$$

λ is the total decay constant for ^{40}K .

λ_ϵ decay constant applies to the process of ^{40}K to $^{40}\text{Ar}^*$ and λ_β for decay of ^{40}K to ^{40}Ca

Thus, λ for ^{40}K is

$$\lambda_\epsilon + \lambda_\beta = \lambda \quad 4.2$$

The values for these decay constants recommended by International Union of Geological Sciences (IUGS), sub-commission on Geochronology (Steiger and Jager, 1977) are:

$$\lambda_\epsilon = 0.581 \times 10^{-10} \text{yr}^{-1}$$

$$\lambda_{\beta} = 4.962 \times 10^{-10} \text{ yr}^{-1}$$

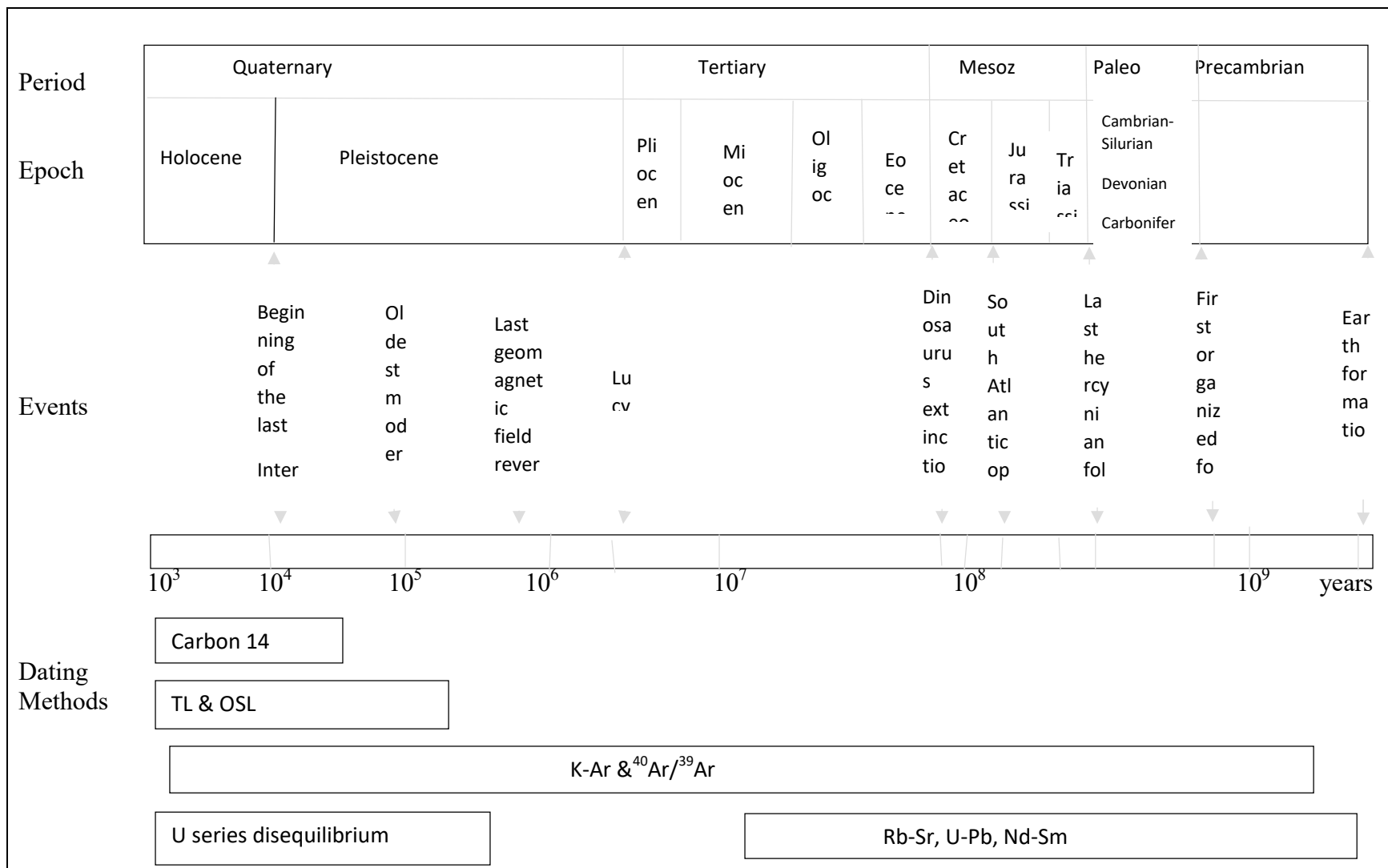


Figure 2.2 Geological times logarithmic scale and radiometric method range of application (After Odin, 1990, 1994)

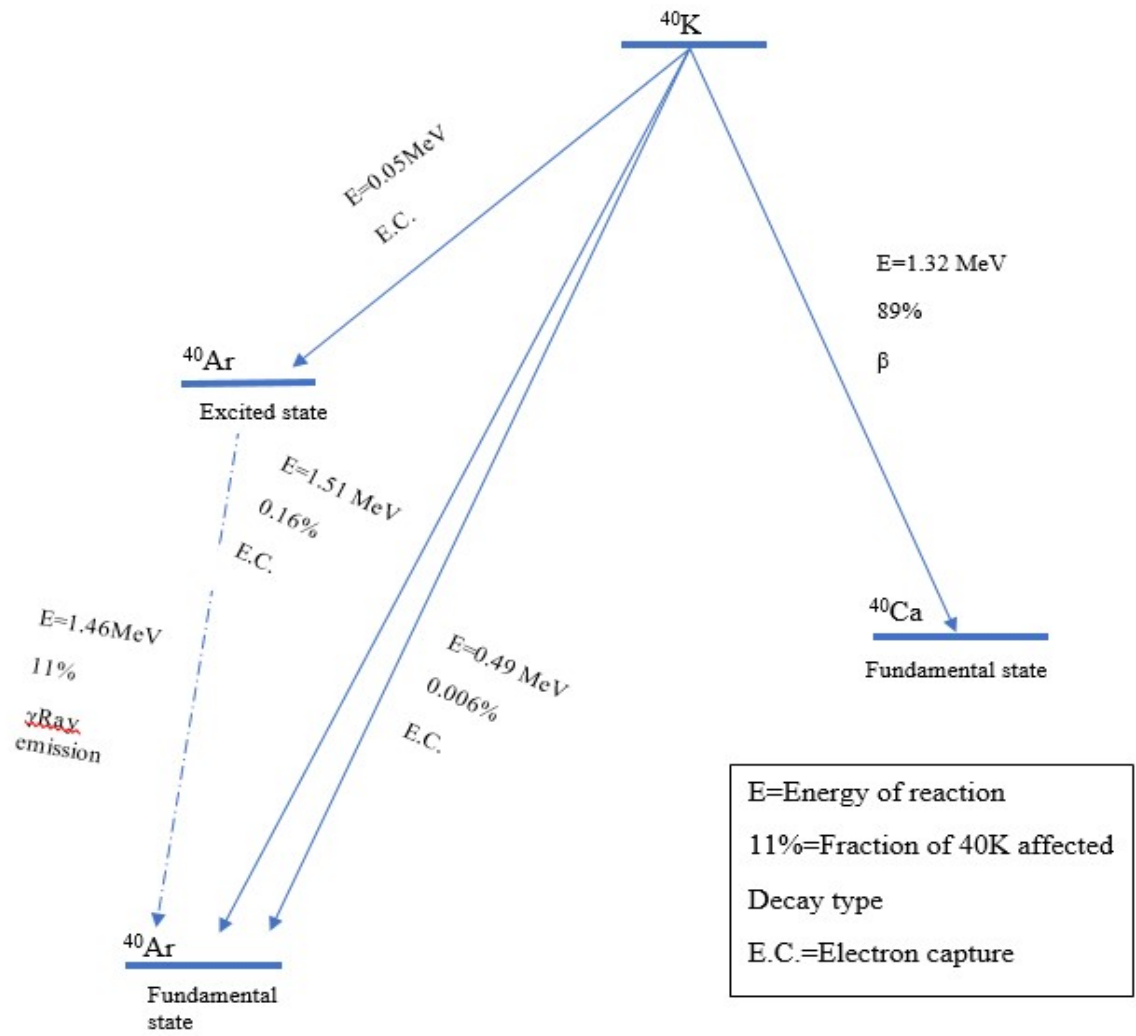


Figure 2.3 Decay scheme of potassium 40, (after Gillot et al., 2006)

Therefore, the total decay constant for ^{40}K is:

$$\begin{aligned}\lambda &= (0.581+4.962) \times 10^{-10} \text{ yr}^{-1} \\ &= 5.543 \times 10^{-10} \text{ yr}^{-1}\end{aligned}$$

The part of ^{40}K that decays to ^{40}Ar is expressed as $(\lambda_{\epsilon}/\lambda)^{40}\text{K}$.

The increase of $^{40}\text{Ar}^*$ atoms in a closed K-bearing rock or mineral is given by this equation:

$$^{40}\text{Ar}^* = \lambda_{\epsilon}/\lambda \ ^{40}\text{K}(e^{\lambda t}-1) \quad 4.3$$

The amount of $^{40}\text{Ar}^*$ and ^{40}K in the rock or mineral of study can be measured in the laboratory.

Then equation 4.3 can be solved for t which is the age of the mineral or rock.

$$(^{40}\text{Ar}^*/^{40}\text{K}) (\lambda/\lambda_{\epsilon}) = e^{\lambda t}-1 \quad 4.4$$

$$(^{40}\text{Ar}^*/^{40}\text{K}) (\lambda/\lambda_{\epsilon}) +1 = e^{\lambda t}$$

$$1/\lambda \ln [(^{40}\text{Ar}^*/^{40}\text{K}) (\lambda/\lambda_{\epsilon}) +1] = t \quad 4.5$$

The following principal assumptions must be true if the calculated value of ‘ t ’ is to be taken as the real age of the mineral, (McDougall and Harrison, 1999).

1. The radioactive potassium, ^{40}K , decays at a rate which is neither dependent on its physical state nor affected by pressure and temperature differences.
2. The ratio $^{40}\text{K}/\text{K}$ in the natural state is the same at all times. As ^{40}K is seldom calculated when ages are measured, this underlying assumption is very important.
3. No radiogenic argon derived from the decay of radioactive potassium in the mineral was lost during its lifetime and none was assimilated by the mineral when it was formed or during a later metamorphic event.

4. The dated mineral became closed to radiogenic argon immediately it was formed. This means the cooling must have been rapid after crystallization unless it crystallized at low temperature.
5. An adequate correction for non-radiogenic ^{40}Ar present in the rock to be dated is applied. The general assumption is that the whole non-radioactive argon is from the atmosphere and $^{40}\text{Ar}/^{39}\text{Ar} = 295.5$.
6. ^{40}K decay is the only process by which isotopic content of potassium in the mineral to be dated was altered.

2.2.2.1 Correction for atmospheric argon contamination.

$^{40}\text{Ar}^*$ resulting from the decay of potassium ^{40}K can be contaminated by atmospheric argon in several ways.

1. Atmospheric argon entrapped inside the mineral at crystallization.
2. During some alteration processes, atmospheric argon may be incorporated in the mineral.
3. Atmospheric argon may be absorbed through the surface of the mineral when the sample is being prepared.

Where ages of younger rock/mineral samples are to be determined, the ability to reduce the level of atmospheric argon contamination is very crucial because the amount of $^{40}\text{Ar}^*$ accumulated in the younger rock is very low compared to the quantity of atmospheric argon that may contaminate it, (Gillot et al., 2006).

The natural abundance of the various isotopes of argon ^{40}Ar , ^{38}Ar and ^{36}Ar is given as 99.60%, 0.063% and 0.337% respectively (Nier, 1950), therefore the relative abundance of these isotopes is $^{40}\text{Ar}/^{38}\text{Ar} = 1535$ and $^{40}\text{Ar}/^{36}\text{Ar} = 296$. The values of ^{38}Ar and ^{36}Ar measured in the laboratory can be used to calculate the amount of ^{40}Ar equal to atmospheric contamination. Thus, the quantity of $^{40}\text{Ar}^*$ can be known by subtracting the amount of ^{40}Ar corresponding to atmospheric contamination from the measured total ^{40}Ar .

$$\text{Total } ^{40}\text{Ar} - ^{40}\text{Ar} (\text{atm. argon}) = ^{40}\text{Ar}^* \quad 4.6$$

This correction for contamination by atmospheric argon can be determined accurately by measuring ^{36}Ar because it is five times greater in abundance to ^{38}Ar (Gillot et al., 2006).

2.2.2.2 Loss of radiogenic argon ($^{40}\text{Ar}^*$)

In accurate dating of minerals, it is assumed that no $^{40}\text{Ar}^*$ resulting from decay of ^{40}K is lost. $^{40}\text{Ar}^*$ loss may occur because argon as a noble gas does not bond with other atoms in a crystal lattice. Generally, argon loss may be due to the following:

1. As temperature reduces and at atmospheric pressure, some mineral lattices are not able to keep argon.
2. Partial or total melting of rocks resulting in the formation of new minerals and argon loss during the event.
3. Metamorphic events at high temperatures and pressures may result in loss of argon.
4. Deep burial and contact metamorphism may cause increase in temperature resulting in argon loss without affecting the physio-chemical condition of the rock.
5. Argon loss and changes in amount of potassium in minerals can result from chemical weathering and alteration caused by aqueous fluids.
6. Minerals exposed to shock waves, damaged by radiation and mechanical breakdown may lose argon. Excessive grinding in the laboratory during preparation of samples for dating may result in loss of argon.

Potassium feldspar loses radiogenic argon easily at low temperatures (even at room temperature) thus it is not appropriate for K/Ar dating method, (Faure, 1977).

2.2.2.3 Presence of excess radiogenic argon ($^{40}\text{Ar}^*$)

Presence of excess radiogenic argon may be due to these reasons.

1. The absorption into the rock of mineral phases earlier crystallized. These may include high equilibrium pressure syngenetic phenocryst or cumulates

concentrated at the root of magma chamber. The $^{40}\text{Ar}^*$ produced previously by ^{40}K in the depth of the earth is absorbed in these mineral phases.

2. Xenoliths of the host rocks are sometimes mechanically absorbed into the magma rising to the surface bringing inherited argon.
3. Basalts formed under high hydrostatic pressure on the floor of the ocean may have excess ^{40}Ar in large quantities in the glassy crust of each pillow especially as argon in the lava is enclosed there by high pressure and quick quenching (Seidemann, 1977).
4. K-Ar dating of minerals having low K content or young minerals is most affected by the presence of excess argon. Minerals like beryl, pyroxene, tourmaline and cordierite often contain excess argon, whereas, feldspar, biotite, hornblende, phlogopite and sodalite seldom have excess argon (Livingston et al., 1967).
5. The presence of fluid inclusions may be another source of excess argon in some minerals (Rama et al., 1965).
6. Minerals in contact with high partial pressure of argon during regional metamorphism may have excess argon especially in pegmatites (Laughlin, 1969).

Overestimation of mineral age usually occur when using K-Ar method of dating where excess argon is present.

2.2.3 K-Ar Isochron dating.

The amount of total ^{40}Ar in rock or mineral of age t bearing potassium can be derived from equations 4.3 and 4.6:

$$^{40}\text{Ar}^* = \lambda_e \lambda^{40}\text{K}(e^{\lambda t} - 1)$$

$$^{40}\text{Ar}^* = \text{Total } ^{40}\text{Ar} - ^{40}\text{Ar} \text{ (atmospheric argon).}$$

$$\text{Total } ^{40}\text{Ar} = ^{40}\text{Ar}_n + \lambda_e \lambda^{40}\text{K}(e^{\lambda t} - 1) \tag{4.7}$$

Where $^{40}\text{Ar}_n$ is the total non-radiogenic component in the rock or mineral, which may consist of argon from various sources like, a) atmospheric argon incorporated into the mineral through microfractures or grain boundaries while open to atmospheric

environment or in the laboratory, b) dissolved argon in the magma from the mantle, c) argon resulting from removal from old minerals containing potassium in the crust, d) Evolved and diffused argon in minerals during later thermal metamorphism.

Conventionally, in K-Ar dating, the initial ^{40}Ar is assumed to be atmospheric and can be subtracted from the measured total ^{40}Ar using the ratio $^{40}\text{Ar}/^{36}\text{Ar}$ which is known to be 295.5. Where the mineral contains other sources of argon like b,c and d above, the estimated age from K-Ar dating will be more than the actual age of the mineral, implying that the mineral has excess argon. The K-Ar isochron dating method can be employed to avoid this problem.

Equation 4.7 can be modified when each term is divided by the amount of ^{36}Ar atoms per unit weight of the mineral sample. Thus equation 4.7 becomes:

$$^{40}\text{Ar}/^{36}\text{Ar} = (^{40}\text{Ar}/^{36}\text{Ar})_n + (\lambda_e/\lambda) ^{40}\text{K}/^{36}\text{Ar}(e^{\lambda t} - 1) \quad 4.8$$

Equation 4.8 gives the measured total ^{40}Ar as the sum of argon derived from the atmosphere and other sources like b,c and d above plus $^{40}\text{Ar}^*$ gathered after the mineral was closed. Generally it is assumed that K-bearing minerals coexisting in the same rock specimen, having experienced the same geological history may have $(^{40}\text{Ar}/^{36}\text{Ar})_n$ ratios that are similar. Also, these coexisting minerals have the same age 't'.

If we compare equation 4.8 with equation of a straight-line $y = b + mx$,

$$y = ^{40}\text{Ar}/^{36}\text{Ar}$$

the intercept is

$$b = (^{40}\text{Ar}/^{36}\text{Ar})_n \quad 4.9$$

$$x = ^{40}\text{K}/^{36}\text{Ar}$$

the slope is

$$m = (\lambda_e/\lambda) (e^{\lambda t} - 1) \quad 4.10$$

From the above, coexisting minerals with the same age and initial $^{40}\text{Ar}/^{36}\text{Ar}$ ratio are depicted by points that form a straight line in coordinates of the measured values of $^{40}\text{Ar}/^{36}\text{Ar}$ and $^{40}\text{K}/^{36}\text{Ar}$.

This type of straight line is known as an isochron because all points on this line have the same age. The age of the mineral can therefore be calculated by solving for 't' in the equation of slope 'm'.

$$m = (\lambda_e/\lambda) (e^{\lambda t} - 1)$$

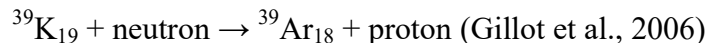
$$t = 1/\lambda \ln [m (\lambda/\lambda_e) + 1] \quad 4.11$$

where ln is the natural logarithm.

Coexisting minerals form isochrons only when all samples have neither lost nor gain Ar and K. Also, all samples must have different potassium content and same initial $^{40}\text{Ar}/^{36}\text{Ar}$ ratio resulting in different $^{40}\text{K}/^{36}\text{Ar}$ ratios so that the slope of the isochron is clearly defined by the data points. The K-Ar isochron dating method seem to be more accurate than the conventional K-Ar method in that the better the data plots on a straight line, the more the assurance that the samples have remain closed to atmospheric argon pollution and that they have similar initial $^{40}\text{Ar}/^{36}\text{Ar}$ ratios.

2.2.4 $^{40}\text{Ar}/^{39}\text{Ar}$ method

The $^{40}\text{Ar}/^{39}\text{Ar}$ method depends on the measurement of daughter and parent isotopes ^{40}Ar and ^{39}Ar respectively. The parent isotope ^{39}Ar is produced when a neutron is activated in a nuclear reactor thus transforming potassium into argon. The ^{39}K which is the naturally dominant isotope of potassium is transformed into ^{39}Ar which will undergo analysis with radiogenic argon and other argon isotopes in the same aliquot. This transformation can be represented by this equation:



This ^{39}Ar produced can be used as proxy for potassium since the abundances of its isotopes in nature are known. So, unlike the case of the conventional K/Ar dating method, instead of measuring absolute abundances, more accurate results are produced when measurements of ratios of different argon isotopes are taken. However, it should be noted that other interference reactions which are undesirable to insignificant occur during the

irradiation of the sample resulting in the production of more argon isotopes from chlorine, potassium, argon and calcium.

Transformation of ^{39}K to $^{39}\text{Ar}_k$ can only take place by fast neutron reaction therefore, all samples to be dated must undergo irradiation in a nuclear reactor core. The quantity of resultant $^{39}\text{Ar}_k$ is dependent on these variables, a) the initial quantity of ^{39}K , b) irradiation period, c) neutron flux density, d) the cross section of the neutron captures for ^{39}K . Although, the independent measurement of these variables is difficult, the samples to be dated are irradiated with a monitor mineral of known age so that by extrapolation from the monitor flux, the flux of the samples can be determined. Thus, the flux ‘J’ is calculated from this equation:

$$J = e^{\lambda t_m} - 1 / ({}^{40}\text{Ar}^*/{}^{39}\text{Ar})_m \quad 4.12$$

Where J = irradiation flux parameter

$({}^{40}\text{Ar}^*/{}^{39}\text{Ar})_m$ = measured ratio in monitor

t_m = age of flux monitor

λ = total decay constant for ^{40}K

e = natural log

Once corrections for argon isotopes produced from calcium, argon, chlorine and potassium in the nuclear reactor are made, the age of the sample is calculated from the ${}^{40}\text{Ar}/{}^{39}\text{Ar}$ age equation:

$$t = 1/\lambda \ln [({}^{40}\text{Ar}^*/{}^{39}\text{Ar})_s J + 1] \quad 4.13$$

where $({}^{40}\text{Ar}^*/{}^{39}\text{Ar})_s$ = determined ratio for sample

equations 4.12 and 4.13 gives:

$$t = 1/\lambda \ln [({}^{40}\text{Ar}^*/{}^{39}\text{Ar})_s e^{\lambda t} / ({}^{40}\text{Ar}^*/{}^{39}\text{Ar})_m + 1]$$

or

$$t = 1/\lambda \ln [1 + ({}^{40}\text{Ar}^*/{}^{39}\text{Ar})_s / ({}^{40}\text{Ar}^*/{}^{39}\text{Ar})_m e^{\lambda t} - 1]$$

2.2.4.1 Benefits of ${}^{40}\text{Ar}/{}^{39}\text{Ar}$ method

1. Since measurement of isotopic ratios is the basis for procedure of analysis, the weight of the sample which yields the argon need not be known.
2. Samples available in very low quantities can be dated because there will be no problem of heterogeneity. This is because the values of ${}^{39}\text{Ar}$ and ${}^{40}\text{Ar}^*$ are determined from the same aliquot of sample.
3. The determination of a sample's age can be carried out without extracting the totality of the argon from the sample by performing incremental degassing with a step-heating procedure (Gillot et al., 2006).

2.2.4.2 Limitations of ${}^{40}\text{Ar}/{}^{39}\text{Ar}$ method

1. Several radioactive elements other than ${}^{39}\text{Ar}$ are produced by several nuclear reactions when samples are irradiated in a fast neutron nuclear reactor. Corrections have to be made for undesirable reactions like artificially produced argon from calcium and chlorine.
2. The J parameter is required in the calculation of the age of a sample by ${}^{40}\text{Ar}/{}^{39}\text{Ar}$ method. It is determined by irradiating a monitor sample of known age with the sample. The K/Ar dating is used to ascertain the age of the standard sample which is then used to calculate the J parameter of the sample of unknown age. The standard sample must be an abundantly available mineral that is homogenous, and easy to date by both potassium-argon and argon-argon methods.

2.2.5 The Cassagnol Technique.

The detection of minute quantities of radiogenic ^{40}Ar requires very precise correction of atmospheric contamination which can be done by reducing the sources of analytical errors to the barest minimum. These errors include factors resulting from spiking in K/Ar method or corrupting influence of isotopes resulting from neutron activation in $^{40}\text{Ar}/^{39}\text{Ar}$ technique. These errors can be reduced by measuring the signal of argon from one aliquot of sample and the signal of pure atmospheric argon at the same level under strictly identical analytical conditions and comparing the results. The proportion of radiogenic argon in the sample is then calculated from the difference between ^{36}Ar signal from the sample, (Figure 2.4), and that from the pure atmosphere for an identical quantity of ^{40}Ar , (Gillot et al., 2006).

In this technique, absolute measurements of argon signals are achieved by mass spectrometer. This procedure corresponds to double comparison with atmospheric argon in that a) ^{40}Ar with signal like that of the sample, is introduced into the mass spectrometer which allows for the determination of radiogenic $^{40}\text{Ar}^*$. b) the use of a known amount of atmospheric argon, to volumetrically determine the number of radiogenic $^{40}\text{Ar}^*$ atoms extracted during fusion of the sample, without comparison to any mineral sample reference.

This more accurate argon isotope measurement which detects radiogenic argon to the tune of 1 ppt in the whole argon is due to the merging of several technical refinements, (Cassagnol and Gillot, 1982). These include a) how pure the gases introduced into the mass spectrometer are, b) the ion-source parameters stability, c) suppressing the signal drift and d) increment of the signal to noise ratio.

a) Gas purity

The ionizing condition in the mass spectrometer can be changed by the presence of active gases which modify the emission of the filament by reacting with it. To ensure the argon is kept pure and the residual active gases remain the same at a low level in the mass

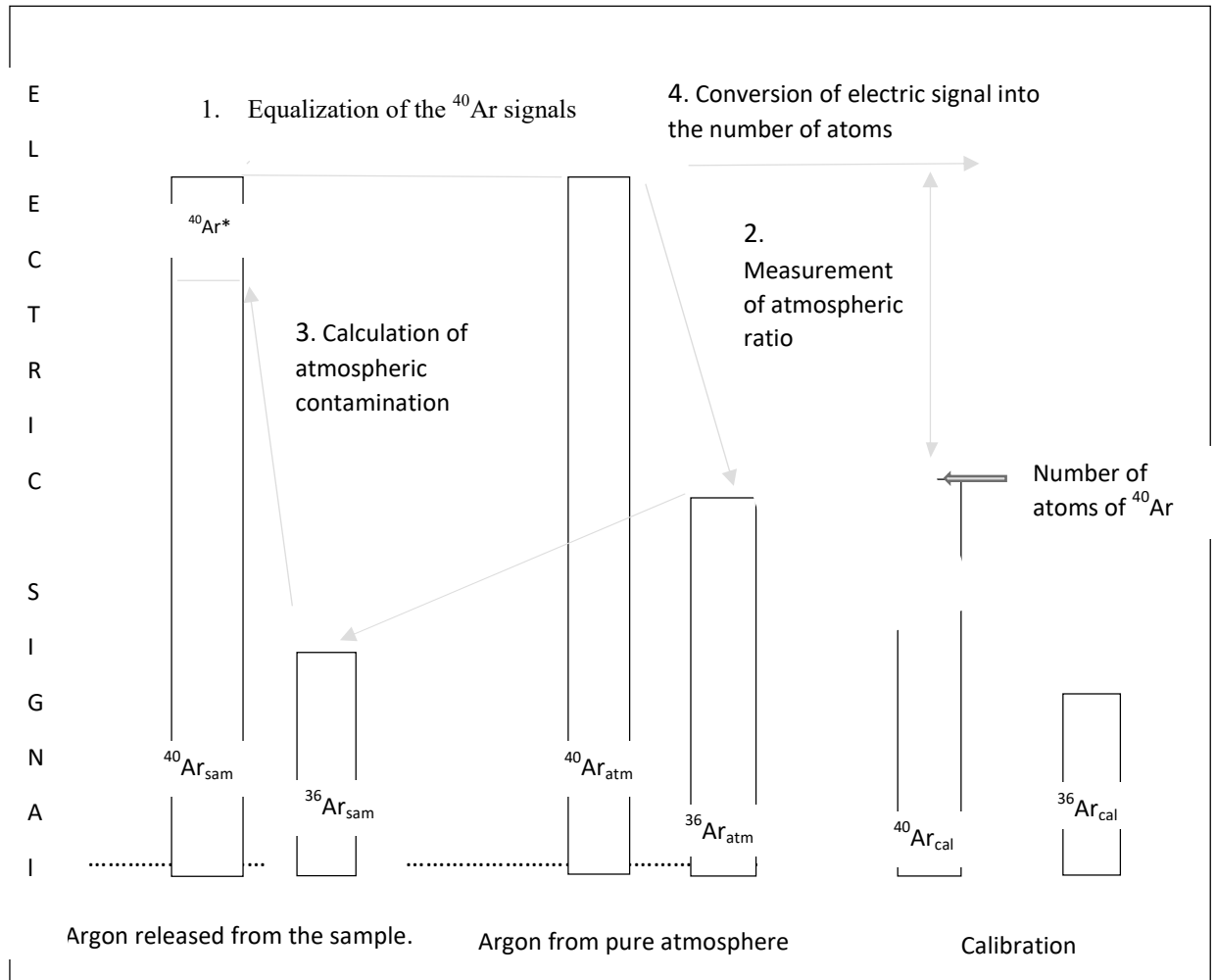


Figure 2.4 Principle of atmospheric correction and signal calibration (after Gillot et al., 2006)

spectrometer, Zr-Al getter pumps (Pisani and Della Porta, 1967) are kept active in the measurement volume throughout the analysis (Cassagnol, 1973). Furthermore, any Helium that infiltrated the line while the titanium sponge is being heated in the initial stage of purifying the sample argon is removed by pumping. Active-charcoal traps cooled with liquid nitrogen absorb argon from the extraction line to the mass spectrometer.

a) Ion source parameters stability

The mass spectrometer contains only pure argon enabling the maintenance of a source in highly uniform ionizing conditions. This kind of stability is possible by constant electricity supply from an electric generator which is not dependent on mains supply and by airconditioner in the laboratory. In addition, the collection of argon masses 36 and 40 at the same time keeps the speed and deflection conditions of the ion beams constant.

b) The suppression of signal drift.

When the argon signals drift, there is a limitation in the precision because of the production of variance in isotopic ratio. A part of the drift results from the presence of active gases in the mass spectrometer which changes the ionizing conditions when argon is measured. Another reason for argon signal drift is memory effects from the mass spectrometer resulting from implantation and desorption phenomena. This signal drift can be avoided by maintaining a balance between the memory of the mass spectrometer and the pressure of argon equivalent to the sample at the initial state before measurement. This can be done in two ways.

1. First is to limit the bombarded surface areas in order to quickly obtain the saturation of the ion beams during implantation. Only three surfaces are targets hit constantly by the ion beams because the three argon masses, 36, 38 and 40 are collected at the same time.
2. The second way is to prepare the mass spectrometer memory to be at equanimity with the sample argon. This is to ensure that the mass spectrometer is running permanently with argon pressure equivalent to that of the sample to be measured. The mass spectrometer

must be emptied and filled rapidly to forestall any change in the memory equilibrium (Gillot and Cornette, 1986).

c) The increase in the signal to noise ratio.

The stable prevailing ionizing conditions makes way for the operation of the amplifiers at high impedance. It is necessary for the instrument to be at its highest luminosity so that 36 and 38 argon masses can be measured accurately for the correction of contamination. The luminosity is increased by expanding the collector slits of the mass spectrometer to collect the most ionic current. This allows the ^{40}Ar peak to be better defined and ensures a precise adjustment of the accelerating voltage. Under these conditions, an accuracy of at least

$5 \cdot 10^{-4}$ for the measurement of ^{36}Ar and an amendment for atmospheric pollutants exact to 0.1% are achieved (Gillot and Cornette, 1986).

2.3: Previous works review

One of the earliest studies on Nigeria pegmatites was carried out by Jacobson and Webbs, (1946). They concluded that pegmatites of Nigeria are located mainly along a 400km NE-SW direction.

Cameron et al., (1949), studied the internal structure of granitic pegmatites, and they devised a classification and described the pattern of internal zones present in granitic pegmatites.

Jahns, (1955), in the study of pegmatites, concluded that the features in many pegmatite bodies, pertaining especially to complex mineralogy can be explained by combining two processes. These include the progressive crystallization of injected magma subjected to limited system conditions, with interaction between the crystalline phase and the remaining fluid. The second process include renewed residual fluid boiling, vapour condensation at various points within the system, and partial replacement of the crystalline phase at the condensate.

Jahns and Burnham, (1969), carried out studies on the genesis of pegmatite. A model was derived for the crystallization and derivation of granitic pegmatites which highlighted the roles of water (and /or other relatively volatile substances) both as constituent dissolved in granitic magma and as the major constituent of a separate fluid phase that is in the supercritical state under most conditions of pegmatite formation.

Gordiyenko, (1971) worked on the content of lithium, rubidium and caesium in K-feldspar and muscovite as attribute for evaluating the enrichment of rare metals in granitic pegmatites.

Matheis and Caen-Vachette, (1983) worked on the pegmatites of Egbe, Ijero and Wamba, in Nigeria. In their research, using Rb-Sr isotopic dating method, they discovered a 100Ma time gap between the tantalum enriched pegmatites which intruded conformably into a sequence of basic to ultrabasic amphibolite and the pegmatite of the main phase of near older granite.

Gaupp et al., (1984) in the study of the geology of tantalum pegmatites of Untersuchungen, reported that genetic features and rare metal potentials could be delineated from fresh samples of the pegmatite whole rock, extracts of muscovite, feldspar and tourmaline are useful for the same purpose.

Moller and Morteani, (1987), tested the geochemical and morphological characteristics of albite, k-feldspar, and white mica from pegmatites of Canada, South Africa, and Europe for their applicability as exploration tools for locating Ta pegmatites. They concluded that metasomatically albitised pegmatites enriched in Ta and Cs are appropriate as targets for exploration.

Kuster, (1990), studied the mineralized pegmatites of Wamba, central Nigeria, he reported that muscovite-quartz-microcline pegmatites are enriched in metals like Ta, Nb, and Sn, during late Pan-African orogeny (± 550 Ma) which also controlled by shear tectonics the emplacement of granites and pegmatites.

Geochemical discrimination studies by Garba, (2003), of complex and simple pegmatites in the Pan-African 600 ± 150 Ma newly discovered in the basement of Northern Nigeria, reveal high content of Rb and Cs and variable content of Ga, Be, and Li as distinctions between the mineralized and barren pegmatites.

Okunlola and Ocan, (2009) did a study on the mineralised pegmatite of Keffi area, northcentral Nigeria to reveal and explain their petrographic features and mineralization. Analytical results reveal different mineralogical zones with rare metal mineralization in specific zones. These zones include albite and tourmaline zone with Ta enrichment, lepidolite and microcline zone with Li enrichment, and lepidolite-microcline-tantalum zone with highest enrichment value has affinity for Sn.

Akintola et al., 2012 worked on Precambrian pegmatites of Ago-Iwoye to determine the compositional features and likely economic potential of this rock. A silica rich pegmatite whole rock and mica extract depleted in silica was reported. The pegmatites have noticeable enrichment in Rb, Sr, Zr, but depleted in the rare metals Ta, Nb, W, Cs and Sn and the plots of Ta vs Nb and Ta vs K/Cs also indicate lack of rare metal mineralization. Thus, pegmatites of Ago-Iwoye are incomparable with rare-metal pegmatites across the globe.

Ale et al., (2014) studied Ijero pegmatite in Ekiti state located in Southwestern Nigeria and discovered its industrial mineral potentials in feldspar, sheet mica, Ta-Nb, lithium minerals and gemstones.

Edem et al., (2015) studied the Precambrian pegmatites of Southern Obudu, Southeastern Nigeria with the aim of identifying the geochemical signatures and its potential for mineralisation. Their study revealed that the pegmatite belongs to the muscovite class, and it exhibits low-level rare metal mineralization potential.

Adetunji et al., (2016) worked on the pegmatites of Ede and reported that U-Pb zircon dating of the pegmatites gave a discordant age of 709 Ma which can be attributed to their emplacement.

Okunlola, (2016) in the study of geochemical characteristics and economic potential of rare metal Ta-Nb-Sn Precambrian pegmatite of southwestern Nigeria, unravelled the trend of enrichment of mineralization and delineated preferred prospective targets in these pegmatite fields.

Olisa et al., (2018) studied the Igangan area pegmatites in southwestern Nigeria and reported that these pegmatites are depleted in rare metals and rare earth elements also the value of 177 for one of the fractionation indices, K/Rb, depicts low mineralization.

While working on the mass spectra of alkali metals, Aston, (1921) did some studies on the isotopic composition of potassium which led to the discovery of ^{39}K and ^{41}K . However, the evidence pointing to the existence of radioactive isotope of potassium (^{40}K) was presented by Nier, (1935).

In 1937, a German physicist von Weizsacker, discovered that ^{40}K decay into two isotopes, ^{40}Ca and ^{40}Ar . He postulated that old K-bearing minerals should contain excess ^{40}Ar . Aldrich and Nier, (1948) confirmed the postulation of von Weizsacker by demonstrating that orthoclase, microcline, langbeinite and sylvite contain radiogenic argon. This formed the theoretical basis for dating by K-Ar method.

Schaeffer and Zahringer, (1966) compiled the works of several scientists on the principles, techniques, and application of K/Ar dating.

In 1969, Dalrymple and Lanphere, made a review of physical principles underlying the potassium-argon dating methods including the open-system method leading to discussion on argon loss.

Damon, (1970) studied the real K/Ar clock and the need to consider it as a system open to an external environment with a partial pressure of argon isotopes.

Hunziker, (1979) posited that the principle governing the conventional K-Ar method is simple. His conclusion is that since ^{40}K decays to ^{40}Ar , if the decay constants are known and the parent and daughter isotopes can be accurately measured, then an age for the mineral or rock can be calculated.

Cassignol and Gillot, (1982) worked on a new analytical technique of K-Ar dating method known as the Cassignol technique which was developed to date very recent volcanic rocks. The Cassignol technique yielded results comparable with those from thermoluminescence and radiocarbon dating methods and the correction for atmospheric contamination from this technique is acceptable.

Applications of Cassignol technique (unspike K-Ar dating method) include dating of new volcanic rocks from Southern Italy, (Gillot and Cornette, 1986) and young volcanics from Loihi and Pitcairn hot spot seamounts, (Guillou et al., 1997).

Umeji and Caen-Vachette, (1984) worked on the Pan-African NassarawaEggon geochronology, Northcentral Nigeria, and Mkar-Gboko granites, Southeastern Nigeria. NassarawaEggon granite yielded a Rb-Sr whole rock isochron age of 535 ± 8 Ma, while Mkar-Gboko granite gave a Rb-Sr age of 547 ± 38 Ma.

Okunlola and Udoudo, (2005) did some studies on the geological occurrence, petrochemical characteristics, and dating of rare metal (Ta-Nb) minerals of Komu areapegmatites, Southwestern Nigeria. The study revealed an age of 502.8 ± 13 Ma – 514.5 ± 13.2 Ma by K/Ar dating for the mineralization of muscovite extracted from the Komu area pegmatites. It was concluded that since this age represent the cooling age of muscovite, the pegmatites may not be syngenetic with the associated Pan-African granitoids.

Goodenough et al., (2014), worked on the Pan-African granitoids formed after collision and Western Nigeria pegmatites enriched in rare metals. They presented granitoids of three different ages as follows; an early phase of magmatism having a new U-Pb zircon age of 790-760 Ma around Minna, which is associated with continental rifting or to

continental margin subduction. Peraluminous biotite-muscovite granites formed mainly by crustal melting were intruded at 650-600 Ma probably when orogenic belt regional shearing occurred. The youngest age of 590 Ma marks the beginning of the period after orogenic extension with the emplacement of metaluminous granitoids.

Adetunji et al., (2016), studied the geochemistry of the pegmatites in Ede area, Southwestern Nigeria. Also, the rock was dated using the U-Pb zircon dating method and it was reported that these are the oldest Pan-African rocks reported thus far in Southwestern Nigeria. The Ede pegmatites gave U-Pb zircon age of $709 \pm 27/-19$ Ma.

2.4 Regional geological setting of Nigeria

Nigeria has three main litho-stratigraphic components, namely the rocks of the Pan-African mobile belt, situated between Congo and West African cratons and south of the Tuareg shield (Black, 1980), called the Nigerian basement complex, the Younger Granites, which are calc-alkaline ring complexes of Mesozoic age intrude into the basement complex in Northcentral Nigeria and extend towards Niger republic. Cretaceous and younger sediments are overlain unconformably on these units (Figure 2.5). The basement rock which occupies the rejuvenated region resulting from collision between the inactive West African Craton and the active Pharusian continental margins (Dada, 2006) was reworked by the 600 Ma Pan-African orogeny. A regional metamorphism yielding migmatites, syntectonic granites and homogeneous gneisses is linked with the Pan-African deformation (Abaa, 1983). The last stages of this deformation were accompanied by late granitoid tectonic emplacement and accompanying contact metamorphism with faulting and fracturing as features of the last part of the orogeny (Olayinka, 1992).

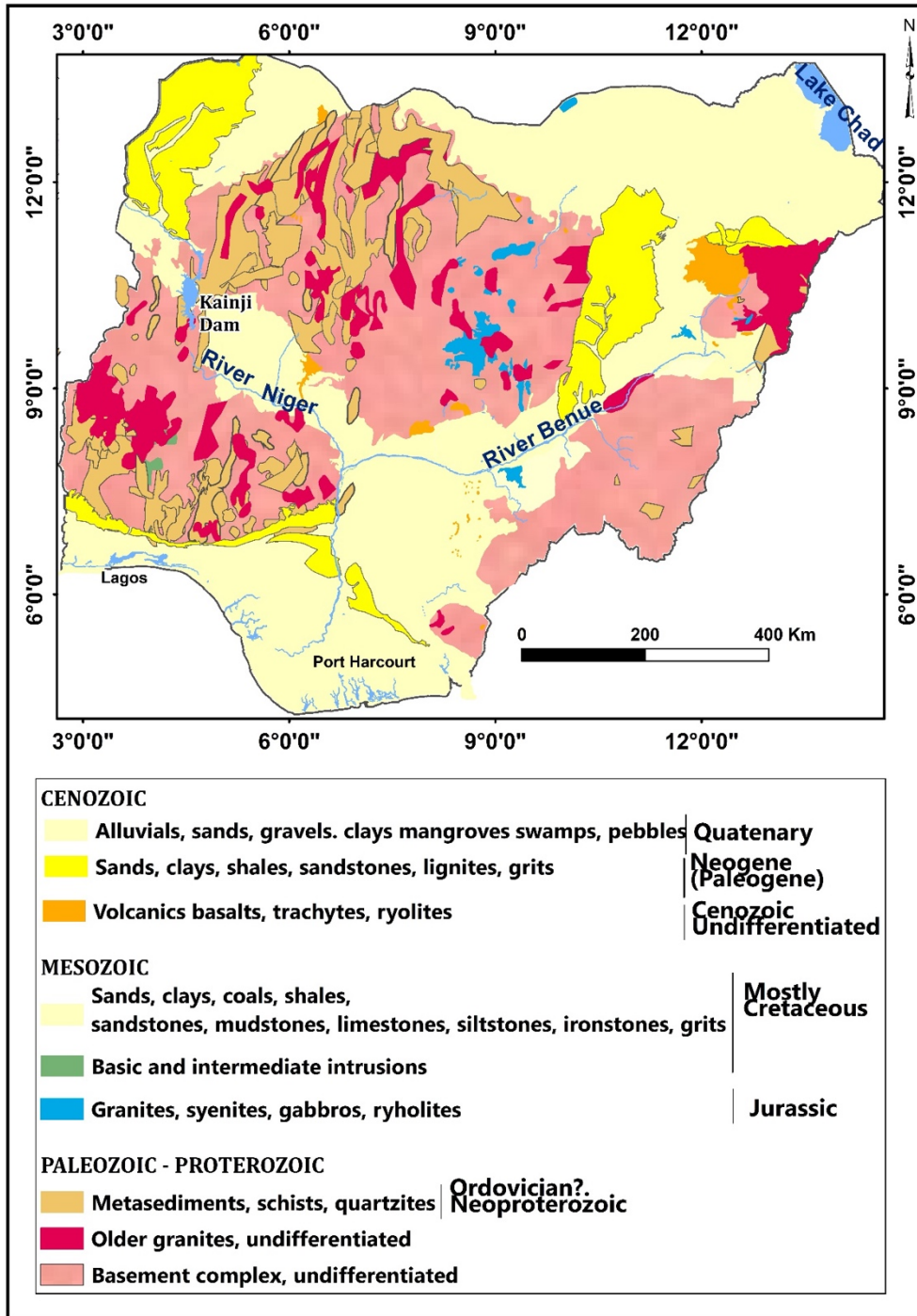


Figure 2.5 Generalized map of the geology of Nigeria (after Obaje, 2009).

2.4.1 The Basement Complex.

The basement complex consists of four main lithological units discussed below.

The Migmatite – Gneiss – Quartzite Complex (MGQC)

The Migmatite–Gneiss-Quartzite Complex is the lithological unit that is most widespread. It consists of migmatites, para and orthogneisses, and basic and ultrabasic metamorphosed rocks. Petrographic examination reveals recrystallization of the minerals present in the rocks of Migmatite–Gneiss-Quartzite Complex because of partial melting during Pan-African orogeny with evidence of metamorphism of medium to upper amphibolite facies. Pan-African to Eburnean ages have been assigned to the rocks of Migmatite–Gneiss-Quartzite Complex

About sixty percent of the Nigerian basement is made up of Migmatite-Gneiss-Quartzite Complex (Rahaman and Ocan, 1978), and these rocks show evidence of three major geological events. The earliest geological event involved processes beginning crust formation, sedimentation and orogeny at 2,500 Ma resulting in crustal growth; this is followed by the Eburnean characterized by the granite gneisses of Ibadan at $2,000 \pm 200$ Ma; the third geological event is the Pan-African event which produced granite gneisses, migmatites and other rock types with ages ranging from 900 to 450 Ma which resulted in recrystallization of many minerals and restructuring of features used for dating in the earlier rocks, (Rahaman and Lancelot, 1984).

The Birrimian of the West African Craton and Migmatite-Gneiss-Quartzite complex developed at the same time. While Birrimian rocks are mineralized, the rocks in Nigeria of same age are not. Rocks with same lithology in Northeastern and Southeastern Nigeria have yielded only Pan-African ages (Tubosun, 1983).

The Schist Belt

The Schist Belts consist of low grade, metasediment N-S trending belts, best exposed in western Nigeria. These belts are made of supracrustal rocks of late Proterozoic age folded into the older rocks and their components include fine to coarse grained clastics, phyllites, pelitic schists, banded iron formation, carbonate rocks, and amphibolites.

Rahaman, (1976) and Grant, (1978) postulated that sediments of the schist belts were deposited in many basins but Oyawoye, (1972) and McCurry, (1976) reported that the schists belts are relics of a deposit overlying the crust. Another thought is that the schist belts were rift-like structures controlled by faults (Olade and Elueze, 1979).

According to Turner, (1983), sediments are of different ages which are based on evidence of structural and lithological associations. However, Ajibade et al., (1979) in disagreement with the above assertion demonstrated that both structural and lithological characteristics of sediments have similar deformational histories, and the schist belt rocks are of Upper Proterozoic age.

The belts are limited to a 300 km wide zone in the NNE direction. Gneisses and migmatites occur at the west of the zone making up the Dahomeyan, (Burke and Dewey, 1972). Furthermore, schist belts are not reported at the east of the zone, but several schist belts occur in Cameroun, of Upper Proterozoic age, and are found north of the Congo Craton in the Pan-African granite-migmatite terrain. Mapping and detailed studies have been undertaken on the schist belts in these locations: Anka, IseyinKazaure, Zuru, Kushaka, Iwo, Zungeru, Maru, Kuseriki, Oyan and Ilesha where they are linked with gold mineralization. (Figure 2.6).

The Older Granites

Falconer, (1911) named the intrusive, concordant to semi-concordant granites of the Basement Complex 'Older Granite' to distinguish it from younger granites that are discordant with tin mineralization located in Northern Nigeria. The Older Granites are

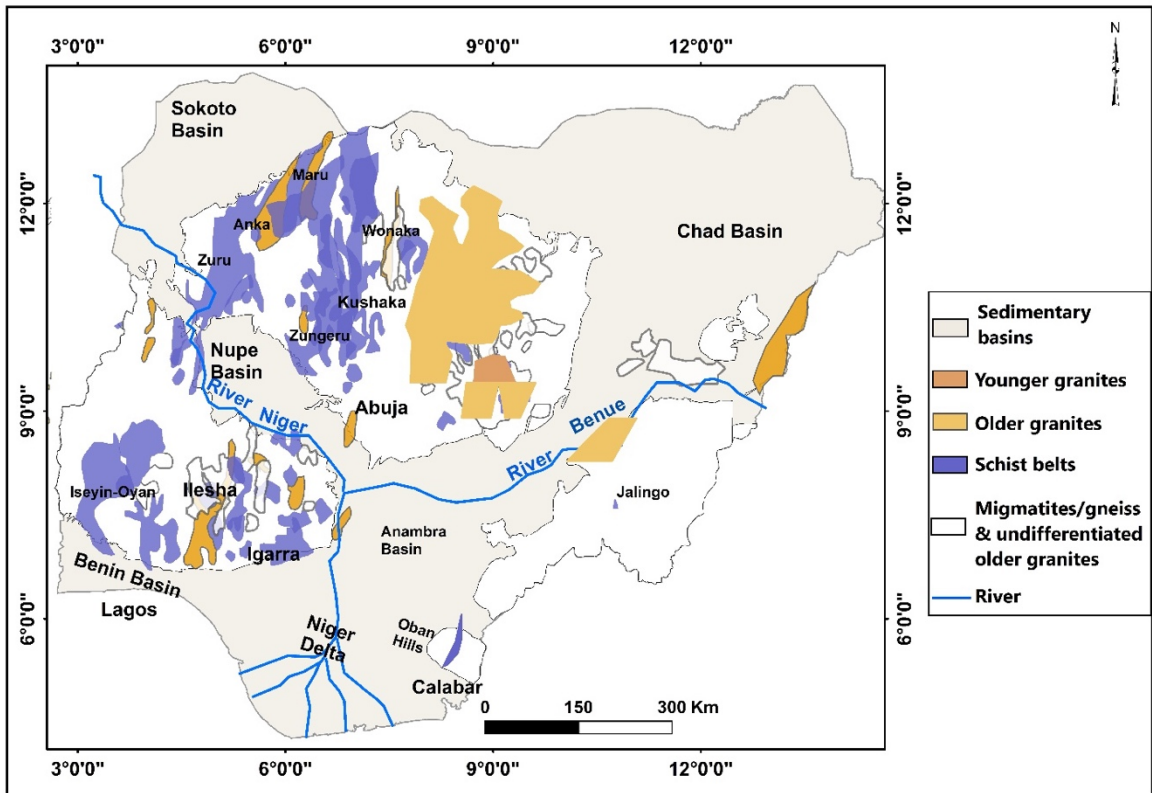


Figure 2.6 Map of Schist belts of Nigeria (after Woakes et al., 1987)

rocks with ages between 750-450 Ma and varying composition intruding the older rocks of the basement complex. The rocks of the older granites include tonalites, diorites, associated with rocks of the older granite. The Older Granites suite is noted for little or no mineralization although hydrothermal effects may be an agent of mineralizing fluids mobilization (Obaje, 2009).

The Older Granites are the most important evidence of the Pan-African orogeny and are important additions to crustal materials and about seventy percent addition in some locations, (Rahaman, 1988). Classification of Older Granites using orogenic event periods is correct for only little distances because features displayed at rock contacts of Older Granites suite indicate the presence of magmas of various contents. It is evident from AFM diagram that these granites are calc-alkaline rocks, though they have appreciable quantity of alkalis, sometimes these granites are slightly corundum normative. Pan-African orogeny period witnessed formation of late granites due to wide-ranging mobilisation and reactivation of older basement rocks.

Undeformed acid and basic dykes

These dykes are late to post-tectonic Pan African crosscutting older basement rocks.

These dykes include:

- a. Felsic dykes linked with mineralized pegmatites, aplites, microgranites, and syenite dykes, (Dada, 2006)
- b. Basic dykes which are the youngest rock type in the basement complex of Nigeria which include dolerite and felsite dykes.

The suggested age for basic dykes is put at ca. 500 Ma, (Grant, 1970) but felsite dykes have whole rock Rb-Sr age of 580-535 Ma, (Dada, 2006). While the structural and dating significance of basic dykes is not considered important in Nigeria, it is of high chronological value elsewhere, (Dada, 2006). Where the dykes cut across the basement,

they are useful in deducing the age of metamorphic structures like faults and folds relative to the age of rock suites, they are also excellent guide to get samples for isotopic studies, (Dada, 2006)

2.4.2 Younger Granite

The Younger Granite of Nigeria are Mesozoic ring complexes extending from Afu in central Nigeria to Kano in the North, (Figure 2.7). Dating of the younger granite using the Rb/Sr method yielded Ordovician age for the oldest complex, which is found in the northern part of Niger, while the rocks get younger southwards so that at the extreme south Late Jurassic age is derived for Afu ring complex (Bowden et al., 1976). The disposition of the individual complexes is controlled by a group of underground NE-SW lineaments of nascent fissures as revealed by aeromagnetic anomalies, (Ajakaiye, 1983).

Comprehensive field mapping of the younger granite has revealed continuous magmatic activity from volcanism to emplacement of principally granitic melts in the upper crust. The entire province possesses an outstanding petrographic feature which is the pronounced acidic character of the rocks and the occurrence of similar rock types such as rhyolites, quartz-syenites or granites which are more than 95% of the rocks found in the area while the rest are basic rocks, (Obaje, 2009).

Over 50 complexes of 2 - 25 km in diameter are found in Nigeria (Kinnaird, 1981). Each of the ring complexes started as chains of volcanoes and some have centres that overlap, while some have individual centres, (Bowden and Kinnaird, 1984). The complexes developed when large amounts of acid lavas, tuffs, and ignimbrites intrude the older rocks, with only some parts preserved now because of subsidence along ring faults. The metamorphic basement is overlain by the rhyolitic rocks, suggesting formation of the younger granites in areas uplifted and eroded. Most complexes are composed of granitic ring dykes. Granitic outcrops have been exposed in the complexes located at the extreme south of the area due to erosion of the volcanics, and this also explains why some ring complexes have no associated volcanics at all.

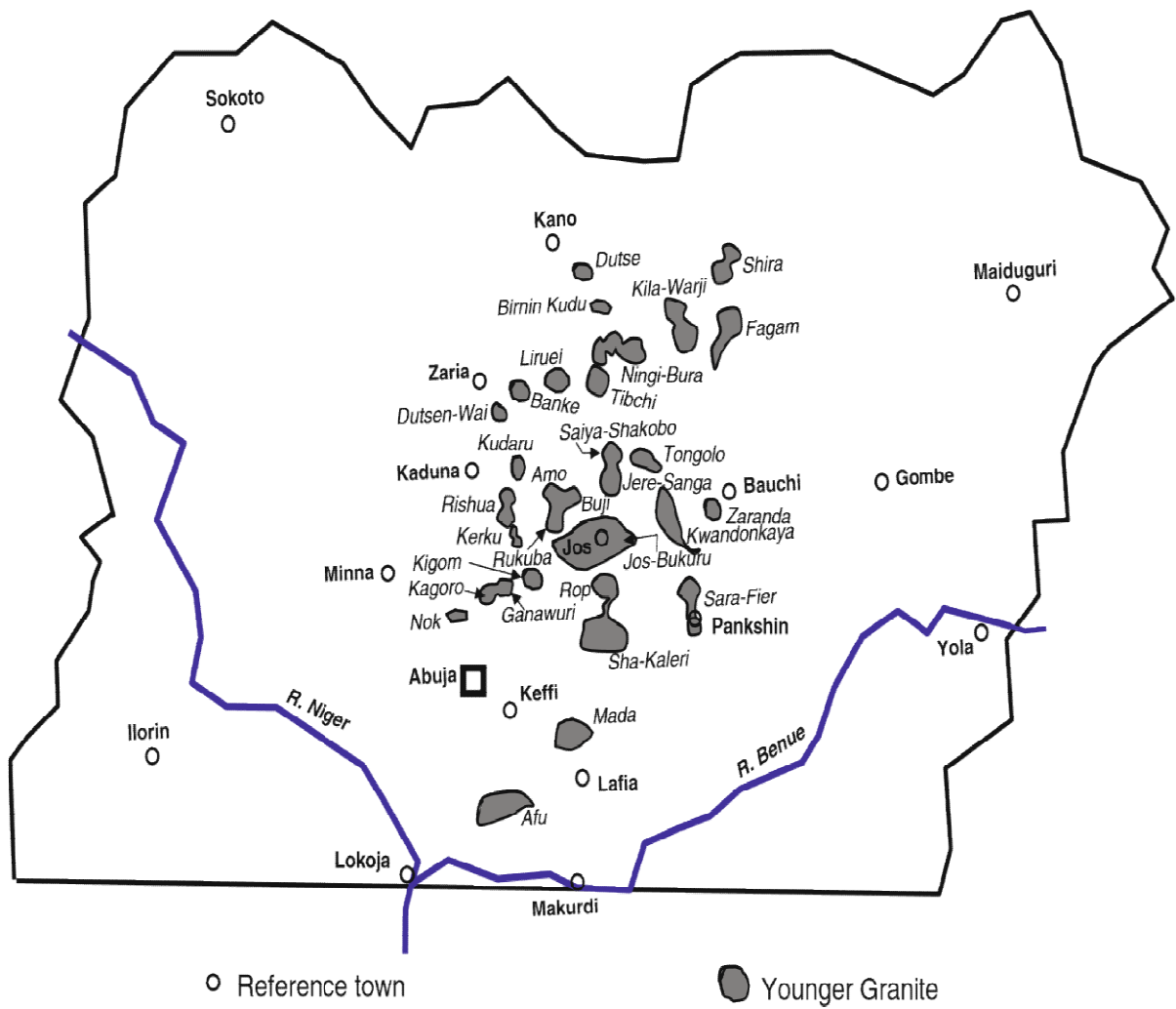


Figure 2.7 Major Younger Granites localities in Nigeria (after Obaje, 2009.)

2.4.3 Sedimentary Basins

Sedimentary basins occur in six locations in Nigeria. These are the Benue Trough, the Chad basin, Iullemeden basin otherwise referred to as Sokoto basin, the Mid-Niger basin known as Bida basin, Dahomey basin and the Niger Delta.

The Benue Trough is a rift basin extending NNE–SSW with dimension of 800km by 150km. It is located between the southern end of the Chad Basin and the north of the Niger Delta. The trough holds sediments of Cretaceous to Tertiary ages with those after the mid-Santonian having folds, faults, and upliftment in several places.

The Bornu Basin is the name given to the portion of the Chad Basin in Nigeria and lies at the extreme northeastern part of Nigeria and constitute about 10% of the Chad Basin land space. The Chad Basin is part of the African Phanerozoic sedimentary basins whose origin is associated with the dynamic process of plate divergence.

The Chad Basin is intra-cratonic, with Niger Republic and Chad Republic hosting over half this land area. The basin is part of a series of rift basins located in Central and West Africa which originates in association with the opening of the South Atlantic and is of Cretaceous and later ages, (Obaje et al., 2004).

“Sokoto Basin” is the local name given to the Iullemeden Basin in northwestern Nigeria. Sedimentation in the Iullemeden Basin occurred in four depositional phases. The grits and clays making up Illo and Gundumi Formations overly the Pre-Cambrian Basement unconformably forming the PreMaastrichtian “Continental Intercalaire” of West Africa. Mudstones and friable sandstones which are Taloka and Wurno Formations with the fossiliferous, shelly Dukamaje Formation deposited in between, together constituting the Maastrichtian Rima Group, is overlain unconformably on the Illo and Gundumi Formation. The Paleocene Sokoto Group, which represents the third phase of sedimentation consists of Dange and Gamba shaly Formations with calcareous Kalambaina Formation in between. The Post-Paleocene Continental Gwandu Formation are gently dipping sediments which increases in thickness to a maximum extent of more than 1,200m towards the northwest by the border with Niger Republic, (Obaje, 2009).

The Bida or Mid-Niger Basin, is a sedimentary basin within the craton trending NW to SE stretching from Kontagora to Lokoja area and towards the south. Bida Basin combines with Anambra basin in the south and Sokoto basin in the north in sedimentary fill consisting of post orogenic molasse facies and marine sediments while at the northeast and southwest it is bordered by basement complex (Adeleye, 1974).

The Dahomey Basin is an inland/coastal/offshore basin extending from southeastern Ghana to southwestern Nigeria. Between the Niger Delta and the Dahomey Basin is Okitipupa Ridge which is a subsurface basement high. A basal sequence without fossils, overlain by coal cycles, clays and marls containing fossiliferous horizons, lies on the Precambrian basement complex. An offshore sandstone sequence which is part of the basin, 1,000m thick, overlain by black shales containing fossils was dated pre-Albian - Maastrichtian (Billman, 1976).

The Cenozoic Niger Delta is located where the Benue Trough intersect the South Atlantic Ocean at a triple junction which developed when the continents of South America and Africa separated in the late Jurassic, (Whiteman, 1982). The Niger Delta evolved in early Tertiary times during increase in clastic river input, (Doust and Omatsola, 1989). The sediments of Niger Delta are sourced from weathered continental basement outcrops through the drainage basin of river Niger and Benue.

The Niger Delta is one of the world's largest deltas having an overall upward transition from Akata Formation consisting of marine shales through Agbada Formation, a sand-shale paralic interval to the continental sands of Benin Formation, (Obaje, 2009). The early Niger Delta is classified as a river-dominated delta, while the post-Oligocene delta is typically wave-dominated. It has a well-developed shoreface sands, tidal channels, beach ridges, freshwater, and mangrove swamps.

CHAPTER THREE

METHODOLOGY

3.1 Field Mapping

Field mapping at the scale of 1:25,000 was undertaken to identify, study the field occurrence and collect samples, of pegmatite and associated rocks in Osogbo-Okinni area, (Figure 3.1). Fresh rock samples were hammered out of exposed outcrops for hand specimen examination. Field identification of component minerals was done using hand-held magnifying lens. Strike and dip direction measurements were taken with compass-clinometer and the coordinates of every sampling location by using hand-held Global Positioning System (GPS). Sixty-three samples were taken from pegmatite and associated rock outcrops in the study area, (Figure 3.1).

3.2 Sample preparation

For the petrographic studies, slides were prepared from the field samples by cutting the samples into thin flat pieces (chips) with a micro-cutting machine, polishing the chips on glass ground plate using carborundum to get the required thickness and smooth surface and the chips mounted with glue on a clean glass slide.

Samples were prepared for laboratory analysis by crushing and grinding selected samples into powder using porcelain mortar and pestle at the Geochemistry Laboratory, Department of Geology, University of Ibadan in Nigeria. The pulverized samples include 22 whole rock, 22 feldspar, and 17 mica extracts. 5 mica books were extracted from different pegmatite samples for K-Ar dating.

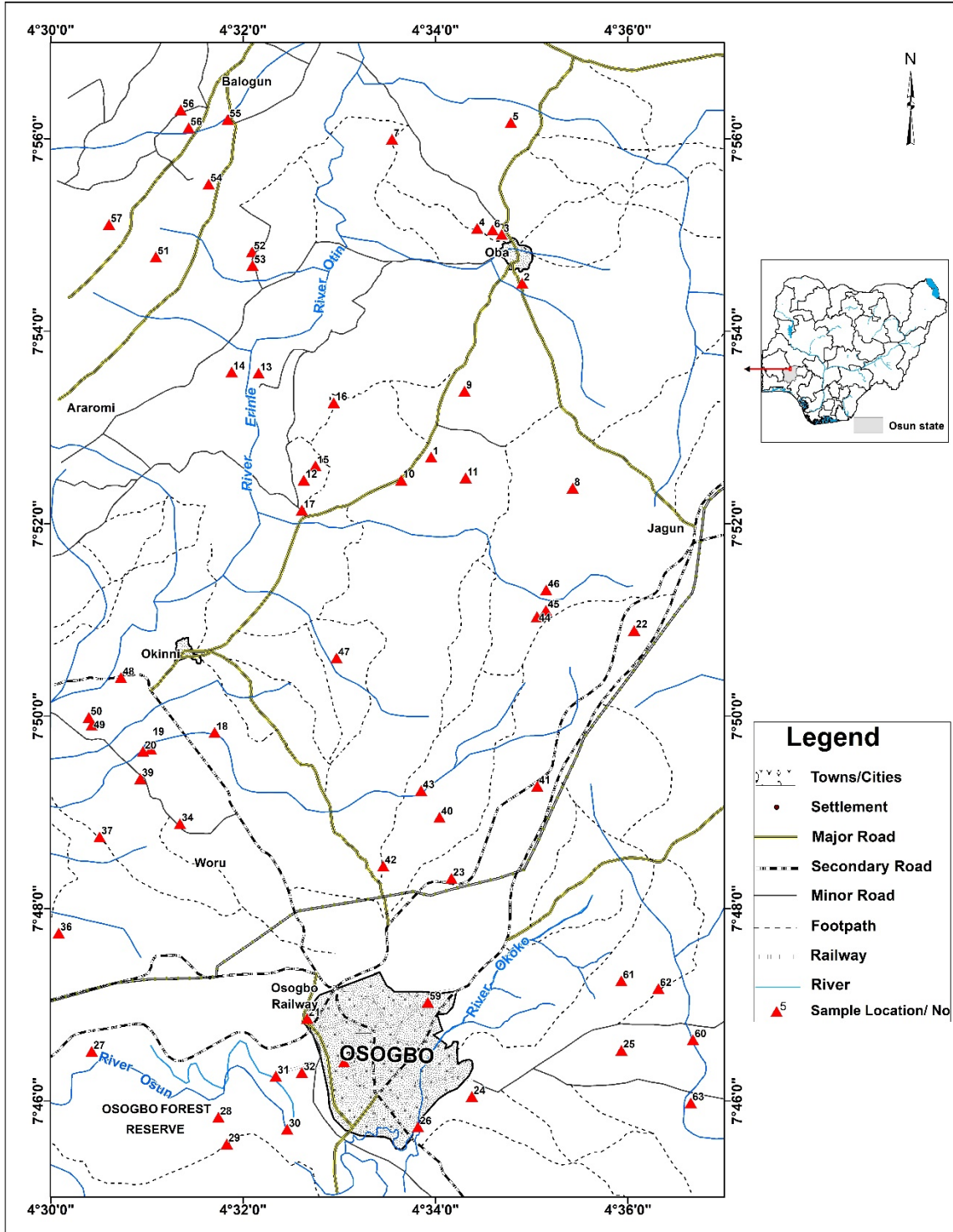


Figure 3.1 Map of Osogbo-Okinni area showing the sample locations.

3.3 Petrographic studies

Prepared slides were examined under a petrological microscope in the Petrographic Laboratory of Geology Department of the University of Ibadan, to identify the mineral constituent of the rock samples and mineralogical features not seen with naked eyes, with a view to naming and classifying these rock samples.

3.4 Geochemical analysis

The analysis was undertaken using Inductively Coupled Plasma Emission Spectroscopy/Mass Spectroscopy (ICP-ES/MS) analytical technique, to give near accurate values for all elements, at Bureau Veritas Mineral Laboratories, Vancouver, Canada. Sample weighing 0.25 g is heated in HNO₃, HClO₄, HF unto fuming and dried. The residue is dissolved in HCl. For some Cr and Ba minerals and oxides of Al, Fe, Mn, Sn, Ta and Zr digestion is partial. Volatilization may result in loss of As, S, Se, Sb during fuming. The concentrations of major elements in whole rock and minerals are given in weight percentage % and in parts per million, ppm, for trace and rare earth elements.

3.5 Geochronology.

Five muscovite samples extracted from the Osogbo-Okinni pegmatites were dated using the conventional K-Ar method modified by Cassinot and Gillot, 1982, called the Cassinot technique for potassium-argon dating. Analysis of the muscovite samples for potassium content was carried out using Inductively Coupled Plasma Emission Spectroscopy/Mass Spectrometry (ICP-ES/MS) analytical method (described in 3.4 above) at Bureau Veritas Mineral Laboratories, Vancouver and utilized at the Geochronological Research Center, Institute of Geosciences, University of Sao Paulo, Brazil, for application in the dating technique. Ar extraction from the muscovite samples, purification and Ar isotope measurement were carried out also at the above-named Institute in Brazil.

Argon measurement

Argon was extracted from 1-2g samples using radio frequency heating induction in high vacuum glass line and purification done with titanium sponge and SAES Zr-Al getter pumps. Extracted argon is held and concentrated by condensation in cooled active-charcoal traps in a modular glass line near the mass spectrometer to get better signal, (Cassignol and Gillot, 1982). Helium is eliminated by use of getter pump. The charcoal is rewarmed at room temperature and pure argon is introduced into the mass spectrometer immediately after rapid pumping. Isotopic analyses were carried out on Ar quantities ranging from $1 \cdot 10^{-11}$ to $2 \cdot 10^{-10}$ mol, using a 186° , 6cm radius mass spectrometer operated at an accelerating potential of 620V. The spectrometer was made to perform in a semi-static mode where data were measured on a double faraday collector in sets of 100 using a 1s integration time. Thus, the measurements are done in a semi-static mode, (Guillou et al., 1997). The Cassignol technique of dating does not utilize spiking of isotopes with ^{38}Ar , therefore the three isotope masses (36, 38 and 40) could be measured simultaneously.

CHAPTER FOUR

RESULTS AND DISCUSSION

4.1 Geology of Osogbo-Okinni area

Osogbo-Okinni area is situated in the Precambrian basement complex of southwestern Nigeria. Rocks identified in this area include migmatite, granite gneiss, quartzite, amphibolite, granite, and pegmatites. Migmatites in the area, occur as xenoliths, in pegmatites at the northcentral and eastern part of the study area. Granite gneiss is situated at four locations including the west of Osogbo, southwest, extreme northwest and eastern end of the study area. These gneisses and xenoliths of migmatites have the indelible imprints of early to late Precambrian metamorphic episodes. Igneous reactivation of these suites of rocks has been attributed to the Pan-African thermotectonic event, (Okunlola et al., 2007). Quartzite occurs as massive ridges at the northwestern part and as hilly outcrops at the southern end of the study area. Outcrops of amphibolite, which are part of the Proterozoic schist belts of southwestern Nigeria, were found at the northeastern and central parts with large pegmatite vein intrusions (0.5-1.4m width) in some places. Granites outcrop mainly at the south to southeastern part of Osogbo.

Pegmatites occur as distinct dykes of dimension ranging from 10m to 300m in length and 5m to 100m in breadth, intruding the older rocks in the study area, outcropping as low-lying to massive mountainlike plutons, (Figure 4.1a and 4.1b).Pegmatites occupy about 60% of the land mass, occurring without any regular pattern in the study area, extending from the north of Osogbo to Okinni and to Oba at the northern part of the study area, (Figure 4.2).



4.1a



4.1b

Figure 4.1a Quarry face of a massive pegmatite outcrop at Asipa, Okinni area Figure
4.1b Pegmatite outcrop by River Apala, Okinni area.

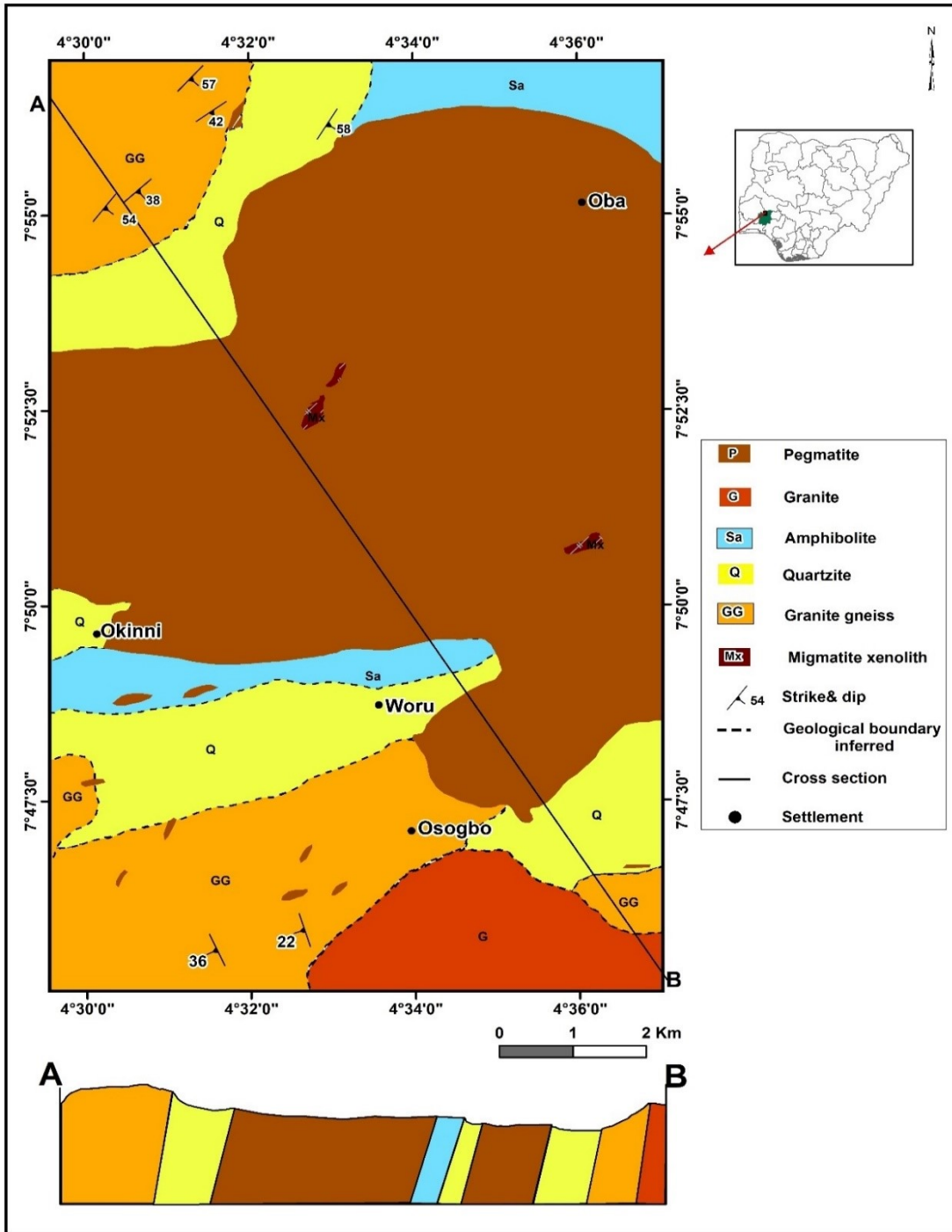


Figure 4.2 Geological map of Osogbo-Okinni area, Southwestern Nigeria.

4.1.1 Migmatite

Field relationship with other rock types reveal migmatite as the oldest rock type in the study area because migmatite gneisses are known to be of 2.8 - 2.0 Ga ages. However, older ages > Ca 3.0 Ga were recently indicated for the Kaduna migmatite (Dada, 1989, Brugurier et al., 1994). Earlier petrographic studies show that migmatite is the result of partial melting and recrystallization of metamorphic rocks like gneisses into which magma has been injected. These rocks show evidence of medium to upper amphibolite facies metamorphism (Mehnert, 1968).

Migmatites in the study area occur as xenoliths which are remnants of the older mafic rocks into which the pegmatite intrudes at Dagbolu, south of Oba, and at Asipa, southwest of Oba, (Figures 4.3, and 4.4). The chilled margin of fine-grained texture bordering the xenoliths of localized relics of assimilated migmatite in the pegmatite is clearly visible in the Dagbolu pegmatite outcrop, (Figure 4.3).

Plagioclase, which is mainly albite, is the dominant mineral occurring as subhedral grains and constitute an average of 28% by volume of the rock, (Table 4.1). Other minerals include quartz (21%) which occurs as subhedral to anhedral grains, k-feldspar which is mainly microcline (21%) is observed with its characteristic cross hatch twinning, untwined orthoclase crystal is not observed in the rock. Biotite occurs as platy brownish crystals and accounts for 14%, whilst hornblende (12%) occurs as continuous greenish crystals. Muscovite (4%) is observed as pinkish elongated platy crystals, and the opaque minerals account for about 1% by volume, (Figure 4.5). The minerals seem to be oriented in the same direction, and this is very apparent with the hornblende and mica minerals, due probably to the deformation processes.



Figure 4.3 Chilled margin in pegmatite around the migmatite xenolith (length of pen), (Dagbolu SE of Oba).



Figure 4.4 Migmatite xenoliths in pegmatite shown by arrows (Asipa, SW of Oba)

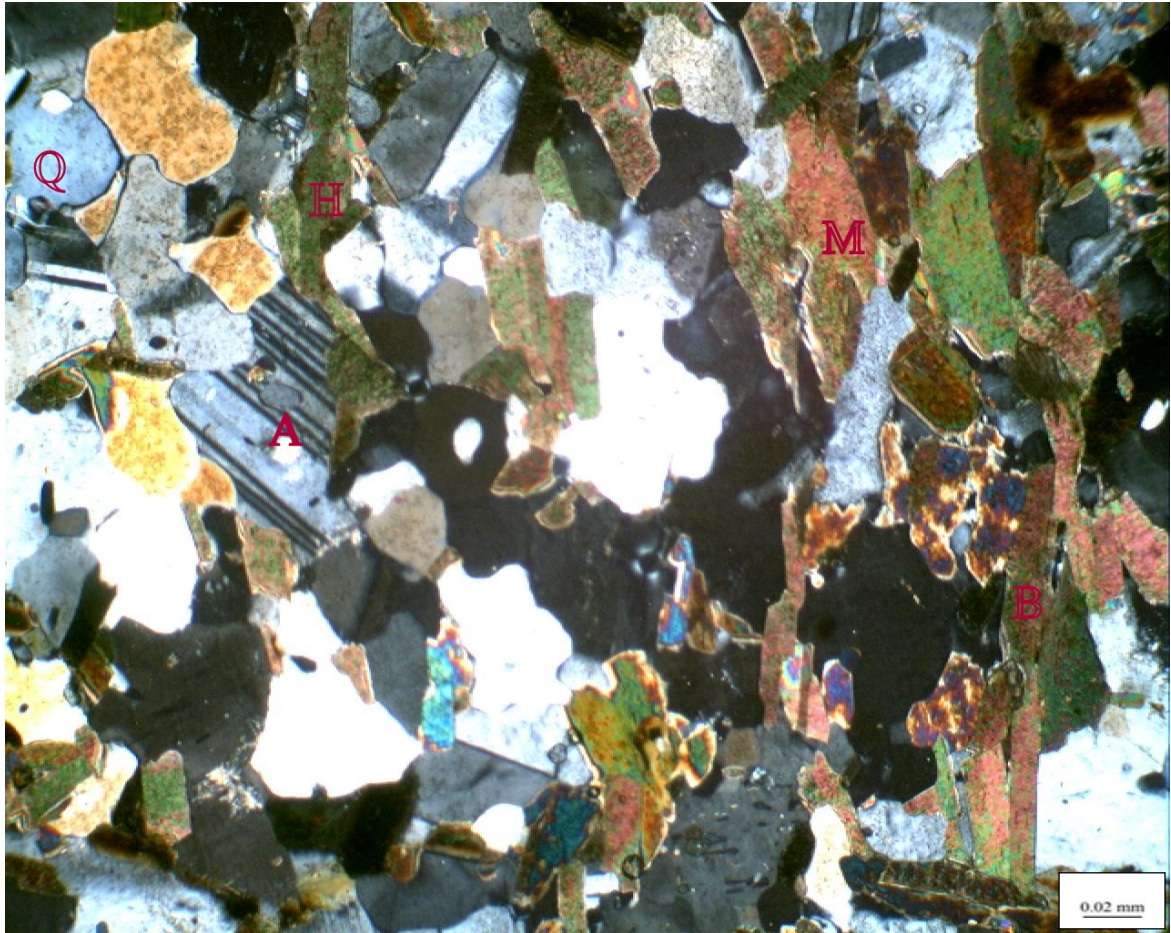


Figure 4.5 Photomicrograph of a section of migmatite in transmitted light showing albite (A), quartz (Q), hornblende (H), biotite (B) and muscovite (M).

Table 4.1 Modal composition of associated rocks

Rock Type	quartz	Microcline	plagioclase	Biotite	Hornblende	muscovite	Opaque	Total
Mig	22	20	27	15	12	4	-	100
Mig	20	21	29	13	12	4	1	100
Amp	14	16	16	20	30	2	1	99
Amp	15	17	20	18	26	3	1	100
Amp	22	20	30	10	12	5	1	100
Amp	20	19	24	19	15	2	1	100
Amp	14	10	20	24	24	7	1	100
Amp	23	23	31	10	8	2	1	98
Amp	18	15	17	19	29	1	1	100
Amp	16	17	19	20	26	1	1	100
GGn	26	24	40	4	--	6	--	100
GGn	23	22	31	7	5	11	1	100
GGn	28	21	33	8	6	3	1	100
GGn	27	22	32	6	4	8	1	100
GGn	27	32	27	9	3	1	1	100
Gra	29	26	36	4	-	5		100
Gra	25	23	38	2	-	12		100
Gra	28	27	37	--	--	8	--	100
Gra	27	24	40	3	--	6	--	100

Mig Migmatite
 Amp Amphibolite
 GGn Granite Gneiss
 Gra Granite

4.1.2 Granite gneiss

Granite gneiss occurs at the northwest, the southwest of Osogbo and the extreme southeastern part of the study area. Outcrops of granite gneiss are low-lying, medium size outcrops having dimensions ranging from 20mX30m to 30mX60m. The light and dark bands of felsic and mafic minerals were observed on the outcrops with joints, pegmatite, quartz and quartzofeldspathic veins intruding the rock along the strike direction generally towards the North, (Figure 4.6).

Granite gneiss is a strongly foliated or banded metamorphic rock derived from igneous (orthogneiss) or sedimentary rocks (paragneiss) mineralogically equivalent to granite.

Petrographic studies reveal that the rock consists of plagioclase, which is mainly albite (27-40%), Quartz (23-28%), microcline (21-32%), biotite (4-9%), muscovite (1-11%) and hornblende (3-6%) volume, (Figure 4.7).

4.1.3 Quartzite

This rock is part of several northerly trending Proterozoic metasedimentary belts mainly composed of pelitic and semi pelitic schists and quartzites in the western part of the Precambrian basement complex of Nigeria, (Egbuniwe, 1982). Quartzite, a schistose rock having predominantly quartz and mica (in minor quantity) minerals is formed from contact or Barrovian metamorphism (or combination of the two) of sandstone.

Quartzite occurs as prominent ridges at the east of Osogbo, the northwestern and central portion of the study area. They are jointed rocks, with discordant intrusion of late quartz veins across the outcrops.



Figure 4.6 Part of granite gneiss outcrop at the northwestern part of the study area.



Figure 4.7 Photomicrograph of a section of granite gneiss in transmitted light, showing quartz (Q), microcline (Mic), biotite (B) and albite (A).

4.1.4 Amphibolite

Amphibolite belongs to the Proterozoic schist belt found in western Nigeria having distinct petrologic and structural features. In the study area amphibolite occurs at the northeastern and central parts as hilly outcrops, one of which is intruded by a large pegmatite vein, (Figure 4.8). These rocks are foliated with alternate green and whitish coloured minerals on some outcrops but banded with the gneissose texture readily seen on the specimen as alternation of mafic minerals, (hornblende and biotite), and felsic minerals, (Quartz, and feldspar) on other outcrops, (Figure 4.9a and 4.9b).

Petrographic studies revealed anhedral grains of quartz, subhedral crystal of plagioclase, and k-feldspar (mainly microcline) in almost equal abundance of 18%, 22%, 17%, respectively by volume in the rock, with plagioclase slightly higher.

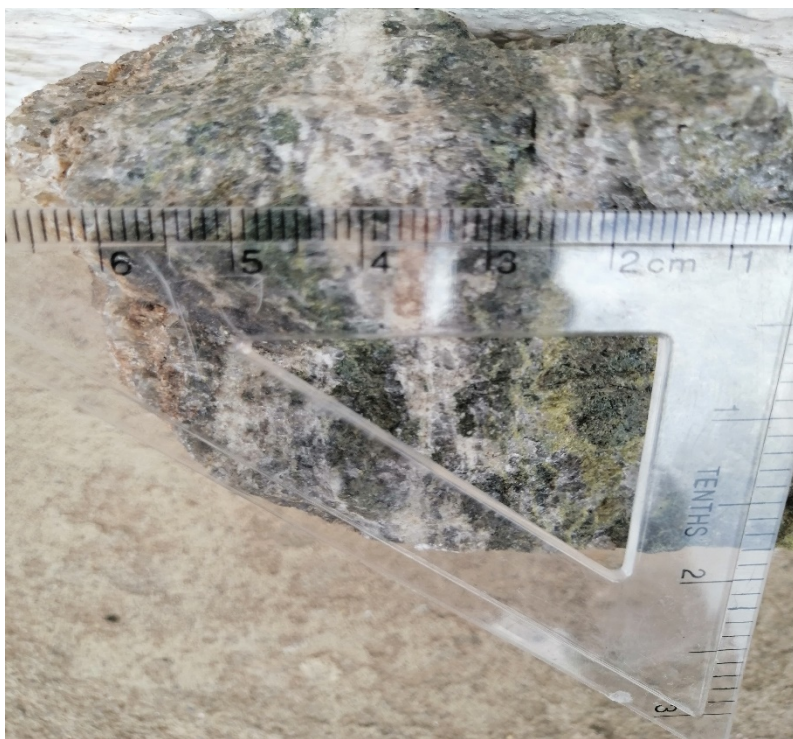
Hornblende which appears as continuous greenish crystals account for 21vol% average content. The characteristic $58^{\circ}/122^{\circ}$ angle between two cleavage planes in hornblende can be observed, (Figure 4.10). Biotite (18vol%) which appears as crystals of brownish coloured grains is slightly less in proportion, while muscovite occurs in minor proportion of 3% by volume, (Table 4.1). The orientation of the mineral grains as seen in transmitted light is towards same direction due to deformation processes, (Figure 4.10).



Figure 4.8 Amphibolite intruded by pegmatite vein (1.4m width, between the marker and pencil).



4.9a



4.9b

Figure 4.9a Specimen of amphibolite (north of Oba) showing foliation of about 1mm thickness

Figure 4.9b Specimen of amphibolite showing banding of about 0.5-1.0cm thickness

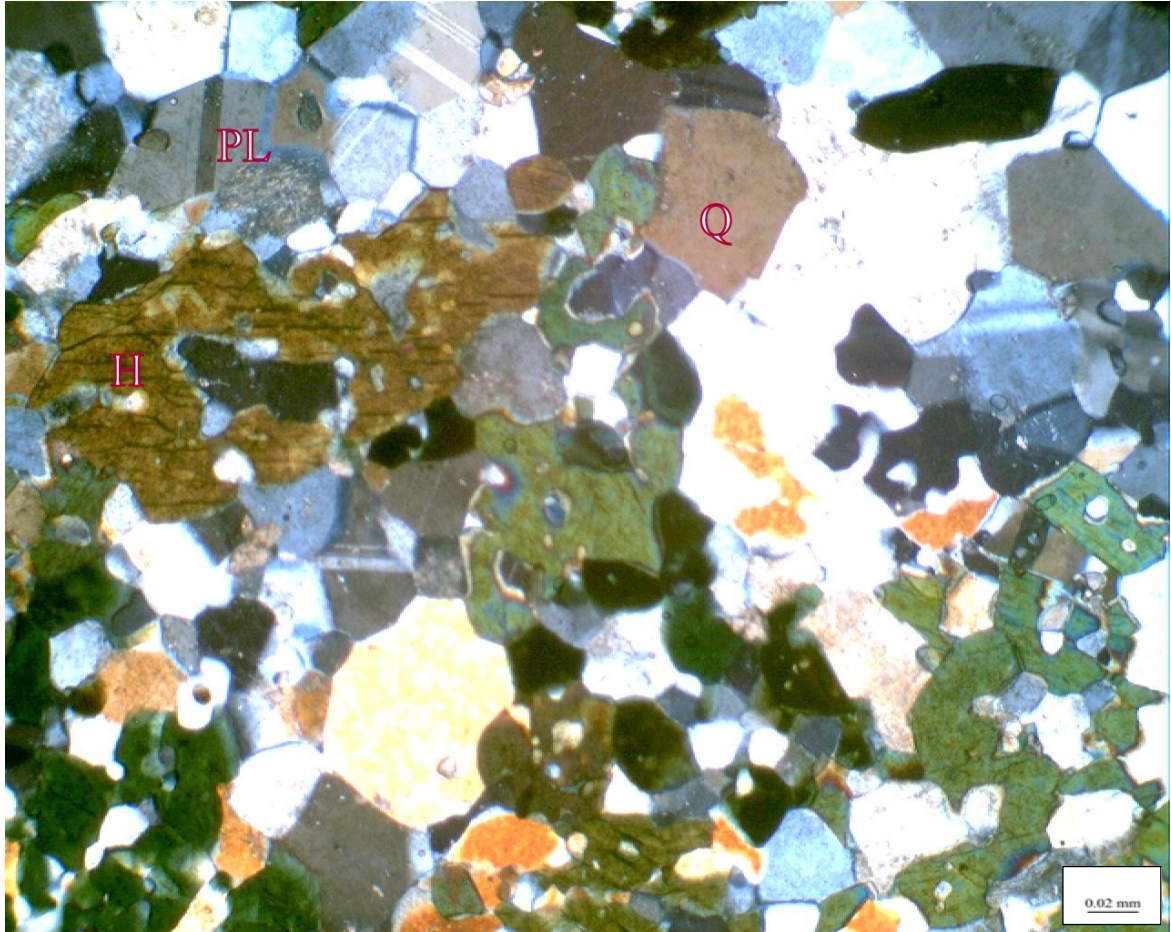


Figure 4.10 Photomicrograph of a section of amphibolite (north of Oba) in transmitted light showing hornblende (H) with cleavage, plagioclase (PL) and quartz (Q) minerals.

4.1.5 Granite

Granite is part of the Older Granites of Nigeria otherwise known as the Pan African granitoids which comprise gabbros, charnokites, diorites, granites and syenites, (Kuster 1990). These granitoids result from oceanic closure, subduction, and tilted collision of the west African craton with the Nigeria shields which intrude into the Pan-African belt during Pan-African orogeny, (Black, 1984).

The granite is a part of the Older Granites and occurs as hilly outcrops southeast of the study area. The rock is fine to medium grained and leucocratic. The average dimension of the outcrops is 30mx50m. Pegmatite, quartz and quartzofeldspathic veins were observed with orientation in various directions. Joints, both open and closed were observed on the outcrops with trends in diverse directions which are probably results of fracturing during emplacement.

The average modal composition is as follows, quartz 28%, plagioclase 34%, microcline 25%, muscovite 5%, biotite 8% by volume. Quartz, plagioclase, and microcline appear as well-formed euhedral grains with crosshatch twinning characterizing microcline. Brownish thin strips of biotite are also observed, (Figure 4.11).

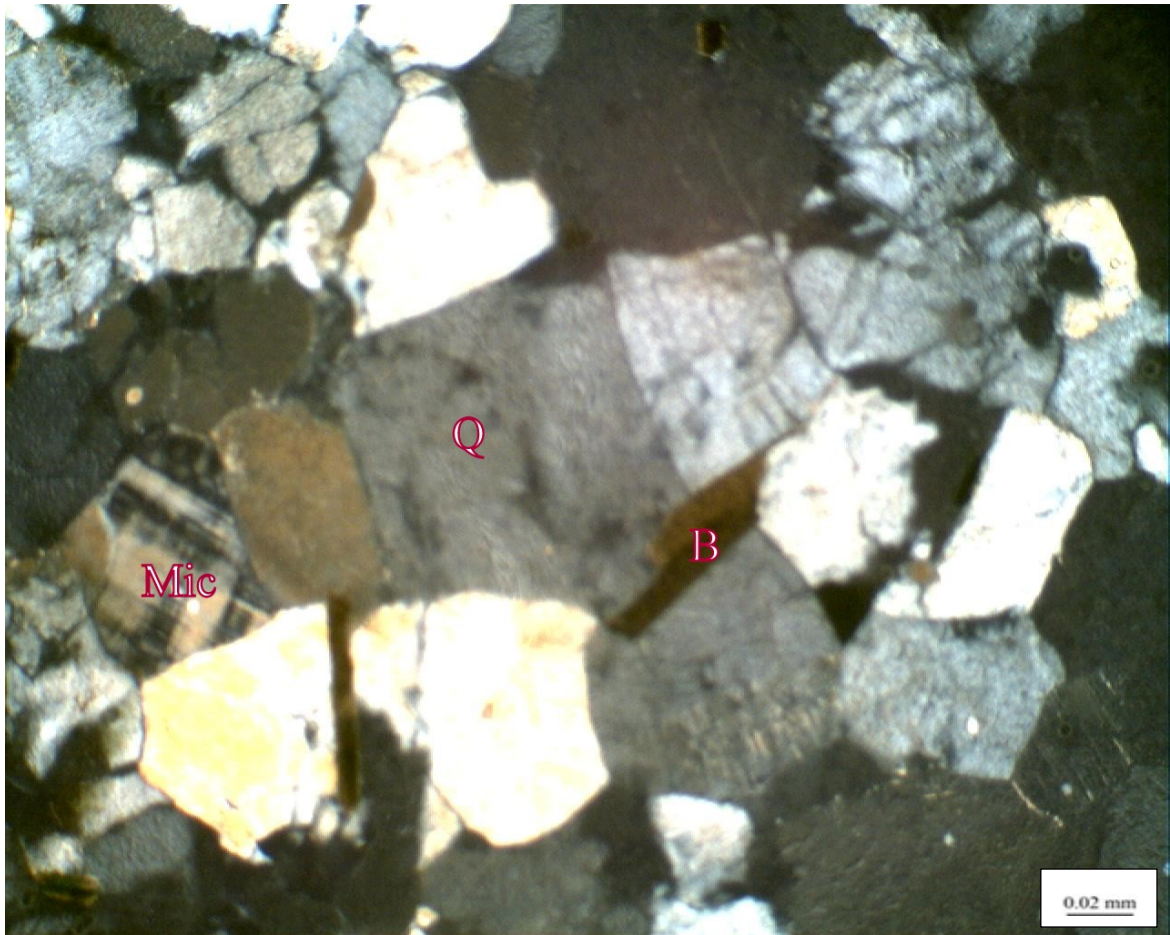


Figure 4.11 Photomicrograph of a section of granite in transmitted light showing Microcline (Mic), Quartz (Q) and Biotite (B).

4.1.6 Pegmatite

4.1.6.1 Field occurrence.

The Pegmatites of Osogbo-Okinni area occur in two major ways, as thin to large veins (1cm-1.4m), intruding granite gneiss, amphibolite, and granite, and as major low-lying to mountainous plutons trending generally NE-SW, with dimensions varying from 10mX30m to 150mX500m, (Figure 4.1a, 4.1b). The latter form of occurrence is the main object of study. Structurally, they are coarse grained, with a graphic texture defined by the interlocking growth of the small to medium grained quartz and feldspar crystals varying in dimension from 5mmx5mm to 6cmx20cm. The outcrops of these rocks are found scattered all over the study area, the bulk of which occupy the area from Osogbo in the south to Oba in the north and Okinni at the southwest spanning about 60% of the area with the older rocks outcropping at the extreme northern and southern edges, (Figure 4.2).

The pegmatites are garnetiferous, euhedral garnet crystals are present on the outcrops with tourmaline mineralisation. For example, dark blue flaring crystals which may be tourmaline mineralisation filled prominently into the later veins/fractures of the pegmatite at Apala river, Okinni, (Figure 4.12) which suggest that the tourmaline mineralisation probably resulted from boron metasomatic phase which came at the end of the pegmatite intrusion. On some other pegmatite outcrops, books of mica occur as aggregates in a part (Figure 4.13) and in some other cases they are scattered on the outcrops with varying thickness of 1cm to 3-4cm and sheets of dimensions of 5x8mm to 2x6cm in places (Figure 4.14). Veins/fractures are filled also with quartz minerals, and these can extend up to over 50m in length as seen in pegmatite of Awosin, to the northeast of Okinni area (Figure 4.15a) and up to 10cm-15cm width in places (Figure 4.15b).

Joints and quartzo-feldspathic veins abound on the pegmatite outcrops trending majorly NE-SW. On some outcrops, the joints have been expanded probably by weathering (Figure 4.21).



Figure 4.12 Pegmatite veins in-filled with tourmaline mineralization (arrows) at Apala river, Okinni.



Figure 4.13 Books of mica aggregate in pegmatite outcrop at Awosin, northeast of Okinni.



Figure 4.14 Hand specimen of pegmatite of Osogbo-Okinni area showing books of muscovite (arrows).



Figure 4.15a Quartz vein in mountainous pegmatite (about 150x500m)at Awosin.



Figure 4.15b. Thick quartz vein and later joints in the vein in pegmatite of Awosin.

4.1.6.2: Petrography

Petrographic studies of Osogbo-Okinni pegmatites revealed quartz (20-28vol%), plagioclase (albite)(23-59vol%) and microcline (14-41vol%) as main minerals whilst muscovite (1-22vol%), biotite (2-18vol%) and tourmaline (4-16vol%) are the minor minerals and zircon, garnet, and opaque minerals as accessories (Table 4.2). Quartz exhibits anhedral to sub-euhedral shape, colourless to cloudy with evidence of poikilitic inclusions of feldspar and other minerals. Plagioclase which is mainly albite with characteristic albite-carlsbad twinning was observed in most samples (Figure 4.16). The nature and type of plagioclase twinning are pointers to the origin of the rock; the nature of twinning in plagioclases of igneous rocks differs from that of plagioclases in metamorphic rocks (Gorai, 1951; Vance, 1961; Tobi, 1961). Gorai, (1951), observed a characteristic difference in the plagioclase twin in magmatic and metamorphic rocks. He identified two types of plagioclase twinning as A-type, and C-type. The A-type twinning which includes lamellar albite, accline and pericline twins are present in both igneous and metamorphic rocks. The C-type twinning include carlsbad, albite-carlsbad and penetration twins which are developed during crystallization and is restricted to the magmatic rocks. The abundance of C-type carlsbad twinning in plagioclases of the pegmatites in the study area may point to their magmatic origin.

Microcline (Figure 4.17) which is a low-temperature polymorph of K-feldspar results from a post-growth change that occurs in K-feldspar below 450°C, where disordered monoclinic sanidine or orthoclase was changed into triclinic microcline. Current concepts have it that primary pegmatitic K-feldspar grows as a partial or fully disordered phase, with associated growth-twins of baveno, manebach or carlsbad laws, and develops the albite-pericline twinning only upon inversion to microcline, (Martin, 1988). It is now believed that most pegmatites crystallize at temperatures close to the temperature at which this inversion takes place. It is therefore possible that some K-feldspar in pegmatites grew with an ordered microcline structure.

Table 4.2 Modal composition of pegmatites

Sample no	Quartz	Microcline	Plagioclase	Biotite	Tourmaline	Muscovite	Opaque	Total
1	21	24	40	5	--	10	--	100
2	21	22	42	4	--	7	--	96
3	26	23	38	3	--	10	--	100
4	23	21	37	6	4	8	1	100
5	21	24	36	7	4	8	--	100
6	20	29	41	5	--	4	--	99
7	26	20	38	5	--	10	--	99
8	20	22	42	4	--	12	--	100
9	26	23	36	6	--	9	--	100
10	25	23	39	3	--	10	--	100
11	20	14	59	2	--	5	--	100
12	20	17	44	3	8	5	--	97
13	23	21	32	10	10	3	1	100
14	24	21	26	15	10	3	1	100
15	25	20	28	12	8	6	1	100
16	28	23	35	6	--	8	--	100
17	25	24	37	8	--	6	--	100
18	27	22	31	9	--	11	--	100
19	25	24	38	7	--	6	--	100
20	20	19	23	18	16	2	1	99
21	29	25	38	2	--	6	--	100
22	24	23	42	2	--	8	--	99
23	27	41	23	--	--	8	--	99
24	28	31	35	--	--	5	--	99
25	25	24	40	4	--	7	--	100
26	27	22	48	--	--	2	--	99
27	29	22	38	6	--	5	--	100
28	24	29	44	--	--	3	--	100
29	24	31	42	2	--	1	--	100
30	24	23	43	--	--	10	--	100
31	26	20	32	--	--	22	--	100
32	29	22	40	3	--	6	--	100
33	26	20	43	--	--	11	--	100
34	28	22	30	10	6	3	1	100
35	26	21	41	--	--	12	--	100
36	26	33	32	2	--	7	--	100
37	25	25	40	4	--	6	--	100
38	28	24	42	3	--	3	--	100
Range	20-28	14-41	23-59	2-18	4-16	1-22	1-1	
Average	25	24	38	6	8	7	1	

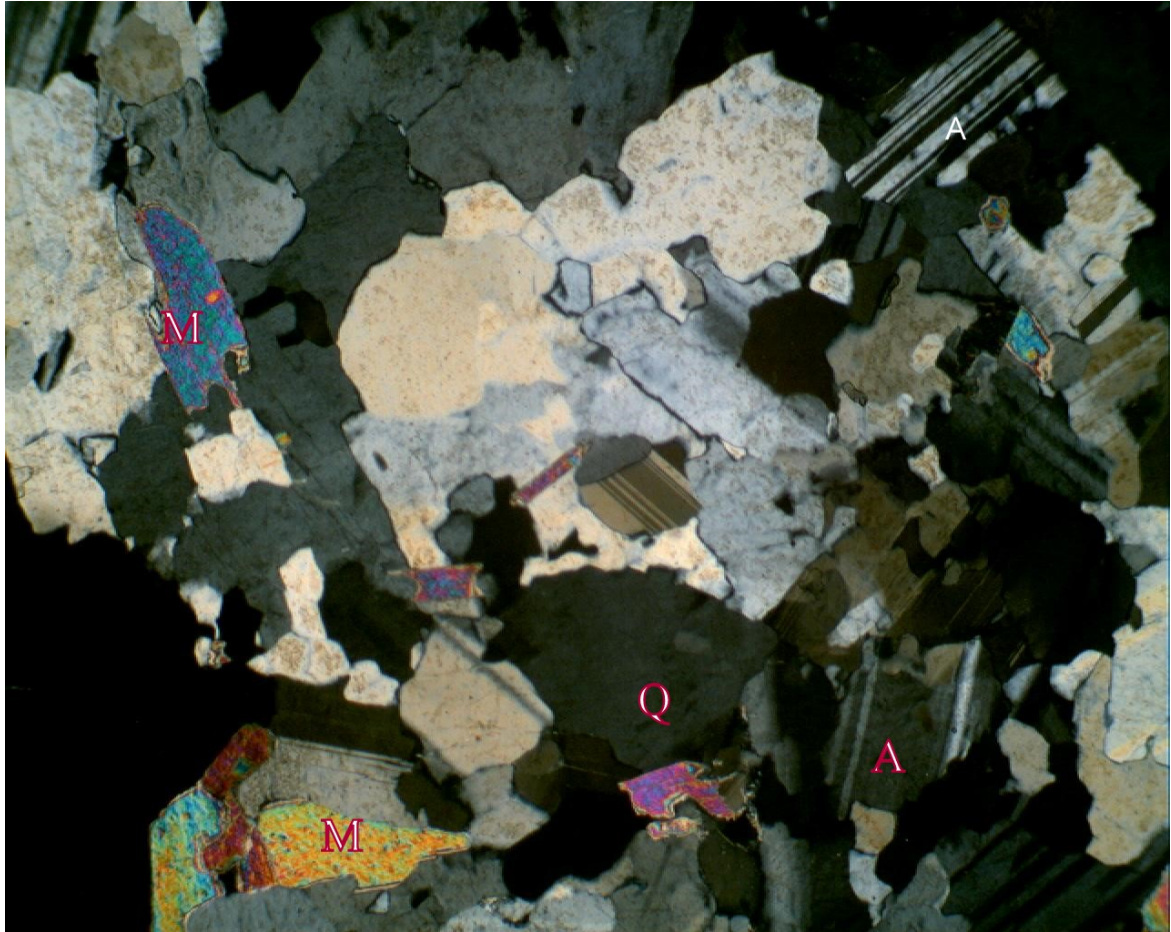


Figure 4.16 Photomicrograph of a section of pegmatite in transmitted light, showing albite (A), muscovite (M) and quartz (Q).

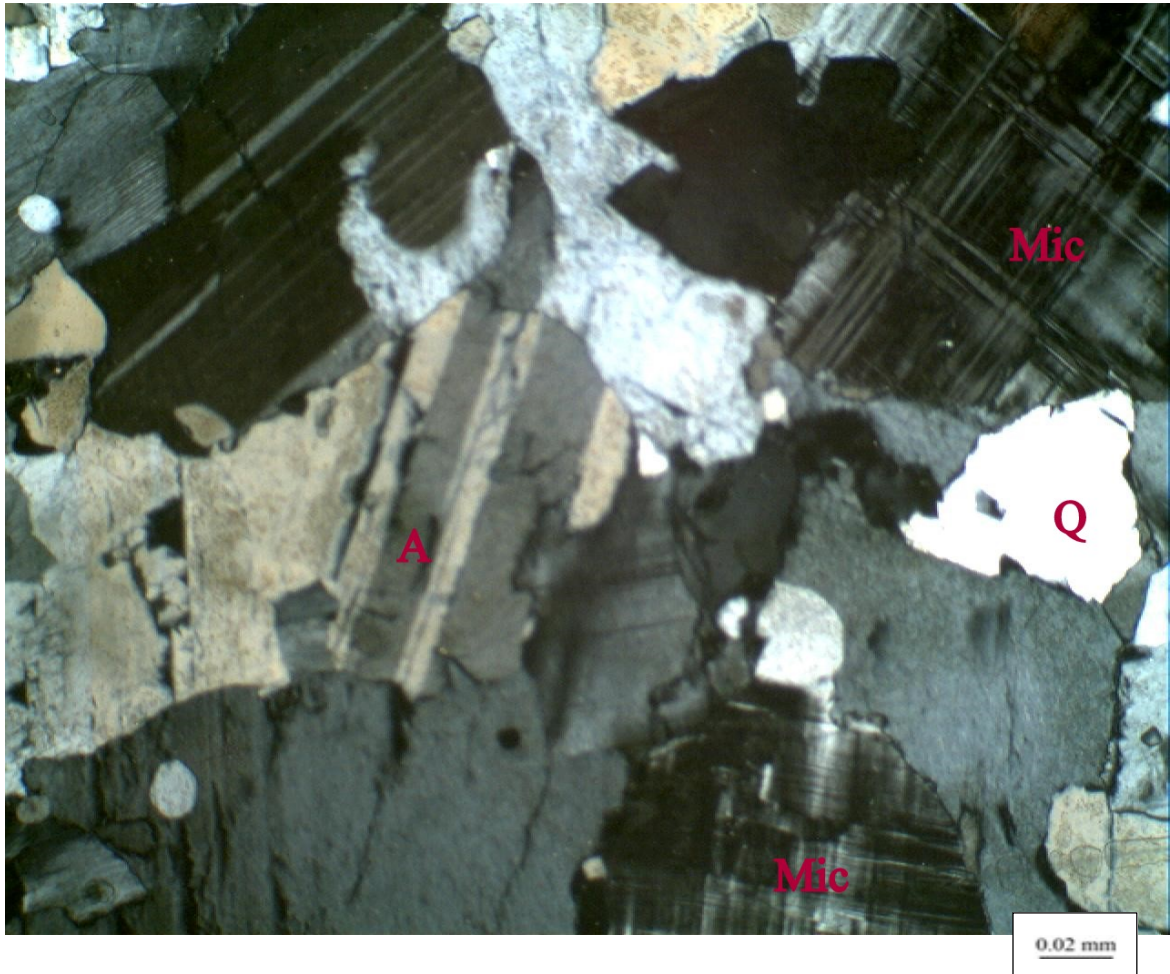


Figure 4.17. Photomicrograph of a section of pegmatite in transmitted light showing large crystals of microcline (Mic), quartz (Q) and albite (A).

Crosshatched twinning which is the result of interpenetrating albite and pericline twins is displayed by microcline with perthitic texture (Figure 4.18a and 4.18b). The formation of

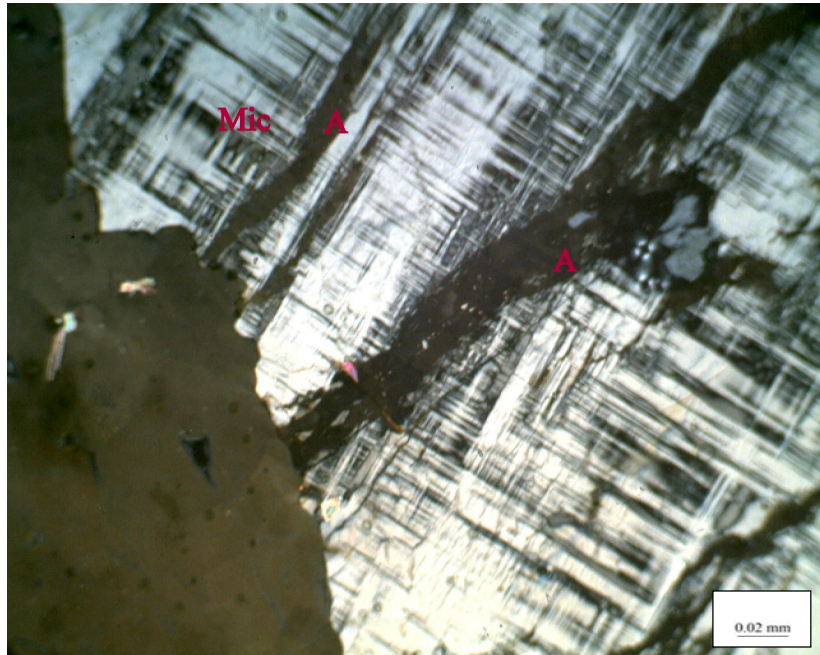
perthitic texture which is the exsolution of albite lamellae within the K-rich host is also a post growth change that reflects extensive recrystallization of the primary phase.

Muscovite, which is more prevalent occur as pink and yellow elongated platy crystals interstitial between other minerals like quartz and feldspar (Figure 4.16). The crystallization of muscovite from melt along with quartz, albite and k-feldspar constrains pegmatites to crystallize at pressures and temperatures within the stability range of this assemblage which is mostly below 650°C to 700°C at pressures of 200 to 400 Mpa H₂O (London, 2008). Biotite was observed as brownish platy minerals that can be separated along the cleavage perfectly in a direction and have strong birefringence colour, (Figure 4.19).

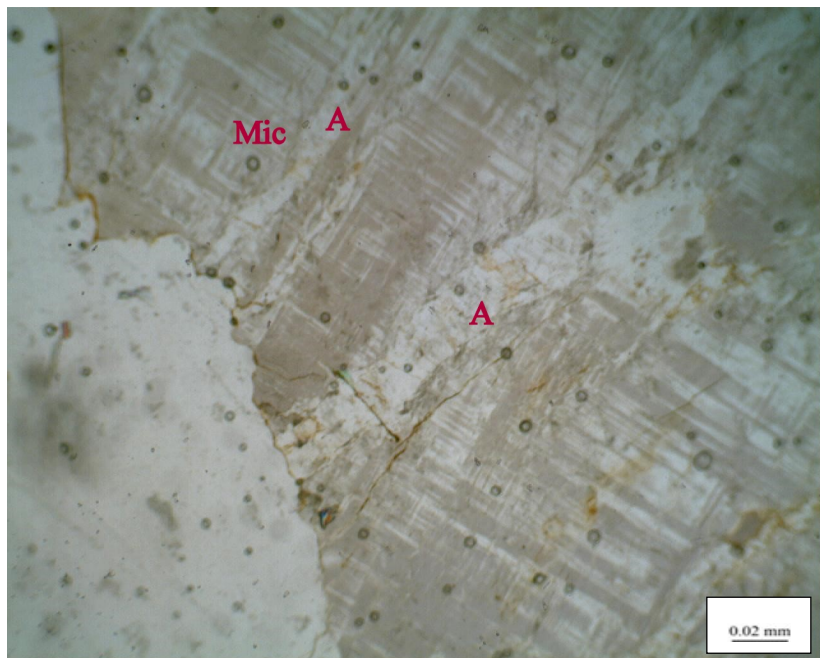
The pegmatites contain primary muscovite which suggests a peraluminous nature of the source magma for this rock type and the abundance of muscovite, which hosts both lithium and caesium, in most samples, points to the classification of these pegmatites as members of LCT family of pegmatites, (London, 2008).

Tourmaline, which is the principal host of boron occurs as accessory mineral. It is dark indigo blue and when found in pegmatite it is known as “schorl” which is a solid solution with substantial amount of schorl, olenite, and foitite components. It occurs most abundantly along the borders of pegmatite, (Figure 4.12) where it forms inwardly pointing and flaring black crystals, (London 2008).

Garnet also occurs as accessory mineral in these pegmatites. It originates from aluminous sources, so it is associated with pegmatites that contain other peraluminous minerals like muscovite and tourmaline. They have strong tendency to form euhedral crystals (Figure 4.20). Though the individual stepped faces are shiny and sharply bounded, this habit arises from the dissolution of the garnet and not from growth, (London, 2008).



4.18a



4.18b

Figure 4.18a Photomicrograph of a section of pegmatite in transmitted light showing microcline with perthitic structure (exsolution of albite lamellae (A) within microcline (Mic)) in cross polarized light, XPL.

Figure 4.18b same as figure 4.17a, but in plane polarized light, PPL.

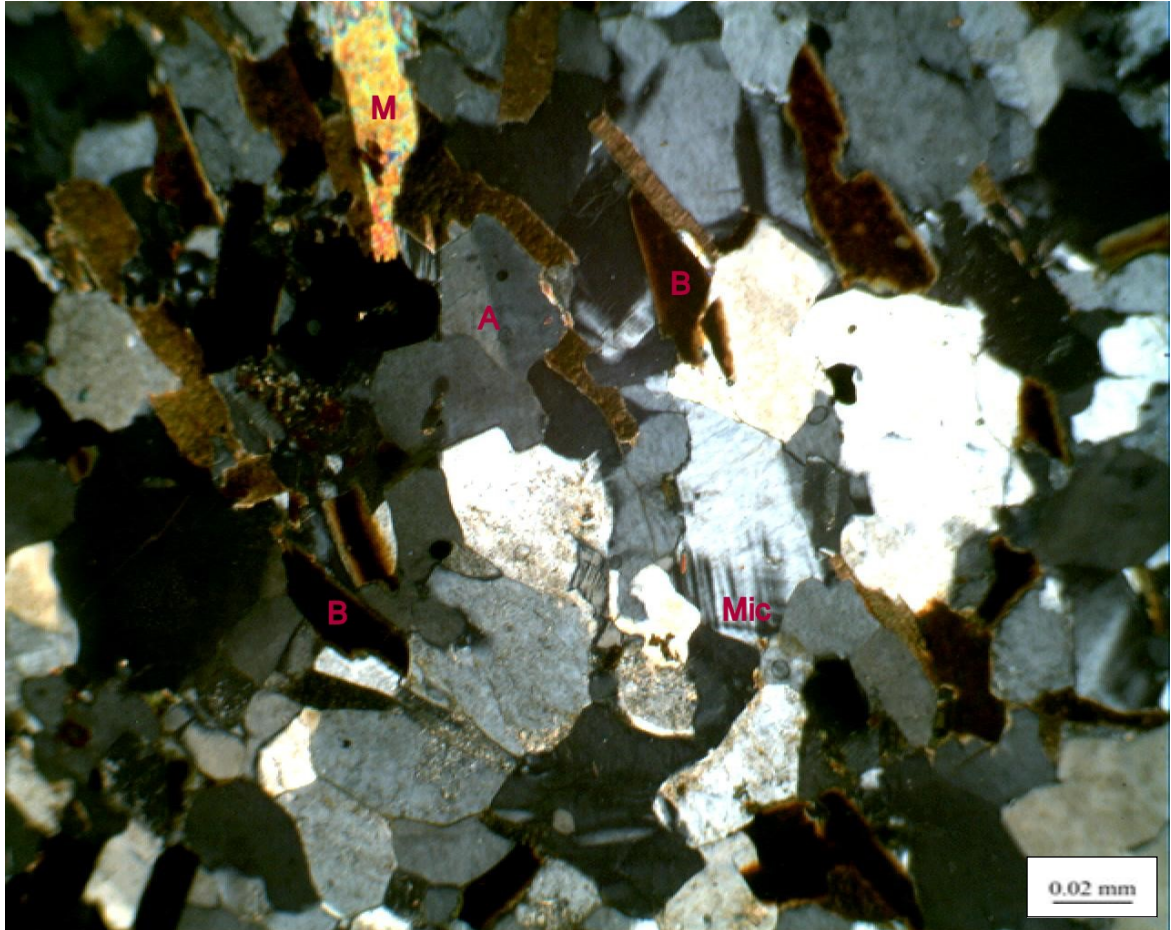


Figure 4.19 Photomicrograph of a section of pegmatite in transmitted light showing albite (A), microcline (Mic), muscovite (M), and biotite (B).

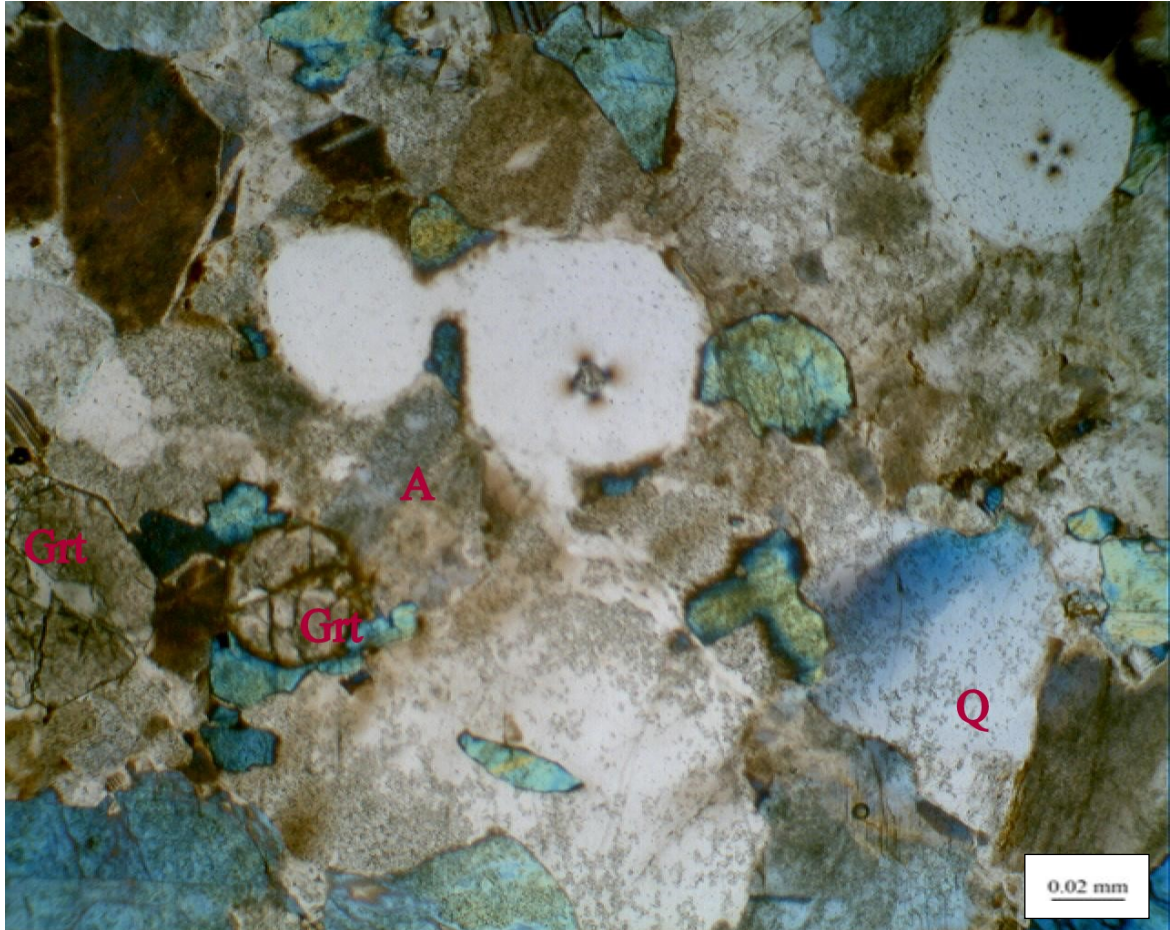


Figure 4.20 Photomicrograph of a section of pegmatite at Dagboluin transmitted light showing garnet (Grt), albite (A) and quartz (Q).

4.2 Structures

The structural features of the basement complex are polycyclic because they have undergone several orogenies. Polycyclic orogenies mean there has been many metamorphism phases, deformation, igneous activities, and mountain-building. The signatures of four major orogenies which affected the Nigerian basement complex have been dated, Liberian of 2700 ± 200 Ma (Oversby, 1975), Eburnean of 2000 ± 200 Ma (Oversby, 1975), Kibaran of 1100 ± 200 Ma (Ekwueme, 1987), and Pan African of 600 ± 150 Ma, (Fitches et al., 1985). The most significant of these is the widespread Pan African orogeny, thermotectonic event, (McCurry,1976) which changed the configuration and signature of the older Precambrian structures. The West African Craton moving eastward collided with the westward mobile plate creating N–S to NE-SW directional structures parallel to the border line of the West African Craton, (Egesi and Ukaegbu, 2010). The Pan African orogeny is a serial event with signatures represented by folds, faults, and lineaments in the Basement Complex of Nigerian and Northern Cameroun, (Toteu et al., 1990). The N-S and NE-SW directional structures are the prevailing Pan African orogeny fabrics which are directly contrary to Achaean or pre-Pan African orogeny structures trending NW-SE direction, (Toteu et al., 1990).

The basement complex of Nigerian was deformed twice, a ductile deformation resulting in folds and planar structures like foliations and a brittle deformation with joints and fractures infilled with veins which are quartzo-feldspathic, pegmatitic and aplitic and dolerite and aplitic dykes.

In the Osogbo-Okinni area, foliations, which are caused by shearing or differential forces resulting in the rock minerals forming repetitive layers which may look like a stack of sheets of paper, were observed in granite gneiss, and amphibolite. The foliation planes consist of bands of dark and light-coloured minerals trending generally in the NNE-SSW direction, attesting to the direction of forces present during the pan African orogeny, (Omosanya et al., 2015).

Joints, which can be described as fractures or breaks in a rock type, naturally occurring and without any measurable displacement, were observed in most rock types and are oriented in varying directions (Figure 4.21). Joints which may occur singly or as a set, differ from faults in that faults display visible and measurable lateral displacement between the opposite faces of the shearing plane. Readings were taken for numerous joints orientation on most outcrops randomly for all rock types. Rose diagrams were plotted for the joints orientation in the different rock types encountered in the area and the result shows that the joints have orientation in two major directions, NW-SE, and NE-SW. This is an attestation of the effects of pre-Pan African orogenies and Pan African orogeny, (Figures 4.22, 4.23 and 4.24).

Rose diagrams were plotted for the orientation of measured quartz veins (Figure 4.25, 4.26 and 4.27). Veins are usually formed when aqueous solution from within the rock, mobilized upwards by hydrothermal flow, precipitate mineral constituents in fractures. The orientation direction is majorly NE-SW and NNE-SSW, except for granite where occurrence of veins in the NW-SE direction are prominent. These again suggest that the quartz veins intrude into the rocks of the area pre- and post-Pan African.



Figure 4.21 Jointed pegmatites of Osogbo-Okinni area (Oba locality).

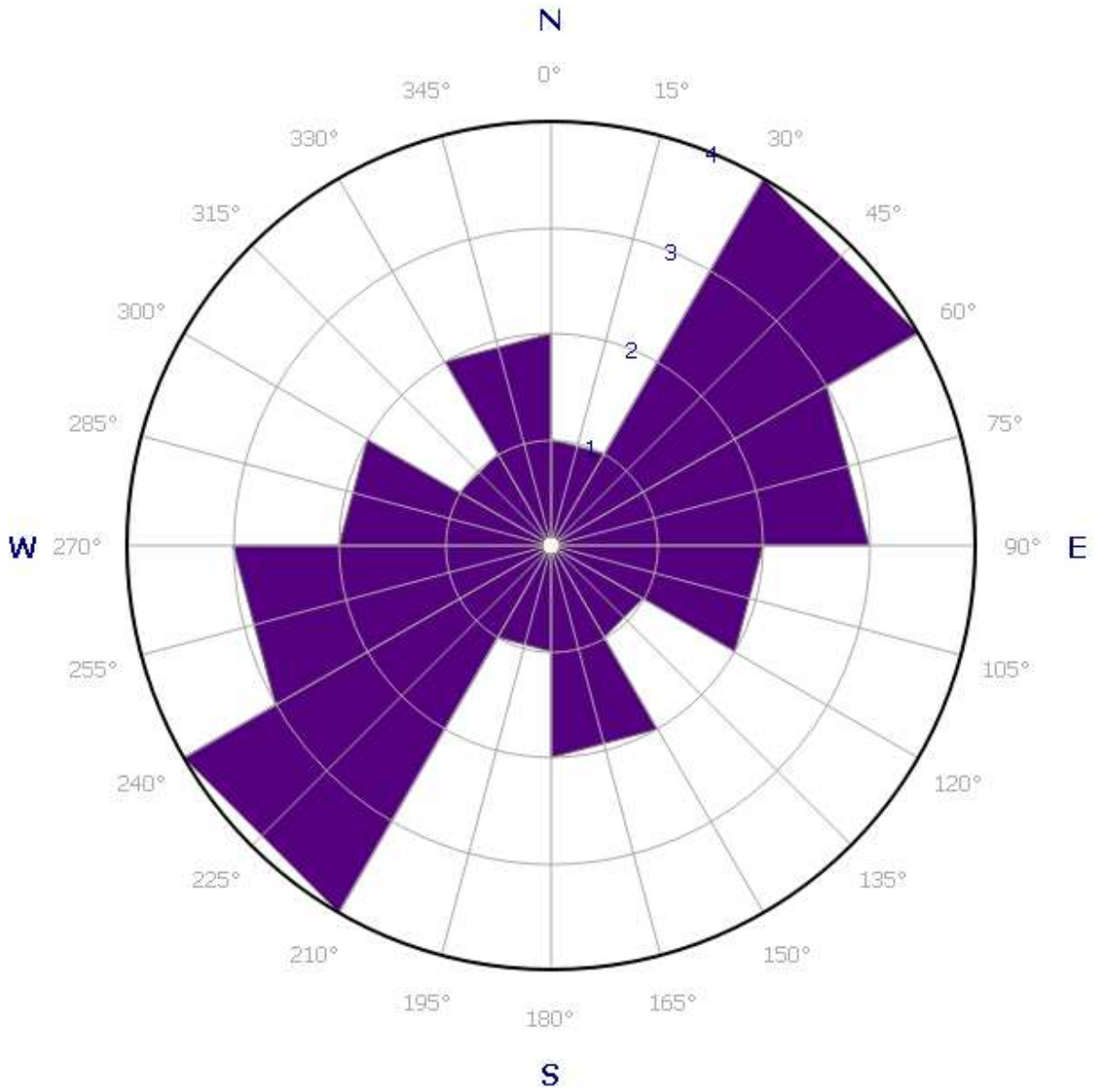


Figure 4.22 Rose diagram for the orientation of joints in granite gneiss of Osogbo-Okinni area

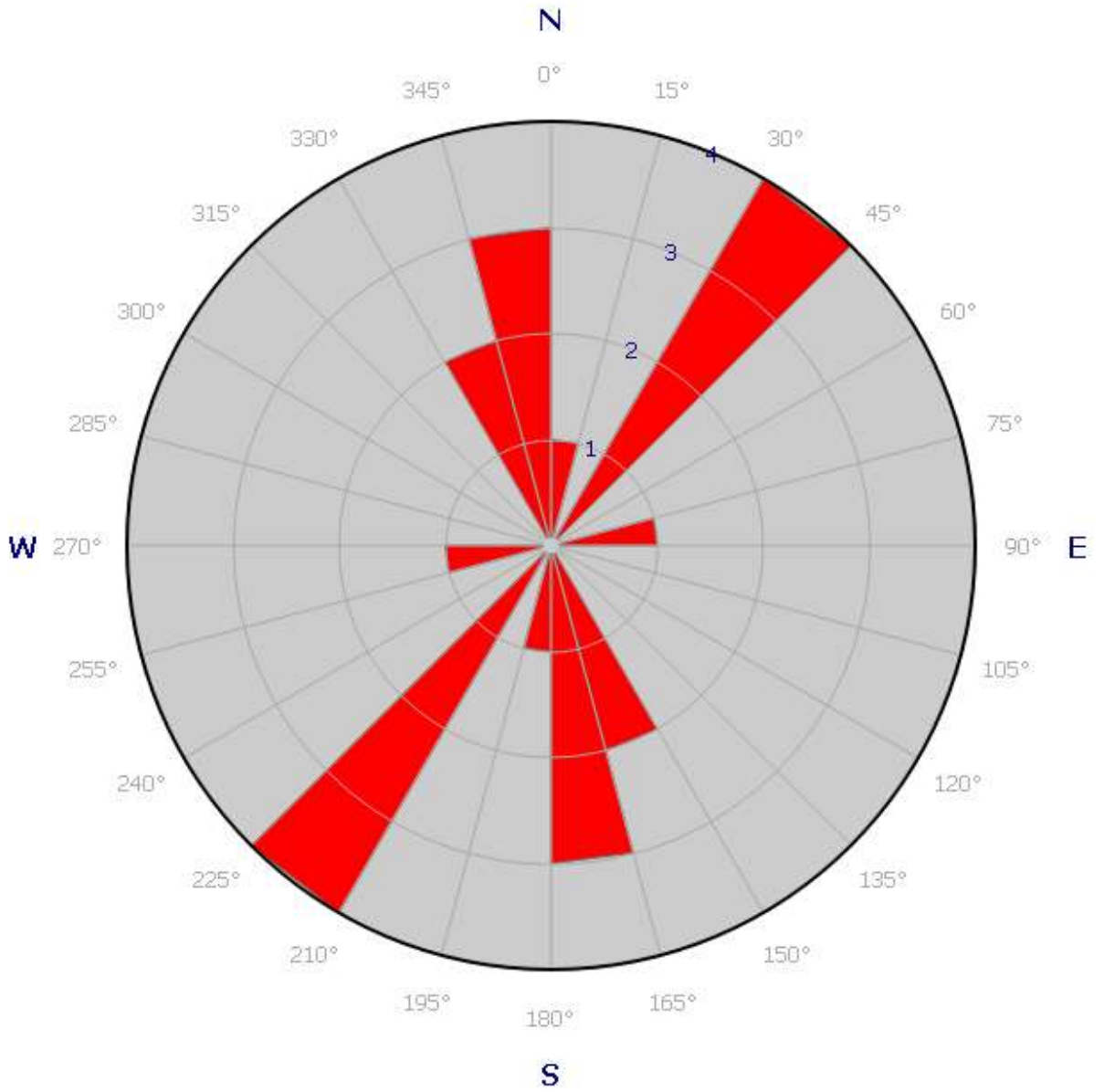


Figure 4.23 Rose diagram for the orientation of joints in granite of Osogbo-Okinni area

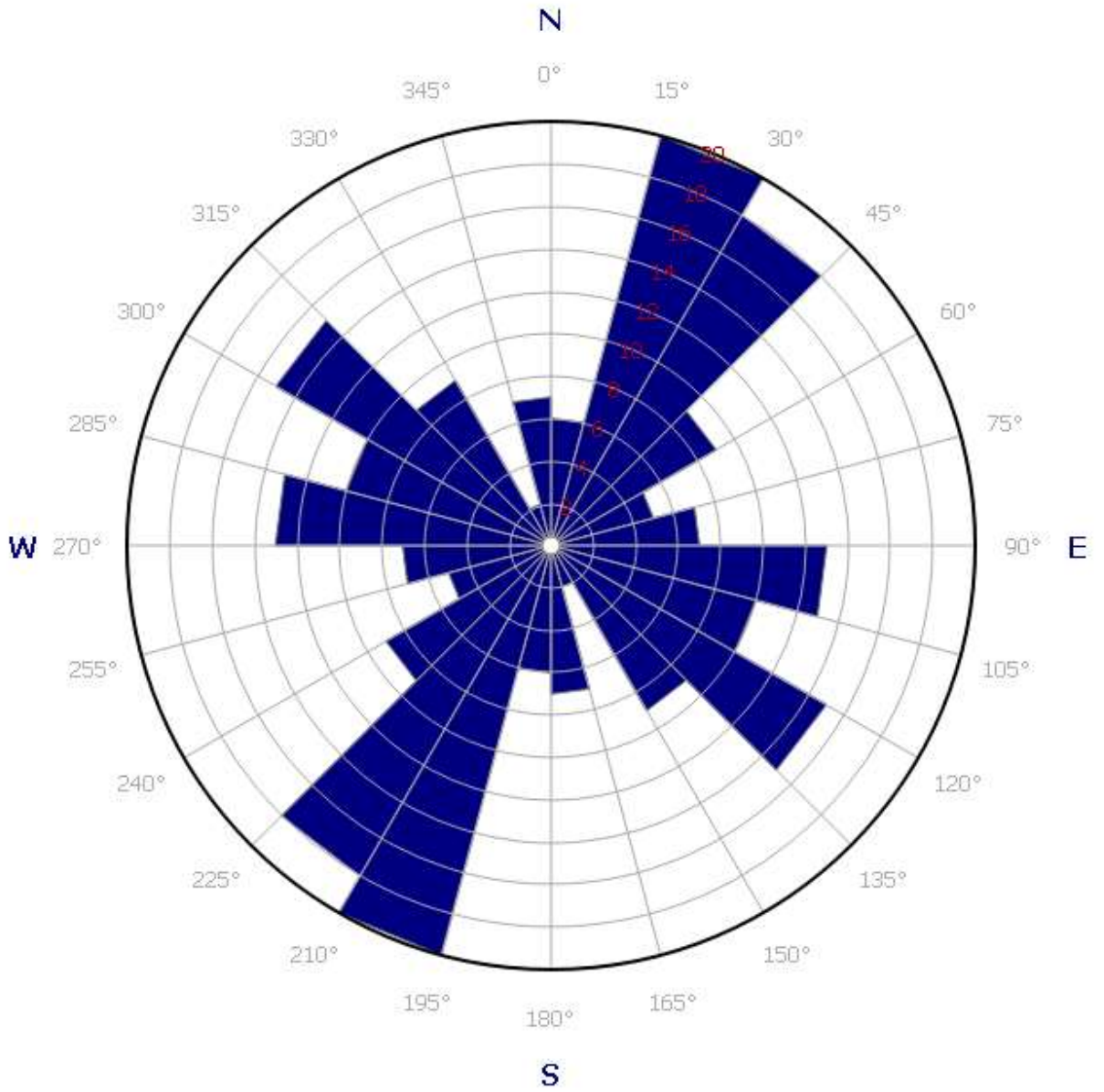


Figure 4.24 Rose diagram for the orientation of joints in pegmatite of Osogbo-Okinni area

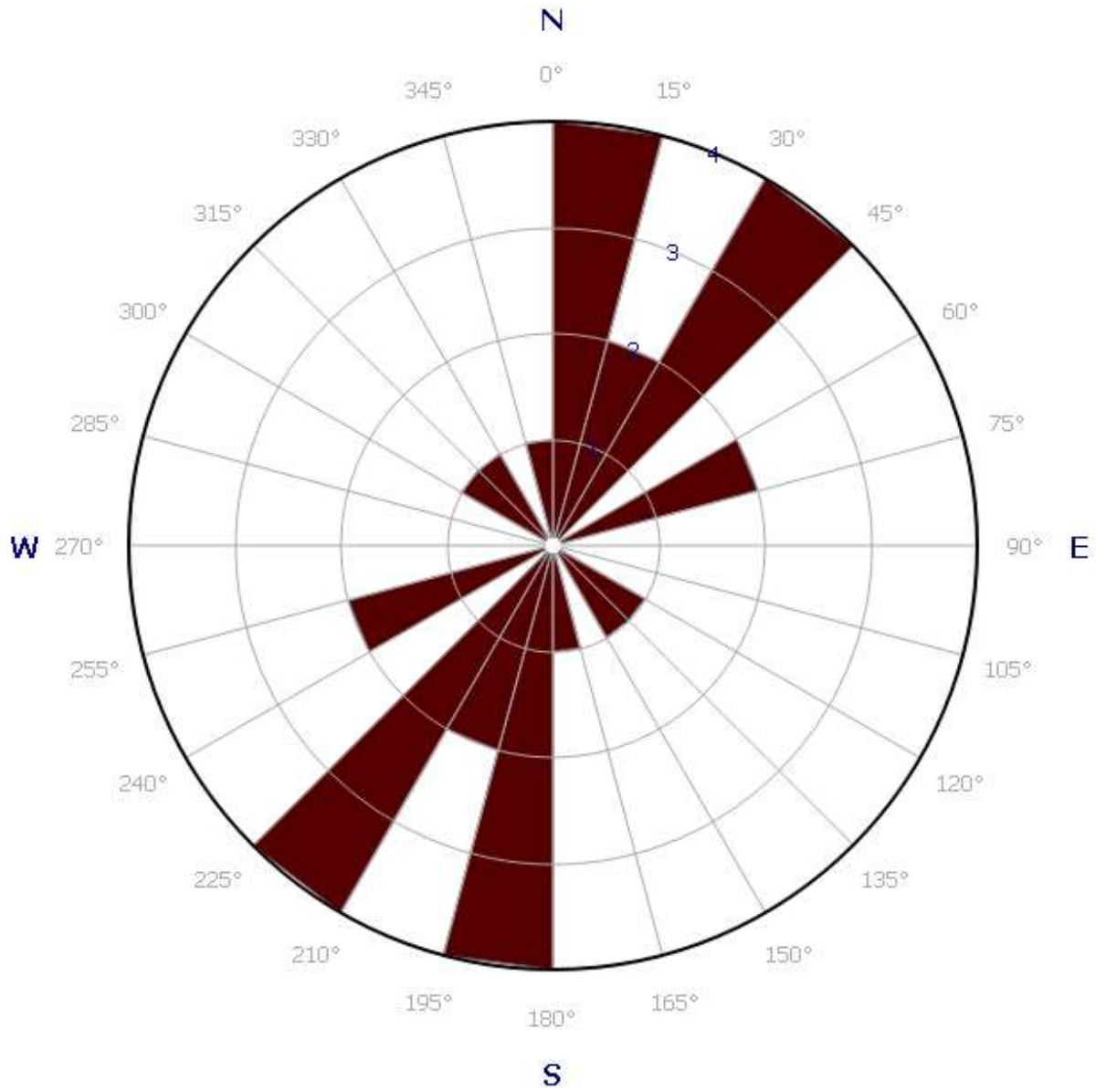


Figure 4.25 Rose diagram for the orientation of veins in granite gneiss of Osogbo-Okinni area

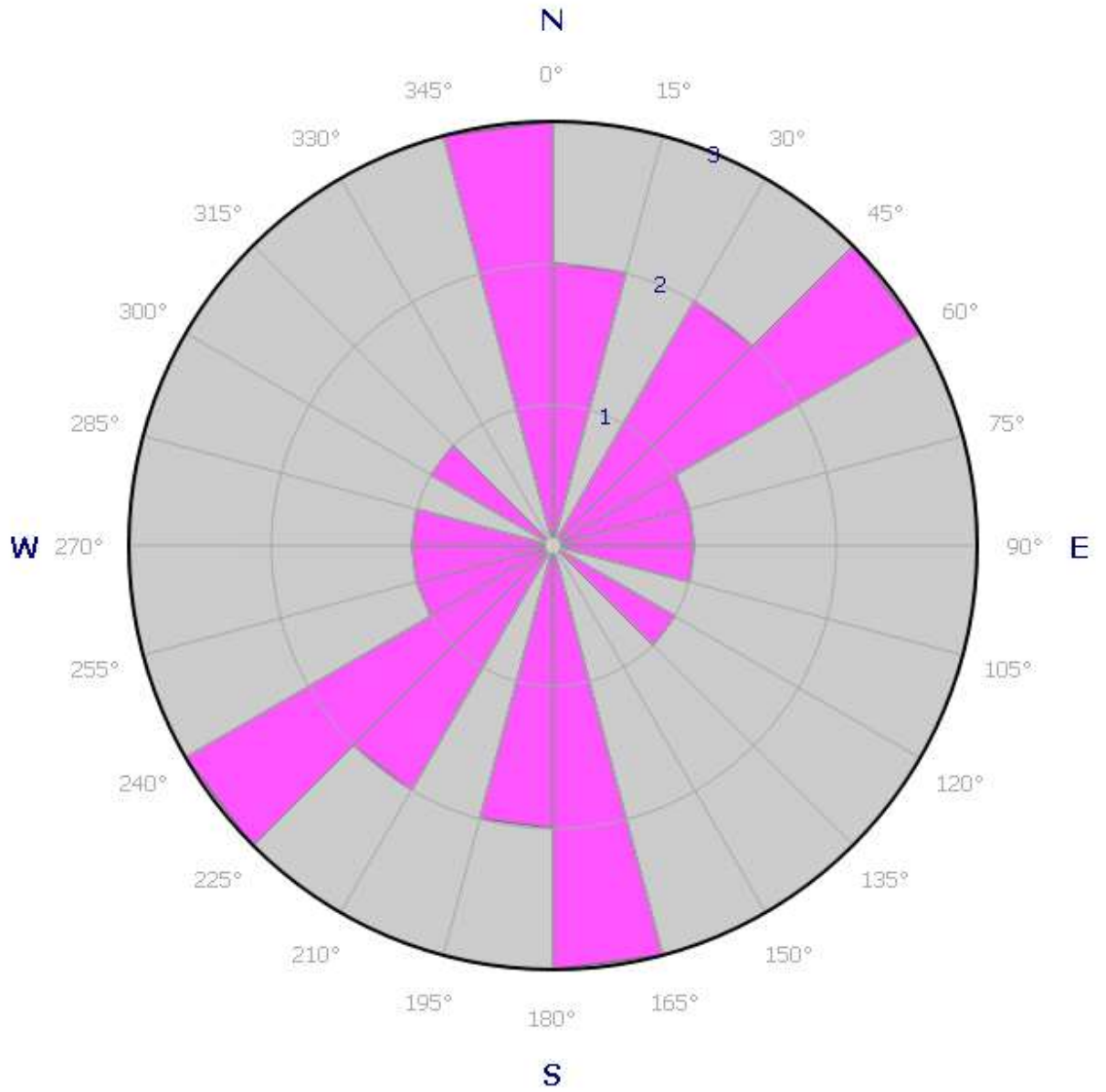


Figure 4.26 Rose diagram for the orientation of veins in granite of Osogbo-Okinni area

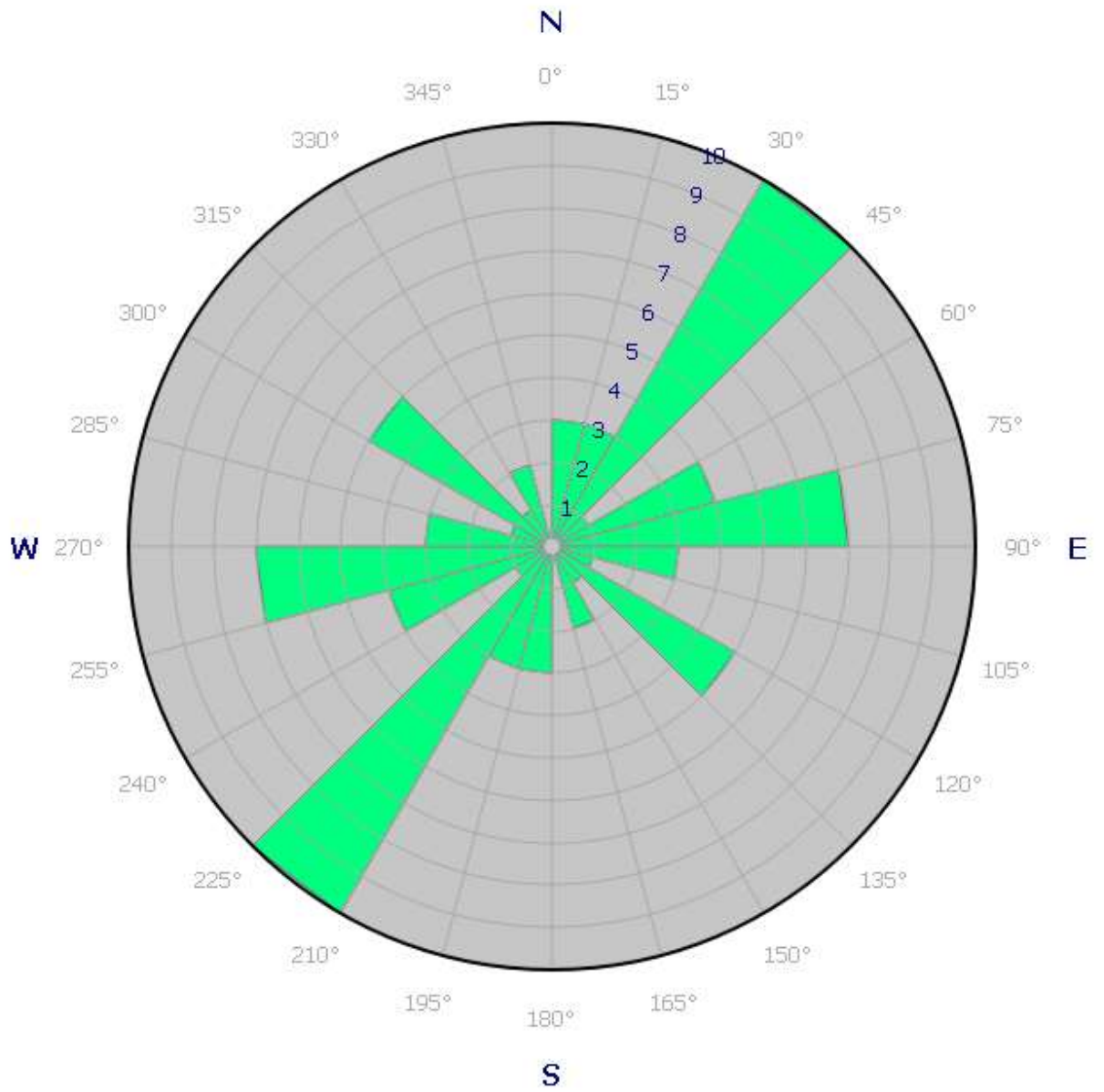


Figure 4.27 Rose diagram for the orientation of veins in pegmatites of Osogbo-Okinniarea

4.3 Geochemistry

4.3.1 Granite Gneiss

Geochemistry of major elements reveals the average composition of granite gneisses as follows; $\text{SiO}_2=69.11\%$, $\text{Al}_2\text{O}_3=14.82$, $\text{Fe}_2\text{O}_3=3.32$, $\text{MgO}=0.72$, $\text{CaO}=1.95$, $\text{Na}_2\text{O}=3.02$, $\text{K}_2\text{O}=4.35$, $\text{TiO}_2=0.32$, $\text{P}_2\text{O}_5=0.17$, $\text{MnO}=0.05$, (Table 4.3). The concentration of SiO_2 , Al_2O_3 , Na_2O and K_2O reflect an abundance of felsic silicates such as Quartz and feldspar compared to the low mafic content of Fe_2O_3 , MgO , MnO , CaO and P_2O_5 . The higher potash content of the gneisses compared to Na_2O , indicate the presence of microcline and biotite, both K-rich rock forming minerals, in the gneisses (Oyinloye, 2011). This property also characterizes granitic rocks of Archaean age, (Martin, 1986). The average aluminium saturation index (ASI) expressed as $(\text{Al}_2\text{O}_3/\text{Na}_2\text{O}+\text{K}_2\text{O}+\text{CaO})$ is 1.13 which indicates the presence of corundum in their norm since the ASI for each rock is greater than one, (Table 4.3). The $\text{MgO}/\text{Fe}_2\text{O}_3+\text{MgO}$ ratios vary between 0.17 and 0.19 with an average of 0.18. The pure primitive mantle has a higher value in the range of 0.68-0.75 and an average of 0.70, (Wilson, 1991). This implies that Mg and Fe were depleted in the melt from which the granite metamorphosed to gneiss crystallized as a result of fractionation of magma or the granitic protolith of the granite gneiss was a product of anatexis of local crust.

Granite gneisses are peraluminous (Figure 4.28) because of deficiency in alkalis content compared to alumina. The protolith of the gneisses are of igneous origin as shown in petrogenetic plot of $\text{Na}_2\text{O}/\text{Al}_2\text{O}_3$ against $\text{K}_2\text{O}/\text{Al}_2\text{O}_3$, (Figure 4.29). In the discriminant plot of $\text{P}_2\text{O}_5/\text{TiO}_2$ against MgO/CaO the gneisses fall in the orthogneisses field confirming their igneous origin (Figure 4.30). Lower values of Fe_2O_3 and MgO compared to the higher values of $\text{Na}_2\text{O}+\text{K}_2\text{O}$ places the gneisses in the Calc-Alkaline magma series as protolith which is confirmed by the AFM diagram, (Figure 4.31). The plot of K_2O versus SiO_2 further classify the protolith as high K Calc-Alkaline magma series (Figure 4.32).

Average Rb concentration of 207.8ppm is reflective of abundance of K-feldspar. Granite gneisses are enriched in Sr and Ba (117ppm and 905.75ppm respectively), (Table 4.4) probably because K is replaced in the K-feldspar by Ba and Ca is replaced by Sr

inplagioclase. Average Y content of 15.9ppm indicates the presence of amphibole which readily accommodates this element. Average Th concentration is 53.45ppm which is reflective of contribution from sedimentary sources to the protolith of this rock. The average contents of compatible elements Ni (6.55ppm), Cr (21.75), and Co (5.8ppm) are too low for rocks emanating from the primitive upper mantle, (Oyinloye, 2011).

The average total rare earth elements (REE) in granite gneiss is 337.71ppm of which the light rare earth elements (LREE) is 330.1ppm and the heavy rare earth elements (HREE) is 7.55ppm, (Table 4.5). The abundance of LREE reflects the presence of REE concentrating minerals like monazite and sphene, (Oyinloye, 2011).

Table 4.3 Major oxide composition of granite gneisses

Oxide Wt%	Granite Gneiss	Granite Gneiss	Granite Gneiss	Granite Gneiss	Average
SiO ₂	70.80	68.22	70.72	66.69	69.11
Al ₂ O ₃	14.07	14.35	13.98	16.87	14.82
Fe ₂ O ₃	3.40	3.91	3.38	2.57	3.32
MgO	0.78	0.79	0.79	0.53	0.72
CaO	2.14	2.17	2.08	1.40	1.95
Na ₂ O	2.97	2.75	2.94	3.40	3.02
K ₂ O	4.51	4.36	4.48	4.03	4.35
TiO ₂	0.36	0.32	0.36	0.24	0.32
P ₂ O ₆	0.20	0.13	0.19	0.17	0.17
MnO	0.04	0.06	0.04	0.04	0.05
LOI	0.5	2.9	0.8	2.6	1.59
ASI	1.03	1.09	1.04	1.35	1.13
MgO/Fe ₂ O ₃ +MgO	0.19	0.17	0.19	0.17	0.18

Table 4.4 Trace element concentration in granite gneisses

Elements Ppm	Granite Gneiss	Granite Gneiss	Granite Gneiss	Granite Gneiss	Average
Mo	0.68	0.62	0.66	0.56	0.63
Cu	11.5	10.8	10.3	10.5	10.78
Pb	21.88	21.58	23.69	36.23	25.85
Zn	23.8	26.6	21.5	32.3	26.05
Ni	6.8	6.4	6.9	6.1	6.55
Co	6.3	5.8	6.4	4.7	5.8
As	1.9	1.1	2.6	1.1	1.68
U	6.6	5.5	6.9	6.8	6.45
Th	56.8	42.1	67.6	47.3	53.45
Sr	220	127	215	146	177
Sb	0.22	0.18	0.26	0.17	0.21
Bi	0.08	0.52	0.09	0.52	0.30
V	52	32	54	34	43
Cr	19	24	24	20	21.75
Ba	1082	732	1066	743	905.75
W	33.2	200	35.6	200	117.2
Zr	82.2	77.3	94.0	71.6	81.28
Sn	3.6	8.3	3.6	35.6	12.78
Be	3	6	3	8	5
Sc	7	10	7.3	10	8.58
Y	17.5	15.2	17.8	13.1	15.9
Hf	2.36	2.67	2.57	3.46	2.77
Li	92.0	108.6	85.4	93.1	94.78
Rb	186.8	198.2	183.2	263.0	207.8
Ta	2.6	2.1	2.1	93.8	25.15

Nb	11.01	8.18	10.62	79.24	27.26
Cs	6.1	5.1	6.1	8.9	6.55
Ga	15.72	26.55	17.48	25.38	21.28
Se	0.4	0.5	0.3	0.3	0.38
Tl	0.92	2.45	0.93	1.36	1.42

Table 4.5. Rare Earth Elements composition of granite gneisses

Elements Ppm	Granite Gneiss	Granite Gneiss	Granite Gneiss	Granite Gneiss	Average
La	107.6	84.6	105.6	77.8	93.9
Ce	179.24	149.16	174.90	129.19	158.12
Pr	19.5	18.1	18.6	13.8	17.5
Nd	55.8	55.6	49.8	38.1	49.83
Sm	7.0	1.8	6.7	4.9	5.1
Eu	1.7	1.3	1.5	1.3	1.45
Gd	4.5	4.2	4.5	3.6	4.2
Tb	0.6	0.6	0.6	0.4	0.55
Dy	3.2	2.8	3.4	2.5	2.98
Ho	0.6	0.6	0.7	0.5	0.6
Er	1.6	1.4	1.9	1.2	1.53
Tm	0.2	-	0.3	0.2	0.18
Yb	1.5	1.6	1.8	1.2	1.28
Lu	0.2	0.1	0.3	0.2	0.2
Eu/Eu*	0.87	1.41	0.79	0.91	1
(La/Yb) _n	43.47	32.05	35.55	39.29	37.59
(La/Sm) _n	8.43	25.78	8.64	8.71	12.89
(Tb/Yb) _n	1.70	1.60	1.42	1.42	1.54
∑REE	383.24	322.09	370.6	274.89	337.71
∑LREE	375.34	314.76	361.6	268.69	330.1
∑HREE	7.9	7.1	9	6.2	7.55

Table 4.6. Ratios and sums of selected major element oxides and trace elements of granite gneisses

Ratio and sums	Granite Gneiss	Granite gneiss	Granite Gneiss	Granite Gneiss	Average
Rb/Sr	0.85	1.56	0.85	1.80	1.27
Nb+Y	28.51	23.38	28.42	92.34	43.16
N+K	7.48	7.11	7.42	7.43	7.36
C+N+K	9.62	7.28	9.5	8.83	8.81
A/N+K	1.88	2.02	1.88	2.27	2.01
A/C+N+K	1.46	1.55	1.47	1.91	1.60
N/A	0.21	0.19	0.21	0.20	0.20
K/A	0.32	0.30	0.32	0.24	0.30
P ₂ O ₅ /TiO ₂	0.55	0.41	0.53	0.71	0.55
MgO/CaO	0.36	0.36	0.38	0.38	0.37
Fe ₂ O ₃ /MgO	4.36	4.95	4.28	4.85	4.61
Zr+Nb+Y	110.71	100.68	122.42	163.94	124.44
Rb/Zr	2.27	2.56	1.95	3.67	2.61

A=Al₂O₃, C=CaO, N=Na₂O, K=K₂O.

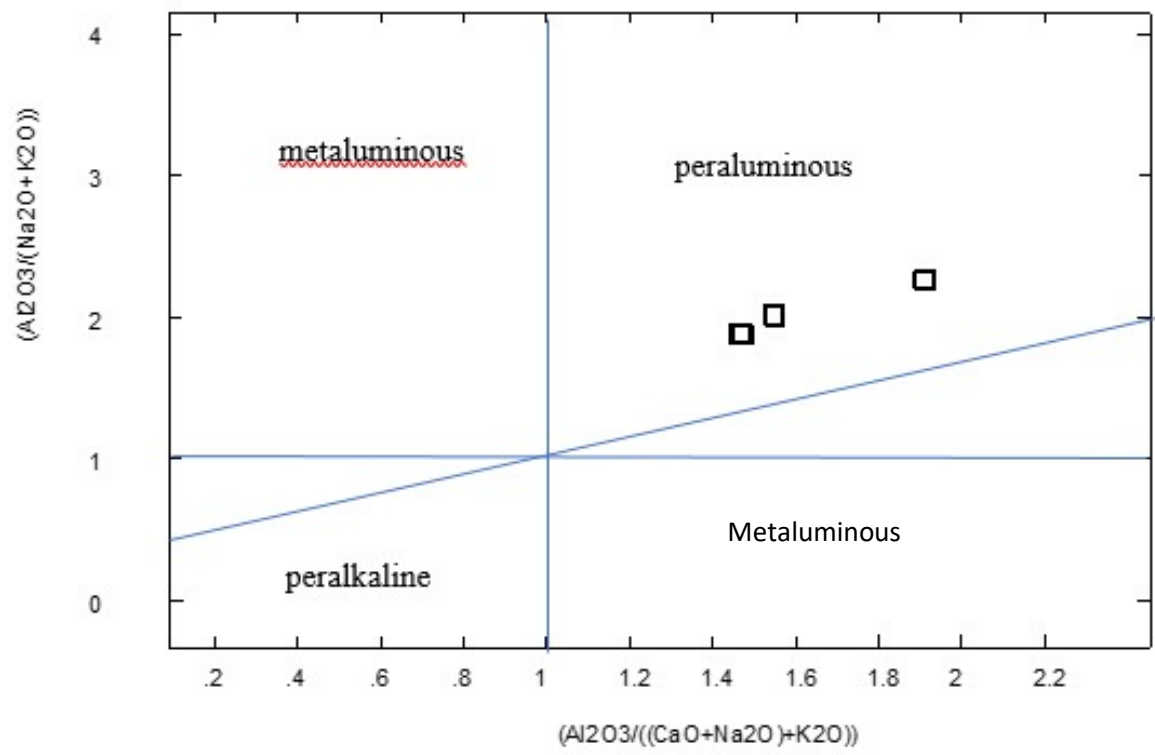


Figure 4.28. Plot of $Al_2O_3/((CaO+Na_2O)+K_2O)$ v $Al_2O_3/(Na_2O+K_2O)$ (after Shand, 1943).

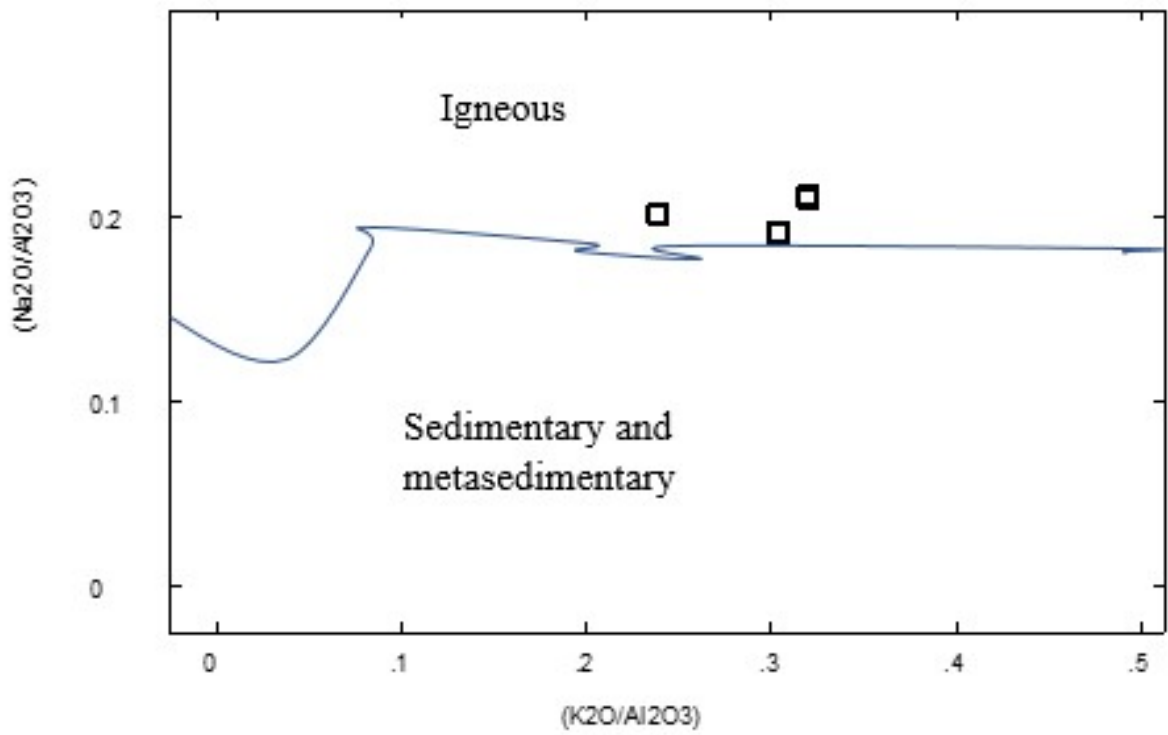


Figure 4.29. Plot of $\text{Na}_2\text{O}/\text{Al}_2\text{O}_3$ vs $\text{K}_2\text{O}/\text{Al}_2\text{O}_3$ (after Garrels and Mackenzie, 1971).

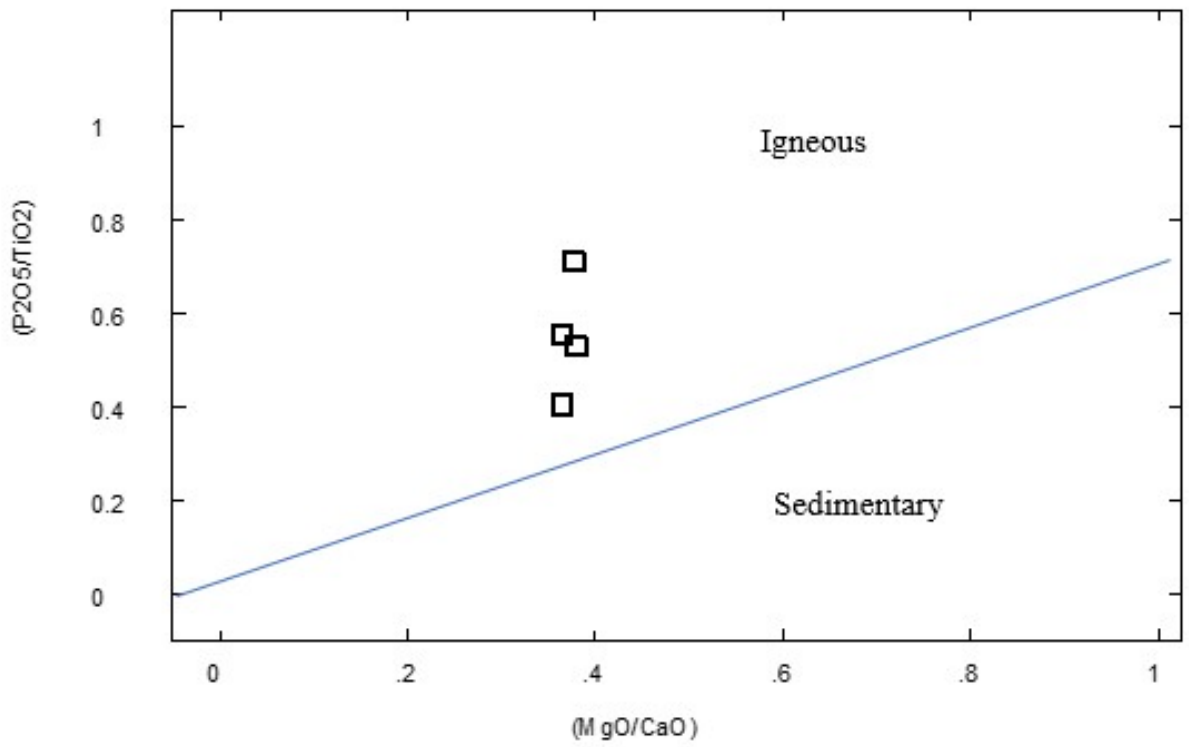


Figure 4.30 Plot of P_2O_5/TiO_2 vs MgO/CaO (after Werner, 1987).

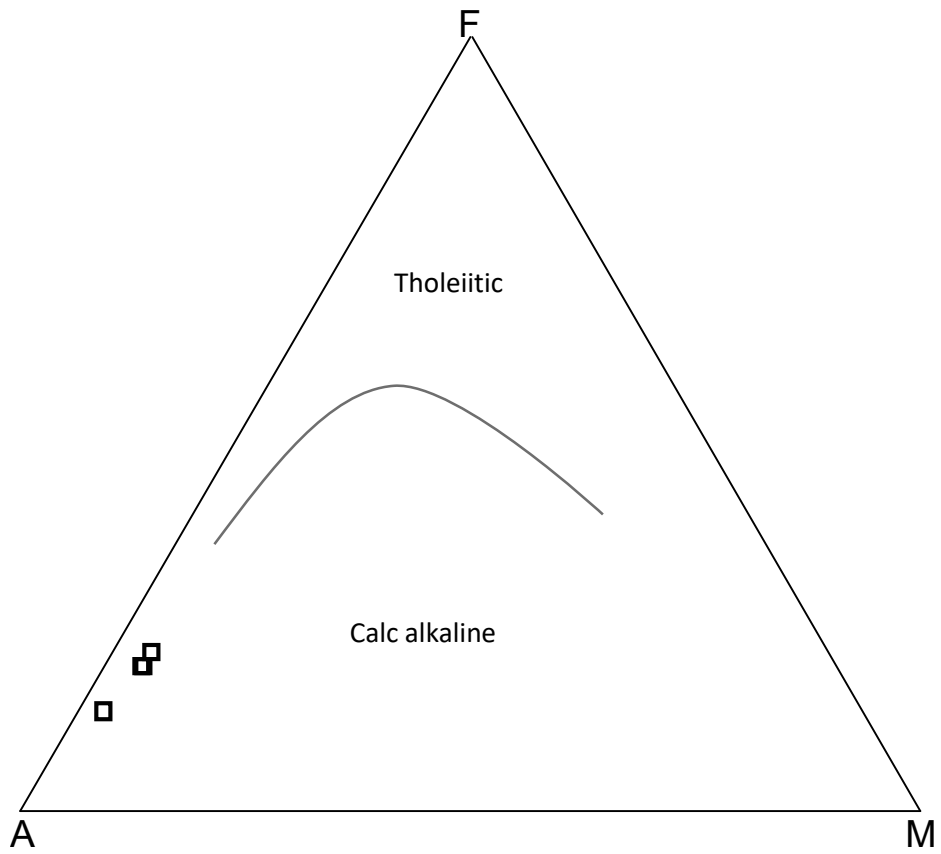


Figure 4.31. AFM ternary plot for granite gneiss, (after Irvine and Baragar, 1971).

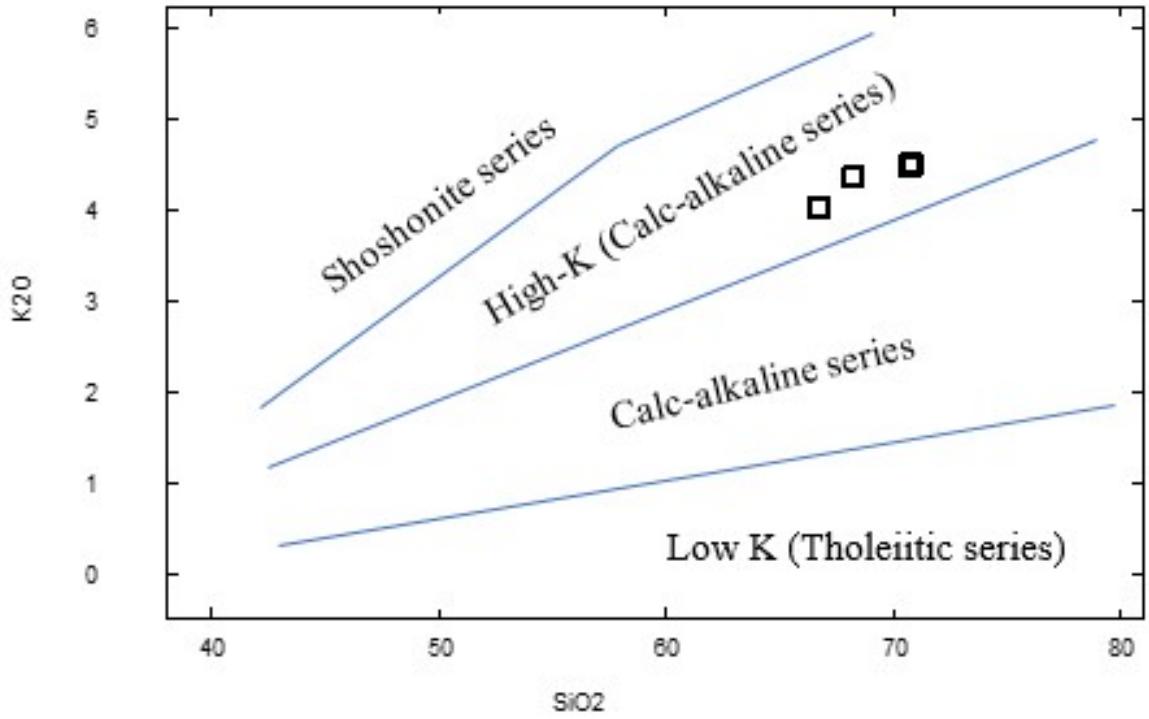


Figure 4.32. Plot of K_2O vs SiO_2 , (after Peccerillo and Taylor, 1976).

Granite gneisses are enriched in Ba, W, Be, Rb, Cs, Sr and Ga compared to average crustal values for trace elements, but are depleted in Y, Zr, and Ni (Table 4.4). The enrichment of these gneisses in Ba, Rb and Sr which are large ion lithophile elements is because they cannot partition into the mantle phase minerals like orthopyroxene and olivine due to their sizes, thus they are concentrated in the igneous melt that produces the parent gneisses (Elatikpo et al., 2013).

The gneisses plot on the fractionated I-type and I-type fields, (Figures.4.33). The High Field Strength Elements (Y+Nb+Zr+Ce) used in this method are not sensitive to low and medium degrees of alteration, (Pearce and Cann, 1973).

In tectonic discrimination diagram Rb vs Nb+Y, granite gneisses plot in the within plate granite field and the volcanic arc granite field, (Figure. 4.34), while in the Nb vs Y plot, the gneisses plot in the volcanic arc granite+syn collisional granite field in the within plate granite field, (Figure 4.35). Trace element data, (Table 4.4) reveals enrichment in large ion lithophile elements, which are usually characteristic of magmas resulting from the mantle modified by subduction component and is typical of volcanic arc environment. Enrichment in Rb and depletion in heavy rare earth elements like Y, Zr and Hf giving a high ratio of Rb/Zr, (Table 4.6) is characteristic of syn-tectonic environment, (Harris et al., 1986).

The chondrite-normalized rare earth elements (REE) patterns show smooth, concave upward shape with enriched LREE and depleted flat HREE for the gneisses, (Figure 4.36). Primitive mantle normalized plot for granite gneiss indicates negative anomaly for Ba, Nb, Sr, and Ti and positive anomaly for Ta and Pb, (Figure 4.37).

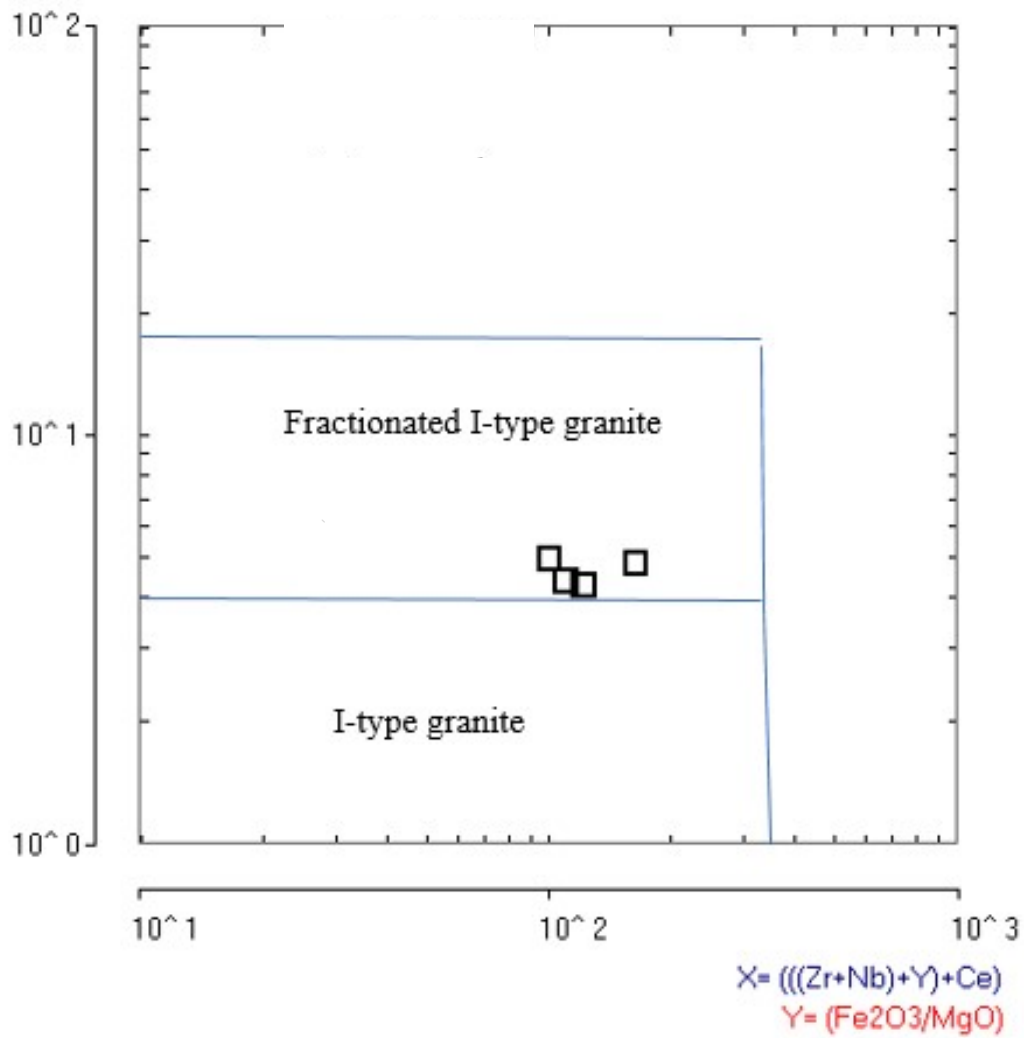


Figure 4.33 Classification plot of Fe_2O_3/MgO vs $(Zr+Nb+Y+Ce)$ for granite gneiss, (after Whalen et al., 1987).

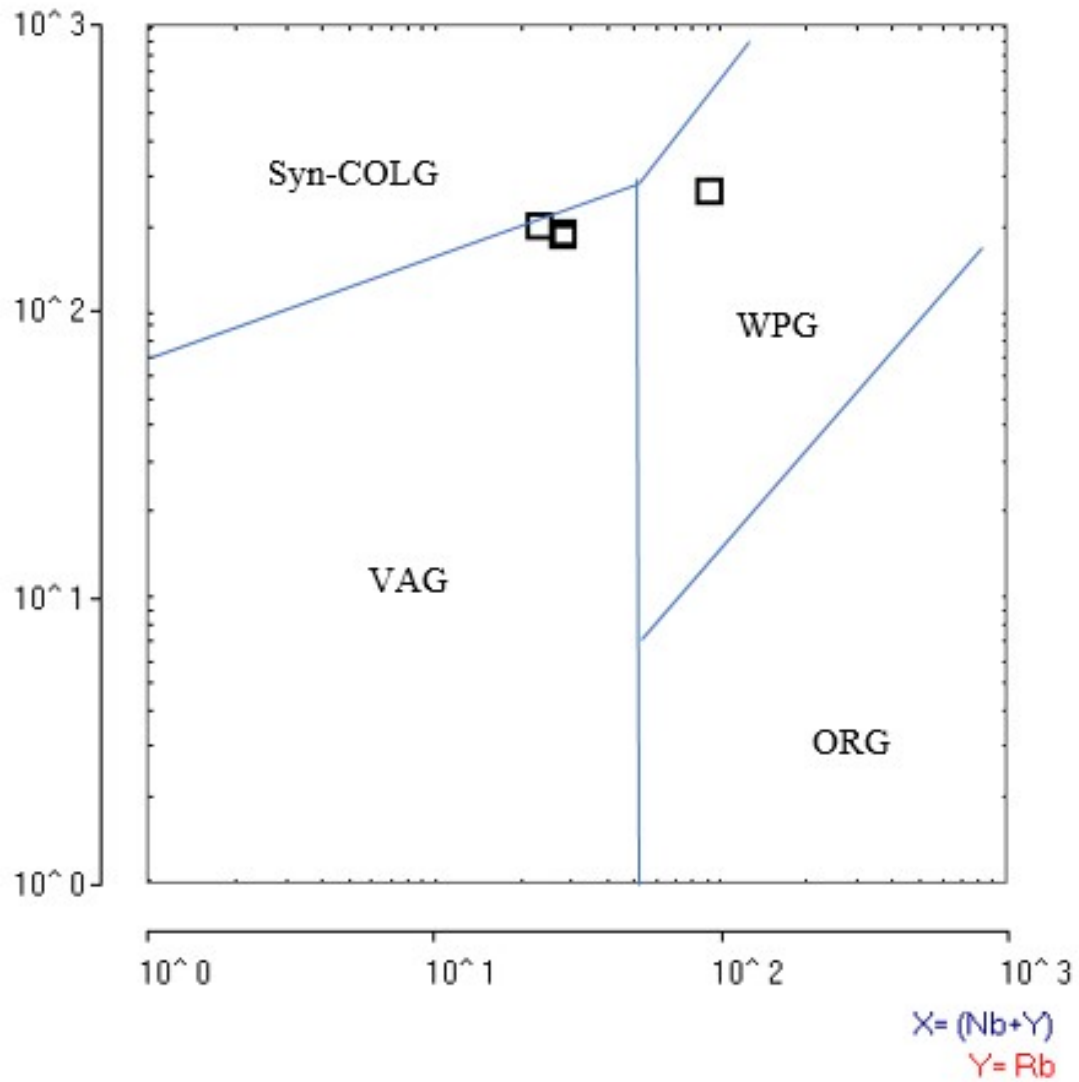


Figure 4.34 Plot of Rb vs Nb+Y tectonic discrimination diagram for granite gneiss.

WPG = Within Plate Granite, ORG = Ocean Ridge Granite, VAG = Volcanic Arc Granite, Syn-COLG = Syn Collisional Granite, (after Pearce et al., 1984).

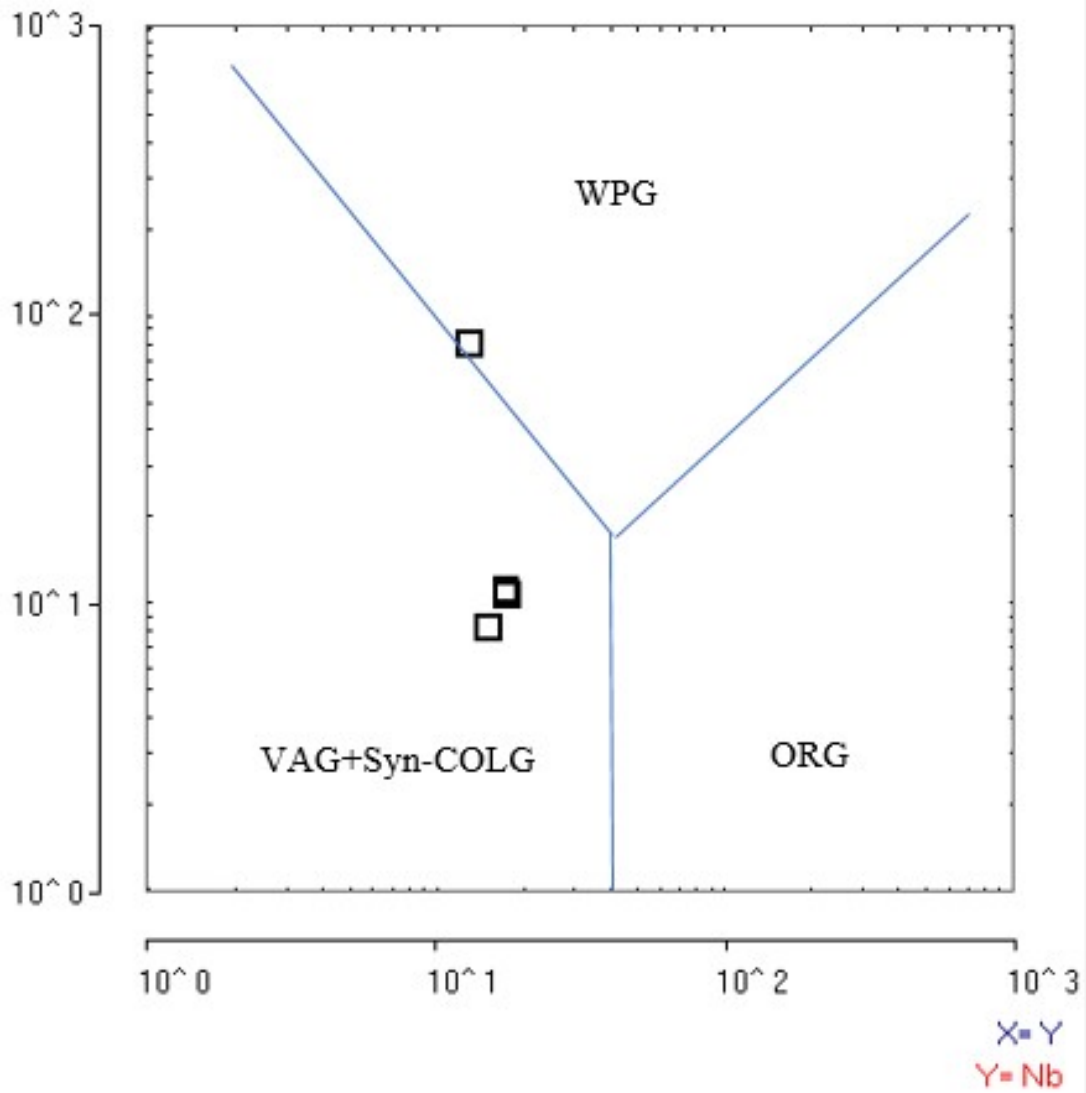


Figure 4.35 Y vs Nb Tectonic discrimination diagram for granite gneiss

WPG =Within Plate Granite, ORG=Ocean Ridge Granite, VAG= Volcanic Arc Granite, Syn-COLG= Syn Collisional Granite. (after Pearce et al., 1984.)

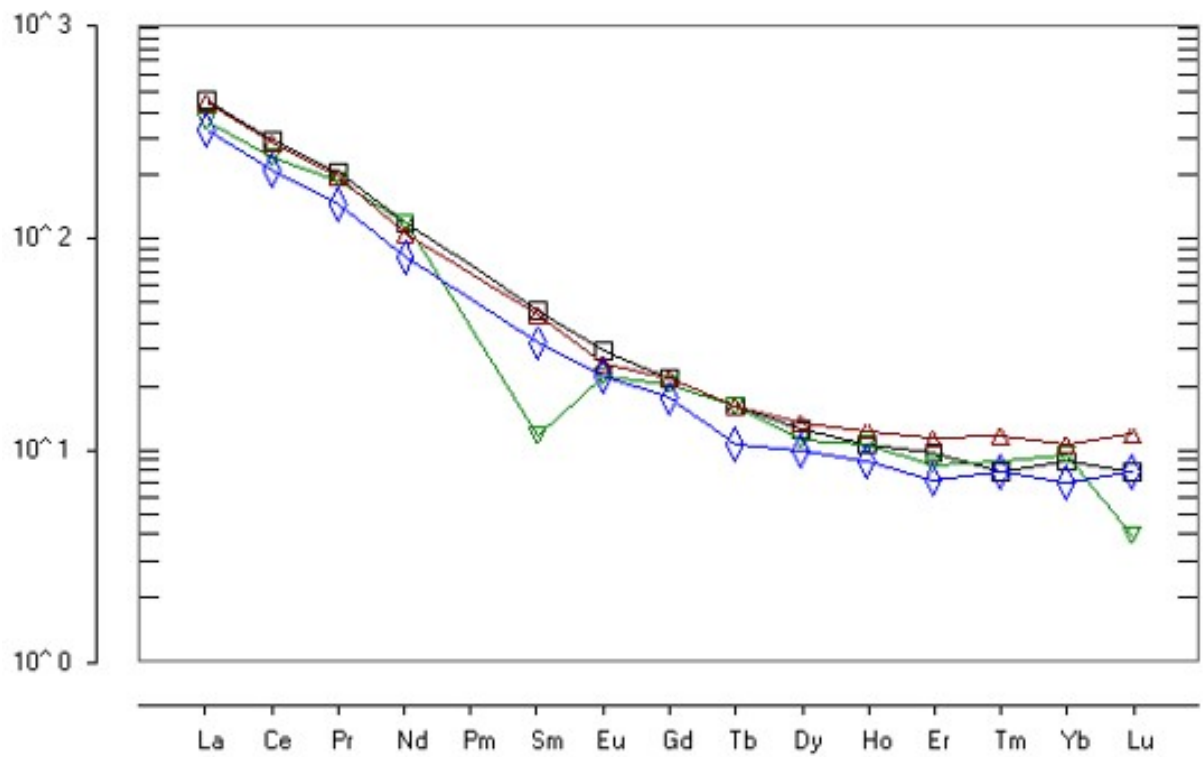


Figure 4.36 Chondrite normalized plot for granite gneiss, (chondrite values after Sun and McDonough, 1989).

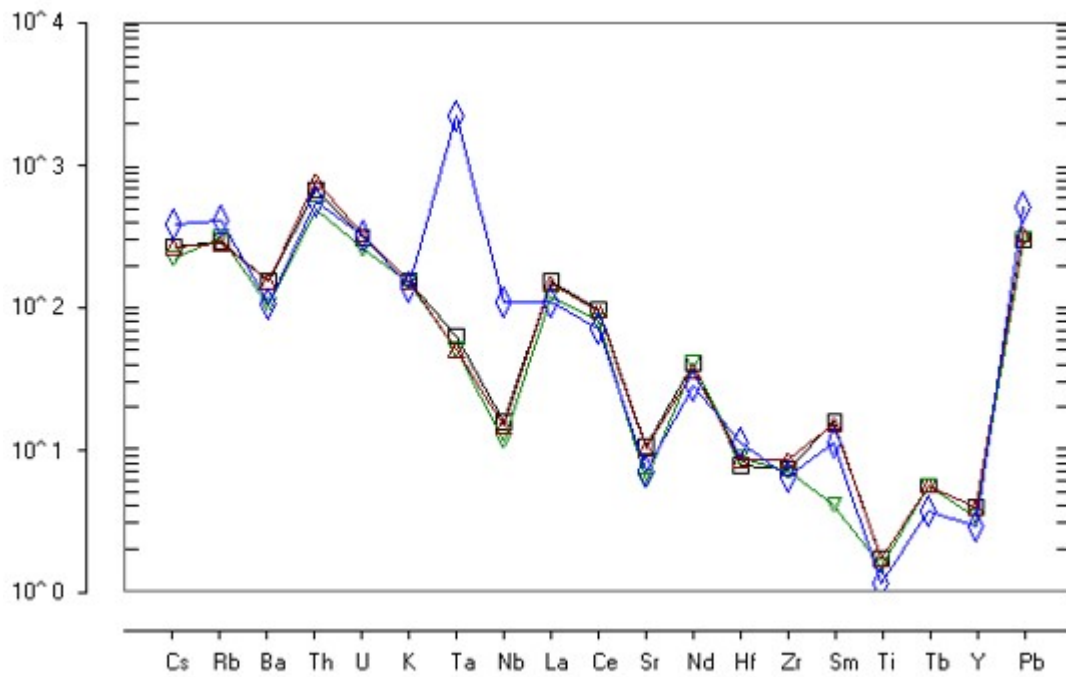


Figure 4.37 Primitive mantle-normalized plot for granite gneiss, (after McDonough et al., 1992)

4.3.2 Granites

Granitic rocks have been construed to be partial melts of crustal rocks derived from sedimentary or igneous origin, or as the outcome of basaltic melts interacting with crustal rocks (Collins, 1996). The granites of Osogbo-Okinni area are characterised by high SiO_2 content which ranges from 70.76 to 74.18% with an average of 72.04%, Al_2O_3 13.18-14.20%, 13.82%; Fe_2O_3 2.55-3.40%, 3.03%; MgO 0.46-0.78%, 0.61%; CaO 1.29-2.10%, 1.65%; Na_2O 2.98-3.65%, 3.28%; K_2O 3.30-4.54%, 3.98%; TiO_2 0.21-0.36%, 0.27%; P_2O_5 0.18-0.21%, 0.19%; MnO 0.01-0.04%, 0.02%, (Table 4.7). The Harker plot of major element abundances show a good linear trend for most of the oxides. The arrows in the plot indicate the increase or otherwise of the oxide concentration during fractional differentiation of the melt considering that SiO_2 concentration increases with differentiation of the melt (Figure 4.38).

The protolith of granites of Osogbo-Okinni area is of igneous origin revealed in the discriminate plot of $\text{Na}_2\text{O}/\text{Al}_2\text{O}_3$ vs $\text{K}_2\text{O}/\text{Al}_2\text{O}_3$, (Figure 4.39). The AFM diagram indicates their calc-alkaline nature, (Figure 4.40) and because of its high potassic nature the granite is classified as High calc alkaline in the plot of K_2O vs SiO_2 , (Figure 4.41). The granites also plot in the sub-alkali field of plot of total alkali vs silica (Figure 4.42).

The granite nomenclature of these rocks is confirmed in the total alkali versus silica diagram, showing the rocks plotting in the fields of granite and granodiorite (Figure 4.43). These granites are peraluminous with aluminium saturation index (ASI) greater than 1.1 (Table 4.7). Generally, peraluminous granites are formed by the melting of metasediments, however, new experimental evidence indicates the formation of peraluminous felsic magma by extended fractionation of mantle derived melt. Also, in altered rocks, peraluminosity can artificially increase because of the easy lixiviation of alkalis, with aluminium remaining fixed in the altered minerals (London, 2008).

Table 4.7 Major oxide composition of granite

Oxide Wt%	1	2	3	4	Average N=4
SiO ₂	70.76	74.18	72.16	71.04	72.04
Al ₂ O ₃	14.10	13.18	13.80	14.20	13.82
Fe ₂ O ₃	3.40	2.55	3.16	3.00	3.03
MgO	0.78	0.46	0.55	0.66	0.61
CaO	2.10	1.29	1.86	1.35	1.65
Na ₂ O	2.98	3.65	3.46	3.04	3.28
K ₂ O	4.54	3.30	3.96	4.12	3.98
TiO ₂	0.36	0.21	0.27	0.22	0.27
P ₂ O ₅	0.18	0.21	0.18	0.19	0.19
MnO	0.04	0.02	0.02	0.01	0.02
LOI	0.5	0.8	0.6	0.5	0.6
ASI	1.47	1.60	1.49	1.67	1.56

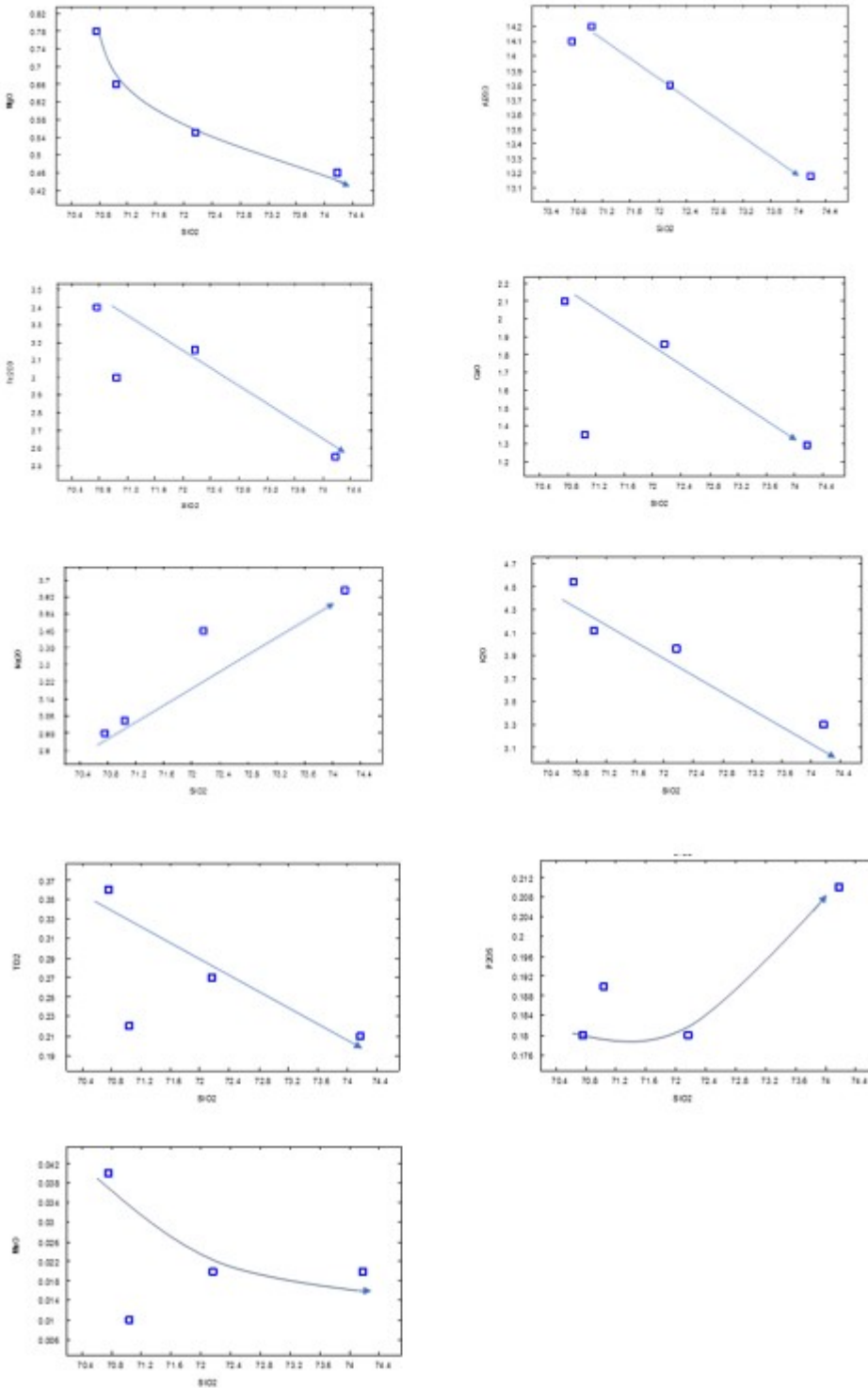


Figure 4.38 Harker diagrams for granite of Osogbo-Okinni area, (arrow shows increasing fractional differentiation).

Table 4.8. Trace elements in granites

Elements Ppm	1	2	3	4	Average N=4
Mo	0.80	0.82	0.78	0.81	0.80
Cu	10.1	10.3	8.2	10.2	9.70
Pb	26.30	20.02	27.10	26.60	25
Zn	21.1	32.3	20.1	28.4	25.48
Ag	28	<20	22	<20	22.50
Ni	7.4	4.9	6.6	4.7	5.9
Co	6.7	3.5	5.8	4.7	5.18
As	1.6	1.3	1.6	1.2	1.43
U	7.1	5.2	7.6	5.4	6.33
Th	63.3	37.8	60.4	46.9	52.1
Sr	221	114	220	112	166.75
Sb	0.24	0.28	0.26	0.28	0.27
Bi	0.08	4.14	0.06	3.15	1.86
V	55	27	46	29	39.25
Cr	22	13	20	16	17.75
Ba	1194	581	1048	795	904.5
W	37.6	66.9	36.4	56.5	49.35
Zr	69.1	39.0	66.7	39.8	53.65
Sn	3.9	5.7	3.9	4.5	4.5
Be	3	3	3	2	2.75
Sc	7.1	4.7	6.8	4.9	5.88
Y	18.0	12.0	16.0	13.0	14.75
Hf	2.03	1.23	1.68	1.45	1.60
Li	93.3	65.0	85.6	65.0	77.23
Rb	198.1	181.6	201.4	188.2	192.33

Ta	2.5	2.7	2.5	2.5	2.55
Nb	10.27	18.62	12.35	14.22	13.87
Cs	6.8	4.4	4.8	6.2	5.55
Ga	16.88	17.02	15.96	17.00	16.72
Se	0.5	0.6	0.5	0.5	0.53
Tl	1.00	0.88	0.86	0.94	0.92
Rb/Sr	0.90	1.60	0.92	1.68	1.15
Ba/Rb	6.03	3.20	5.20	4.22	4.70

Table 4.9. Rare earth elements composition of granite

Elements Ppm	1	2	3	4	Average N=4
La	117.0	63.3	104.2	73.5	89.5
Ce	184.41	105.60	182.44	115.70	147.04
Pr	20.9	10.6	24.3	11.6	16.85
Nd	56.4	28.3	50.4	31.6	41.68
Sm	7.3	4.4	7.2	5.4	6.08
Eu	1.7	0.9	1.6	0.7	1.23
Gd	4.1	2.5	3.6	2.7	3.23
Tb	0.6	0.3	0.6	0.4	0.48
Dy	3.3	1.8	3.1	2.0	2.55
Ho	0.7	0.4	0.9	0.4	0.6
Er	1.6	1.0	1.7	1.1	1.35
Tm	0.3	0.2	0.3	0.3	0.28
Yb	1.7	1.1	1.6	1.3	1.43
Lu	0.3	0.1	0.3	0.3	0.25
Σ REE	400.31	220.5	382.24	247	312.55
Σ LREE	391.81	215.6	373.74	241.2	305.61
Σ HREE	8.5	4.9	8.5	5.8	6.94
LREE/HREE	46.10	44	43.97	41.59	44.04
(La/Yb)N	68.82	57.54	65.13	56.54	62.59

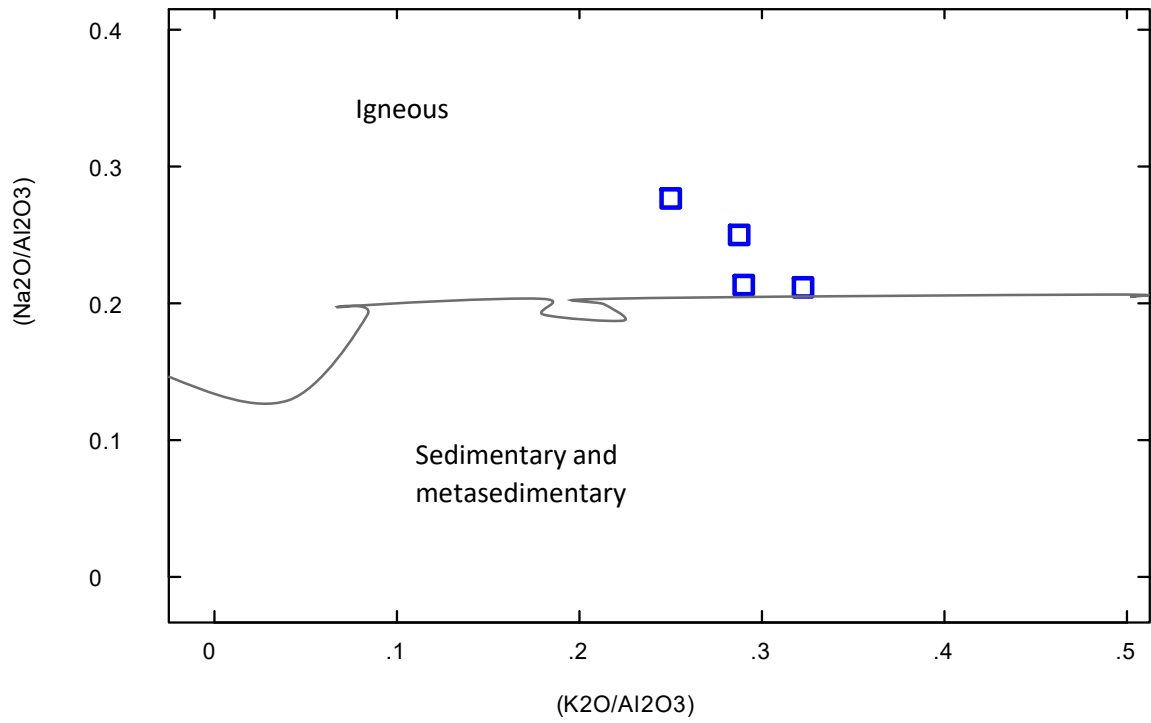


Figure 4.39 Plot of $\text{Na}_2\text{O}/\text{Al}_2\text{O}_3$ vs $\text{K}_2\text{O}/\text{Al}_2\text{O}_3$ (after Garrels and MacKenzie, 1971).

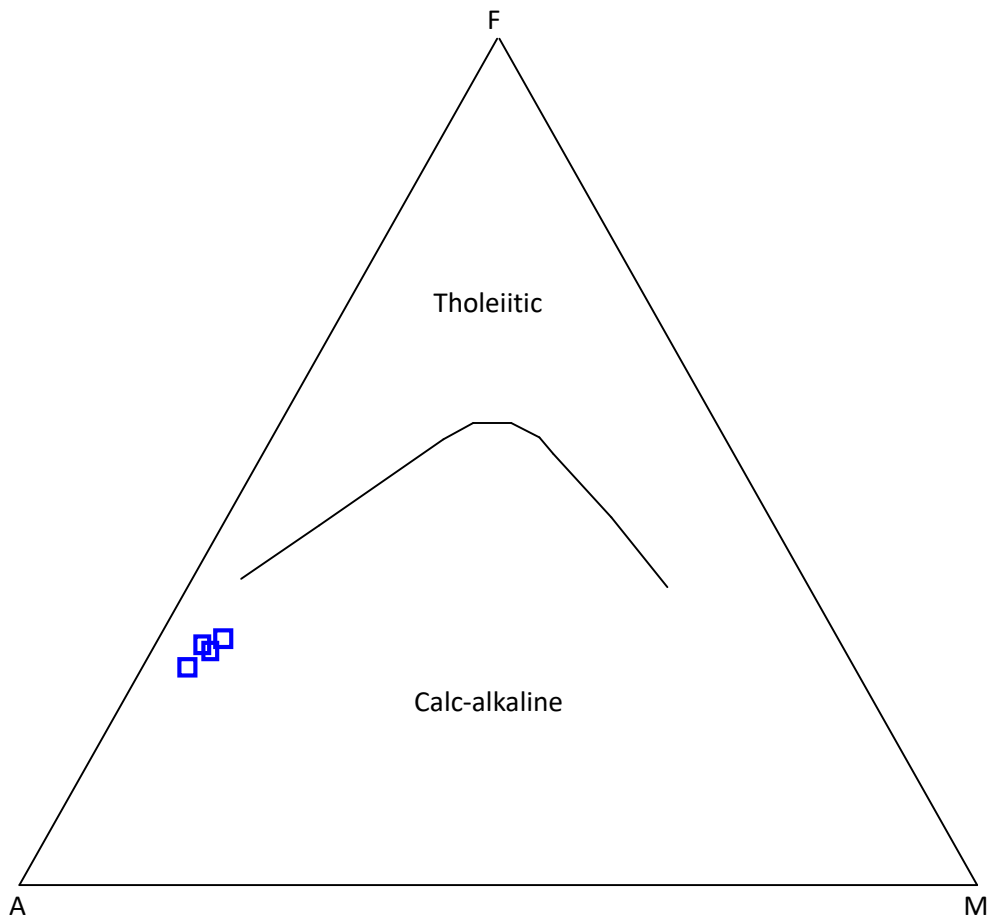


Figure 4.40 AFM diagram for granite of Osogbo-Okinni area, (after Irvine and Baraga, 1971).

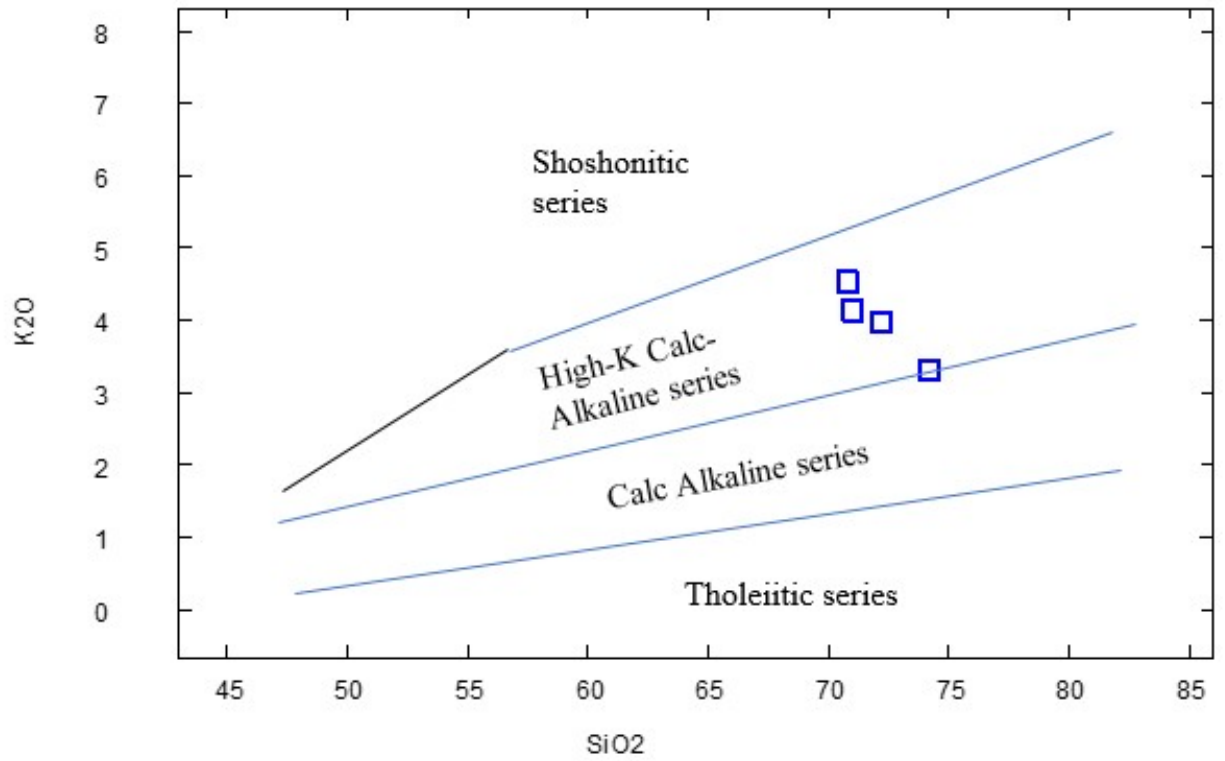


Figure 4.41. Plot of K_2O vs SiO_2 for granite of Osogbo-Okinni area, (after Le Maitre et al., 1989).

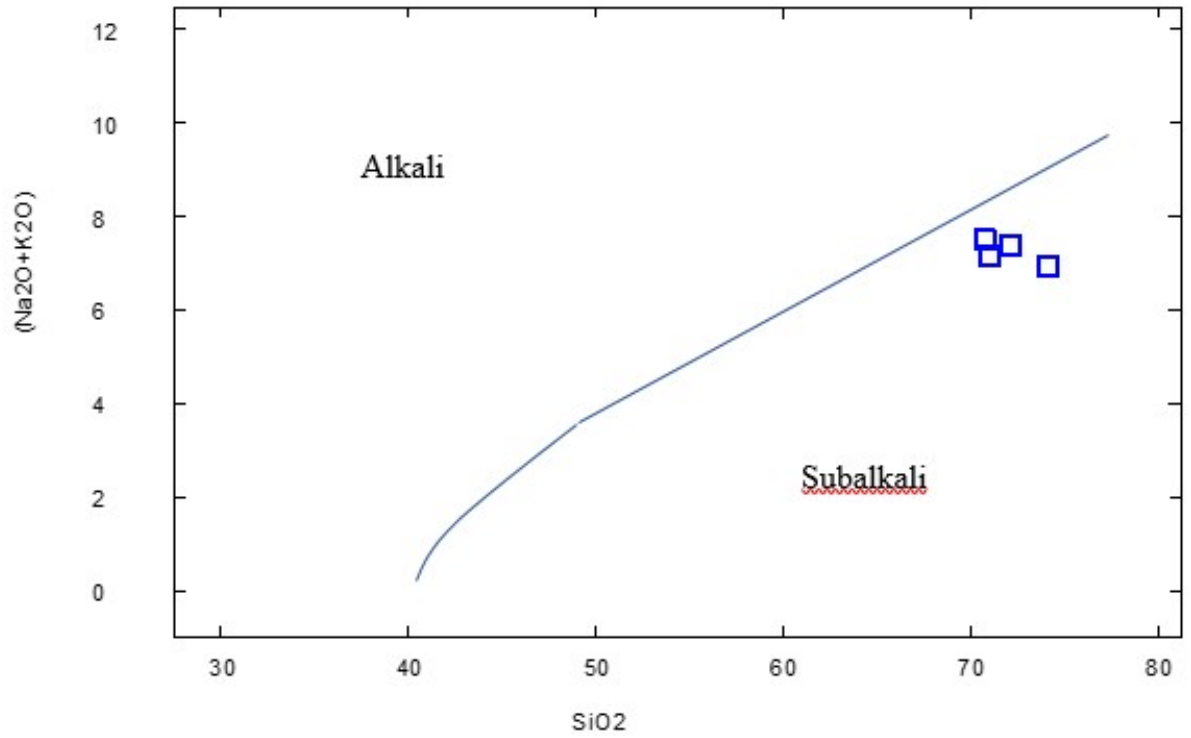


Figure 4.42 Plot of total alkali vs silica for granites of Osogbo-Okinni area, (after Cox et al., 1979)

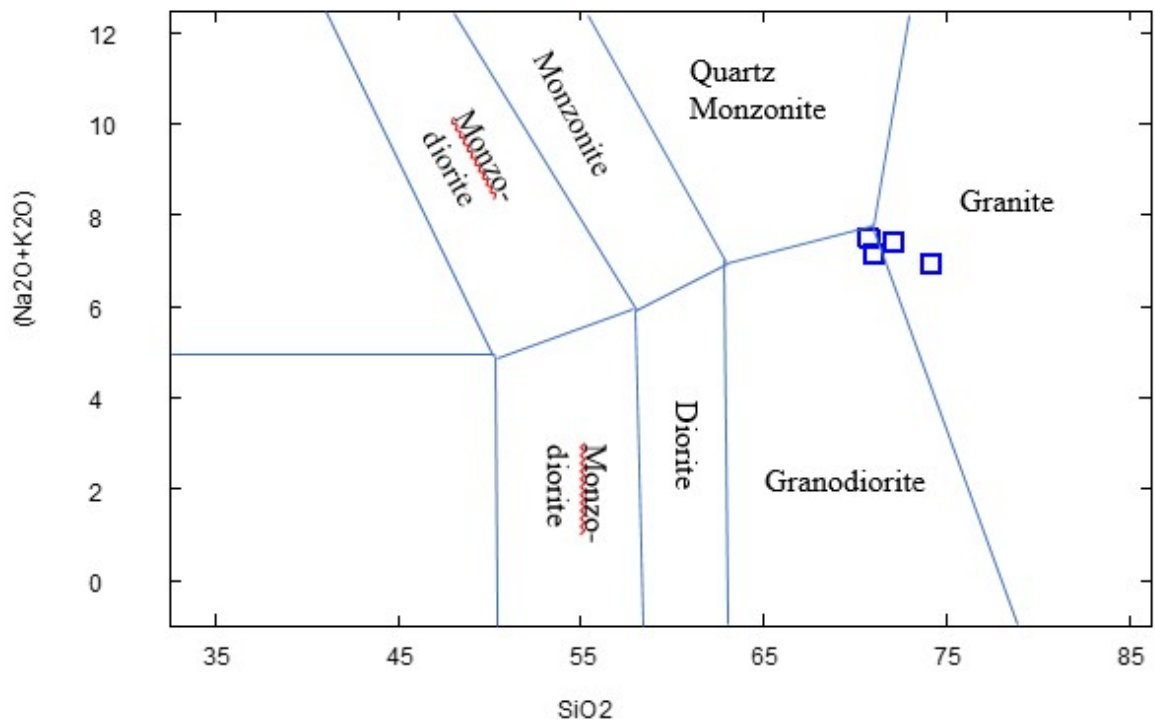


Figure 4.43. $\text{Na}_2\text{O}+\text{K}_2\text{O}$ vs SiO_2 diagram for granite of Osogbo-Okinni area, (after Middlemost, 1994).

The SiO₂ content of granite of the study area compares favourably with the SiO₂ content of granites of other areas in Nigeria, such as the Assob muscovite-biotite granite (Wright, 1970), the Mai-Lumba fine-grained granite (Olawajaju and Rahaman, 1982), the Igbebi coarse-grained granodiorite (Rahaman et al., 1983), Kayarda granodiorite (Olawajaju and Rahaman, 1982), and Idiko-ile porphyritic granite (Popoola, 2016). However, TiO₂ and CaO concentrations in granites of study area are lower than that of the Kayarda granodiorite, while the K₂O content of granite of the other locations are higher than that of the granites of the study area (Table 4.10).

Low Rb content indicates low K-feldspar concentration, while Sr substitutes for Ca in plagioclase whilst the presence of high amount of Ba results from Ba substituting for K in K-feldspar, (Table 4.8). Mineralized granite possesses high Rb/Sr and low Ba/Rb ratios because of high fractionation and increasing hydrothermal volatile activities, (Imeokparia, 1981). The Rb/Sr and Ba/Rb ratios of the granite of Osogbo-Okinni area indicate low and high values respectively contrary to the conclusion of Imeokparia, 1981 consequently these granites are not mineralized (Table 4.8).

Trace elements content often may be used to discriminate what tectonic activity took place resulting in magmatic intrusion in the formation of intermediate-acid intrusive rocks (Pearse et al., 1984). This applies to the granites of Osogbo-Okinni area which falls in VAG + Syn-COLL field of Nb vs Y diagram (Figure 4.44), indicating that their protolith is the source of their geochemical characteristics typical of syn-collisional environment. A clearer discrimination plot of Rb versus Yb+Ta of Pearse et al., 1984, put Osogbo-Okinni granites in the syn-collisional field (Figure 4.45). The depth of emplacement of just below 30km to more than 30km for the Osogbo-Okinni area granites is given by the plot of Rb versus Sr (Figure 4.46).

The Chondrite-normalized patterns for rare earth element of granites (Normalization values after Sun and McDonough, 1989) reveals enrichment of LREE and depletion of HREE, with the patterns appearing concave upwards from the LREE to flattening out at the HREE (Figure 4.47). The Chondrite-normalised diagram of incompatible trace elements

for granite of Osogbo-Okinni area also reveals enrichment of Rb, Th, K, La, Ce relative to low content of Sr, Hf, Zr, Ti and Y, (Figure 4.48).

Table 4.10. Average major element composition of Osogbo-Okinni granite compared to other older granites in Nigeria

Oxides Wt%	Present Study	A	B	C	D	E
SiO ₂	72.04	72.45	72.24	69.67	67.07	70.40
TiO ₂	0.27	0.25	0.36	0.29	0.75	0.42
Al ₂ O ₃	13.82	14.05	14.1	15.17	14.53	13.53
Fe ₂ O _{3t}	3.03	1.88	1.98	3.77	4.93	3.84
MnO	0.02	0.05	0.02	0.05	0.08	0.07
MgO	0.61	0.57	0.37	0.38	0.68	0.35
CaO	1.65	1.4	1.18	1.71	2.32	1.58
Na ₂ O	3.28	3.18	3.93	2.56	3.2	4.31
K ₂ O	3.98	5.75	4.88	5.28	5.44	5.14
P ₂ O ₃	0.19	0.16	0.11	0.31	0.23	0.17

Present study- Osogbo-Okinni granite

A – The Assob muscovite-biotite granite (Wright, 1970)

B – The Mai-Lumba fine-grained granite (Olaewaju and Rahaman, 1982)

C – The Igbeti coarse-grained granodiorite (Rahaman et al., 1983)

D – The Kayarda granodiorite – (Olaewaju and Rahaman, 1982)

E – The Idiko-Ile porphyritic granite (Popoola, 2016)

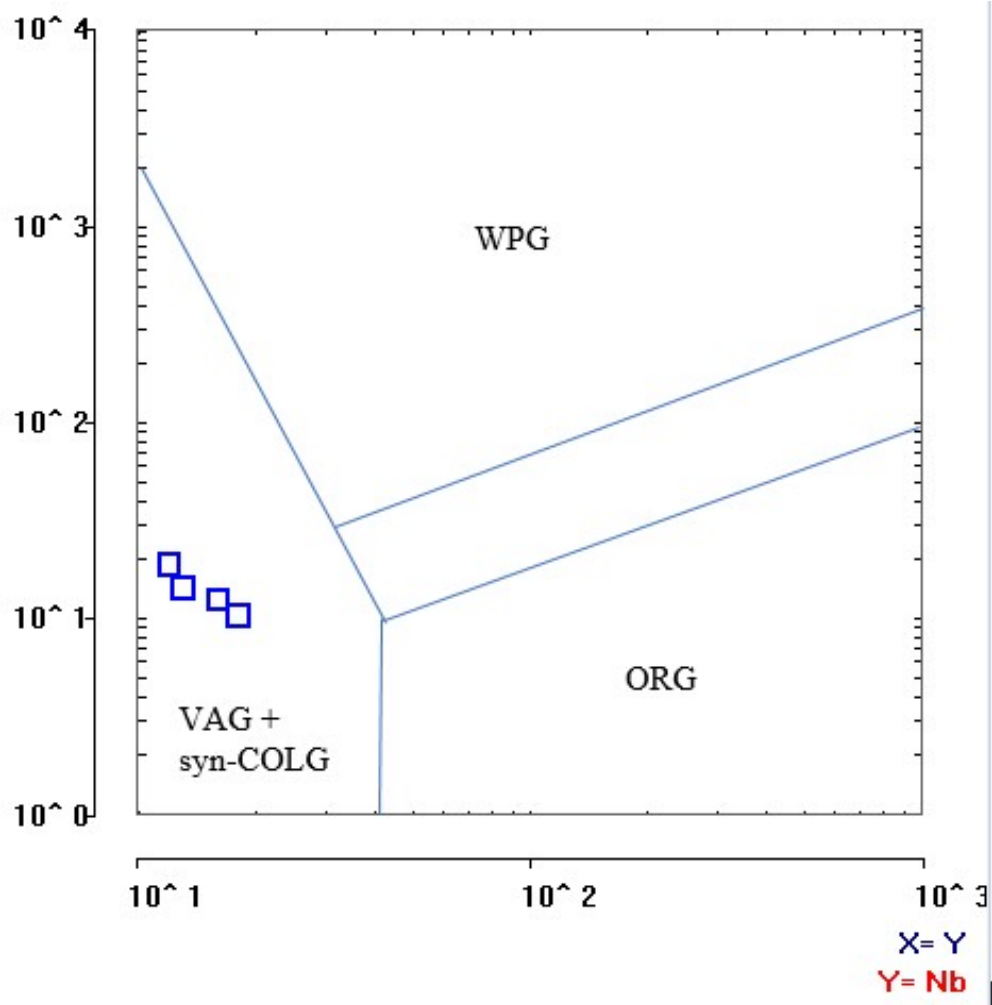


Figure 4.44. Plot of Nb vs Y for granite of Osogbo-Okinni area, (after Pearce et al., 1984)

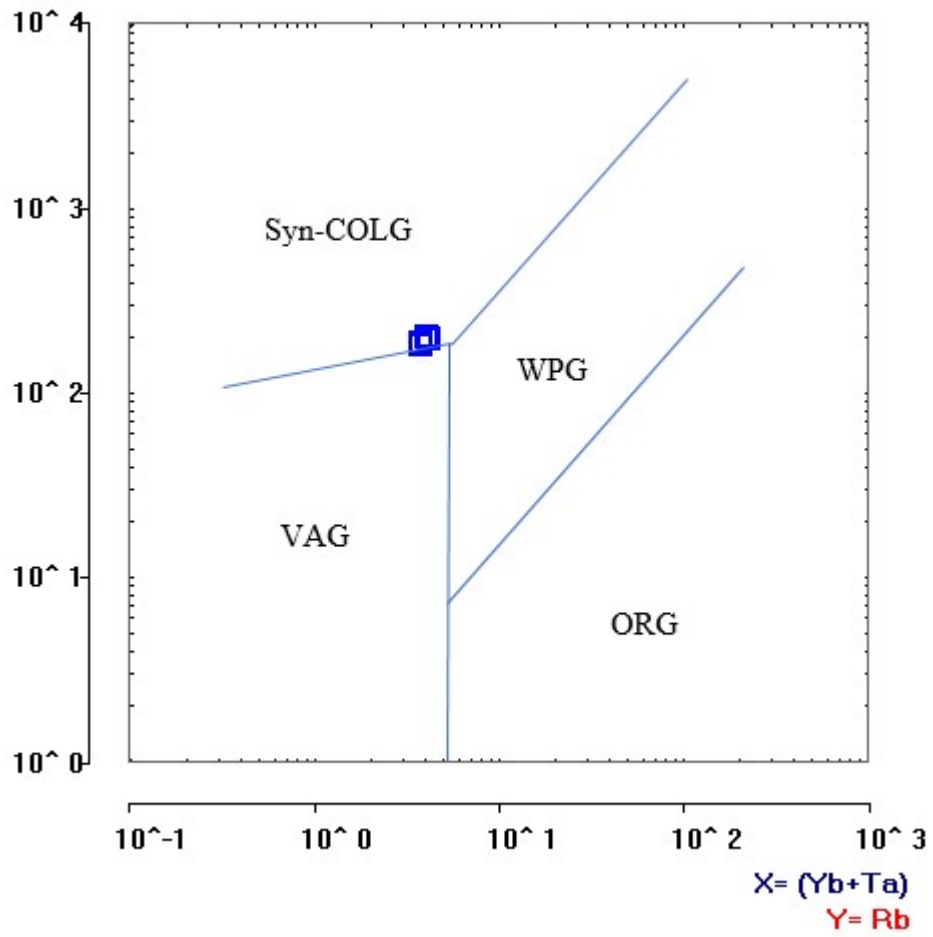


Figure 4.45. Plot of Rb vs Yb+Ta for granite of Osogbo-Okinni area, (after Pearce et al., 1984)

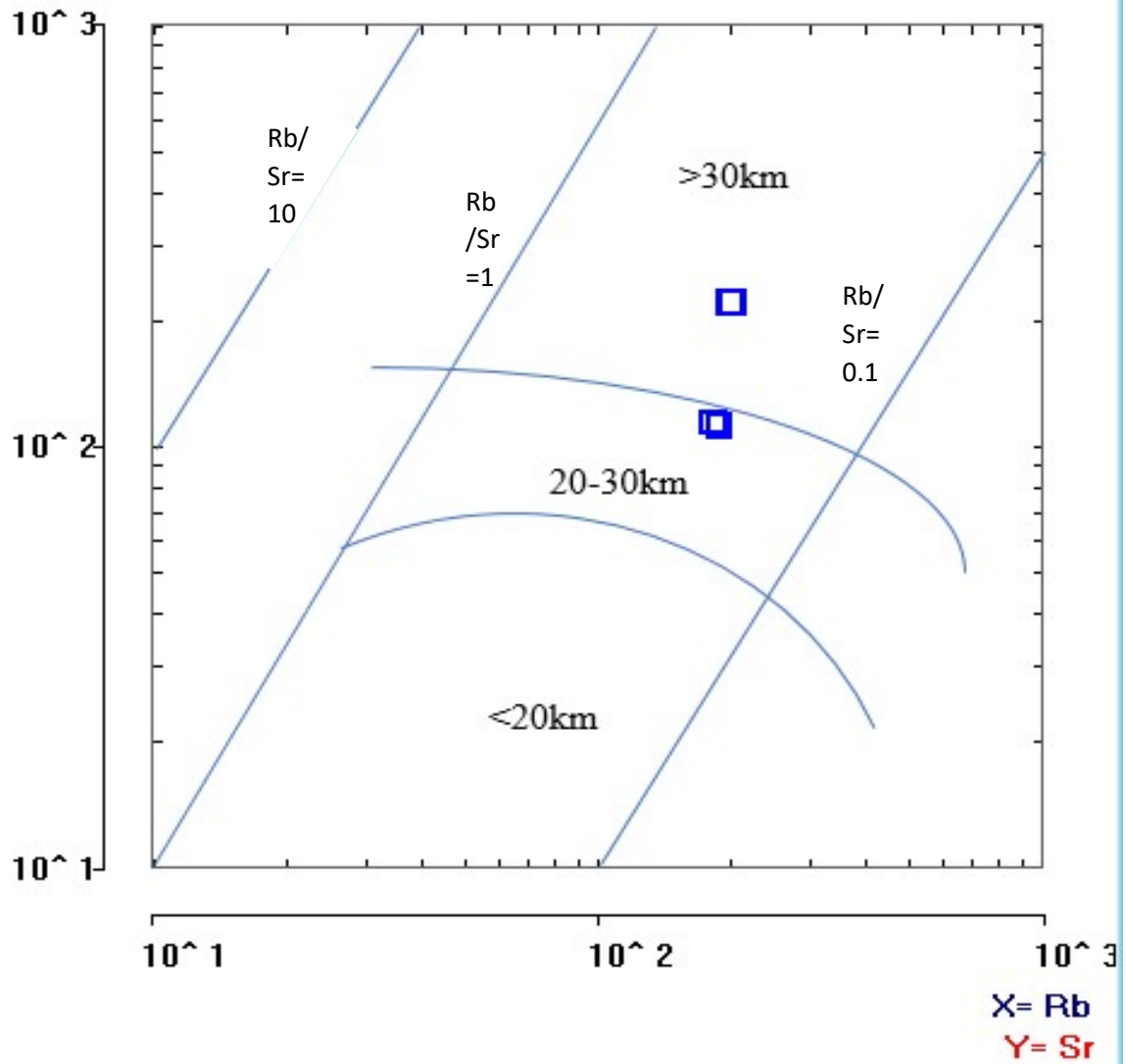


Figure 4.46. Plot of Rb vs Sr for granites of Osogbo-Okinni area showing the depth of emplacement (after Condie, 1973).

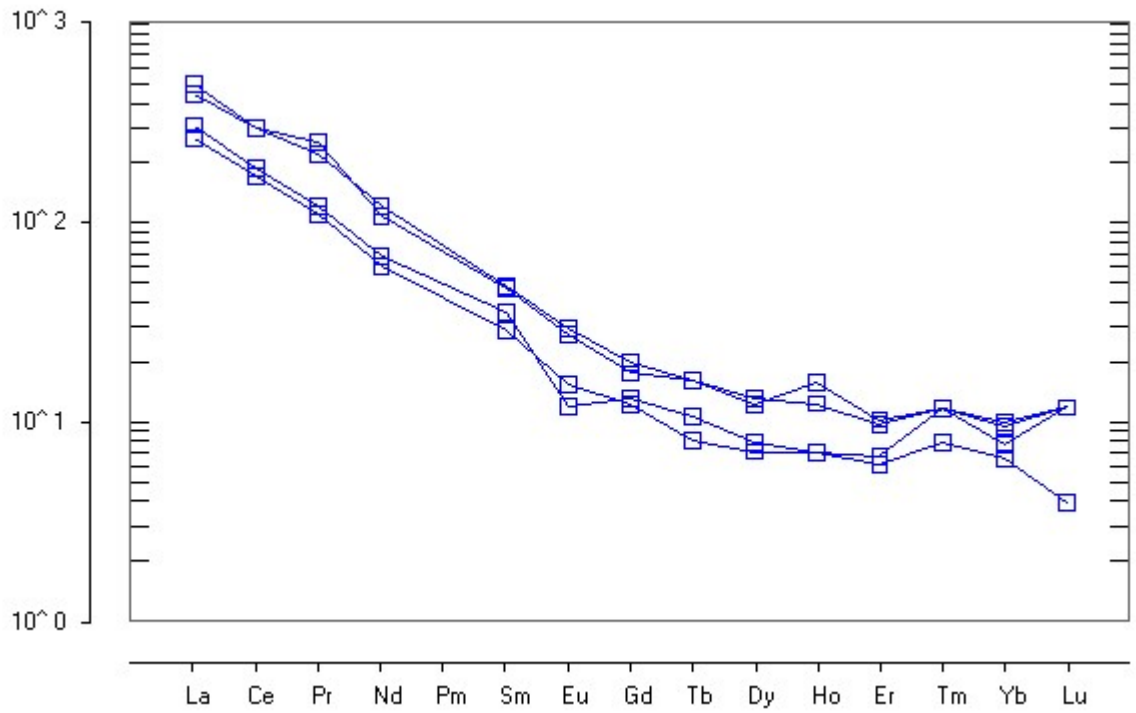


Figure 4.47. Chondrite-normalized rare earth element pattern for granites of Osogbo-Okinni area, (normalization values after Sun and McDonough, 1989)

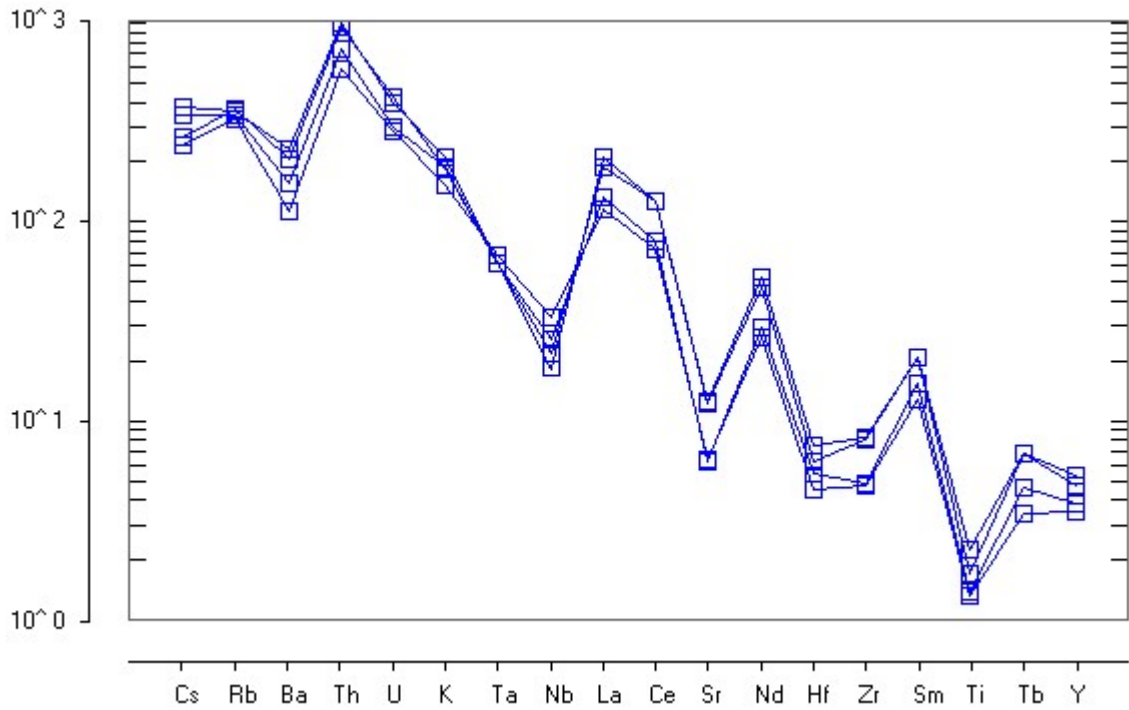


Figure 4.48. Chondrite-normalised plot of incompatible trace elements for granite of Osogbo-Okinni area, (normalization values after Taylor and McLennan, 1985).

4.3.3 Pegmatite

4.3.3.1 whole rock chemistry

Geochemical analysis results of the major element composition of whole rock samples, (Table 4.11) reveals that the Osogbo-Okinni pegmatite are siliceous with SiO_2 values ranging from 59.12wt% to 79.01wt% and an average value of 70.92wt% and about 70wt% have $\text{SiO}_2 > 70\text{wt}\%$. Some samples have lower SiO_2 contents of between 59.12wt% and 64.74wt%. In the plot of total alkali vs silica diagram, the pegmatites fall majorly in the granite field, (Figure 4.49). Al_2O_3 content ranges between 11.93wt% and 22.97wt% with an average of 15.95wt%. K_2O content is next in abundance with a range of 1.74wt% to 10.59wt% and an average of 4.23wt%. Na_2O content ranges from 2.05wt% to 4.53wt% with 3.50wt% average whilst CaO content ranges from 0.17wt% to 0.33wt% with an average of 0.28wt%. The Fe_2O_3 values range from 0.62wt% to 1.40wt% with average of 1.15wt%. P_2O_5 values range from 0.11wt% to 0.57wt% with an average of 0.19wt% while MgO contents range from 0.03wt% to 0.10wt% with an average of 0.08wt%, TiO_2 values range from 0.02wt% to 0.03wt% with an average of 0.02wt%, MnO values range from 0.01wt% to 0.06wt% with an average of 0.04wt%. K_2O is the dominant alkali in the whole rock (Table 11).

The SiO_2 content of the feldspar extracts are lower than that of whole rock with a range of 54.51wt% to 64.76wt% and an average of 56.81wt%. However, the Al_2O_3 content is much higher than that of the whole rock with a range of 21.02wt% to 29.57wt% and an average of 27.03wt%. The K_2O content is slightly higher than the whole rock content with a range of 0.67 to 10.04% and an average of 4.70%, while all the other major element oxides in the feldspar extracts have lower contents than in the whole rock. Na_2O values vary between 0.46wt% and 8.98wt% and mean of 3.04wt%; Fe_2O_3 values range from 0.05wt% to 1.09wt% and mean of 0.55wt%; MgO values range from 0.02wt% to 0.05wt% and mean of 0.03wt%; CaO values range from 0.05wt% to 0.22wt% and mean of 0.10wt%; TiO_2 values range from 0.01wt% to 0.02wt% and mean of 0.01wt%; P_2O_5 values range from

Table 4.11. Major elementwt% content of whole rock, feldspar extracts and mica extracts

Oxides (wt%)	Whole rock pegmatite		Feldspar extracts		Mica extracts	
	Range (N=22)	Average	Range (N=22)	Average	Range (N=22)	Average
SiO ₂	59.12 - 79.01	70.92	54.51 - 64.76	56.81	41.37 - 53.56	43.55
Al ₂ O ₃	11.93 - 22.97	15.95	21.02 - 29.57	27.03	26.99 - 29.71	29.01
TiO ₂	0.02 - 0.03	0.02	0.01 - 0.02	0.01	0.03 - 0.14	0.12
Fe ₂ O ₃	0.62 - 1.40	1.15	0.05 - 1.09	0.55	1.29 - 3.22	2.88
MgO	0.03 - 0.10	0.08	0.02 - 0.05	0.03	0.08 - 0.52	0.46
MnO	0.01 - 0.06	0.04	0.03 - 0.08	0.07	0.03 - 0.07	0.03
CaO	0.17 - 0.33	0.28	0.05 - 0.22	0.10	0.11 - 0.22	0.19
Na ₂ O	2.05 - 4.53	3.50	0.46 - 8.98	3.04	0.58 - 3.05	0.87
K ₂ O	1.74 - 10.59	4.23	0.67 - 10.04	4.70	2.86 - 8.75	8.10
P ₂ O ₅	0.11 - 0.57	0.19	0.11 - 0.35	0.21	0.11 - 0.15	0.12

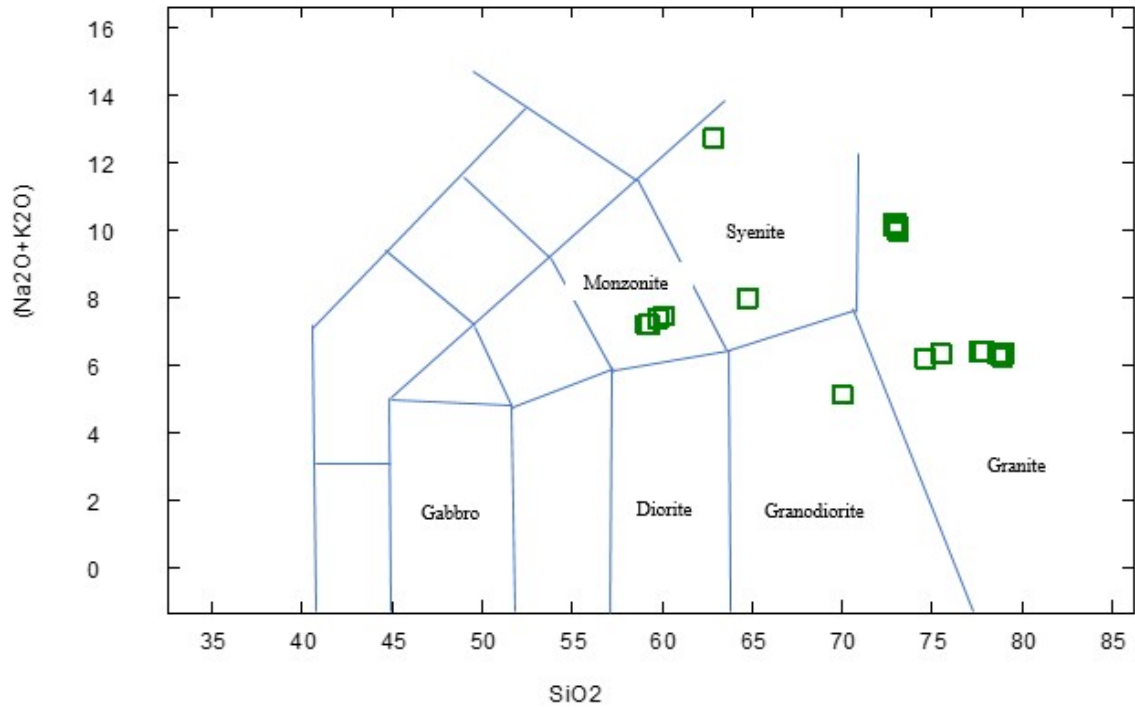


Figure 4.49 Na₂O+K₂O vs SiO₂ diagram for whole rock pegmatites (after Gillespie and Styles, 1999).

0.11wt% to 0.35wt% and mean of 0.21wt%; MnO values range from 0.03wt% to 0.08wt% and mean of 0.07wt%.

The mica extract is enriched in the following major element oxides when compared to the whole rock and feldspar extracts, Al_2O_3 with a range of 26.99wt% to 29.71wt% and an average of 29.01wt%, K_2O with a range of 2.86wt% to 8.75wt% and an average of 8.10wt%, Fe_2O_3 with a range of 1.29wt% to 3.22wt% and an average of 2.88wt%, MgO with a range of 0.08wt% to 0.52wt% and an average of 0.45wt%, TiO_2 with a range of 0.03wt% to 0.14wt% and an average of 0.12wt%. It is however depleted in SiO_2 with a range of 41.37wt% to 53.56wt% and an average of 43.55wt%, Na_2O with a range of 0.58wt% to 3.05wt% and an average of 0.87wt% and P_2O_5 with a range of 0.11wt% to 0.15wt% and an average of 0.12wt%.

The Osogbo-Okinni pegmatites are peraluminous in bulk composition, $\text{Al}_2\text{O}_3 / \text{CaO} + \text{Na}_2\text{O} + \text{K}_2\text{O} > 1$, (Table 4.12). LCT family pegmatites have been observed to have a mild to extremely peraluminous granitic composition parent (Cerny, 1992). As the A/CNK ratio increases the alumina content also increases, and garnet and muscovite rich in aluminium become more abundant. A/CNK values are low in barren granites, increases moderately for fertile granites while rare-element pegmatites have high A/CNK values. The graph of A/NK vs A/CNK (Figure 4.50), also shows the peraluminous composition of the pegmatites.

When compared with the major element oxides of other pegmatites of Nigeria, the SiO_2 content of Osogbo-Okinni area compares favourably with those of the pegmatites of Southern Obudu, Oban, Oke-Asa, Itakpe, but generally higher than that of Komu, Igbeti, Sepeteri, and Awo, while the Oro pegmatites have a higher content of SiO_2 , (Table 4.13). Sepeteri and Awo pegmatites are characterized by higher Al_2O_3 content than that of Osogbo-Okinni pegmatites which however compares favourably with those of Southern Obudu, Oban, Oke-Asa, Itakpe, Komu, and Igbeti pegmatites. The Fe_2O_3 content in pegmatites of the study area compares favourably with Oban, Oke-Asa and Itakpe

pegmatites, but is enriched in Komu, Igbeti, Sepeteri, Awo, and Oro pegmatites. The Na₂O content of Igbeti pegmatite is like that of the study area but depleted in the others. The K₂O content of pegmatites of the study area compares with that of Oban, Itakpe, and Komu pegmatites but is depleted in the others. Komu and Igbeti pegmatites are characterized by higher CaO content than the pegmatites of Osogbo-Okinni, while Sepeteri and Oro pegmatites compares with it, but CaO content is lower in the others. Of significance is the TiO₂ concentration of the Osogbo-Okinni pegmatites which is relatively lower than those of all other pegmatites of Nigeria as given in Table 4.13.

The major element oxide composition of Osogbo-Okinni pegmatites compares favourably with that of pegmatitic leucogranite and potassic pegmatite of Greer Lake, Manitoba, Canada and pegmatite from the Spruce Pine district, North Carolina, US, with some exceptions. The values SiO₂ 70.92wt%, Al₂O₃ 15.95wt%, Na₂O 3.50wt%, K₂O 4.23wt% for Osogbo-Okinni pegmatites agree with SiO₂ 75.15wt%, Al₂O₃ 14.55wt%, Na₂O 3.98wt%, K₂O 3.76wt% for pegmatitic leucogranite and SiO₂ 76.13wt%, Al₂O₃ 14.75wt%, Na₂O 3.43wt%, K₂O 3.52wt% for potassic pegmatite of Greer Lake, Manitoba (Cerny et al., 2005) and SiO₂ 73.79wt%, Al₂O₃ 15.11wt%, Na₂O 4.71wt%, K₂O 4.02wt% for pegmatite of the Spruce Pine district, (Jahns and Burnham, 1969). However, the Fe₂O₃ and MgO content of Osogbo-Okinni pegmatite at 1.15wt%; 0.8wt% are much higher than those of pegmatitic leucogranite, potassic pegmatite of Greer Lake and pegmatite of the Spruce Pine District at 0.54wt%; 0.03wt% and 0.58wt%; 0.06wt%; and 0.26wt%; 0.07wt% respectively.

Trace element composition in whole rock is used to evaluate level of fractionation in pegmatites. Comparison of trace element concentrations in whole rock with feldspar and mica extracts reveal enrichment of whole rock in Be, Sr, Ba, W and Ta. Normal fractionation tends to induce higher silica content in the melt, and the ratio Nb/Ta reduces. This trend enriches the residual melt in Ta over Nb which results in oxides richer in Ta, this is consistent with chemical variations observed in granites and their pegmatites,

(London, 2008) this probably explains the enrichment of whole rock in Ta. For Be, Sr and Ba the trend in enrichment is whole rock > Feldspar > mica. Zn, Sn, Sc, Li, Rb and Nb are

Table 4.12 Elemental ratios of selected major element oxides of whole rock

E/R	Range	Average (n=22)
K_2O/Na_2O	0.40-4.93	1.61
Na_2O/Al_2O_3	0.11-0.38	0.23
K_2O/Al_2O_3	0.10-0.61	0.28
CaO/Na_2O	2.37-4.85	3.78
$CaO+Na_2O+K_2O$	5.39-13.02	8.01
Al/CNK	1.26-3.15	2.08
Na_2O+K_2O	5.14-12.74	5.90

Oxides	This Study	A	B	C	D	E	F	G	H	I
SiO ₂	70.92	71.90	71.02	71.46	70.17	68.26	63.02	66.17	54.95	86.43
Al ₂ O ₃	15.95	15.44	15.99	13.90	15.68	14.02	15.03	25.51	25.77	6.86
Fe ₂ O ₃	1.15	0.48	1.5	1.49	1.15	1.95	5.58	3.91	2.44	2.05
MgO	0.08	<0.01	0.056	0.12	-	0.16	0.18	0.19	1.61	0.23
CaO	0.28	0.12	0.063	0.03	0.13	1.49	2.75	0.37	0.06	0.22
Na ₂ O	3.50	0.88	0.38	1.11	1.19	1.38	4.25	0.35	0.30	2.09
K ₂ O	4.23	2.43	4.43	2.08	3.26	3.42	2.93	1.18	1.28	0.45
TiO ₂	0.02	7.42	4.83	8.77	6.05	4.64	4.10	1.16	3.74	0.30
P ₂ O ₆	0.19	0.05	0.01	0.01	0.04	0.20	0.75	0.73	0.06	0.08
MnO	0.04	0.05	0.51	0.26	0.02	0.03	0.30	0.02	0.14	0.03

Table 4.13 Major element oxide content of Osogbo-Okinni pegmatites compared to pegmatites from various locations in Nigeria

A = Southern Obudu pegmatites (Edem et al., 2015)

B = Oban pegmatites (Ero and Ekwueme, 2009)

C = Oke-Asa pegmatites (Okunlola and Akinola, 2010)

D = Itakpe pegmatites (Okunlola and Somorin, 2005)

E = Komu pegmatites (Okunlola and Udoudo, 2005)

F = Igbeti pegmatites (Okunlola and Oyedokun, 2009)

G = Sepeteri pegmatites (Okunlola and Akintola, 2007)

H = Awo pegmatites (Akintola et al., 2011)

I = Oro pegmatites (Oyebamiji, 2014)

enriched in mica and Zn, Li, Rb and Nb enrichment trend is mica > feldspar > whole rock, (Table 4.14). Mica enrichment over feldspar and whole rock in these elements may be due to their compatibility in mica and incongruent melting of mica at source and recrystallization and accumulation of the elements in pegmatite. Ce is enriched in feldspar probably because feldspar is a principal reservoir for Ce, (London, 2005b).

K/Rb, K/Cs, and Nb/Ta are elemental ratios which are excellent fractionation indicators. The lower the values of these ratios the greater the mineralization potential of pegmatites. In the plot of K/Rb v Cs (Figure 4.51) all samples plot in the muscovite class. This put Osogbo-Okinni pegmatites in the muscovite class of pegmatites. The values for the elemental ratios stated above for some samples of Osogbo-Okinni pegmatites compare favourably with the values for fertile granite (Cerny, 1989a), (Table 4.16).

Another indicator of fractionation of granites and pegmatites is Mg/Li ratio for whole rock. Mg/Li ratio <30 is evidence of high level of fractionation, (Beus, et al., 1968 and Cerny, 1989a). Mg/Li ratio \geq 50 means abundance of Mg in a barren granite, while Mg/Li ratio <10 points to high Li content in an evolved rock, that is, fertile pegmatite. Li-rich rocks have high economic potential because of their association with Ta mineralization. Applying the Mg/Li ratio as indicated by Beus, et al. (1968) and Cerny, (1989a), 3 out of 22 pegmatites of Osogbo-Okinni outcrop samples can be termed barren, while 12 have high degree of fractionation but not necessarily fertile and 7 can be said to have Ta mineralization. This points to the fact that Osogbo-Okinni pegmatites can be grouped into mineralized and unmineralized or barren in Ta mineralization, (Figures 4.52, 4.53).

Simple bivariate plots of one trace element against another from the whole rock sample of a pegmatite outcrop can reveal the fertility or otherwise of the rock. For example, bivariate plots of Ta vs Ga (Figure 4.52) and Ta vs Cs (Figure 4.53) after Moller and Morteani, 1987, reveal that major percentage of the pegmatite whole samples fall below

the Beus line for Ta mineralization while about one-third plot above the Gordiyenko line of Ta mineralization.

Table 4.14 Trace element content (ppm) of whole rock, feldspar, and mica extracts

Trace Elements	Whole rock pegmatite		Feldspar extracts		Mica extracts	
	Range (N=22)	Mean	Range (N=22)	Mean	Range (N=17)	Mean
Mo	0.29 - 0.93	0.66	0.05 - 0.20	0.08	0.19 - 0.43	0.34
Cu	6.70 - 22.80	13.09	1.40 - 10.40	5.17	4.70 - 11.90	6.17
Pb	13.72 - 67.14	31.77	8.05 - 56.34	32.22	4.97 - 37.76	12.01
Zn	6.50 - 57.90	34.29	9.10 - 106.60	51.13	129.10 - 286.60	239.17
Ag	33.00 - 77.00	52.12	-	-	-	-
Ni	1.90 - 7.60	2.96	0.60 - 13.50	8.22	2.00 - 10.60	3.01
Co	0.50 - 4.00	1.21	0.20 - 6.60	3.32	1.00 - 4.80	1.63
As	0.40 - 3.60	1.75	0.30 - 1.80	0.86	0.50 - 1.70	0.97
U	1.40 - 6.70	3.76	0.80 - 12.80	4.52	0.20 - 4.60	0.81
Th	0.50 - 2.60	1.14	0.20 - 2.10	0.60	0.50 - 1.10	0.67
Sr	7.00 - 97.00	34.50	2.00 - 17.00	9.18	5.00 - 14.00	7.18
Cd	0.02 - 0.11	0.06	0.05 - 0.14	0.07	0.02 - 0.06	0.04
Sb	0.11 - 0.30	0.23	0.03 - 0.12	0.06	0.05 - 0.18	0.12
Bi	0.23 - 9.24	3.82	0.17 - 2.07	0.93	0.04 - 1.48	0.27
V	2.00 - 3.00	2.18	1.00 - 3.00	2.30	5.00 - 10.00	8.76
Cr	3.00 - 13.00	7.04	1.00 - 6.00	3.31	3.00 - 10.00	6.76
Ba	30.00 - 861.00	283.95	14.00 - 102.00	53.45	16.00 - 93.00	29.29
W	73.50 - 178.00	101.94	0.20 - 6.60	2.24	9.20 - 58.70	27.16
Zr	4.10 - 81.80	25.85	0.90 - 131.80	28.41	4.30 - 19.10	6.83
Sn	5.40 - 89.40	25.78	4.50 - 20.70	11.63	123.80 - 615.80	510.86
Be	3.00 - 737.00	40.64	5.00 - 386.00	34.41	10.00 - 25.00	13.71
Sc	0.40 - 12.10	3.65	0.30 - 0.80	0.47	19.80 - 133.40	104.86
Y	1.20 - 9.80	5.66	0.60 - 9.90	3.83	0.90 - 7.30	1.59
Hf	0.15 - 10.04	2.75	0.09 - 8.95	2.01	0.42 - 1.91	0.76

Li	15.40 - 202.40	59.61	53.90 - 121.40	74.15	138.70 - 448.30	376.88
Rb	161.40 - 387.20	257.42	67.90 - 1998.30	528.46	473.80 - 1601.60	1101.97
Ta	0.20 - 259.00	70.35	6.50 - 72.40	28.59	20.00 - 123.90	38.20
Nb	1.83 - 202.96	63.00	3.86 - 164.71	77.30	136.65 - 313.06	272.41
Cs	2.40 - 20.80	7.65	1.90 - 117.90	48.78	14.80 - 54.20	35.53
Ga	13.45 - 44.33	23.64	21.23 - 47.13	33.48	68.16 - 68.16	68.16
Tl	0.77 - 16.41	2.21	0.32 - 26.29	11.03	2.84 - 10.61	5.06

Table 4.15 Rare earth element content (ppm) of whole rock, feldspar extracts, mica extracts

	Whole Rock Pegmatite		Feldspar		Mica	
	Range N=22	Average	Range N=22	Average	Range N=17	Average
La	1.40 - 10.40	4.59	0.20 - 0.90	0.47	0.70 - 2.70	1.58
Ce	2.70 - 14.62	7.67	0.41 - 1.93	1.03	1.57 - 5.39	3.38
Pr	0.20 - 1.80	0.94	0.10 - 0.30	0.23	0.30 - 0.70	0.42
Nd	1.00 - 6.70	3.61	0.20 - 2.00	1.14	1.20 - 3.50	1.99
Sm	0.20 - 2.00	0.89	0.10 - 0.60	0.40	0.30 - 1.00	0.46
Eu	0.30 - 0.50	0.39	0.10 - 0.10	0.10	0.10 - 0.20	0.17
Gd	0.40 - 1.50	0.83	0.20 - 0.50	0.35	0.10 - 0.60	0.33
Tb	0.10 - 0.20	0.13			0.20 - 0.20	0.20
Dy	0.30 - 1.20	0.75	0.10 - 1.00	0.51	0.10 - 0.70	0.30
Ho	0.10 - 0.30	0.16	0.20 - 0.20	0.20	0.20 - 0.20	0.20
Er	0.30 - 0.90	0.50	0.10 - 0.90	0.40	0.10 - 0.60	0.16
Tm	0.10 - 0.10	0.10	0.10 - 0.10	0.10	0.10 - 0.10	0.10
Yb	0.10 - 0.90	0.48	0.10 - 1.00	0.53	0.10 - 1.00	0.20
Lu	0.10 - 0.10	0.10	0.10 - 0.20	0.12	0.10 - 0.10	0.10
∑REE	7.3 - 41.22	21.14	2.01- 9.73	5. 58	5.17-16.99	9.59
∑LREE	6.2 – 37.52	18.92	1.31 – 6.33	3.72	4.27 – 14.09	8.33
∑HREE	1.1 – 3.7	2.22	0.7 – 3.4	1.86	0.9 – 2.9	1.26

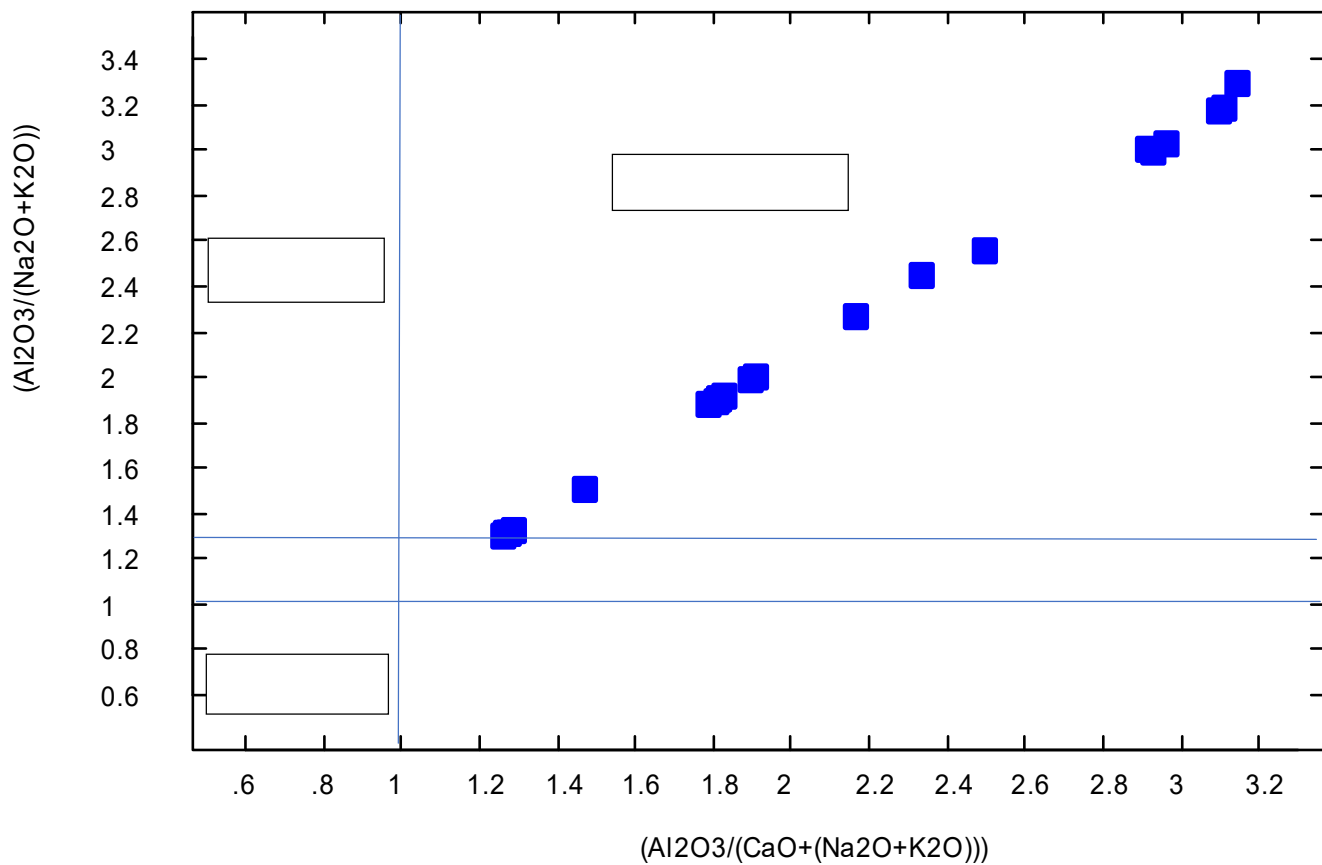


Figure 4.50 Plot of $Al_2O_3/(Na_2O+K_2O)$ against $Al_2O_3/(CaO+Na_2O+K_2O)$ (after Maniar and Piccoli, 1989).

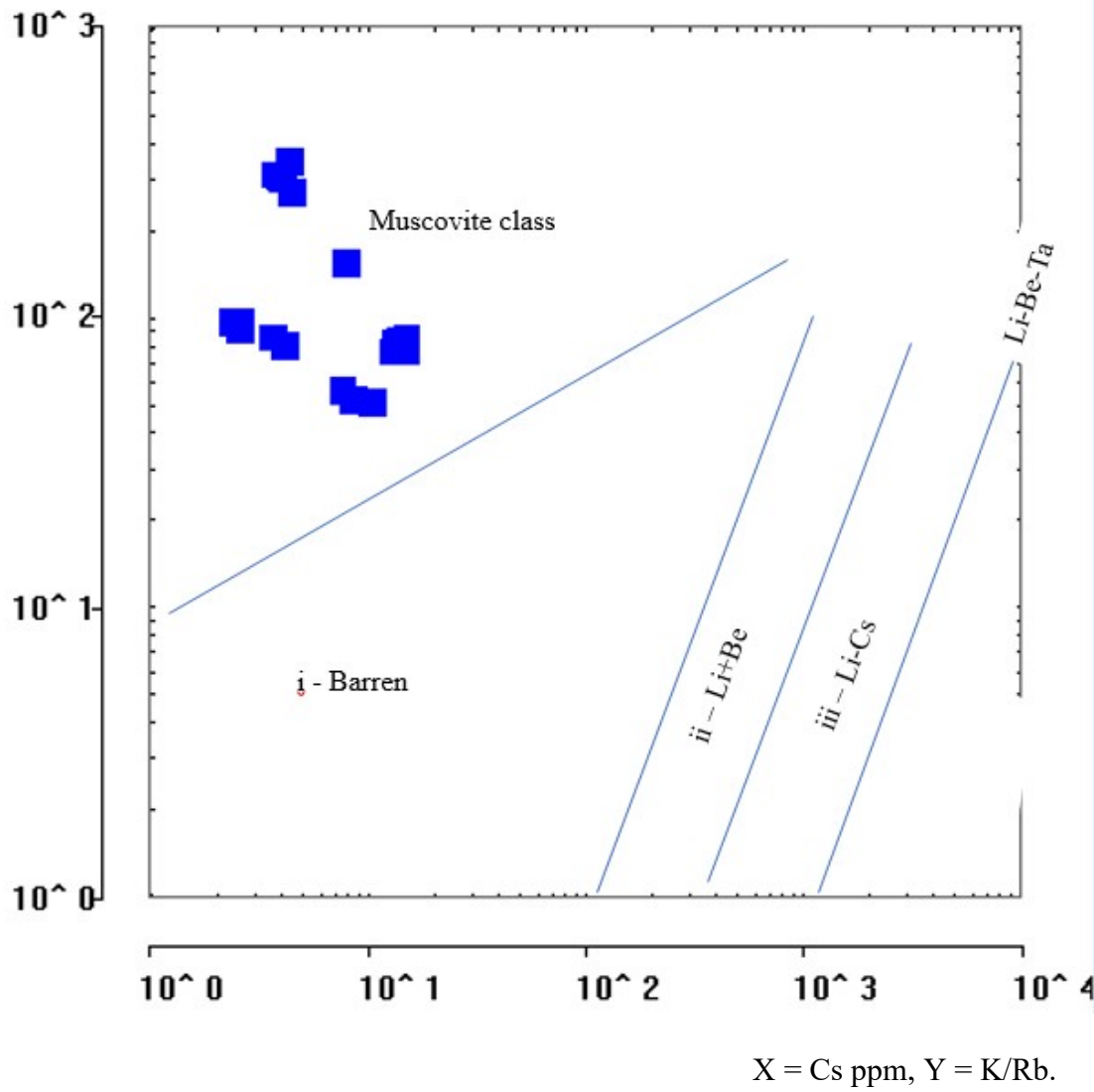


Figure 4.51 K/Rb vs Cs diagram, (after Cerny, 1982).

Table 4.16 Range of selected trace elements content and elemental ratios in whole rock of fertile granites and average value for Upper Continental Crust compared to that of Osogbo-Okinni pegmatites.

Elements/ Elemental ratio	*Fertile granite	Osogbo-Okinni pegmatites N=22	#Average upper continental crust
Be	1-604	3.00-737.00	3
Cs	3-51	2.40-20.80	3.7
Ga	19-90	13.45-44.33	17
Li	1-3,540	15.40-202.40	20
Nb		1.83-202.96	25
Rb	32-5,775	161.40-387.20	112
Sn	<1-112	5.40-89.40	5.5
Ta		0.20-259.00	2.2
K/Rb	42-270	50.37-340.77	252
K/Cs	1,600-15,400	1375.22-17,645.77	7,630
K/Ba	48-18,200	77.98-1171.78	
Rb/Sr	1.6-185	2.13-43.03	
Mg/Li	1.7-50	1.23-36.54	
Zr/Hf	14-64	5.23-30.00	
Nb/Ta		0.58-10.46	11.4

*Cerny, 1989a

#Taylor and McLennan, 1985

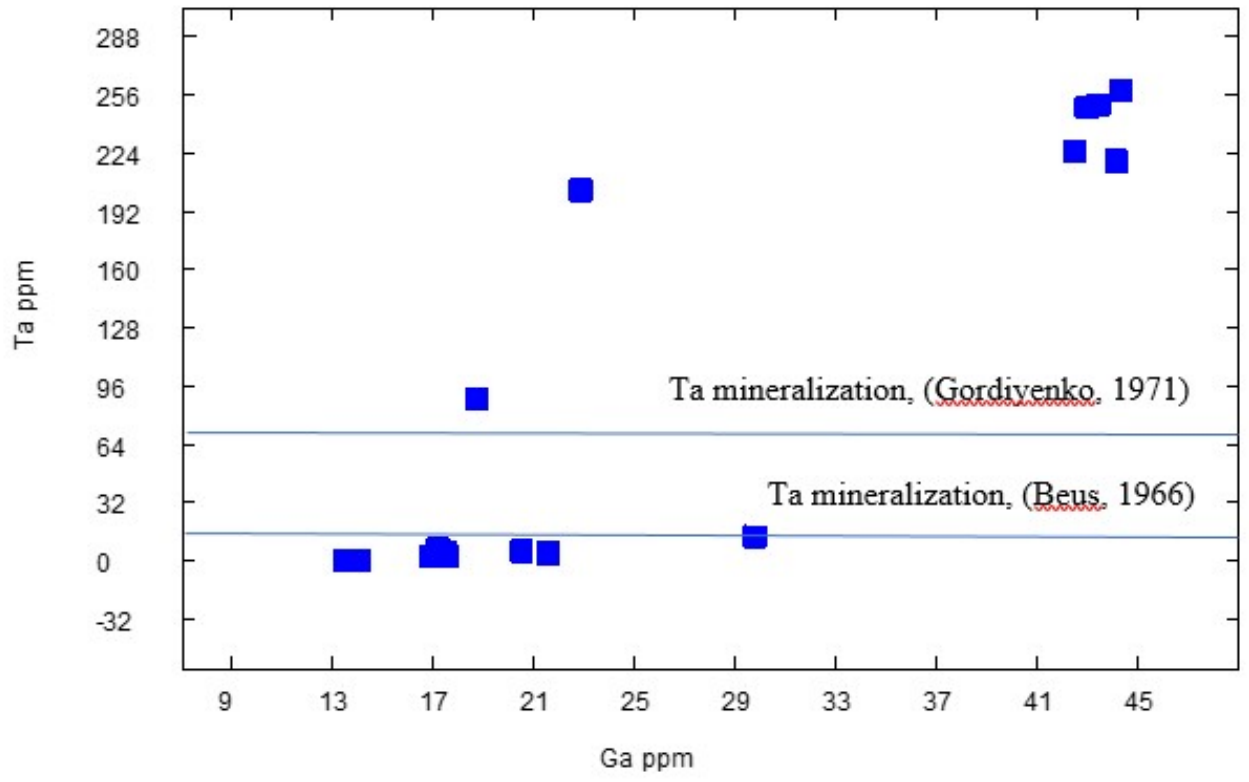


Figure 4.52 Plot of Ta vs Ga, (after Moller and Morteani, 1987).

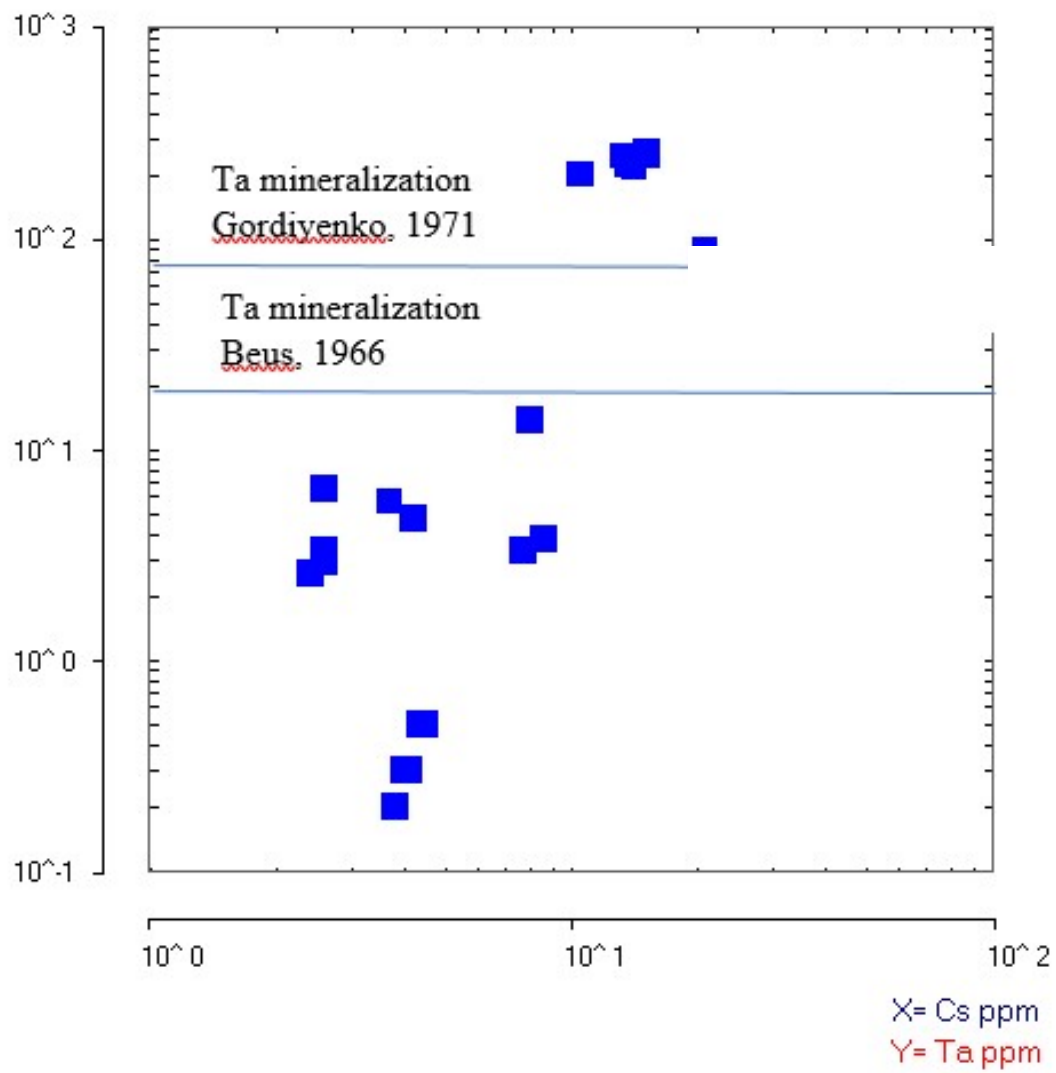


Figure 4.53 Plot of Ta vs Cs, (after Moller and Morteani, 1987).

The plots of Ta vs Cs+Rb, Ta vs Rb, and Ta vs K/Cs (Figures 4.54, 4.55 and 4.56) for the whole rock, feldspar and mica extracts respectively revealed that a fraction of all the whole rock and mica extracts samples plot over the mineralization line of Gordiyenko (1971), this indicates that some pegmatites of Osogbo-Okinni have tantalum mineralization, while the major part of the feldspar and mica extracts plot above the Beus line of mineralization. Generally, in igneous rocks, REE have preferential accumulation in ultrabasic and basic rocks formed early as compared to intermediate and acidic rocks which are formed later, (Randive et al., 2014). Acidic rocks like granites have low to moderate REE content ($\sum\text{REE} = 8\text{-}1977\text{ppm}$) and low to moderate LREE/HREE ratio ($(\text{La/Lu})_{\text{cn}} = 0.54\text{-}137$). Positive Eu anomalies are not common (Henderson, 1984).

The whole rock of Osogbo-Okinni pegmatites has $\sum\text{REE} = 7.3\text{-}41.22\text{ppm}$, $\text{La/Lu} = 14\text{-}104$ (Table 4.14) and positive Eu anomalies ($\text{Eu/Eu}^* = 0.61\text{-}1.52$) and this agrees with Henderson, (1984). These pegmatites have abundant light rare earth elements (LREE), ($\sum\text{LREE} = 6.2\text{-}37.52\text{ppm}$) when compared with their heavy rare earth elements (HREE) content, ($\sum\text{HREE} = 1.1\text{-}3.7\text{ppm}$). This points to high fractionation of the pegmatites ($(\text{La/Yb})_{\text{n}} = 2.06\text{-}9.00$), (Figure 4.57).

The ratio of $\sum\text{REE}$ in whole rock compared to feldspar and mica extracts is whole rock $\sum\text{REE}$ ($7.33\text{-}41.22\text{ppm}$) > mica $\sum\text{REE}$ ($5.17\text{-}16.99\text{ppm}$) > feldspar $\sum\text{REE}$ ($2.01\text{-}9.73\text{ppm}$), this trend is same for $\sum\text{LREE}$ where whole rock $\sum\text{LREE}$ ($6.2\text{-}37.52\text{ppm}$) > mica $\sum\text{LREE}$ ($4.27\text{-}14.09\text{ppm}$) > feldspar $\sum\text{LREE}$ ($1.31\text{-}6.33\text{ppm}$) but different for $\sum\text{HREE}$, where whole rock $\sum\text{HREE}$ ($1.1\text{-}3.7\text{ppm}$) > feldspar $\sum\text{HREE}$ ($0.7\text{-}3.4\text{ppm}$) > mica $\sum\text{HREE}$ ($0.9\text{-}2.9\text{ppm}$). The trend for $\sum\text{REE}$ where whole rock $\sum\text{REE} > \text{mica } \sum\text{REE} > \text{feldspar } \sum\text{REE}$ may be because mica probably concentrates more of the REE and thus control the REE content during melting or crystallization, (Rollinson, 1993).

Weak Eu anomalies are indicated in the REE pattern for whole rock, these may be used to distinguish presence or otherwise of mineralization in the pegmatites.

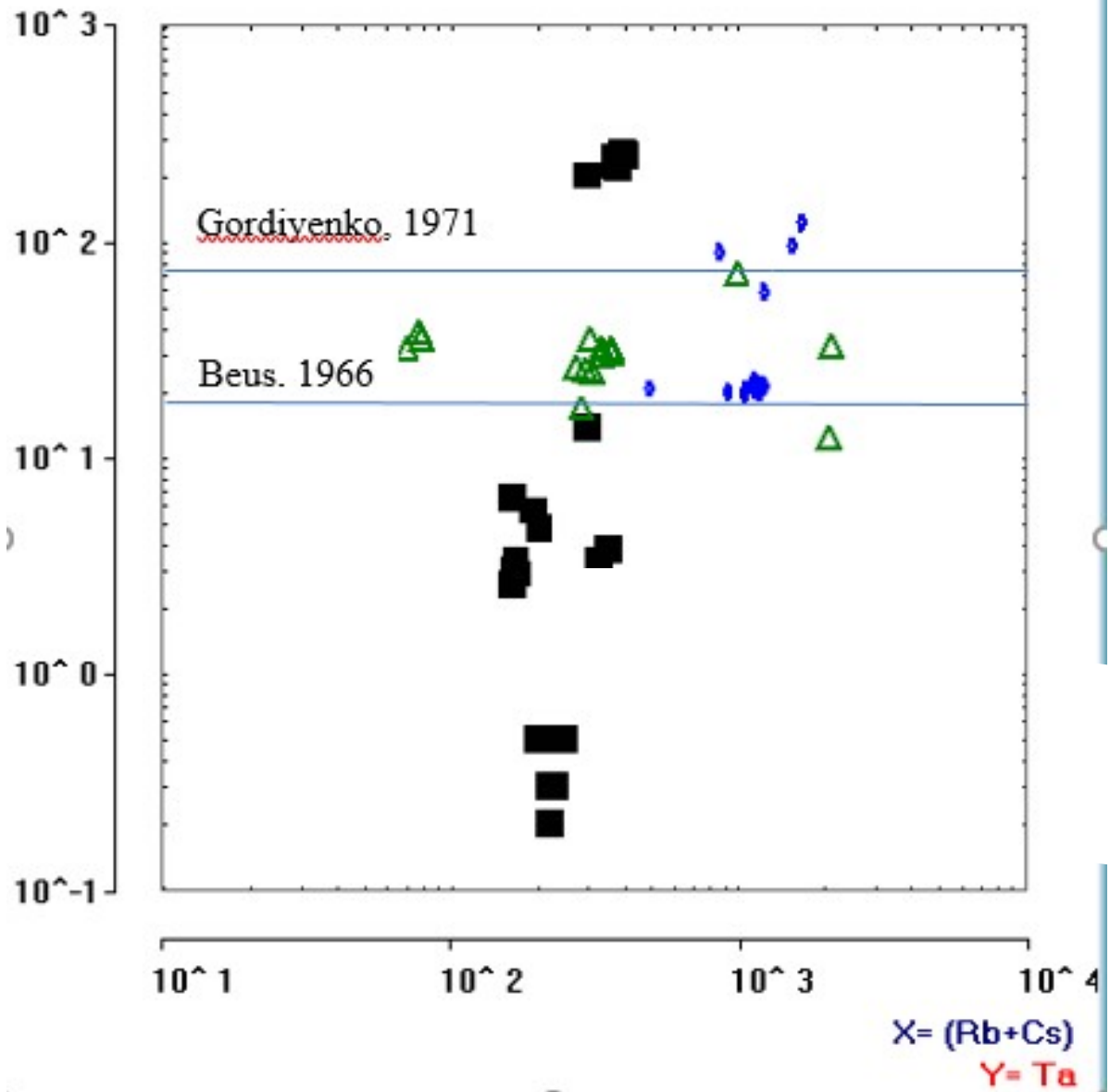


Figure 4.54 Ta vs Rb+Cs diagram for whole rock, feldspar, and mica extracts showing Ta mineralization (mineralization lines after Beus, 1966, and Gordiyenko, 1971).

- Black square – whole rock
- ▲ Green triangle – feldspar extracts
- ◆ Blue diamond – mica extracts

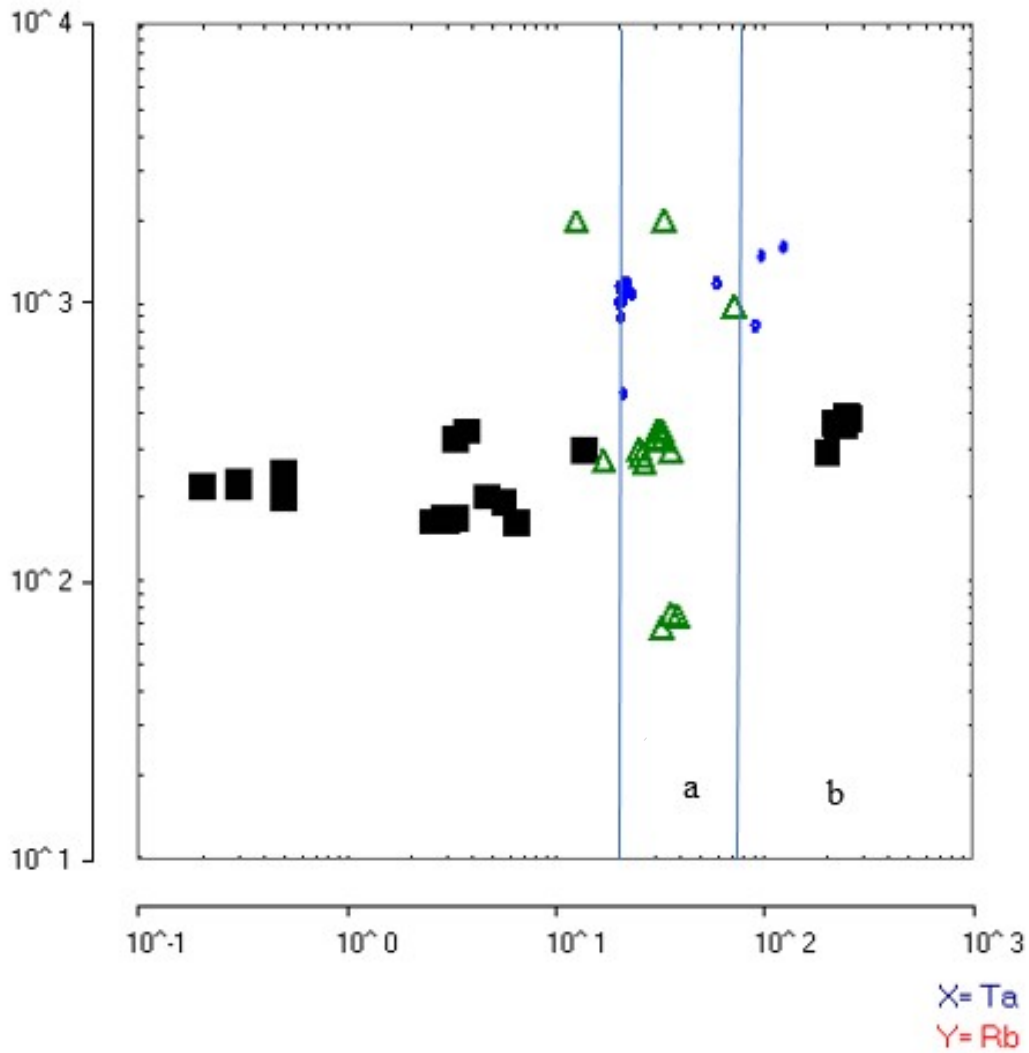


Figure 4.55 Ta vs Rb diagram for whole rock, feldspar, and mica extracts showing Ta mineralization, (mineralization lines after Beus, 1966, and Gordiyenko, 1971).

- a). Ta Prospect >Beus' line;
- b). Ta mineralized >Gordiyenko line

■ black square – whole rock
 ▲ green triangle – feldspar extracts
 ◆ blue diamond – mica extracts

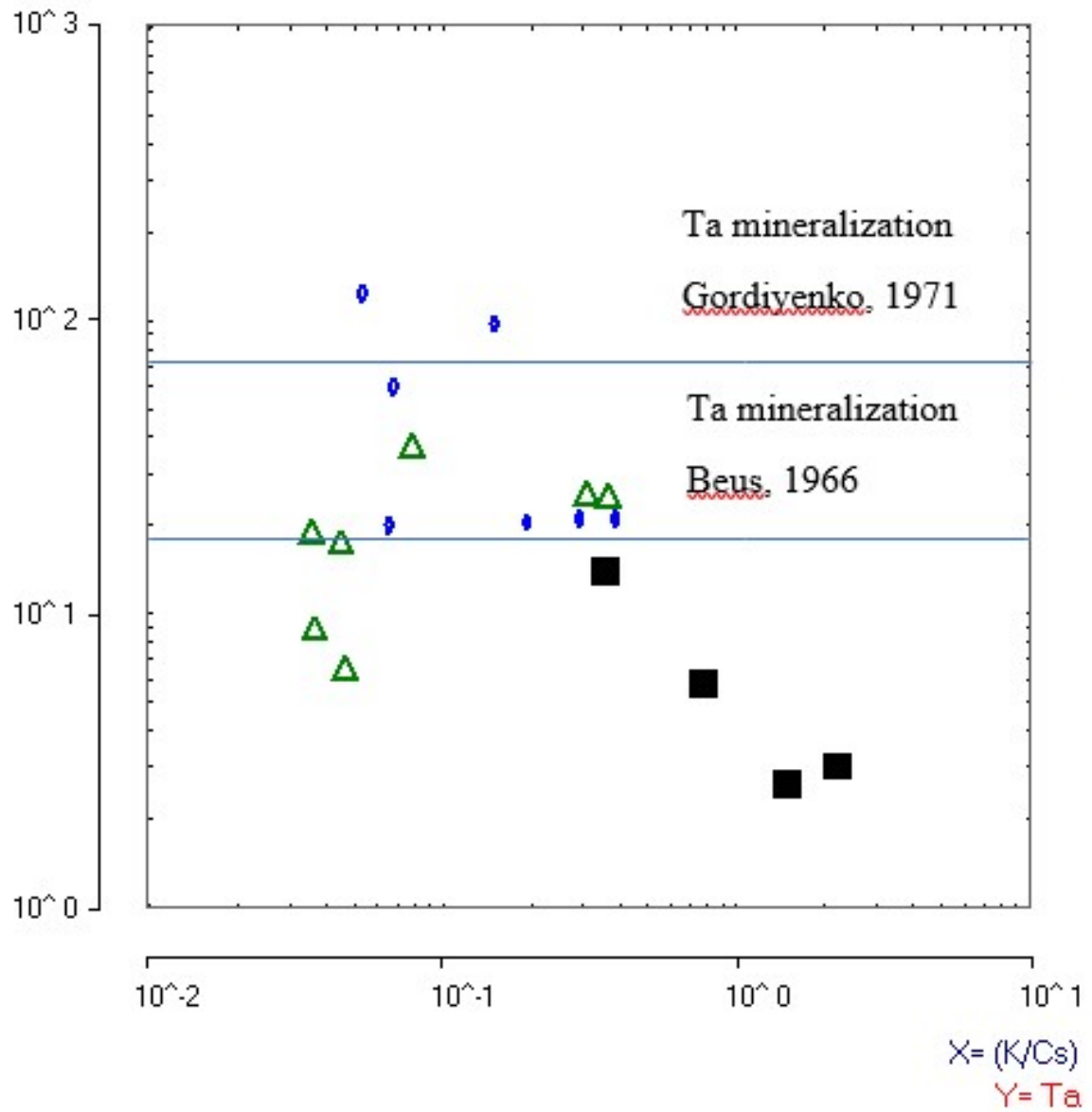


Figure 4.56 Plot of Ta vs K/Cs for whole rock, feldspar, and mica extracts showing Ta mineralization.

- Black square – whole rock
- ▲ Green triangle – feldspar extracts
- ◆ Blue diamond – mica extracts

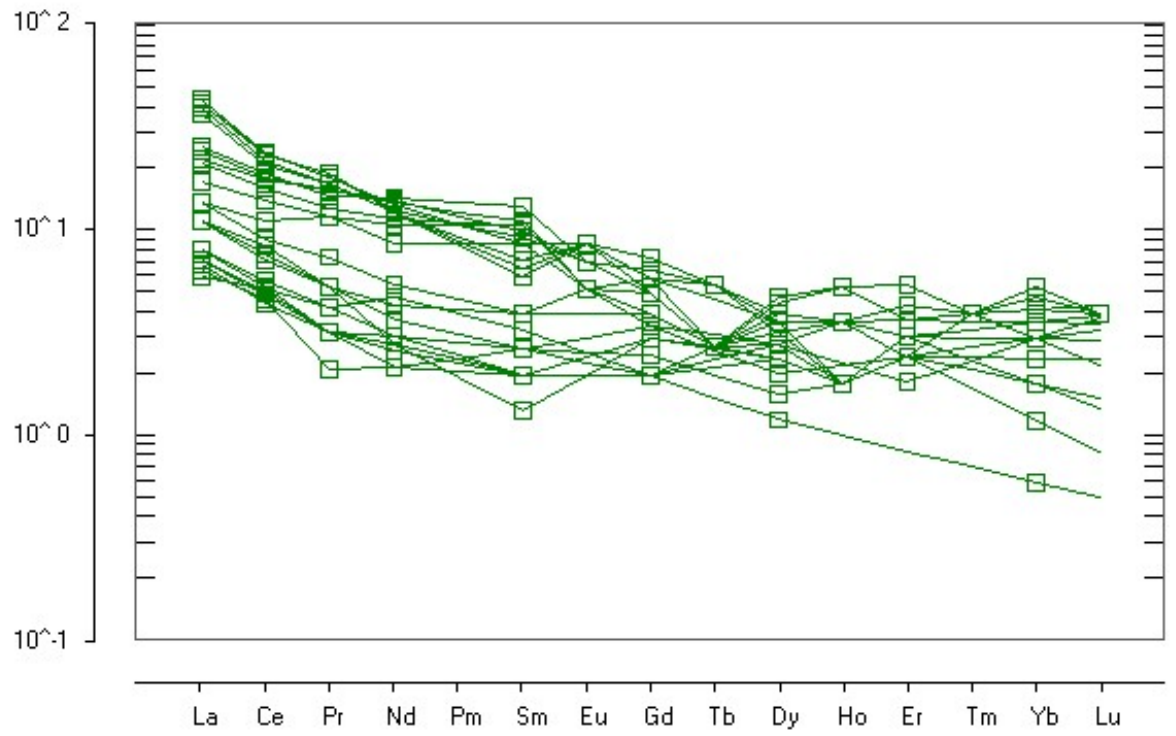


Figure 4.57 REE pattern of Osogbo-Okinni pegmatites

4.3.3.2 Mineral chemistry

4.3.3.2.1 Feldspar

Geochemical analysis of K-feldspar which is a constituent of fertile granites and rare element pegmatites is an excellent mineral exploration tool, (Morteani and Gaupp, 1989). In geochemical analysis, enriched Na content in K-feldspar indicate albite contamination, quartz contamination is revealed by elevated silica content, while high composition of Rb and Cs is indicative of feldspar from high pegmatite fractionation, (Selway et al., 2005). Other elements such as Sr and Ba partition into primary K-feldspar, while Rb and Pb remain in the melt because of their incompatibility during the differentiation of felsic igneous rocks. The trend of compatibility of elements in K-feldspar is Rb, (least compatible) to Ba and then Sr (the most compatible), (Icenhower and London, 1996).

The elemental ratio K/Rb in K-Feldspar is a good indicator of a pegmatite body evolution (Gordiyenko, 1971; Cerny et al., 1985) because they are interpreted as fractional crystallization products of a granitic protolith (Cerny et al., 2012b). It should be noted however, that other processes like low-degree partial melting may result in characteristics of similar nature. Plagioclase contains little amount of trace elements, probably because of the small size of Na^+ (Cerny, 1994) and generally no connection exists between the trace element content of plagioclase and type of pegmatite (Alfonso et al., 2003), K-Feldspar is therefore the relevant mineral for trace element content analysis.

The standard plot K/Rb versus Cs measure the level of fractionation of pegmatite, and it indicates the level of replacement of K with Rb in the K-feldspar crystal lattice. Little quantities of albite contamination effect no change in K/Rb ratio because K and Rb are not incorporated into albite crystal structure (Selway et al., 2005). As a result of the incompatibility of Rb, as fractionation increases its content in K-feldspar increases while Sr and Ba content decreases. (Icenhower and London, 1996). Rb are usually incompatible in peraluminous melts, it partitions into micas at crystallization (Icenhower and London, 1995, 1996). Barren pegmatites characterised by low amounts of Rb in feldspars may be the result of Rb partitioning into biotite earlier. The K-feldspar in highly fractionated

Pegmatites has Rb value of >3000ppm, K/Rb < 30, and Cs value >100ppm which is evidence of Li-Cs-Ta mineralization (Tindle et al., 2002).

Pegmatites with feldspar extracts having the highest K/Rb values are the most primitive while the most evolved have the lowest K/Rb values. In Osogbo-Okinni area, two groups of pegmatites can be identified in the plot of K/Rb versus Cs. This plot shows group 'a' pegmatite with low level of fractionation and therefore low mineralization potential and group 'b' pegmatite with high level of fractionation and therefore high mineralization potential, (Figure 4.58). The pegmatites of Osogbo-Okinni area compare favourably with fertile granites in enrichment of Rb and Cs and K/Rb ratio, (Table 4.17).

In many pegmatite fields, strontium in K-feldspar has negative correlation with rubidium (Abad Ortega et al., 1993; Kontak and Martin, 1997). This means in highly evolved pegmatites with high rubidium values, strontium values will be lower. This is the case with some samples of feldspar extracts of the study area (Figure 4.59). The Ba/Rb ratio (Figure 4.60) follow the same trend as the Rb/Sr ratio in evaluating granitic pegmatite evolution while Pb concentration increases as the pegmatite evolve (Figure 4.61). As a result of the Rb incompatibility, fractionation increases Rb content of K-feldspar(Figure 4.62a). K/Rb values of feldspar extracts from Osogbo-Okinni pegmatites plot in a similar pattern (Figure 4.62a) with those from Scotland, Finland, and Canada, but these values are not as low as the values for the highly mineralized pegmatites of Canada.

4.3.3.2.2 Mica

Muscovite books occur in fertile and rare element pegmatites, it is therefore an excellent exploration tool and a direct pointer to likely Ta mineralization, (Gordiyenko, 1971). K, Li, Ta, Rb, and Cs are elements important in the analysis of muscovite. Ta versus Cs plot is a good indicator of Ta mineralization because mica extract in pegmatite with Ta value >65ppm, and >500ppm Cs has a high possibility of Ta-Nb mineralization.

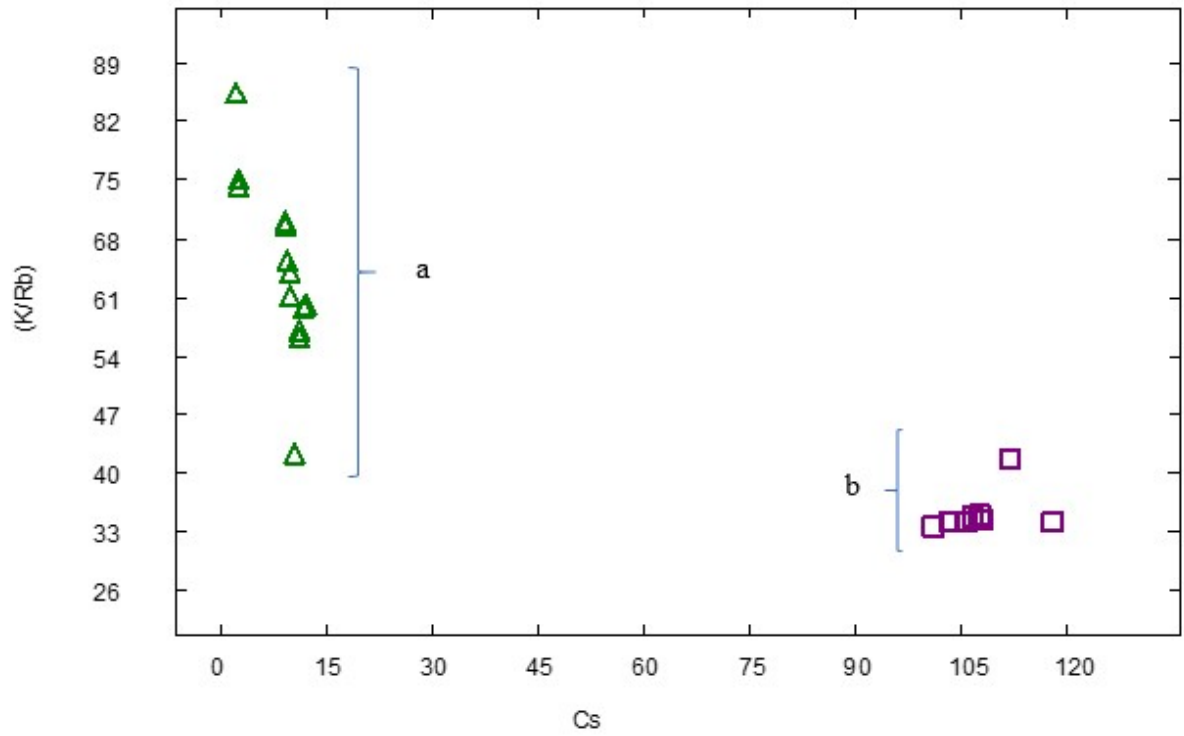


Figure 4.58 Plot of K/Rb vs Cs in K-feldspar showing groups 'a' and 'b' pegmatites, (after Breaks et al, 2003).

□ Complex pegmatites

△ Simple pegmatites

Table 4.17 Selected trace element contents and elemental ratio of K-feldspar of barren, fertile, and rare element pegmatites compared to Osogbo-Okinni pegmatite.

K-feldspar	Barren granite	Fertile granite	Rare element Pegmatite	Osogbo-Okinni Pegmatite N=22
Rb	<400	500-3,000	>3,000	68-1998
Cs	<10	20-100	>100	49
K/Rb	>150	30-150	<30	61

Data of Barren, fertile and rare element pegmatites from Tindle et al., 2002

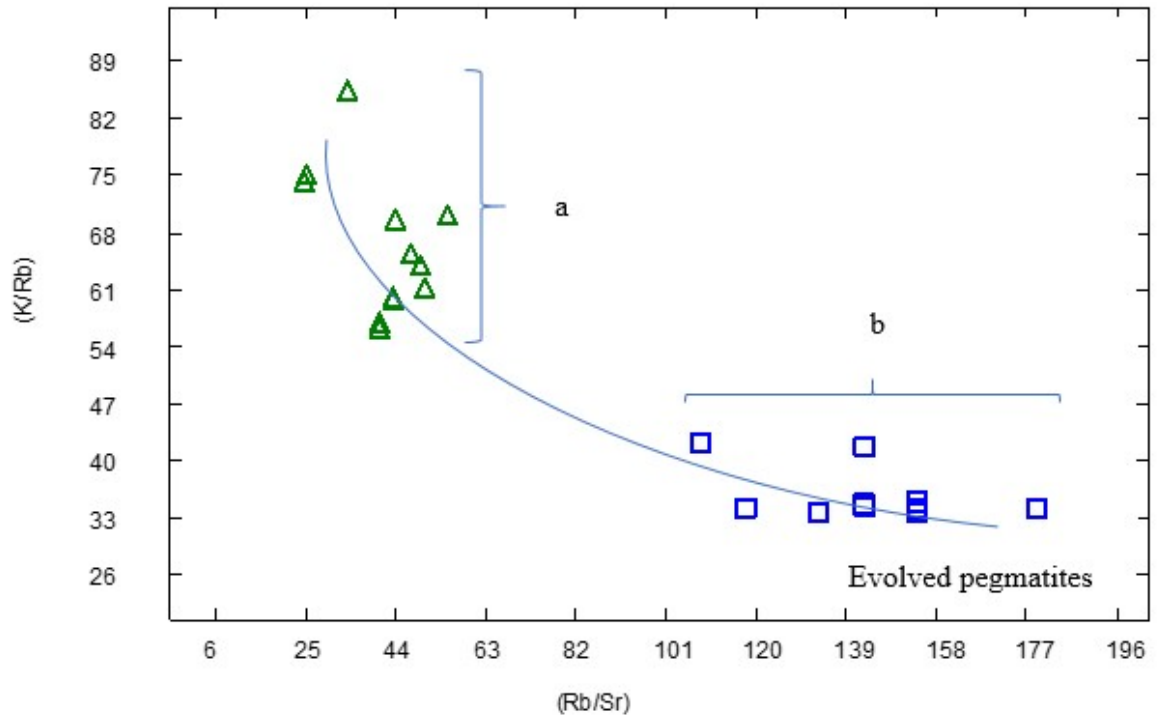


Figure 4.59 Plot of K/Rb vs Rb/Sr for K-feldspar showing trend of evolved pegmatites, (after Larsen, 2002)

△ Simple pegmatites

□ Complex pegmatites

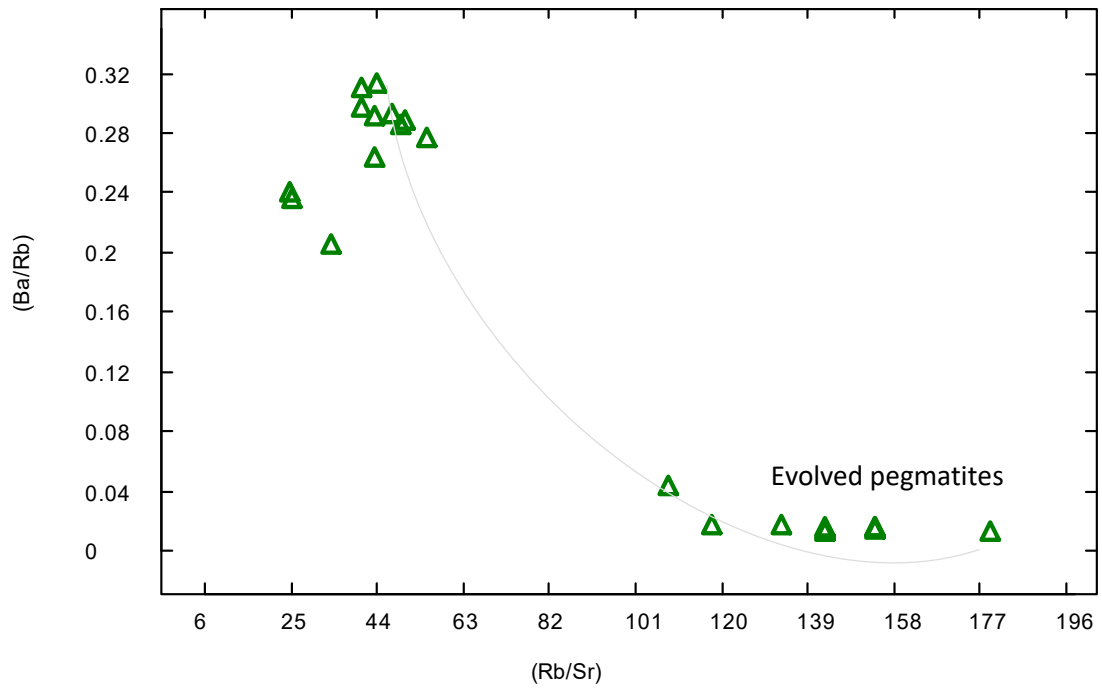


Figure 4.60 Plot of Ba/Rb vs Rb/Sr for K-feldspar showing trend of evolution, (after Larsen, 2002).

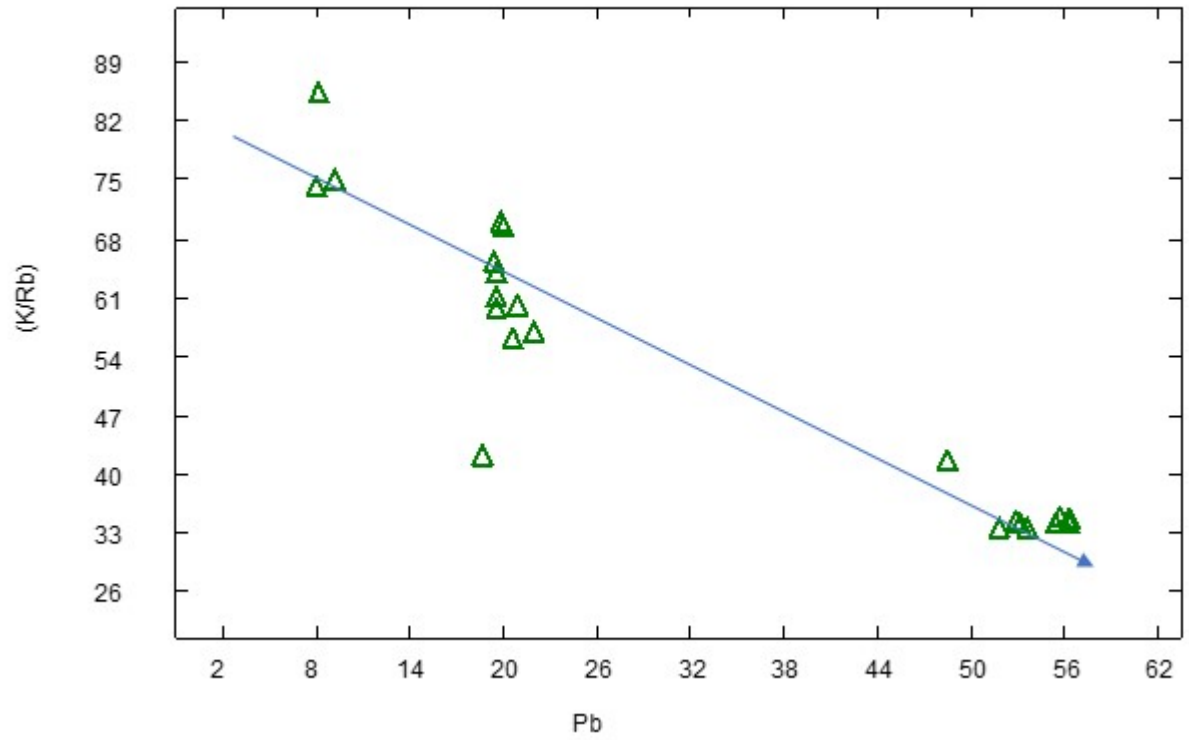


Figure 4.61 Plot of K/Rb vs Pb showing the evolution trend of pegmatites with increase in Pb concentration in feldspar extract, (after Larsen, 2002).

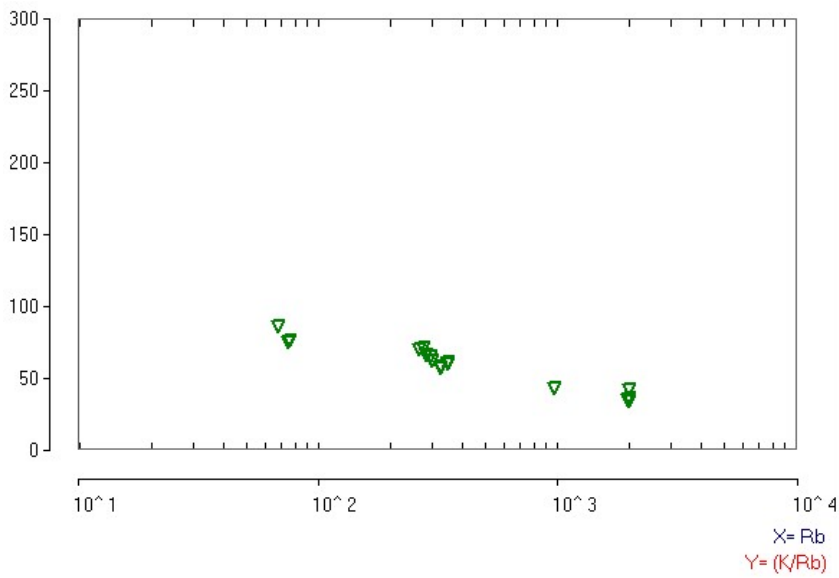


Figure 4.62a Plot of K/Rb vs Rb in Feldspar extracts of Osogbo-Okinni pegmatite

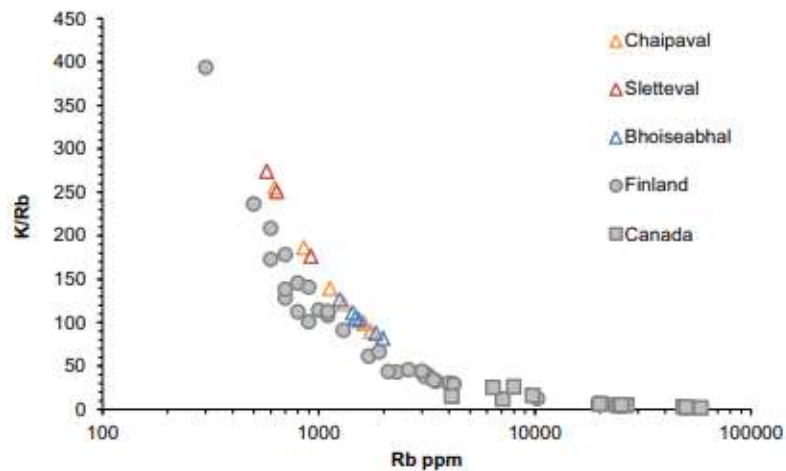


Figure 4.62b Plot of K/Rb vs Rb in K-feldspar from Chaipaval, Sletteval, Bhoiseabhal in Scotland (Shaw et al., 2016), Kaatiala, Finland (Lappalainen and Neuvonen, 1968) and Canada (Cerny et al., 2012b).

(Selway et al., 2005). Only three mica extract samples of Osogbo-Okinni pegmatites have values of Ta >65ppm while none have value of Cs >500ppm (Figure 4.63). High content of Li, Rb, Cs, and Ta in mica extracts of pegmatites of Osogbo-Okinni compare favourably with that of fertile granite, (Table 4.18).

The K/Rb versus Cs in mica is an excellent indicator of the pegmatite fractionation (Cerny, 1991). The measure of the change of K to Rb in mica crystal lattice is given by K/Rb. The arrow in Figure 4.64 indicates the pegmatites with high degree of fractionation.

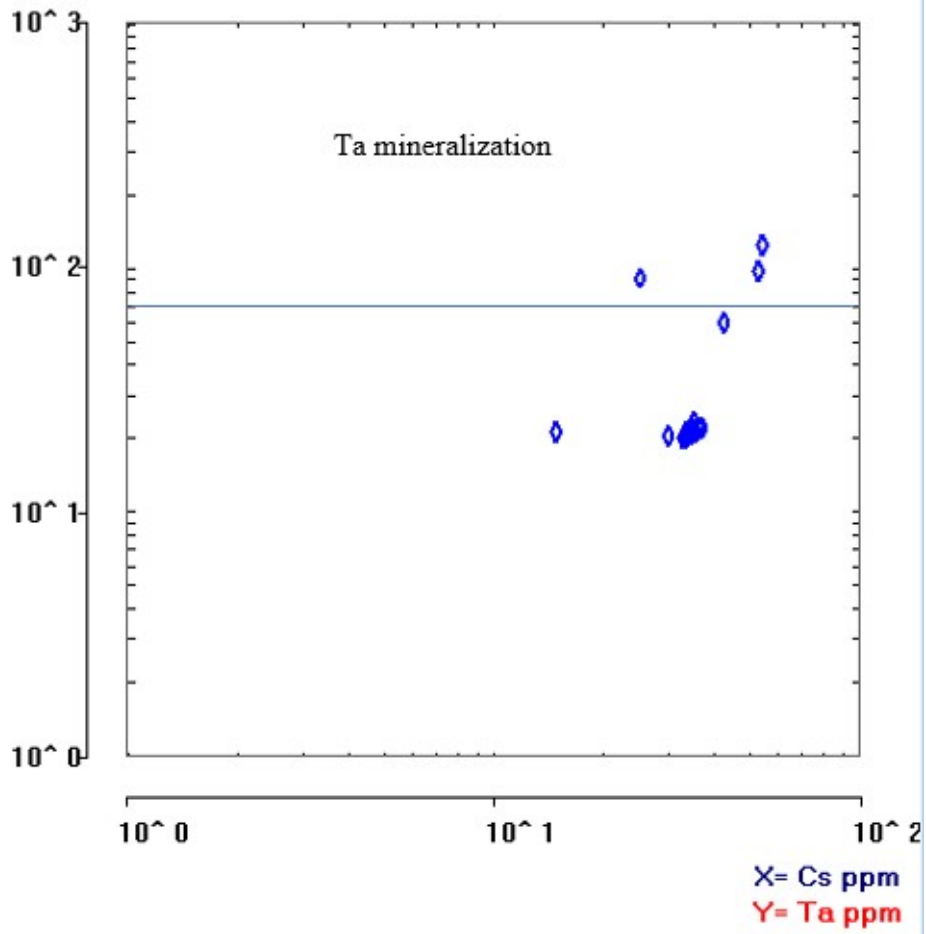


Figure 4.63 Ta mineralization in some mica extract samples above Gordiyenko, (1971) mineralization line.

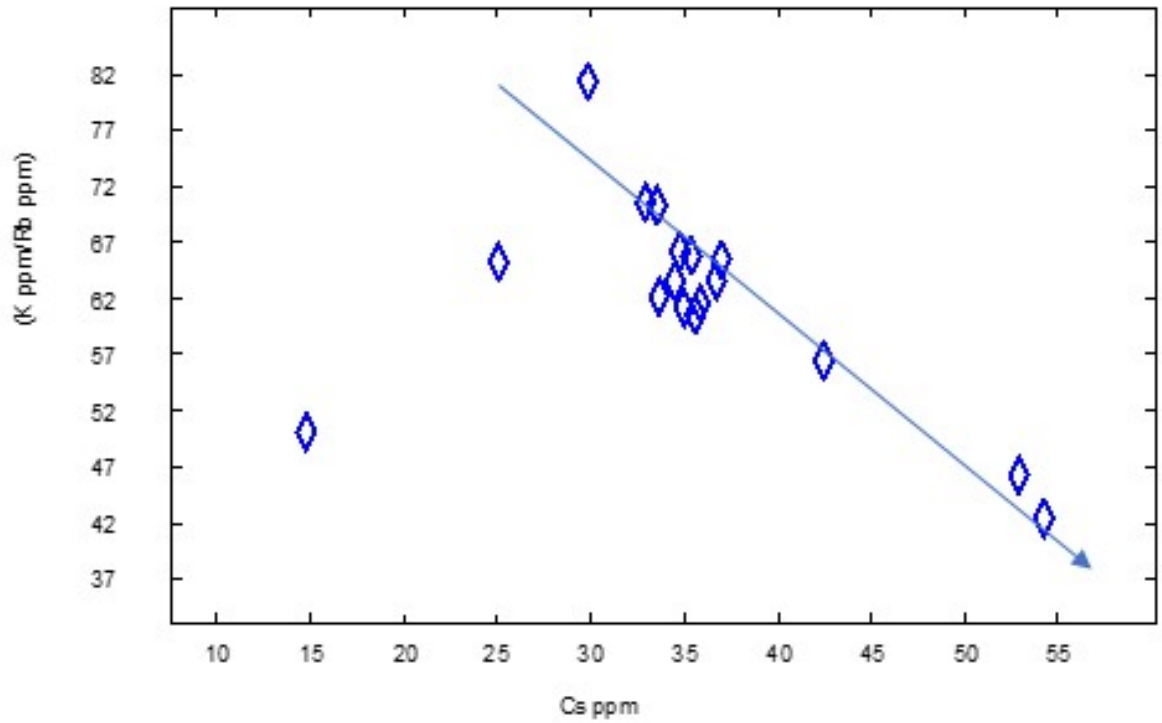


Figure 4.64 Plot of K/Rb vs Cs showing positive correlation between cesium and rubidium and degree of fractionation in mica extract of Osogbo-Okinni pegmatites, (after Breaks et al., 2003).

Table 4.18 Selected trace element contents, and elemental ratio of mica extracts of fertile granite, beryl-type, and spodumene-subtype pegmatites compared to Osogbo-Okinni pegmatite.

Elements/elemental ratios	Fertile granite	Beryl-type pegmatite	Spodumene-type pegmatite	Osogbo-Okinni pegmatite
Li	200-500	500-2,000	>2,000	139-448
Rb	1,000-1,500	1,500-10,000	>10,000	474-1602
Cs	10-100	100-500	>500	15-54
Ta	10-65	10-65	>65	20-124
K/Rb	50-100	20-50	<20	42-81

Data from Tindle et al., 2002b

4.3.4 The pegmatite groups of Osogbo-Okinni area.

The pegmatites of Osogbo-Okinni area can be classified as complex and simple types. The complex type has been identified by tantalite-niobium, tin and lithium mineralization in the whole rock, feldspar, and mica extracts. In the whole rock, the silica concentration of the complex pegmatites is lower than that of the simple, Fe_2O_3 concentration also have the same trend, while the Al_2O_3 content is higher in the complex pegmatites (Table 4.19). The complex pegmatites are characterized by enrichment in Sn, Sc, Hf, Rb, Li, Ta, Nb, Cs, and Be and depletion of Y, Ba, Cr, and Sr in whole rock relative to the simple type (Table 4.19). The mineralization maps of Osogbo-Okinni pegmatites shows the location and concentration of niobium, lithium, tin, and tantalum mineralization in the study area (Figures 4.65-4.68).

Beus, et al., (1968) and Cerny, (1989a) reported that pegmatites with Mg/Li ratio <10 are highly evolved with high potential for mineralization. The complex pegmatite type has high lithium content thus their Mg/Li ratio has a range of 1.23-10.64, while that of simple is between 13.75 and 36.54.

The whole rock is enriched in tantalum and niobium in the complex type to between $<100\text{ppm}$ to $>200\text{ppm}$.

Another differentiating factor between the complex and simple pegmatites is the positive Eu anomalies (Figure 4.69) exhibited by REE patterns of the simple pegmatites compared to the negative Eu (Figure 4.70) anomalies seen in the REE patterns of the complex pegmatites. The negative Eu anomalies may be an indication of plagioclase fractionation, or the melting of a source material depleted in plagioclase (Shaw et al., 2016). The simple pegmatite samples have lower Rb concentration indicating lower fractionation than the complex samples and the REE pattern which is like that from partially melted igneous rock may be controlled to a larger extent by the protolith than by a gaseous phase that may be introduced from the melt, (Tindle and Pearce, 1983).

Table 4.19. Comparison of selected oxides and trace elements in complex and simple pegmatites of Osogbo-Okinni area.

	Complex n=8 (wt%)		Simple n=14 (wt%)	
	Range	Average	Range	Average
SiO ₂	59.12-69.97	61.95	72.82-79.01	76.05
Al ₂ O ₃	16.96-22.97	21.18	11.93-15.08	12.97
Fe ₂ O ₃	0.62-1.19	0.95	1.08-1.40	1.26
	Ppm		Ppm	
Sn	11.00-89.40	57.55	5.40-8.90	6.84
Sc	0.40-12.10	7.41	0.90-2.00	1.50
Hf	1.53-10.04	6.87	0.15-0.72	0.39
Li	62.40-202.40	105.73	15.40-48.30	33.26
Rb	286.70-2000	553.84	161.40-344.20	212.51
Ta	89.40-259	188.76	0.2-6.5	2.69
Nb	52.19-202.96	139.50	1.83-36.81	19.29
Cs	10.50-20.80	13.81	2.40-8.60	4.13
Ga	18.75-44.33	36.10	13.45-21.53	16.53
Zr	8-81.8	55.64	4.10-16.40	8.83
Th	0.70-2.60	1.64	0.50-1.80	0.85
U	1.40-6.70	5.13	1.6-4.3	3
Y	1.20-9.80	4.30	4.80-8	6.44
Ba	55-434	217.86	30-861	321.71
Cr	3-9	5.25	6-10	8.07
Sr	11-46	27	7-97	38.79
Mg/Li	1.23-10.64		13.75-36.54	
K/Cs	1,375.22-5,570.54		2,065.04-17,645.77	
K/Rb	50.37-152.88		51.60-309	

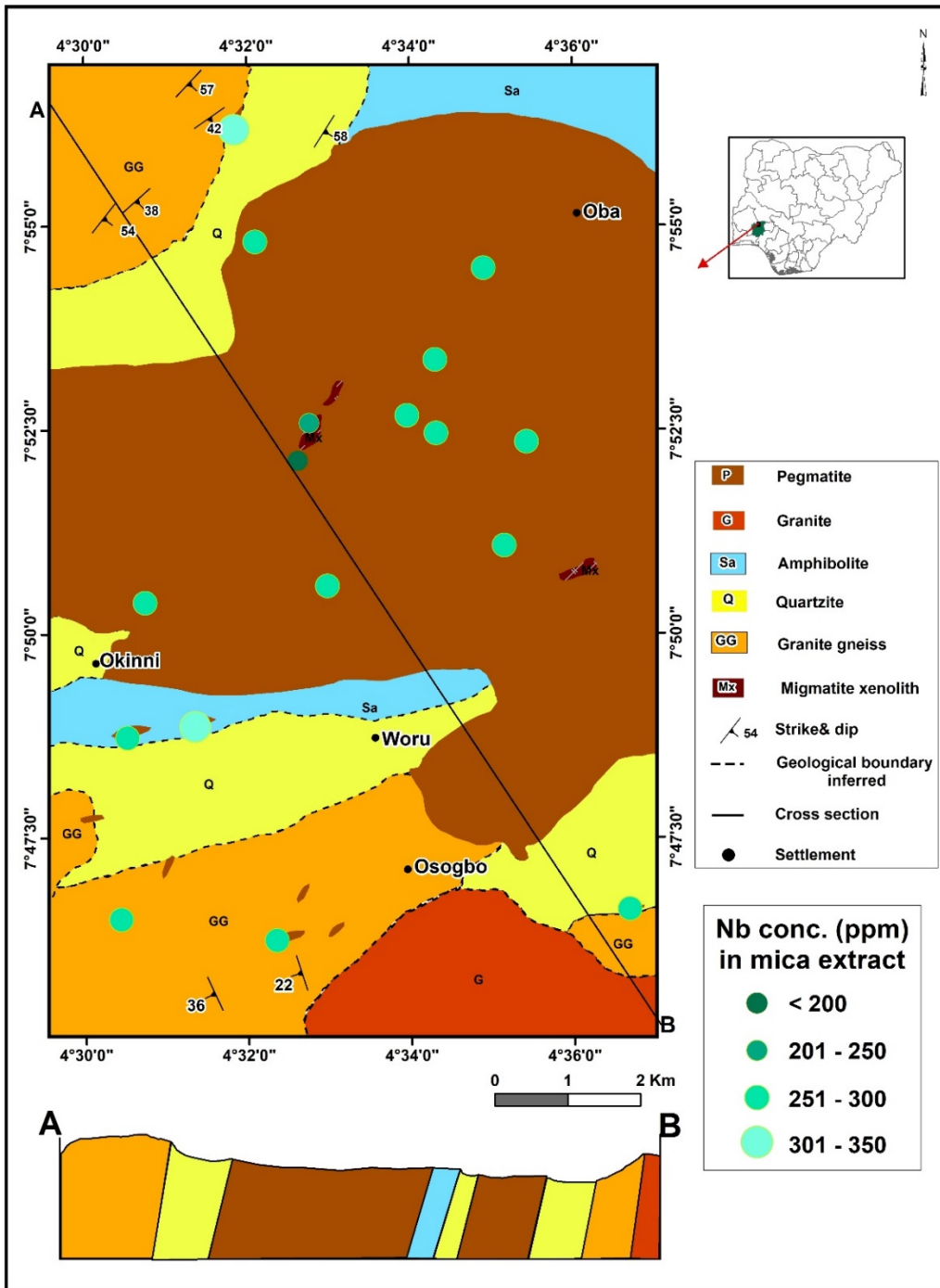


Figure 4.65 Distribution map of Niobium concentration in pegmatites of Osogbo-Okinni area

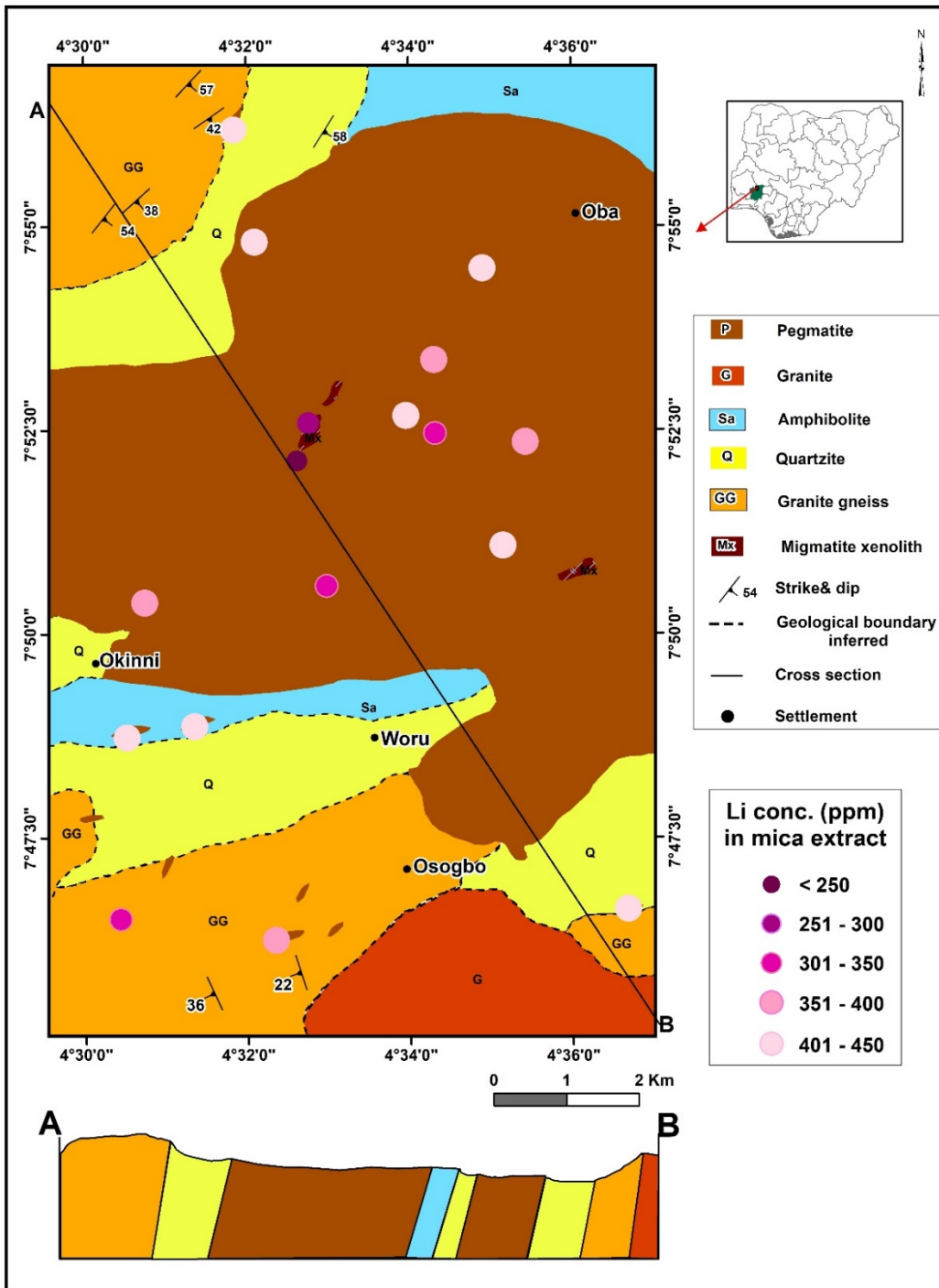


Figure 4.66 Distribution map of Lithium concentration in pegmatites of Osogbo-Okinni area

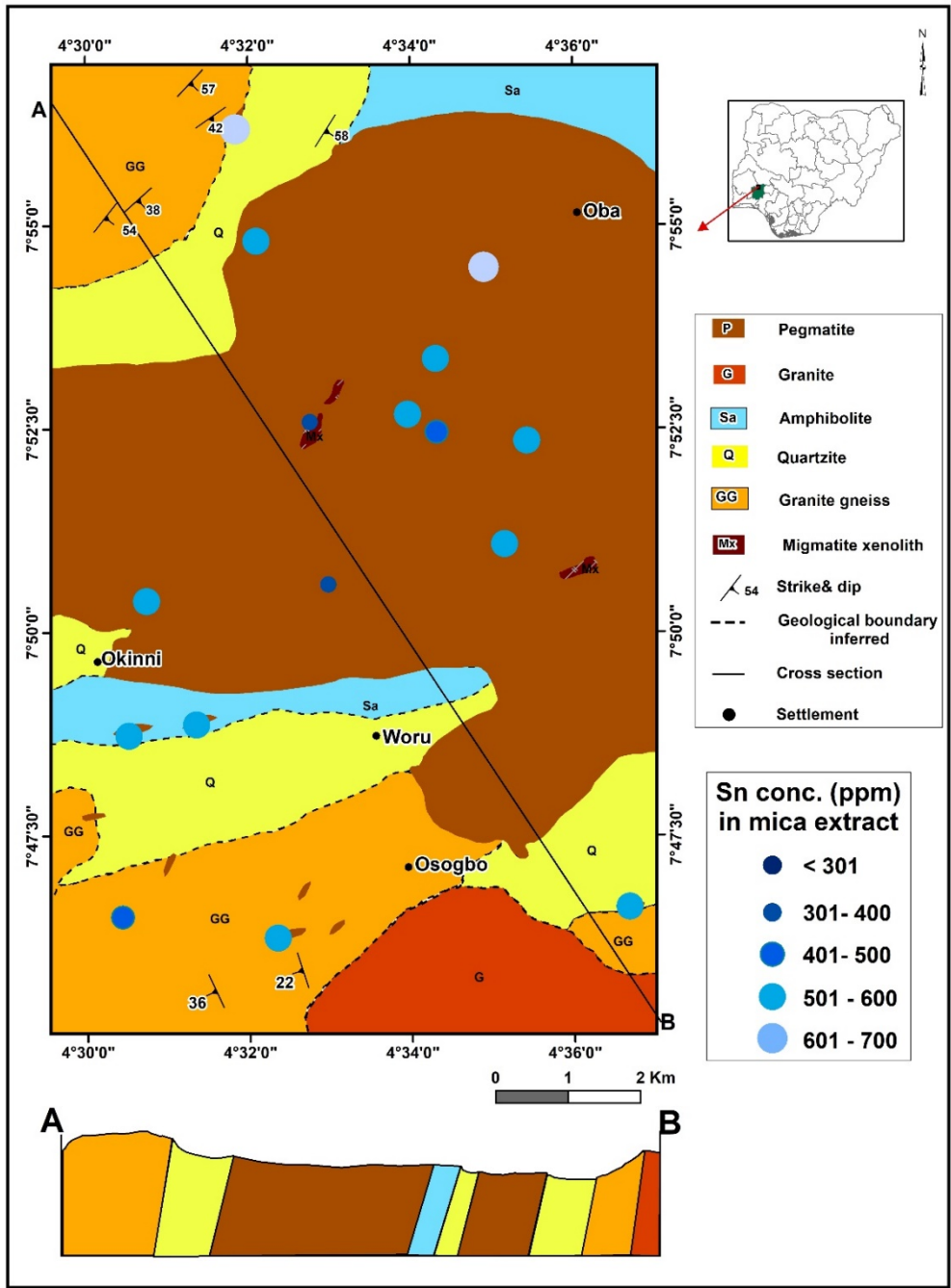


Figure 4.67 Distribution map of Tin concentration in pegmatites of Osogbo-Okinni area

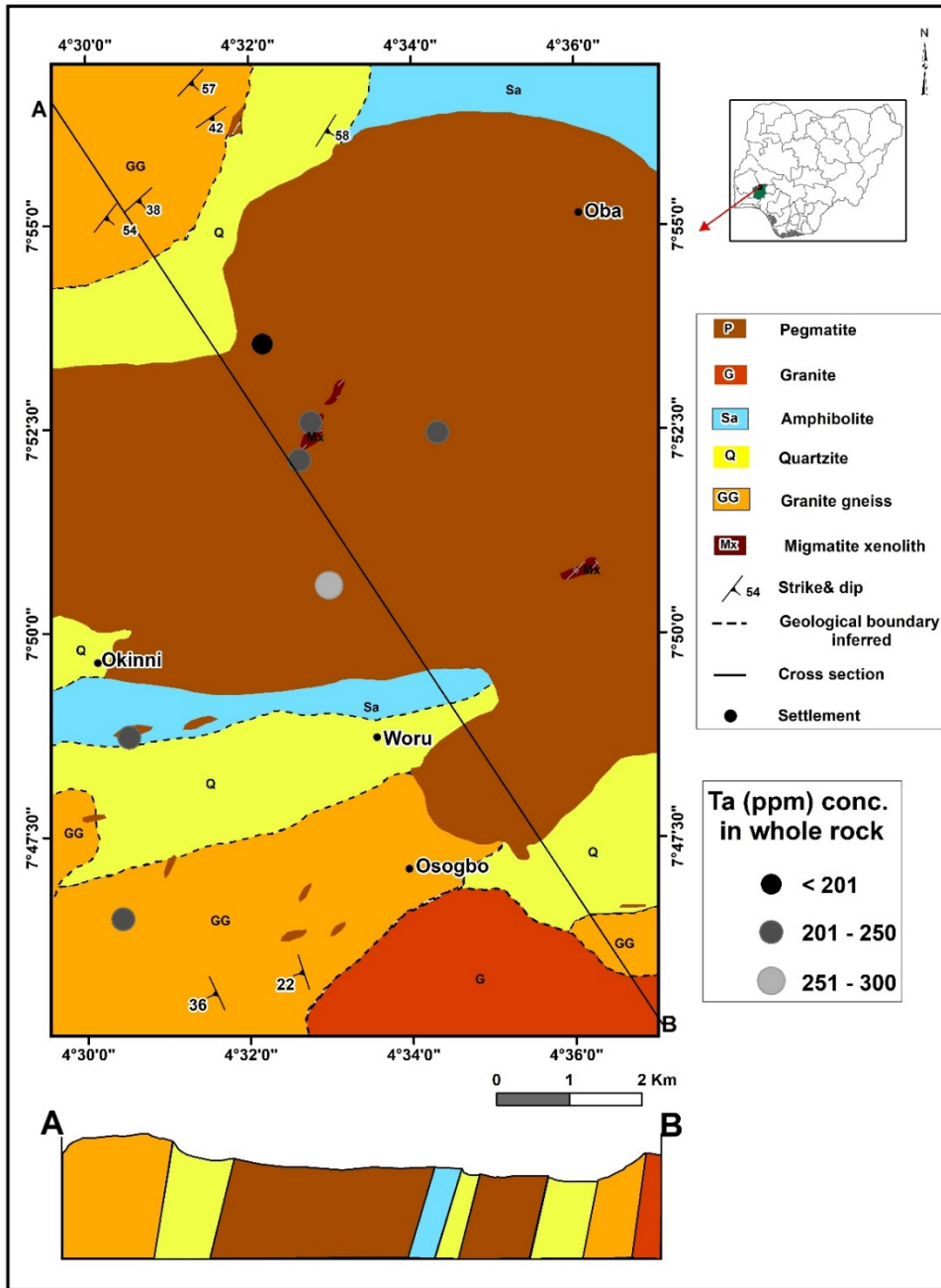


Figure 4.68 Distribution map of Tantalum concentration in pegmatites of Osogbo-Okinni area

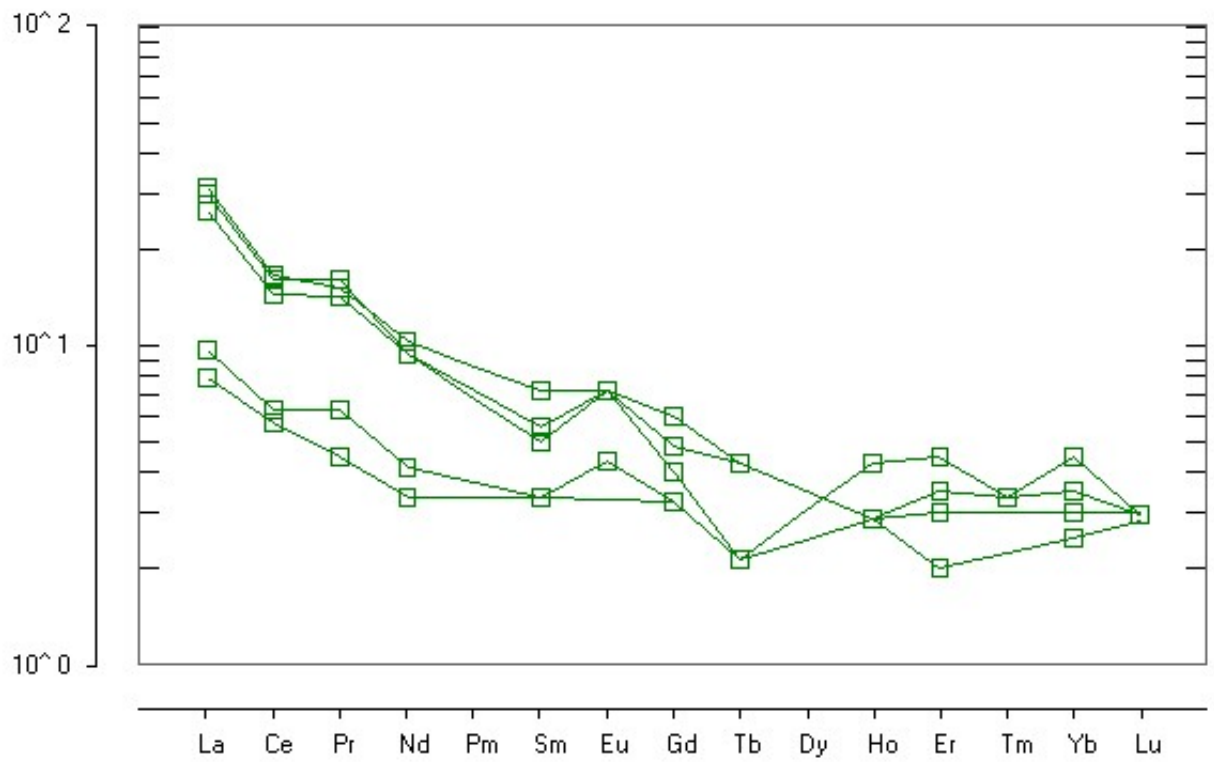


Figure 4.69 Spider diagram of REE content of some simple pegmatites of Osogbo-Okinni area showing positive Eu anomalies.

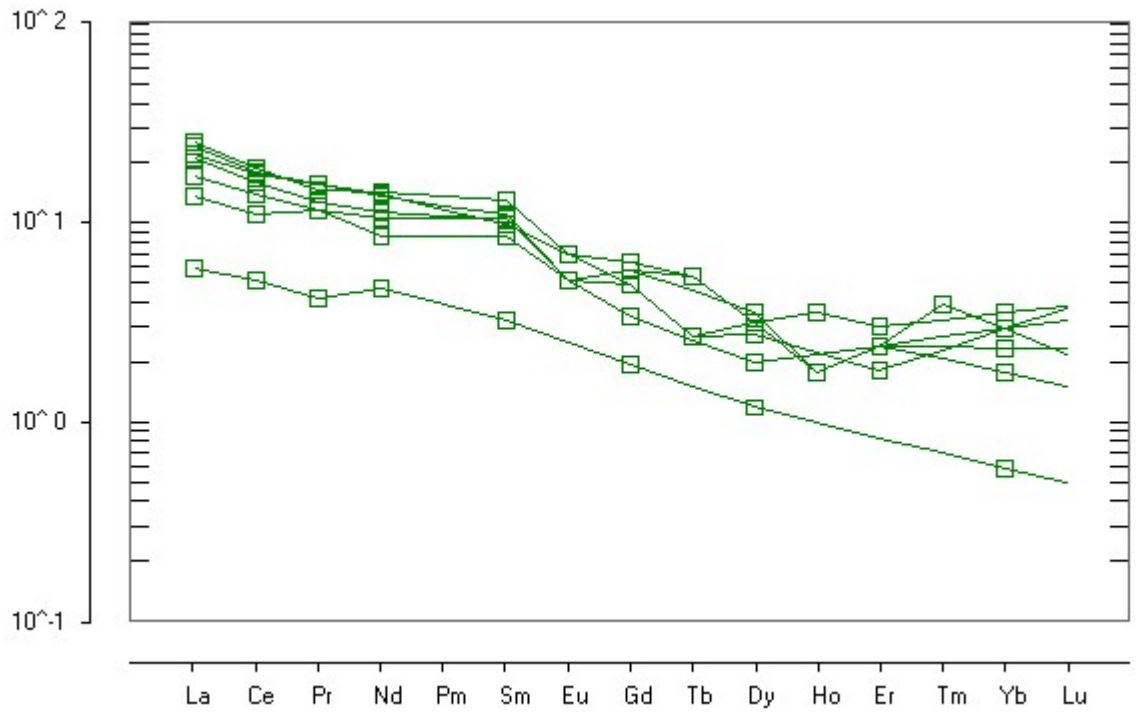


Figure 4.70 Spider diagram of REE content of complex pegmatites of Osogbo-Okinni area showing negative Eu anomalies.

The pegmatites of Osogbo-Okinni area intrude older gneissic and granitic rocks can be interpreted to be due to the proximity of a granitic protolith in the area. Also it could be due to the possibility that the complex or rare-metal pegmatites resulted from fractional crystallization of the granitic magma. Another explanation may be that the pegmatites were derived from fractionation of localized granitic bodies derived from crustal melting. A third possibility may be that spatial changes in local crustal materials control the pegmatite content. The possible occurrence of numerous source materials in the area explains the occurrence of the two types of pegmatites.

A model put forward by Shaw et al., 2016, may be found suitable to explain the formation of Osogbo-Okinni area pegmatites. It was suggested that the host rock forming these pegmatites melted at depth, and the magma combined into small magma bodies which became fractionated, and the enriched magma rose upwards to intrude into the country rock as pegmatites.

Harris et al., 1986 suggested a model like this where syn-collisional granites containing muscovite form during crustal-thickening periods. It was proposed that fluids enriched in volatiles rising into the crustal pile during tectonic movement may initiate partial melting by interacting with the over-riding sheet. Melts enriched in Rb, Ta, B and F are likely to result, and these elements are then moved by the gaseous phase.

Therefore, in an area of formation of partially melted granites and pegmatites in a large compression zone and thick crust, the source materials available for melting may control the composition of pegmatite rather than magmatic processes like fractional crystallization. There is a likelihood the content rather than the volume of protoliths, to be melted and fractionated over a long period, is more essential for the formation of rare-metal pegmatites.

Similarity in major oxide concentrations and some trace element concentrations in granites and pegmatites of Osogbo-Okinni area seems to indicate formation by anatexis of source materials and some amount of fractional crystallization, (Table 4.20).

Table 4.20 Major oxides and some trace element concentration of granite compared with those of the pegmatites of Osogbo-Okinni area.

Major oxides (wt%)	Granite	Pegmatite
SiO	72.04	70.91
Al ₂ O ₃	13.82	15.95
Fe ₂ O ₃	3.03	1.14
MgO	0.61	0.07
CaO	1.65	0.27
Na ₂ O	3.28	3.49
K ₂ O	3.98	4.23
TiO	0.27	0.02
Trace elements (ppm)		
Mo	0.80	0.66
Cu	9.70	13.09
Pb	25	31.77
Zn	25.48	34.29
Th	52.1	1.14
Sr	166.75	34.50
Ba	904.5	283.95
W	49.35	101.94
Zr	53.65	25.85
Sn	4.5	25.78
Y	14.75	5.66
Hf	1.60	2.75
Li	77.23	59.61
Rb	192.33	257.42
Ta	2.55	70.35
Nb	13.87	63
Cs	5.55	7.65
Ga	16.72	23.64
∑REE	312.55	21.14
∑LREE	305.61	18.92
∑HREE	6.94	2.22

The pegmatite is enriched in Al_2O_3 , Cu, Pb, Zn, Cs, W, Ta, Sn, Rb, Nb, and Ga and is depleted in Fe_2O_3 , MgO, TiO, Ba, Zr, Sr, Y and REE, which are left in the melt residue, when compared to granite which may indicate fractionation of the granite.

When compared to some well-studied pegmatites around the globe, Osogbo-Okinni pegmatite have very low concentration of K, Rb, Cs and Ga. However, it compares favourably in Ta concentration with that of Liberia, South Dakota, Namaqualand, and New Mexico. The ratios K/Rb and K/Cs is very high when compared to that of the others because of its depletion in Rb and Cs indicating comparatively lower fractionation, (Table 4.21).

Table 4.21. Geochemical characteristics of some well-studied pegmatites compared with Osogbo-Okinni Pegmatites

	Liberia	TipTop Dakota (low Ta)	Tanco Manitoba (high Ta)	Noumas Namaqualand	Harding New Mexico (low Ta)	Wamba Central Nigeria	Osogbo- Okinni
K (%)	8.08	8.52	8.33	8.21	9.47	n.d	3.51
Rb (%)	0.70	0.36	2.45	0.36	0.63	0.32	0.03
Cs (ppm)	556	222	2420	566	1917	116	7.65
Ta (ppm)	57	56	240.9	74.2	64	53	70.35
Ga (ppm)	163	175	433	92	123	n.d	24
K/Rb	12.6	24	3.4	23	15	25	117
K/Cs	198	384	34	145	49	800	4,590
No of samples	11	13	19	2	21	51	22

4.4 K-Ar geochronology

In Southwestern Nigeria, Pan African events have been divided into three age intervals by Rahaman, (1988), as pre 600Ma, 560 ± 40 Ma and 500Ma. Also, Caby, (1989), divided Pan-African tectono-metamorphic events in Northern Nigeria into threefold time interval, 750-700Ma – early Pan African orogenic event, 630-580Ma – main Pan-African episode and 580-520Ma – Late Pan-African orogenic event. These Pan-African events resulted in orogenic belts created during the Gondwana formation between the Neoproterozoic and Cambrian. These belts span the African continent to the Brasiliano orogen of South America (Stern, 1994; Jacob and Thomas, 2004). The Brasiliano orogeny of South America occur in three age intervals of Brasiliano I – 790Ma and 730-700Ma; Brasiliano II – 640-620Ma and 600Ma; Brasiliano III – 595-560Ma and 520-500Ma (Da Silva, et al., 2005).

The Pan-African orogenic belts consist of rocks of Archaean and Proterozoic age which have gone through Neoproterozoic to Cambrian orogenesis, plus a mixed portion of young materials. These belts are made up of extensive post-collisional granitoid plutons. The plutons are potassic and of magmatic protolith resulting from mixed materials of mantle and crust which form major content of the upper crust during Gondwana formation (Kuster and Harm, 1998).

Dating of five samples of pegmatite of Osogbo-Okinni area was undertaken using the K-Ar methodology known as Cassinot dating technique. Duplicate analyses were made for each sample using muscovite extracts from the pegmatites. The duplicates show different ages in the pair, which may be a result of inhomogeneity of the potassium content in the muscovite extract leading to differing radiogenic ^{40}Ar content. All analyses yielded 0.3-2.7% atmospheric ^{40}Ar content. This means the whole ^{40}Ar signal is potentially from radiogenic ^{40}Ar or may be a combination of radiogenic and inherited ^{40}Ar from the source of the pegmatite. K content is 5.45-7.26%, radiogenic ^{40}Ar , 336-483ppm and $^{36}\text{Ar}/^{38}\text{Ar}$, 0-10. All samples gave Neoproterozoic ages between Ediacaran and Tonian, $774-692 \pm 10$ Ma (Table 4.22)

The ages derived for the Osogbo-Okinni pegmatite samples by unspike K-Ar dating technique which is 774-692 Ma compare favourably with ages of early Pan African rocks identified in the basement complex of Nigeria (Table 4.23). Some examples include, Snelling, (1966), with a K/Ar age of 780 ± 40 Ma on hornblende derived from coarse porphyritic granite of Southern Kano, a part of the older granites identified in Northern Nigeria. Whole rock granite with foliations in Panyam area of Northcentral Nigeria was dated 677 ± 161 Ma by Rb/Sr method (Van Breemen et al., 1977). A whole rock isochron Rb/Sr age of 665 ± 65 Ma was reported by Ogezi, (1977), on hornblende granite and granodiorite around Mainci. Pegmatites of Wamba, central Nigeria and pegmatites of Osu, southwestern Nigeria were dated 750Ma and 700Ma respectively by Matheis and Caen-Vachete, 1983.

Old Pan African rocks, 730Ma, were reported by Ferre et al., (2002), in Eastern Nigeria and were correlated with the Eastern Hoggar using the U-Pb zircon dating technique. Signature of an early phase of magmatism at 790-760Ma was recorded in Batholith of older granite in Minna, Northwestern Nigeria (Goodenough, 2014). U-Pb zircon dating of pegmatites of Ede area, Southwestern Nigeria, gave $709 \pm 27/-19$ Ma (Adetunji et al., 2016).

This Neoproterozoic Pan-African suite of rocks are present in Pan-African province of Madagascar as syntectonic (750-600Ma) and post tectonic (500Ma) pegmatites (Petters, 1991). Also, the Tazigzaout complex within BouAzzer inlier of Anti-Atlas orogenic belt of Morocco consist of metagabbro, augen granite gneiss, syn-tectonic leucogranite, closely banded granite gneiss with sheeted muscovite-biotite granite crosscutting the meta-igneous rocks. The muscovite-biotite granite gave $705 \pm 2/-3$ Ma age (D'Lemos et al., 2006). Stratigraphic sequence derived from volcanic and sedimentary events in Borborema province of Brazil has signatures of Neoproterozoic magmatism with age at 780-770Ma. This is believed to be associated with break apart through faulting due to plate tectonics around continental margins (Fetter et al., 2003; Arthaud et al., 2008)

Table 4.22 Unspike K-Ar ages of Osogbo-Okinni pegmatites

Sample No.	% atm- ⁴⁰ Ar	error	% K content	rad_ ⁴⁰ Ar (ppb)	Error	³⁶ Ar/ ³⁸ Ar	Error Error	Unspiked Age
1	2.7	0.3	6.69	442	6	10	30	760 10
2	0.6	0.2	6.89	403	5	2	6	692 8
3	0.2	0.3	7.26	478	7	0	100	760 10
4	1.2	0.3	5.45	336	5	2	4	720 10
5	0.3	0.3	7.2	483	5	0	300	774 8

Table 4.23 Derived absolute age of Osogbo-Okinni pegmatites compared to other Neoproterozoic rocks of Nigeria, Africa, and South America

	Rock Type and Location	Dating Method	Age	Reference
1	Muscovite extract in Osogbo-Okinni pegmatite	Unspike K-Ar (Cassignol Technique)	774-692 \pm 10 Ma	This study
2	Pegmatite of Wamba, Central Nigeria		750 Ma	Matheis and Caen Vachette, 1983
3	Osu pegmatite, Southwestern Nigeria		700 Ma	=ditto=
4	Ede pegmatite, Southwestern Nigeria	U-Pb Zircon	709 \pm 27/-19 Ma	Adetunji et. al., 2016
5	Komu pegmatite, Southwestern Nigeria	K/Ar	515-503 \pm 13 Ma	Okunlola and Udo udo, 2006
6	Hornblende in Coarse Porphyritic granite of Southern Kano, Nigeria	K/Ar	780 \pm 40 Ma	Snelling, 1966
7	Whole rock granite of Panyam area, Northcentral, Nigeria	Rb/Sr	677 \pm 161 Ma	Van Breemen et al., 1977
8	Whole rock hornblende granite and granodiorite around Maiinci, Northern Nigeria	Rb/Sr	665 \pm 65 Ma	Ogezi, 1977
9	Early phase magmatism in older granite of Minna, Northwestern Nigeria		790-760 Ma	Goodenough, 2014
10	Biotite granite of Morocco	U-Pb Zircon	705 \pm 2/-3 Ma	D'Lemos et al., 2006
11	Volcano-sedimentary rock of Borborema Province, Brazil		780-770 Ma	Fetters et al., 2003; Arthaud et al., 2008

4.5 Indications from the study

Field study of Osogbo-Okinni area was undertaken by geological mapping to a scale of 1:25,000. The rock types identified are migmatite, which occur as xenoliths of relicts of assimilated old mafic rocks in pegmatites in some locations, granite gneiss, quartzite, amphibolite, granite, and pegmatites. Granite gneisses occur as low-lying outcrops at the extreme northwestern and southwestern part of the area and a part of southeast. Quartzite occupies the northeastern part as inselbergs, in the southwest and southeast as ridges north of the granite gneisses. Amphibolite occurs as low-lying outcrops north of the quartzite at the southwestern and at the extreme northeastern part. Granites occur at the extreme southeastern part of the area. This indicate that Osogbo-Okinni pegmatites intrude these older rocks which are in proximity and may have their protolith from one or combination of the older rocks, especially granite.

Quartz, plagioclase, microcline are the main minerals in these rock types with biotite, muscovite, hornblende as minor minerals with zircon, garnet, and opaque minerals as accessories from petrographic studies. However, amphibolite has, in addition to quartz, plagioclase and microcline, as main minerals biotite and hornblende with average modal composition of 17.5% and 21.25% respectively. The pegmatites contain no hornblende as usual indicating a felsic composition. The high content of feldspar, plagioclase and microcline makes the pegmatites suitable for exploitation for industrial use.

Geochemical analysis reveals the composition of granite gneisses as SiO₂ (69.11%), Al₂O₃ (14.82%), Fe₂O₃ (3.32%), MgO (0.72%), CaO (1.95%), Na₂O (3.02%), K₂O (4.35%), TiO₂ (0.32%), P₂O₅ (0.17%), and MnO (0.05%). the gneisses are peraluminous, of igneous origin as indicated by the plot of Na₂O/Al₂O₃ vs K₂O/Al₂O₃ and have protolith with calc-alkaline nature as specified by AFM diagram. The plot of Rb vs Nb+Y put the gneisses in the VAG and WPG tectonic fields. Granite geochemical content include SiO₂ (72.04%), higher than the gneisses and amphiboles, Al₂O₃ (13.82%), Fe₂O₃ (3.03%), MgO (0.61%), CaO (1.65%), Na₂O (3.28%), K₂O (3.98%), TiO₂ (0.27%), P₂O₅ (0.19%), and MnO (0.02%). The granites are peraluminous, of igneous origin and have high potassic nature

as revealed by the plot of K_2O vs SiO_2 . Na_2O+K_2O vs SiO_2 diagram put the rock in the granite and granodiorite fields. Granites are depleted in some fractionation indicator trace elements like Sn (4.5ppm), Li (77.23ppm), Rb (192.33ppm), Ta (2.55ppm) and Nb (13.87ppm). Low Rb/Sr and high Ba/Rb elemental ratios points to absence of mineralization in the granites. The granites plot in the tectonic field of VAG + Syn-COLL. The Rb vs Sr give an emplacement depth of <30km - >30km for the granites.

Pegmatites occur as thin to large veins intruding the older rocks and as low-lying to mountainous plutons with dimensions up to 100mx50m in some cases, occupying the central part of the area. Mineral composition include quartz, plagioclase, microcline, biotite, muscovite, tourmaline and opaque.

Geochemical analysis results reveal that the pegmatites are granitic with high silica average content of 70.92% in the whole rock, while the feldspar and mica extracts have average lower content of 56.81% and 43.55% respectively, Na_2O content in the same trend is 3.49% in whole rock, 3.04% in feldspar and 0.86% in mica extracts. However, Al_2O_3 content increases from 15.95% in whole rock to 27.03% in feldspar and 29% in mica extracts, similarly K_2O content increases from 4.23% in whole rock, to 4.70% in feldspar and 8.10% in mica extracts. Mica extracts have the highest content in Fe_2O_3 (2.88%), MgO (0.45%) and TiO_2 (0.12%).

The average content of trace elements in whole rock such as Sr (34.50ppm), Ba (283.95ppm), W (101.94ppm) and Ta (70.35ppm) are higher than those for feldspar and mica extracts, while mica extracts have average higher content of Zn (239.17ppm), V (8.76ppm), Sn (510.86ppm), Sc (104.86ppm), Li (376.88ppm), Rb (1101.97ppm), Nb (272.41ppm) and Ga (68.16ppm) than whole rock and feldspar extracts. The average REE content of whole rock (21.14ppm) and is higher than that of mica extracts (9.59ppm) and feldspar extracts (5.58pp). The plot of Al_2O_3/Na_2O+K_2O against $Al_2O_3/CaO+Na_2O+K_2O$ reveal the peraluminous nature of these pegmatites, and the variation plot of Na_2O/Al_2O_3 against K_2O/Al_2O_3 suggest a granitic-igneous source. The presence of granite and granite gneiss at the South to Southwest and Northwest of the study area may affirm this

postulation. K/Rb against Cs diagram put the pegmatites in the muscovite class of the LCT pegmatite family. High rubidium and low K/Rb values indicate that some of these pegmatites are highly fractionated resulting in tantalum mineralization in whole rock samples of some pegmatites in the area and tin, lithium, and niobium mineralization in mica extracts of some of the pegmatites, in the plots of Ta against Rb+Cs, Ta against Rb and Ta against K/Cs where the mineralized samples fall above the Beus, (1966) and Gordiyenko, (1971) lines.

The pegmatites have been grouped into complex and simple. The complex pegmatites are enriched in Sn, Sc, Hf, Rb, Li, Ta, Nb, Cs and Be and are depleted in Y, Ba, Cr and Sr. The values of ratio Mg/Li <10 indicate mineralization and the complex group have Mg/Li values in the range of 1.23-10.64, while that of simple is 13.75-36.54. Also, positive Eu anomalies are exhibited by REE patterns of the simple pegmatites compared to negative Eu anomalies in REE patterns of complex pegmatites. The mineralisation of the complex pegmatites may be the result of continuous and progressive fractionation of a large protolith of granitic composition buried deep below in the area. Another possibility is the melting of the protolith at depth and the resultant magma combined into small magma bodies which became fractionated, and the enriched magma rose upwards to intrude into the country rock as pegmatites.

A model where syn-collisional granites containing muscovite form during crustal-thickening periods was suggested by Harris et al., 1986. It was proposed that fluids enriched in volatiles rising into the crustal pile during tectonic movement may initiate partial melting by interacting with the over-riding sheet. Melts enriched in Rb, Ta, B and F are likely to result, and these elements are then moved by the gaseous phase.

The process of partial crustal melting is further explained by Pearce, (1996). This process involves not just partial melting of the crust but also effective separation of the melt from residue. The principal controls on the composition of the resulting magma are the composition of the crust undergoing melting and the nature of the residue from melting. The principal controls on the degree of melting includes the presence or absence

of free fluid, the mineralogy of the protolith and the temperature and pressure. In general, small degrees of melting give the most siliceous products and the lowest concentrations of those elements that depend on minor phase solubility. Given a sufficient degree of melting, the yield strength of the resultant mush may be sufficiently reduced that the whole crust (melt and restite) is mobilised (Arzi, 1978). The resulting granite body then has the composition of the original crust and can evolve by separation of melt from restite as well as by crystallisation of the melt fraction.

Five samples of muscovite extracts from the pegmatites were used to date the pegmatites using a K-Ar dating method called the Cassinol dating technique. This yielded an age range between Ediacaran and Tonian, $774-692 \pm 10$ Ma. This age is agreeable with the ages of early Pan African rocks identified in the basement complex of Nigeria, like 750 Ma for pegmatites of Wamba, central Nigeria, and early phase of magmatism (790-760 Ma) reported in batholith of older granite in Minna, Northwestern Nigeria.

CHAPTER FIVE

SUMMARY, CONCLUSION AND RECOMMENDATION

5.1 SUMMARY

Geological mapping of Osogbo-Okinni area to a scale of 1:25,000 reveal the presence of migmatite, granite gneiss, quartzite, amphibolite, granite, and pegmatites. Petrographic studies indicated the main mineral constituent of Osogbo-Okinni pegmatites to be quartz, plagioclase and microcline with biotite, muscovite, and tourmaline as minor minerals while zircon, garnet and opaque minerals are accessories.

Geochemical analysis result reveals the granitic nature of the pegmatites with high silica and alumina content, low major alkali, and alkaline earth contents. Trace elements such as tantalum are enriched in whole rock, while zinc, tin, lithium, rubidium and niobium are enriched in mica extracts.

Osogbo-Okinni pegmatites are peraluminous and have granitic-igneous protolith. They belong to the muscovite class of the LCT pegmatite family. Some whole rock samples of these pegmatites contain tantalum mineralization while mica extracts of some samples have high contents of tin, lithium, and niobium. The pegmatites of Osogbo-Okinni area have been grouped into two based on their enrichment or otherwise in rare metals. The complex pegmatites have rare metal mineralisation in whole rock and mica extracts, but the simple pegmatites do not.

The Cassinoli dating technique of K-Ar dating method was used to date five samples of mica extracts from these pegmatites. The result of the dating was $774-692 \pm 10$ Ma, an age range between Ediacaran and Tonian which is early Pan African.

5.2 CONCLUSION

The pegmatites of the study area low-lying to mountainous plutons of igneous origin, peraluminous, and belong to the muscovite class of the LCT pegmatite family. They have been grouped into two, mineralized and unmineralized based on the enrichment of Ta, Sn, Li and Nb. K-Ar dating using Cassinol technique yielded Neoproterozoic age of 774 - 692 \pm 10Ma.

5.3 RECOMMENDATION

In view of its high modal composition of plagioclase (23-59%) and microcline (14-41%) from petrographic studies, the pegmatites of Osogbo-Okinni area is recommended for exploitation of its feldspar for industrial uses such as ceramic wares, floor tiles, glass making, filler and extender in paints, plastic, and rubber. In addition, through different extraction processes, the rare metals Ta-Nb-Sn-Li can be exploited especially from the mica extracts as revealed by geochemical studies of these pegmatites. Further exploration work to calculate the reserve of feldspar and mica is also recommended. All these are in line with the nation's quest to increase its foreign exchange earnings by diversifying its economy with solid mineral exploration and exploitation.

Further academic research can be undertaken in the underlisted areas of interest.

1. Fluid inclusion studies should be carried out to decipher the characteristics of the mineralizing fluid to delineate the mineralizing processes.
2. More isotopic studies should be carried out to compare the age from the K-ArCassinol technique dating.
3. Studies on comparison of geochemical features and absolute age between the pegmatites of Nigeria and Brazil on the east coast of South America.

5.4 CONTRIBUTIONS TO KNOWLEDGE

1. Geological map of Osogbo-Okinni area at the scale of 1:25,000

2. Delineation of simple and complex pegmatites in the area
3. Location of Ta-Nb-Sn-Li mineralization, location maps with mineralization concentration.
4. Dating of the pegmatites - $774 - 692 \pm 10$ Ma.

REFERENCES

- Abaa S.I., 1983. The structure and petrography of alkaline rocks of the Mada Younger Granite Complex, Nigeria. *J Afr Earth Sci* 3:107–113
- Abad Ortega, M.D.M., Hach-Ali, P.F., Martin-Ramos, J.D. and Ortega-Huertas, M., 1993. The feldspar of the Sierra Albarrana granitic pegmatites, Cordoba, Spain. *Can. Minerals*. 31, 185-202
- Adeleye, D.R., 1974. Sedimentology of the fluvial Bida Sandstones (Cretaceous), Nigeria. *Sediment Geol* 12:1–24
- Adetunji, A., Olarewaju, V.O., Ocan, O.O., Ganev, V.Y. and Macheva, L., 2016. Geochemistry and U-Pb Zircon geochronology of the pegmatites in Ede area, SouthWestern Nigeria: A newly discovered oldest Pan African rock in SouthWestern Nigeria. *Journal of African Earth Science*
- Agboola, S.A., 1979. An agricultural atlas of Nigeria. *Oxford University Press, Nigeria* p.248
- Ajakaiye, D.E., 1983. Deep structures of alkaline ring complexes from geophysical data. *In: Abstract, international conference on alkaline ring complexes in Africa. Zaria, Nigeria*
- Ajibade, A.C., Fitches, W.R. and Wright, J.B., 1979. The Zungerumylonites, Nigeria: recognition of a major unit. *Rev de GeolGeog Phys* 21:359–363
- Akintola, A.I., Ikhane, P.R., Okunlola, A.O., Akintola, G.O. and Oyebolu, O.O., 2012. Compositional features of Precambrian pegmatites of Ago-Iwoye area, Southwestern Nigeria. *Journal of Ecology and the Natural Environment* 4.3:71-87
- Ale, P.T, Dada, J.A. and Adewumi, A.J., 2014. Industrial Minerals Potentials of Ijero Pegmatite in Ekiti State, Southwestern Nigeria *World Applied Sciences Journal* 29 (3): 415-420, 2014
- Aldrich, L.T. and Neir A.O., 1948. Argon 40 in potassium minerals. *Rev.*, 74, 876-877

- Alfonso, A.P., Melgarejo, J.C., Yusta, I. and Velasco, F., 2003. Geochemistry of feldspars and muscovite in granitic pegmatite from Cap de Creus field, Catalonia, Spain. *Can. Mineral.* 41, 103-116
- Arthaud, M.H., Caby, R., Fuck, R.A., Dantas, E.L. and Parente, C.V., 2008. Geology of the Northern Borborema Province, NE Brazil, and its correlation with Nigeria, NW Africa, in: Pankhurst, R. J., Trouw, R. A. J., Brito Neves, B. B., De Wit, M. J. (Eds.) West Gondwana: Pre-Cenozoic Correlations across the South Atlantic Region. *Geological Society, London, Special Publication 294*, pp.49-67.
- Arzi, A.A., 1978. Critical phenomena in the rheology of partially molten rocks: *Tectonophysics*, v. 44, pp. 173-184
- Aston, F.W., 1921. The mass spectra of the alkali metals. *Phil. Mag., ser. 6*, 42. 436-441
- Beus, A.A., 1966. Distribution of tantalum and niobium in muscovites from granitic pegmatites. *Geokhimiya* 10. 1216-1220
- Beus, A.A., Berengilova, V.V., Grabovskaya, L.I., Kochemasov, G.G. and Leont'yeva, L.A., and Sitnin, A.A., 1968. Geochemical exploration for endogenic deposits of rare elements (citing tantalum as an example). *Geological Survey of Canada Library, Ottawa, Ontario*.
- Billman, H.G., 1976. Offshore stratigraphy and paleontology of the Dahomey embayment. *Proceedings, 7th African micropaleontology colloquium, Ile-Ife*
- Black, R., 1980. Precambrian of West African. *Episode, Vol No. 4*, 3-8
- Black, R., 1984. The Pan African event in the geological framework of Africa. *Pangea* 2, 6-16
- Bowden, P., van Breemen, O., Hutchison, J. and Turner, D.C., 1976. Palaeozoic and Mesozoic age trends for some ring complexes in Niger and Nigeria. *Nature* 259:297-299
- Bowden, P. and Kinnaird, J.A., 1984. Geology and mineralization of the Nigerian anorogenic ring complexes. *Geologisches Jahrb (Hannover)* B56, 3-65

- Bruguier, O., Dada, S., and Lancelot, J.R., 1994. Early Archaean component (.3.5 Ga) within a 3.05 Ga orthogneiss from northern Nigeria: U-Pb zircon evidence. *Earth and Planetary Science Letters*, 125, 89–103
- Breaks, F.W., Selway, J.B., and Tindle, A.G., 2003. Fertile peraluminous granites and related rare element mineralization in pegmatites, Superior province, northwest, and northeast Ontario: Operation treasure hunt. *Ontario Geological Survey, open file report 6099, 179p*
- Burke, K.C., Dewey, J.F., 1972. Orogeny in Africa. In: Dessauvage TFJ, Whiteman AJ (eds), Africa geology. *University of Ibadan Press, Ibadan, pp 583–608*
- Caby, R., 1989. Precambrian terranes of Benin-Nigeria and Northeast Brazil and the late Proterozoic South Atlantic fit, in: Dallmeyer, R.D. (Eds), Terranes in the Circum-Atlantic Palaeozoic Orogens. *Geological Society of America Special Paper 230, pp. 145-158.*
- Cameron, E.N., Jahns, R.H., McNair, A.N. and Page, L.R., 1949. Internal structure of granitic pegmatites. *ECON. GEOL. MONOGR*
- Cassagnol, C., 1973. Remarks on mass spectrometric measurements of argon isotope peaks. *Fortschr. Mineral.*, 50: 57 (abstract).
- Cassagnol, C. and Gillot, P.Y., 1982. Range and effectiveness of unspiked potassium-argon dating: experimental groundwork and applications. In: G.S. Odin (Editor), *Numerical Dating in Stratigraphy*. Wiley, Chichester, pp. 159-179.
- Cerny, P., 1982. Petrogenesis of granitic pegmatites. In *Granitic Pegmatites in Science and Industry* (P. Cerny, ed.). *Mineral Assoc. Can., Short course handbook 8, 405-461*
- Cerny, P., 1989a. Exploration strategy and methods for pegmatite deposits of tantalum. In *Lanthanides, Tantalum and Niobium*. Edited by P. Moller, P. Cerny and F. Saupe. *Springer-Verlag, New York, p. 274-302*
- Cerny, P., 1991. Fertile granites of Precambrian rare-element pegmatite fields: is geochemistry controlled by tectonic setting or source lithologies? *Precamb. Res.* 51, 429–468.

- Cerny, P., 1991a. Rare-element granite pegmatites. Anatomy and internal evolution of pegmatite deposits. *Geoscience Canada* 18, 49-67.
- Cerny, P., 1992. Geochemical and petrogenetic features of mineralization in rare element granitic pegmatites in the light of current research. *Appl. Geochem.* 7, 393–416.
- Cerny, P., 1994. Rare-element Granitic Pegmatites. Part 1: Anatomy and Internal evolution of Pegmatite Deposits. *Prec. Res.; Vol. 53, pp. 29–62.*
- Cerny, P. and Ercit, T.S., 2005. The classification of granitic pegmatites revisited. *Canadian Mineralogist* 43, 2005-2026.
- Cerny, P., Blevin, P.L., Cuney, M., and London, D., 2005. Granite related ore deposits. *Econ. Geol. 100th Anniv.*, 337-370
- Cerny, P., Teertstra, D.K., Chapman, R., Selway, J.B., Hawthorne, F.C., Ferreira, K., Chackowsky, L. E., Wang, X. J. and Meintzer, R. E., 2012b. Extreme fractionation and deformation of the leucogranite-pegmatite suite at Red Cross Lake, Manitoba, Canada (IV. Mineralogy). *Can. Mineral.* 50, 1839–1875.
- Chappell, B.W. and White, A.J.R., 1992. I- and S-type granites in the Lachlan fold belt. *Transactions of the Royal Society of Edinburgh, Earth Science* 83, 1-26.
- Chappell, B.W. and White, A.J.R., 2001. Two contrasting granite types. 25 years later. *Australian Journal of Earth Sciences* 48, 489-499.
- Collins, B.W., 1996. Lachlan fold belt granitoids; products of three component mixing. In: Brown, M., Candela, P. A., Peck, D. L., Stephens, W. E., Walker, R. J. & Zen, E-an (Eds.). Third Hutton Symposium on the Origin of Granites and Related Rocks. *Geological Society of America, Special Papers* 315, 171-181
- Condie, K.C. 1973. Archean magmatism and crustal thickening. *Geological Society of America Bulletin* 84: 2981-2992
- Cox, K.G., Bell, J.D. and Paunkhurst, R.J. 1979. The interpretation of Igneous rocks. *London: Allen and Unwin.* 450

- da Silva, L.C., McNaughton, N.J., Armstrong, R., Hartmann, L. A. and Fletcher, I. R., 2005. The Neoproterozoic Mantiqueira Province and its African connections: a zircon-based U-Pb geochronologic subdivision for the Brasiliano/Pan African systems of orogens. *Precambrian Res.* 136, 203-240
- Dada, S.S., 1989. Evolution de la croûte continentale au Nord Nigeria: apport de la géochimie, de la géochronologie U-Pb et des traceurs isotopiques Sr Nd et Pb. *Doctorate Thesis, Université des Sciences et Techniques du Languedoc, Montpellier, France.*
- Dada, S.S., 2006. Proterozoic evolution of Nigeria. In: Oshi O (ed) The basement complex of Nigeria and its mineral resources (*A Tribute to Prof. M. A. O. Rahaman*). Akin Jinad & Co. Ibadan, pp 29-44
- Dalrymple, G.B. and Lanphere, M.A., 1969. Potassium-Argon Dating. *W.H. Freeman, San Francisco, Calif., 258 pp.*
- Damon, P.E., 1970. A theory of 'real' K-Ar clocks. *Eclogae Geol. Helv.*, 63. 69-76
- D'Lemos, R.S., Inglis, J.D., and Samson, S.D., 2006. A newly discovered orogenic event in Morocco: Neoproterozoic ages for supposed Eburnean basement of the BouAzzer inlier, Anti-Atlas Mountains. *Precambrian Research* 147 (2006) 65-78
- de Wit, M.J., Stankiewicz, J. and Reeves, C., 2008. Restoring Pan-African-Brasiliano connections: more Gondwana control, less Trans-Atlantic corruption in: Pankhurst, 789 R.J., Trouw, R.A.J., Brito Neves, B.B., De Wit, M.J. (Eds.), Pre-Cenozoic 790 Correlations Across the South Atlantic Region. *The Geological Society, London, pp. 791 399-412.*
- Deschamps, Y., Hocquard, C., Pelon, R., Milési, J.P. and Ralay, F., 2006. Geology and Ta Ore Deposits (Africa). *BRGM, Map 1:10,000,000.*
- Doust, H. and Omatsola, E., 1989. Niger Delta. *AAPG Memoir* 48:201-238
- Edem, G.O., Ekwueme, B.N. and Ephraim, B.E. 2015. Geochemical signatures and mineralization potentials of Precambrian pegmatite of Southern Obudu, Bamenda Massif, Southeastern Nigeria. *International Journal of Geophysics and Geochemistry* 2.3: 53-67

- Egbuniwe, J.G., 1982. Geotectonic evolution of the Maru belt, N.W. Nigeria. *Unpublished P.HD. Thesis, University college of Wales. Aberyswith 400p.*
- Egesi, N. and Ukaegbu, V.U., (2010). Petrologic and Structural Characteristics of the Basement Units of Bansara Area, southeastern Nigeria. *Pacific Journal of Science and Technology (PJST) 11(1):510 – 525.*
- Ekwueme, B.N., 1987. Structural orientations and Precambrian deformation episodes of Uwet area, Oban Massif, SE Nigeria *Prec. Res. 34, 269-289*
- Elatikpo, S.M., Danbatta, U.A. and Najime, T., 2013. Geochemistry and petrogenesis of Gneisses around Kafur-YariBori-Tsiga area within Malumfashi schist belt, Northwestern Nigeria. *Journal of Environment and Earth Science, vol 3, no.7.*
- Elueze, A.A., 2002. Compositional character: A veritable tool in the appraisal of geomaterials. *An inaugural lecture. University of Ibadan; 43p.*
- Ercit, T.S., 2005. REE-enriched granitic pegmatites. In rare-element Geochemistry and Mineral deposits (R.L. Linnen& I.M. Samson, eds.) *Geological Association of Canada, Short Course Notes 17, 175-199.*
- Ero K.A. and Ekwueme B.N., 2009. Mineralization of pegmatites in parts of the Oban Massif, Southeastern Nigeria: A preliminary analysis [J]. *Chinese Journal of Geochemistry. 28, 146 – 153.*
- Falconer, J.D., 1911. The geology and geography of Northern Nigeria. *Macmillan, London: 135pp.*
- Faleyimu, O.I., Agbeja, B.O. and Akinyemi, O., 2013. State of forest regeneration in Southwest Nigeria. *Africa Journal of Agricultural Research. Vol 8 (26) pp 3381-3383*
- Faure, G., 1977. Principles of isotope geology (Bk)
- Ferré, E.C., Gleizes, G. andCaby, R., 2002. Obliquely convergent tectonics and granite emplacement in the Trans-Saharan belt of Eastern Nigeria: a synthesis. *Precambrian Research 114, 199-219.*

- Fetherston, J.M., 2004. Tantalum in Western Australia: *Western Australia Geological Survey, Mineral Resources Bulletin 22, 162 p.*
- Fetter, A.H., dos Santos, T.J.S., Van Schmus, W.R., Hackspacher, P.C., Brito Neves, B.B., Arthaud, M.H., Neto, J.A.N. and Wernick, E., 2003. Evidence for Neoproterozoic Continental Arc Magmatism in the Santa Quitéria Batholith of Ceará State, NW Borborema Province, NE Brazil: Implications for the Assembly of West Gondwana. *Gondwana Research 6, 265-273.*
- Fitches, W.R., Ajibade, A.C., Egbuniwe, I.G., Holt, R. W. and Wright, J. B., 1985. Late Proterozoic schist belts and plutonism in NW Nigeria. *J. Geol. Soc. London, 142, 319-337.*
- Foley, S., 1991. High-pressure stability of the fluor- and hydroxy-endmembers of pargasite and K-richterite. *Geochimica et Cosmochimica Acta 55, 2689-2694.*
- Garba, I. 2002. Late Pan African tectonics and origin of gold mineralization and rare metal pegmatite in the Kushaka schist belt, northwestern Nigeria. *Journal of Mineral and Geol. 38:1-12*
- Garba, I., 2003. Geochemical discrimination of newly discovered rare metal bearing and barren pegmatites in the Pan-African 600 ± 150 Ma basement of Northern Nigeria. *Applied Earth Sc. Transaction Inst. Of Mining and Metallurgy; 13: Vol. 112, pp. 287–292.*
- Garner, E.L., Murphy, T.J., Gramlich, J.W., Paulsen, P.J. and Barnes, I.L., 1975. Absolute isotopic abundance ratios and the atomic weight of a reference sample of potassium. *Journal of research Natl. Bur. Standards – A. Physics and chemistry. 79A. No. 6, 713-725*
- Garrels, R.M. and Mackenzie, F.T., 1971. Evolution of Igneous and Sedimentary rocks. *New York: W. W. Norton and Company Inc. 397*
- Gaupp, R., Moller, P. and Morteani, G., 1984. Geology, Petrology and Geochemistry of Tantalum Pegmatites of untersuchungen. *Monograph series, Min. Deposit 23, 124p. Borntraeger Berlin Stuttgart.*

- Gillespie, M.R. and Styles, M.T., 1999. Rock Classification Scheme Volume 1, Classification of Igneous Rocks, *British Geological Survey Research Report (2nd ed.)*. British Geological Survey, Keyworth, Nottingham.
- Gillot, P.Y. and Cornette, Y. (1986). The “Cassignol technique” for potassium-argon dating, precision, and accuracy: examples from the Late Pleistocene to recent volcanics from Southern Italy. «*Chem. Geol. (Isot. Geos. Sect.)*», 59, 205-222
- Gillot, P.Y., Hildenbrand, A., Lefevre, J.C. and Albore-Livadie, C., 2006. The K/Ar dating method: Principle, analytical techniques, and application to holocene volcanic eruptions in Southern Italy. *Acta Vulcanologica*. Vol. 18 (1-2), 2006: 55-66
- Ginsburg, A.I., 1984. The geological condition of the location and the formation of granitic pegmatites. *International Geological Congress, 27th proceedings 15*, 245-260.
- Goodenough, K.M., Lusty, P.A.J., Roberts, N.M.W., Key, R.M. and Garba, A., 2014. Post-collisional Pan-African granitoids and rare metal pegmatites in Western Nigeria: age, petrogenesis and the pegmatite conundrum. *Litos 200-201*, 22-34
- Gorai, M., 1951. Petrological studies on Plagioclase twins. *Am. Mineral.*, 36, 884-901.
- Gordiyenko, V.V., 1971. Concentration of Li, Rb, and Cs in potash feldspar and muscovite as criteria for assessing rare metal mineralization in granite pegmatites. *Int. Geology Rev. Vol.13*, 134-142.
- Grant, N.K., 1970. Geochronology of Precambrian basement rocks from Ibadan, Southwestern Nigeria. *Earth Planet Sci Lett*, 10:19-38.
- Grant, N.K., 1978. Structural distinction between a metasedimentary cover and an underlying basement in the 600 my old Pan-African domain of Northwestern Nigeria. *Geol Soc Am Bull* 89:50-58
- Guillou, H., Michael, O.G. and Laurent, T., 1997. Unspiked K-Ar dating of young volcanic rocks from Loihi and Pitcairn hot spot seamounts. *Journal of Volcanology and Geothermal research* 78 (1997) 239-249
- Harris, N.B.W., Pearse, J.A. and Tindle A.G., 1986. Geochemical characteristics of

- collision-zone magmatism. *Geological society, London. Special Publications 19, 67-81*
- Heier, K.S., and Adams J.A.S., 1964. The geochemistry of the alkali metals. *In Physics and Chemistry of the Earth. Vol. 5, 253-381. Pergamon Press. Oxford*
- Henderson, P. (Ed.), 1984. Rare Earth Element Geochemistry. *Elsevier, Amsterdam, 510p*
- Hofmeister, A.M. and Rossman, G.R., 1985a. A spectroscopic study of amazonite: structurally hydrous, Pb-bearing feldspar. *American Mineralogist 70, 794-804.*
- Hunziker, J.C., 1979. Potassium argon dating. In E. Jager and J. C. Hunziker, eds., *Lectures in Isotope Geology, 52-76. Springer-Verlag, Berlin, 329p*
- Icenhower, J. and London, D., 1995. An experimental study of element partitioning among biotite, muscovite, and coexisting peraluminous silicic melt at 200 MPa (H₂O). *Am. Mineral. 80, 1229–1251.*
- Icenhower, J. and London, D., 1996. Experimental partitioning of Rb, Cs, Sr, and Ba between alkali feldspar and peraluminous melt. *Am. Mineral., p. 719.*
- Imeokparia, E.G., 1981. Cluster analysis of geochemical data from Tin-Tungsten bearing Afu Younger Granite Complex, Central Nigeria. *Journal of Mining and Geology 18(1): 198-203.*
- Irvine, T.N. and Baragar, W.R.A., 1971. Guide to the chemical classification of the common volcanics. *Canadian Journal of Earth Sciences 8: 523-545*
- Jacobs, J. and Thomas, R.J., 2004. Himalayan-type indenter-escape tectonics model for the Southern part of the late Neoproterozoic-early Palaeozoic East African-Antarctic orogen. *Geology 32, 721-724.*
- Jacobson, R.R.E. and Webb, J.S., 1946. The pegmatites of Central Nigeria *Geol. Surv. Nig. Bull.; Vol. 17, pp. 40–61.*
- Jahns, R.H. 1955. The study of pegmatites. *ECON. GEOL. 50TH ANNIVERSARY VOLUME. 1025-1130*
- Jahns, R.H. and Burnham, C.W. 1969. Experimental studies of pegmatite genesis: A

- model for the derivation and crystallisation of granitic pegmatites. *ECON. GEOL.* 64, 843-864
- Kinnaid, J.A., 1981. Geology of the Nigerian Anorogenic Ring Complexes 1:500,000 geological map. *John Bartholomew and Sons*
- Kontak, D.J. and Martin, R.F., 1997. Alkali feldspar in the peraluminous South Mountain batholith, Nova Scotia: trace element data. *Can. Mineral.* 35, 959-977
- Koppen, W. and Geiger, R., 1936. Das geographische system der Klimate. In *Koppen, W. and Geiger, R. (eds) Handbuch der Klimatologie, Berlin, Verlag von Gebrüder Borntraeger, Vol. 1, Part C:1-44*
- KPMG. 14th June 2017. Nigerian Mining Sector: An Overview.
- Kuster, D., 1990. Rare metal pegmatites of Wamba, central Nigeria their formation in relationship to late Pan-African granites. *Mineral Deposita; Vol.25, pp. 25-28*
- Küster, D. and Harms, U., 1998. Post-collisional potassic granitoids from the southern and northwestern parts of the Late Neoproterozoic East African Orogen: a review. *Lithos* 45, 177-195.
- Lappalainen, R. and Neuvonen, K.J., 1968. Trace elements in some Finnish pegmatitic potassium feldspars. *Bull. Geol. Soc. Finland* 40, 59-64
- Larsen, R.B., 2002. The distribution of rare-earth elements in K-feldspar as an indicator of the petrogenetic processes in granitic pegmatites: examples from two pegmatite fields in Southern Norway. *Can. Mineral.* 40, 137-151
- Laughlin, A.W., 1969. Excess radiogenic argon in pegmatite minerals. *J. Geophys. Res.*, 74. 6684-6690
- Le Maitre, R.M., Batman, P., Dudek, A.M., Keller, J., Lameyre Le Bas, M.J., Sabine, P. A., Schmid, R., Sorensen, H., Streikensen, A., Wolley, A.R. and Zenettin, B., 1989. Classification of Igneous rocks and glossary of terms. Recommendations of the international union of Geological Sciences sub-commission on the systematic of Igneous rocks. *Oxford: Blackwell Scientific Publications.* 193
- Livingston, D.E., Damon, P.E., Mauger, R.L., Bennett, R. and Laughlin, A.W., 1967.

- Argon 40 in cogenetic feldspar-mica mineral assemblages. *J. Geophys. Res.*, 72, 1361-1375
- London, D., 1995. Geochemical features of peraluminous granites, and rhyolites as sources of lithophile metal deposits. In Magmas, Fluids and Ore deposits (J.F.H. Thompson, ed.) *Mineralogical Association of Canada, Short Course Handbook 23*, 175-202
- London, D., 2005. Granitic pegmatites: An assessment of current concepts and directions for the future *LITHOS. Vol. 8*, pp. 281-303.
- London, D., 2005b. Geochemistry of alkalis and alkaline earths in ore-forming granites, pegmatites, and rhyolites. In Rare-Element Geochemistry of Ore deposits (R. Linnen & I. Samson, eds). *Geological Association of Canada, Short Course Handbook 17*, 17-43
- London, D., 2008, Pegmatites: The Canadian Mineralogist Special Publication 10, 347 p.
- Maniar, P.D. and Piccoli, P.M., 1989. Tectonic discrimination of granitoids, *Geol. Soc. Am. Bull.* 101, 635-643
- Martins, H., 1986. Progressive alteration associated with auriferous massive sulphide bodies at the Dumagami, Abitibi greenstone belt, Quebec. *Econ. Geol. Vol. 85*, pp 746-764
- Martin, R.F., 1988. The K-feldspar mineralogy of granites and rhyolites: a generalized case of pseudomorphism of the magmatic phase. *Rendiconti della Societa Italiana di Mineralogia e petrologia* 43, 343-354
- Martin, R.F. and De Vito, C., 2005. The patterns of enrichment in felsic pegmatites ultimately depend on tectonic setting. *Canadian Mineralogist* 43, 2027-2048
- Martin, R.F., De Vito, C. and Pezzotta, F., 2008. Why is amazonitic K-feldspar an earmark of NYF-type granitic pegmatites. Clues from hybrid pegmatites in Madagascar. *American Mineralogist* 93, 263-269.
- Matheis, G. and Caen-Vachette, M., 1983. Rb-Sr Isotopic Study of rare-metal bearing and barren pegmatites in the Pan-African reactivation zone of Nigeria. *J. Afr. Earth Sci.* 1, 35-40

- McCurry, P., 1976. The geology of the Precambrian to Lower Palaeozoic Rocks of Northern Nigeria – A Review. In: *Kogbe CA (ed) Geology of Nigeria. Elizabethan Publishers, Lagos, pp 15–39*
- McDougall, I., and Harrison, T.M., 1999, Geochronology and thermochronology by the $^{40}\text{Ar}/^{39}\text{Ar}$ method: *New York, Oxford University Press, xii, 269p*
- McDonough, W.F., Sun, S., Ringwood, A.E., Jagouzt, E. and Hofmann, A.W., 1992. K, R and Cs in the earth and moon and the evolution of earth's mantle. *Geochimica et Cosmochimica Acta, Ross Tylor Symposium volume, 1001-1021*
- Mehnert, K.R., 1968. Migmatites and origin of granitic rocks. *Elsevier, New York, x +394pp Illus.*
- Melcher, F., Graupner, T., Gabler, H.E., Sitnikova, M., Henjes-Kunst, F., Oberthur, T., Gerdes, A. and Dewaele, S., 2013. Tantalum-(niobium-tin) mineralisation in African Pegmatites and rare metal granites: Constraints from Ta-Nb mineralogy, geochemistry and U-Pb geochronology. *Ore Geology Review*
<http://dx.doi.org/10.1016/j.oregeorev.2013.09.003>
- Middlemost, E.A.K., 1994. Naming materials in the magma, Igneous rock system. *Earth Science Review 37: 215-224*
- Moller, P. and Morteani, G., 1987. Geochemistry exploration guide for Tantalum pegmatites. *Economic Geology, Vol.42, pp. 1885-1897*
- Morteani, G and Gaupp, R., 1989. Geochemical evaluation of the tantalum potential of pegmatites. In Lanthanides, Tantalum and Niobium. Edited by P. Moller, P. Cerny and F. Saupe. *Springer-Verlag, New York, p.303-310*
- Nier, A.O., 1935. Evidence for the existence of an isotope of potassium of mass 40. *Phys. Rev., 48. 283-284*
- Nier, A.O., 1950. A redetermination of the relative abundances of the isotopes of carbon, nitrogen, oxygen, argon, and potassium. *Phys. Rev., 77, 789-793*
- NMGRL, 2019. New Mexico geochronology research laboratory. Data acquisition and processing framework for Ar-Ar geochronology and noble gas mass spectrometry.
- Norton, J.J., 1966. Ternary diagrams of the quartz-feldspar content of pegmatites in

- Colorado, US. *Geological Survey, Bulletin 1241, D1-D16.*
- Obaje, N.G., Wehner, H., Scheeder, G., Abubakar, M. B. and Jauro, A., 2004. Hydrocarbon prospectivity of Nigeria's inland basins: from the viewpoint of organic geochemistry and organic petrology. *AAPG Bull* 87:325–353
- Obaje, N.G., 2009. Geology and Mineral Resources of Nigeria, *Lecture Notes 1 in Earth Sciences 120, DOI 10.1007/978-3-540-92685-6 _1, C Springer-Verlag Berlin Heidelberg 2009*
- Odin, G.S., 1990. Echelle numérique des temps géologiques. «*Geochronique, Soc.Geol. Fr.*», 35, 12-21.
- Odin, G.S., 1994. Geological time scale. «*C.R. Acad. Sci. Paris*», s.ii, 318, 1, part 2, 59-71.
- Ogezi, A.E.O., 1977. Geochemistry and Geochronology of Basement Rocks from Northwestern Nigeria. *Unpublished Ph.D. Thesis, University of Leeds*
- Okunlola, O.A., 2005. Metallogeny of Tantalite-Niobium Mineralization of Precambrian Pegmatites of Nigeria. *Mineral Wealth; 104/2005, pp. 38-50.*
- Okunlola, O.A., 2010. 'Ifewara Gold Exploration Report Nigeria Geological Survey Agency'' *Technical Report. pp 5-6*
- Okunlola, O.A., 2016. Geochemical characteristics economic potential and prospectivity assessment of rare metal Ta-Nb-Sn of Precambrian Southwestern Nigeria. *Abstracts Volume International Geological Conference, Cape Town. Pp.356*
- Okunlola, O.A., 2017. Riches beneath our feet: mineral endowment and sustainable development of Nigeria. *Inaugural lecture, University of Ibadan, Ibadan, Nigeria.*
- Okunlola, O.A., and Ogedengbe, E., 2003. Investment potential of gemstones occurrences in southwestern Nigeria. *Prospects for investment in mineral resources of southwestern Nigeria. A.A. Elueze. Eds. 41-45.*
- Okunlola, O.A. and Somorin, E.B., 2005. Compositional features of Precambrian

- pegmatites of Itakpe area, Central Nigeria. *Global Journal of Geological Sciences* 4.2;2006
- Okunlola, O.A. and Akintola, A.I., 2007. Geochemical features and rare metal (Ta-Nb) potentials of Precambrian pegmatites of Sepeteri area, Southwestern Nigeria. *Ife Journal of Science* 9:2:203-214
- Okunlola, O.A. and Akintola, A.I., 2008. Composition features and rare metal Ta-Nb potentials of Precambrian pegmatite of Lema-Ndeji area Central Nigeria. *Mineral Wealth* 149/2008 pp43-53
- Okunlola, O.A. and Ocan, O.O., 2009. Rare metal (Ta-Sn-LI-Be) distribution in precambrian pegmatites of Keffi area, Central Nigeria. *Nature and Science*, 7 (7) pp90-99
- Okunlola, O.A. and Jimba, S., 2006. Compositional trends in relation to Tantalum-Niobium mineralization in PreCambrian pegmatites of Aramoko-Ara-Ijero area, Southwestern Nigeria. *Journal of Mining and Geology Vol 42 (2) 2006; pp. 113-126*
- Okunlola, O.A., Akintola, A.I. and Egbeyemi, R.O., 2007. Geological setting, petrochemistry and petrogenetic affinity of Precambrian amphibolite of Lema-Ndeji area, Central Nigeria. *Quarterly publication of the scientific society of the mineral wealth technologists, July-September 2007.*
- Okunlola, O.A. and Oyedokun, M.O., 2009. Compositional trends and rare metal (Ta-Nb) mineralization potential of pegmatite and association lithologies of Igbeti area, Southwestern Nigeria. *Jour. RMZ- Materials and Geoenvironment, Vol.56, No.1, pp. 38-53.*
- Okunlola, O.A. and Akinola, 2010. Petrochemical characteristics of the Precambrian metal pegmatite of Oke-Asa area, Southwestern Nigeria. Implication for Ta-Nb mineralization. *RMZ- Materials and Geoenvironment, vol 57, No.4 pp 525-538*
- Okunlola, O.A. and Udoudo, O.B., 2005. Geological setting, petrographic features and

- age of rare-metal mineralization of pegmatites of Komu area, southwestern Nigeria. *UNESCO-ANSTI African Journal of Science and Technology Engineering Series 7. 1: 96-110*
- Ola, A.B. and Adewale, Y.Y., 2014. Infrastructural vandalism in Nigeria Cities: The case of Osogbo, Osun State. *J. Res. Humanities Soc. Sci. 4(3): 49-60.*
- Olade, M.A. and Elueze, A.A., 1979. Petrochemistry of the Ilesha amphibolite and Precambrian crustal evolution in the Pan-African domain of SW Nigeria. *Precambrian Res 8:303–318*
- Olarewaju, V.O. and Rahaman, M.A., 1982. Petrology and Geochemistry of Older Granites from some parts of Northern Nigeria. *Journal of Mining Geology 16.1: 97-107*
- Olayinka, A.I., 1992. Geophysical siting of boreholes in crystalline basement areas of Africa. *J Afr Earth Sci 14:197–207*
- Olisa, O.G., Okunlola, O.A. and Omitogun, A.A., 2018. Rare metals (Ta-Nb-Sn) mineralization potential of pegmatites of Igangan area, Southwestern Nigeria. *Journal of Geoscience and environment protection, 6, 67-88.*
<https://doi.org/10.4236/gep.2018.64005>
- Omosanya, K.O., Ariyo, S.O., Kaigama, U., Mosuro, G.O. and Laniyan, T.A., 2015. An outcrop evidence of polycyclic orogenies in the basement complex of Southwestern Nigeria. *Journal of geography and geology, Vol 7, No.3, 2015.*
- Oversby, V.M., 1975. Lead isotopic study of Aplites from the Precambrian basement rocks near Ibadan, Southwestern Nigeria. *Earth and planetary science letters, 37, 90-96.* [http://doi.org/10.1016/0012-821X\(75\)90027-8](http://doi.org/10.1016/0012-821X(75)90027-8)
- Oyawoye M.O., 1972. The basement complex of Nigeria. In: *Dessauvagine TFJ, Whiteman AJ (eds) African geology. Ibadan University Press, pp 66–102*
- Oyebamiji, A.O., 2014. Petrology and Petrochemical characteristics of rare metal pegmatites around Oro, Southwestern Nigeria. *Asia Pacific Journal of Energy and Environment, Volume 1, no.1*
- Oyinloye, O. A., 2011. Geology and Geotectonic setting of the Basement Complex Rocks

- in Southwestern Nigeria: Implications on provenance and evolution. *I.A. Dar. Ed. Earth and Environmental Sciences* 97-118
- Pearce, J.A., 1996. Sources and settings of granitic rocks. *Episodes, Vol. 19, No.4*
- Pearce, J.A. and Cann, J.R., 1973. Tectonic setting of basic volcanic rocks determined using trace element analysis. *Earth Planet. Sci. Lett.* 19, 290-300
- Pearse, T.H., Harris, N. B. W. and Tindle, A. D., 1984. Trace element discrimination diagrams for the tectonic interpretation of rocks. *Journal of Petrology*, 25, 956-983
- Peccerillo, A. and Taylor, S. R., 1976. Geochemistry of Eocene calc-alkaline volcanic rocks from the Kastmonu area, Northern Turkey. *Contributions to mineralogy and Petrology*, 58, 63-81
- Petters, S.S., 1991. Regional Geology of Africa, *Lecture Notes in Earth Science*, vol. 40. Springer Verlag, Berlin.
- Pisani, C. and Della Porta, P., 1967. A non-evaporable getter cartridge for use in UHV systems and in appendage pumps. *Nuovo Cimento, Suppl. Vol. 5: 261-273.*
- Popoola, O.A., 2016, Geological setting, petrochemical features of rocks and economic characterization of rare metal (Ta-Sn-Nb) pegmatite around Idiko-Ile, Igangan.
- Rahaman, M.A., 1976. Review of the basement geology of South-Western Nigeria. In: *Kogbe CA (ed) Geology of Nigeria, 2nd edn, Elizabethan Publishers, Lagos, pp 41-58*
- Rahaman, M.A., 1988. Recent advances in the study of the Basement Complex of Nigeria. In *Oluide P.O. (ed.) Precambrian Geology of Nigeria, Geol. Surv. of Nigeria, pp. 241-256*
- Rahaman, M.A. and Ocan, O., 1978. On relationships in the Precambrian Migmatite-gneisses of Nigeria. *Niger J Min Geol* 15:23-32
- Rahaman, M.A., Emofurieta, W.O. and Caen-Vachette, M., 1983. The potassic granites of the Igbeti area: further evidence of the polycyclic evolution of the Pan-African belt in Southwestern Nigeria. *Precamb. Res.* 22: 75-92
- Rahaman, M.A. and Lancelot, J.R., 1984. Continental crust evolution in SW Nigeria:

- constraints from U/Pb dating of pre-Pan-African gneisses. *In: Rapport d'activite 1980–1984 – Documents et Travaux du Centre Geologique et Geophysique de Montpellier 4:pp 41*
- Rama, S.N.I., Hart, S.R. and Roedder Edwin., 1965. Excess radiogenic argon in fluid inclusions. *Journal of Geophysical Research, vol 70, 2, pp.509-511*
- Randive, K.R., Hari, K.R., Dora, M.L., Malpe, D.B. and Bhondwe, A.A., 2014. Study of fluid inclusions: methods, techniques, and applications. *Gondwana Geological Magazine, 29, 19-28.*
- Rollinson, H.R., 1993. Using geochemical data: evaluation, presentation, interpretation. London (Longman scientific and technical). xxvi + 352pp
- Schaeffer, A.O. and Zähringer, J., (1966). Potassium-argon dating, *Berlin-Heidelberg-New York, Springer Verlag, 187pp.*
- Selway, J.B., Breaks, F.W. and Tindle, A.G., 2005. A review of rare-element (Li-Cs-Ta) pegmatite exploration techniques for the Superior Province, Canada, and large worldwide tantalum deposits. *Explor. Min. Geol. 14, 1–30*
- Seidemann, D.E., 1977. K-Ar dating of altered deep-sea igneous rocks from DSDP Legs 2, 34, and 35. *Department of Geology and Geophysics, Yale University, PANGAEA.*
- Shand, S.J., 1943. Eruptive rocks: Their genesis, composition, and classification, and their relation to Ore deposit with a chapter on meteorites. *John Wiley and sons, New York. 444pp.*
- Shaw, R.A., Goodenough, K.M., Roberts, N. M. W., Horstwood, M. S. A., Chenery, S. R. and Gunn, A. G., 2016. Petrogenesis of rare metal pegmatites in high-grade metamorphic terranes: A case study from the Lewisian Gneiss Complex of North-west Scotland. *Precambrian Research 281: 338-362*
- Simmons, W., Webber, K.L., Falster, A.U. and Nizamoff, J.W., 2003. Pegmatology: Pegmatite mineralogy, petrology and petrogenesis. *Rubellite Press, New Orleans, 176p*
- Snelling, N.J., 1966. Geochronology. *In Overseas Geological Survey Annual Report.*

HMSO, London

- Steiger R.H. and Jaeger E., 1977. Subcommission on geochronology: Convention on the use of decay constants in geo- and cosmochronology. «*Earth Planet.Sci. Lett.*», 36, 359-362.
- Stepanov, A., Mavrogenes, J.A., Meffre, S. and Davidson, P., 2014. The key role of mica During igneous concentration of tantalum. *Contributions to mineralogy and petrology* 167, article number:1009 (2014)
- Stern, R.J., 1994. Arc Assembly and continental collision in the Neoproterozoic East African orogeny - implications for the consolidation of Gondwana. *Annual Reviews of Earth and Planetary Sciences* 22, 319-351
- Sun, S.S. and McDonough W.F., 1989. Chemical and isotopic systematics of oceanic basalts: for mantle composition and processes. Magmatism in the Ocean Basins. D. Saunders and M. Norry. Eds. *Geological society of London Special Publications* 42: 313-345
- Taylor, S.R. and McLennan, S.C., 1985. The continental crust: its composition and evolution. *Carlton: Blackwell Scientific Publication*. 312
- Tindle, A.G. and Pearce, J. A., 1983. Assimilation and partial melting of continental crust:evidence from the mineralogy and geochemistry of autoliths and xenoliths. *Lithos*, 16, 185-202
- Tindle, A.G., Breaks, F.W. and Selway, J. B., 2002. Tourmaline in petalite-subtype granitic pegmatites: Evidence of fractionation and contamination from the Pakeagama Lake and Separation Lake areas of Northwestern Ontario, Canada. *Canadian Mineralogist*, 40, p. 753-788
- Tindle, A.G., Selway, J.B. and Breaks, F.W., 2002b. Electron microprobe and bulk analysis of fertile peraluminous granites and related rare-element pegmatites, Superior province, northwest and northeast Ontario: Operation Treasure Hunt, *Ontario Geological Survey, Miscellaneous Release-Data* 111.
- Tobi, A.C., 1961. The recognition of plagioclase twins in sections normal to the composition plane. *Amer.Mineral Vol. 46 (1961) pg1470*

- Totue, S.F., Macaudiere, J., Bertrand, J. M. and Dautel, D., 1990. Metamorphic Zircons from North Cameroon: Implications for the Pan-African Evolution of Central Africa. *Geol. Rundsch.*, 79, 777-788
- Trueman, D.L. and Cerny, P., 1982. Exploration for rare-element granitic pegmatites. In Granitic Pegmatites in Science and Industry (P. Cerny, ed.). *Mineralogical Association of Canada. Short Course Handbook 8*, 463-494.
- Truswell, J.F. and Cope, R.N., 1963. The geology of parts of Niger and Zaria Provinces, Northern Nigeria. *Geol. Survey Nigeria Bull* 29:1-104
- Tubosun, I.A., 1983. Geochronologie U/Pb du Socle Precambrian du Nigeria. *Unpublished 3^{eme} Cycle Thesis, Univ. des Sciences et Techniques du Languedoc. Montpellier*
- Turner, D.C., 1983. Upper Proterozoic schist belts in the Nigerian sector of the Pan-African Province of West Africa. *Precambrian Res* 21:55-79
- Umeji, A.C. and Caen-Vachette, M., 1984. Geochronology of Pan-African Nasarawa Eggon and MkarGboko granites, Southeastern Nigeria. *Precamb. Res.* 23, 317-324
- Van Breemen, O., Pidgeon, R.T. and Bowden, P., 1977. Age and isotopic studies of some Pan-African granites from North-central Nigeria. *Precambrian Res.* 4, 307-319.
- Vance, J.A., 1961. Polysynthetic twinning in plagioclase. *Amer. Mineral* Vol 46 (1961) pp 1097
- Von Knorring, O. and Condliffe, E., 1987. Mineralized pegmatites in Africa. *Geol. J.* 22, 253-270.
- Von Weizsäcker C.F., 1937. Über die Möglichkeit eines durch den β -Zerfall von Kalium. *«Phys. Zeitschr.»*, 38, 623-624
- Werner, C.D., 1987. Saxonian granulites-igneous or lithoigneous. A contribution to

the geochemical diagnosis of the original rocks in high grade metamorphic complexes. *Contributions of the Geology of the Saxonian granulites massif (SochisishesGanulitebirge)*. H. Gerstenberger. Ed. *ZeitschriftMitteillung* 133: 221-250

- Whalen, J.B., Currie, K.L. and Chappel, B. W., 1987. A-type granites: geochemical characteristics, discrimination and petrogenesis. *Contribution to Mineralogy and Petrology* 95: 407-419
- Whiteman, A., 1982. Nigeria: its petroleum geology, resources, and potential. *Graham and Trotman, London, 381 pp*
- Wilson, M., 1991. Igneous petrogenesis global tectonic approach, *Harpar Collins Academy, London second impression pp 227-241*
- Woakes, M., Rahaman, M.A. and Ajibade, A.C., 1987. Some metallogenetic features of the Nigerian Basement. *Journal of African Earth Sciences* 6, 655-664.
- Wright, J.B., 1970. Control of mineralisation in the older and younger tin fields of Nigeria, *Economic Geology*, 65, 945-951.
- Wright, J.B., 1985. Geology and mineral resources of West Africa. *George Allen & Unwin, London, 187*

